Analysis of Adult Hippocampal Neurogenesis in Neurodegenerative disease

Gang Han

Supervisors:
Dr Jeffrey S. Davies
Dr Alwena Morgan

Submitted to Swansea University in fulfilment of the requirements for the Degree of Doctor of Philosophy

Abstract

Neurodegenerative diseases cause severe health and social problems. They create a health and economic burden on individuals and their families. Currently, there is no efficient treatment, apart from some attenuating medicines, for the majority of neurodegenerative diseases. Neurone loss is a consistent characteristic of these diseases. The hippocampal dentate gyrus is one of the regions in the adult mammalian brain capable of generating new neurones throughout life. The neurogenic niche appears to play an important role in the neuronal dysfunction associated with neurodegeneration. However, the detailed mechanisms underpinning this process are still unclear.

To explore the neurogenic niche in Frontal Temporal Dementia (FTD) and Parkinson's disease (PD) we investigated disease-relevant rodent models and donated post-mortem human brain samples. Immunohistochemistry and immunofluorescent assays were developed to allow the quantification of dividing cells and immature neurones in the adult hippocampus of selected tissues.

The TDP43-Q331K knock-in mice, a model of FTD, revealed a significant reduction in the number of dividing cells ($Ki67^{+}$) and immature neurones (Dcx^{+}). Distinct morphological stages of immature neurone development were observed in this disease model. Further rodent neurotoxin-based models were used to characterise neurogenesis in PD. However, contrary to previous reports, these models did not consistently induce significant deficits in adult hippocampal neurogenesis (AHN). Human post-mortem brain samples were used to explore the neurogenic niche, but we were unable to consistently observe immature neurones in non-diseased brain samples.

In summary, this project identified significant AHN deficits in the FTD mouse model. These require further analysis to determine their function and possible role in human disease.

DECLARATION

This work has not previously been accepted in substance for any degree and is not being

Signed .....[redacted]..... (Candidate)

Date .....3.8.2022.....

This thesis is the result of my own investigations, except where otherwise stated. Other sources are acknowledged by footnotes giving explicit references. A bibliography is appended.

Signed .....[redacted]..... (Candidate)

Date .....3.8.2022.....

I hereby give consent for my thesis, if accepted, to be available for photocopying and for inter-library loan, and for the title and summary to be made available to outside organisations.

Signed .....[redacted]..... (Candidate)

Date .....3.8.2022.....

The University's ethical procedures have been followed and, where appropriate, that ethical approval has been granted.

Signed .....[redacted]..... (Candidate)

Date .....3.8.2022.....

ACKNOWLEDGEMENTS

Thanks for the instructions and help from my supervisors Jeff Davies, Alwena Morgan and Lauren Blake. Their research experience directed me to finish my PhD project.

For my research group Luke Buntal, Martina Sassi, Carla Carisi and Luke Roberts, it is my honour to work with all of you. The group helped numerous times. We work together, face problems together, solve problems together and grow up together in the academic world. A lot of happy memories with you will accompany me in my future career.

A huge thanks to some staff from Swansea University Medical School, Singleton Hospital and Morrison Hospital. With your help, I came back to the Lab to complete my project. A big thanks to Richard Summers and Stephen John. Your looking after me changes the way I feel about Swansea.

With the support from Dr Jemeen Sreedharan's group at King's College London, precious collaborating experiences were formed. The opportunity and the efficient professional working mindset made a deep impression and shows me the frontline research direction.

The numerous supports from my parents were the keys to ensuring my project was finished. Although they disagree with my decision to undertake a PhD, they still showed big support to me.

CONTENTS

1 Chapter 1 21
1.1 Frontotemporal dementia 21
1.1.1 Epidemiology 21
1.1.2 Behavioural syndrome (BvFTD) 22
1.1.3 Motor syndrome 23
1.1.4 Primary Progressive Aphasias (PPA) 24
1.1.5 Frontotemporal Dementia with Motor Neurone Disease 24
1.1.6 FTLD (Frontotemporal lobar degeneration) -Tau 26
1.1.7 Pick's Disease (3R Tau) 27
1.1.8 Progressive supranuclear palsy (PSP) (4R Tau) 27
1.1.9 FTLD-TDP (Frontotemporal lobar degeneration) 28
1.1.10 Fused in sarcoma (FUS) 28
1.1.11 Genetics 29
1.1.12 Neurogenesis and FTD 31
1.1.13 Treatments 31
1.1.14 FTD and ALS ..... **Error! Bookmark not defined.**
1.1.15 Frontotemporal Dementia TDP-43 animal model 32
1.2 Parkinson's disease (PD) 37
1.2.1 Epidemiology of PD 37
1.2.2 Syndrome of PD 38
1.2.3 Treatment of PD 39
1.2.4 Cause of PD 41
1.2.5 Pathology of PD 42
1.2.6 Immune system and PD 43
1.2.7 Genetics of PD 44
1.2.8 NSPCs and neurogenesis 45
1.2.9 MPTP 46
1.2.10 6-OHDA 48
1.3 Neurogenesis 51
1.3.1 Characterization of Neurogenesis 53
1.3.2 Neurogenesis in Humans 54

1.3.3 NSCs 55
1.3.4 Microglia and neurogenesis 57
1.3.5 Astrocytes and neurogenesis 58
1.3.6 Ghrelin 60
1.3.7 Environmental Enrichment (EE) and exercise on neurogenesis 61
1.3.8 Ageing and neurogenesis 63
1.3.9 Stress and neurogenesis ..... **Error! Bookmark not defined.**
1.3.10 Diet 63
1.4 Aim and hypothesis 65
2 Chapter 2 Materials & Methods 66
2.1 Animal studies 66
2.2 FTD mice model 66
2.2.1 Generation of an FTD mouse model using CRISPR/Cas9 66
2.2.2 Preparation of DNA for genotyping 67
2.2.3 Breeding of mice 68
2.2.4 Mice feeding 69
2.2.5 Brain exposure and preparation 69
2.2.6 DCX DAB Immunohistochemistry 70
2.2.7 Immunofluorescence co-localization IHC for DCX and PHF1 (PHD finger protein 1) -Tau 71
2.2.8 Ki67 DAB Immunohistochemistry 72
2.3 A rat model of PD using 6-hydroxydopamine (6-OHDA) 74
2.3.1 Housing Conditions and 6-OHDA treatment 75
2.3.2 Group Information 76
2.3.3 Brain sectioning 76
2.3.4 Immunofluorescence co-localization IHC for TH (Tyrosine hydroxylase) and Doublecortin (DCX) (free-floating method) 77
2.4 Generating a mouse model of PD using N-methyl-4-phenyl-1, 2, 3, 6-tetrahydropyridine (MPTP) 79
2.4.1 The generation of Dopamine transporter (DAT) knock-in mice 80
2.4.2 Housing Conditions and MPTP treatment 80
2.4.3 Group information 81
2.4.4 DCX DAB Immunohistochemistry 82
2.5 Analysis of IHC images using ImageJ 82

2.6 ImageJ coding lists 83
2.6.1 FTD disease model, (2 weeks old) DG images, Macro Coding records 83
2.6.2 FTD disease model, (2 weeks old), SVZ images, Macro Coding records 84
2.7 Data calculation & Statistical analysis 85
2.8 Human PD brain 85
3 Chapter 3 - Characterisation of adult hippocampal neurogenesis in a novel mouse model of Frontotemporal Dementia (FTD) 88
3.1 Introduction 88
3.1.1 FTD 88
3.1.2 Chapter aims 90
3.2 Methods and Materials 91
3.2.1 DCX DAB Immunohistochemistry ..... **Error! Bookmark not defined.**
3.2.2 Ki 67 DAB Immunohistochemistry ..... **Error! Bookmark not defined.**
3.2.3 DCX PHF1-Tau Immunofluorescence. **Error! Bookmark not defined.**
3.2.4 Materials used ..... **Error! Bookmark not defined.**
3.3 Results 93
3.3.1 Cell proliferation is not altered in two-week-old female TDP-$43^{Q331K+/Q331K+}$ and wild-type mice. 93
3.3.2 The immunoreactive area of $Ki67^{+}$ cells was increased in 6-month-old female TDP-$43^{Q331K+/Q331+}$ mice compared to wild-type mice. 98
3.3.3 2-week-old female TDP-$43^{Q331K+/Q331K+}$ mice show no reduction in immature neurone numbers 102
3.3.4 Six-month-old TDP-$43^{Q331K/Q331K}$ female mice have significantly reduced numbers of immature neurones in the hippocampus. 106
3.3.5 Six-month-old TDP-$43^{Q331K/Q331K}$ male mice have significantly reduced numbers of immature neurones in the hippocampus. 111
3.3.6 Six-month-old TDP-$43^{Q331K/Q331K}$ mice have significantly reduced numbers of immature neurones in the hippocampus. 115
3.3.7 Twenty-four-month-old male TDP-$43^{Q331K/Q331K}$ mice do not have a significantly reduced number of immature neurones in the hippocampus. 118
3.3.8 The number of immature neurones decreases between 6 - 24 months in both TDP-$43^{Q331K+/Q331+}$ and wild-type male mice. 122
3.3.9 Wild-type male mice generate more immature neurones compared to females at 6 months of age. 124

3.3.10 DCX^{+} cells from 6-month-old TDP-43$^{Q331K+/Q331K+}$ male mice show no difference in morphology in comparison to wild-type mice.....128
3.3.11 The TDP-43$^{Q331K+/ Q331K+}$ mutation affects the morphology of the DCX^{+} cells in 6-month-old female mice. 137
3.3.12 The TDP-43$^{Q331K+/ Q331K+}$ mutation affects the morphology of the DCX^{+} cells in 6-month-old mice. 144
3.3.13 The number of category A & B immature neurones is altered in male TDP-43$^{Q331K+/Q331K+}$ mice in comparison to male wild-type mice at 24 months of age. 150
3.3.14 TDP-43$^{Q331K+/Q331K+}$ mice have impaired immature phospho-Tau^{+} neurones in 6-month-old female mice. 158
3.4 Discussion .....**Error! Bookmark not defined.**
4 Chapter 4 Study of adult hippocampal neurogenesis in Parkinson's disease .166
4.1 Introduction 166
4.1.1 PD.....166
4.1.2 Aim of the Chapter.....170
4.2 Methods and Materials 171
4.2.1 6-OHDA rat model.....**Error! Bookmark not defined.**
4.2.2 MPTP mouse model.....**Error! Bookmark not defined.**
4.2.3 DCX DAB Immunohistochemistry.....**Error! Bookmark not defined.**
4.2.4 DCX TH Immunofluorescence .....**Error! Bookmark not defined.**
4.2.5 Materials.....**Error! Bookmark not defined.**
4.3 Results 172
4.3.1 6-OHDA can generate a PD disease model by reducing immature neurone numbers.....172
4.3.2 Acyl-ghrelin does not regulate adult hippocampal neurogenesis in a mouse MPTP-based model of PD.....177
4.3.3 There was no specific DCX immunostain observed in the post-mortem human hippocampus. 180
4.4 Discussion .....**Error! Bookmark not defined.**
5 Chapter 5 Discussion 184
5.1 FTD 184
5.2 PD.....196
5.3 Human AHN.....200
6 Chapter 6 Appendix 205

List of FIGURES

Figure 1.1 The structure of 3R-Tau and 4R-Tau.....27
Figure 1.2 Schematic of the TARDBP gene and 6 different isoforms of Tau caused by alternate splicing. 35
Figure 1.3 L-Dopa and dopamine pathway. 40
Figure 1.4 Substantia nigra pars compacta region of the adult brain. 42
Figure 1.5 PD disease animal model comparison. 50
Figure 2.1 Schematic of 6-OHDA rats experimental timeline.....76
Figure 2.2 Schematic of AMPK KO mice experimental timeline. 81
Figure 3.1 Ki67^{+} cells in the hippocampus and SVZ of 2-week-old TDP-43$^{Q331K/Q331K}$ and WT mice. IHC-DAB was performed for Ki67 on brain tissue sections from TDP-43$^{Q331K+/Q331K+}$ and wild type mice. Above are example images of the DG from TDP-43$^{Q331K+/Q331K+}$ (A), wild-type (B) mice, followed by example images of the SVZ from TDP-43$^{Q331K+/Q331K+}$ (C) and wild-type (D) mice. Images were taken by 10X objective lens. Representative of positive immunolabelled cells is shown by the arrows. Scale bar equals to 50μm.....94
Figure 3.2 Cell proliferation is similar in 2-week-old TDP-43$^{Q331K+/Q331K+}$ and wild type mice. IHC-DAB was performed for Ki67 on brain sections from male TDP-43$^{Q331K+/Q331K+}$ and wild type mice. The number of Ki67^{+} cells (A), Ki67^{+} immunoreactive area (B), rostral DG (C)(D), caudal DG (E)(F). Ki67^{+} cell number / average DG area (G)(H)(I). SVZ region (J)(K). The experiments comprised of 2 groups. Each Group n=6. Comparison was conducted by student's unpaired t-test. ns = not significant. All data shown are mean ± SEM. 97
Figure 3.3 Ki67^{+} cells in the hippocampus and SVZ of 6-month-old female TDP-43$^{Q331K/Q331K}$ mice and wild type mice. IHC-DAB was performed for Ki67 on hippocampal and SVZ sections from TDP-43$^{Q331K+/Q331K+}$ and wild type mice. Above are example images of the DG region from TDP-43$^{Q331K+/Q331K+}$ (A), wild-type (B) mice, followed by example images of the SVZ from TDP-43$^{Q331K+/Q331K+}$ (C) and wild-type (D) mice. Images were taken by 10X objective lens. Representative of positive immunolabelled cells is shown by the arrows. Scale bar equals to 50μm. 99
Figure 3.4 The area of Ki67+ cells increased in 6-month-old female TDP-43$^{Q331K+/Q331+}$ mice. IHC-DAB was performed for Ki67^{+} on hippocampal and SVZ sections from male TDP-43$^{Q331K+/Q331K+}$ and wild type mice. The number of Ki67^{+} cells were counted across the entire DG (A) immune positive cell area (B), Rostral DGs (C)(D), Caudal DGs (E), immuno positive cell area (F), SVZ (G)(H). The experiments comprised of 2 groups. Wild type mouse n=6, TDP-43$^{Q331K/Q331K}$ mice n=4. Comparison was conducted by student's unpaired t-test. ns = not significant, *P<0.05, **P<0.01. All data shown are mean ± SEM.....101
Figure 3.5 The expression of DCX^{+} cells in the hippocampus of 2-week-old female TDP-43$^{Q331K/Q331K}$ mice. IHC-DAB was carried out for DCX on hippocampal sections from TDP-43$^{Q331K+/Q331K+}$ and wild type mice. Above are example images of the DG

region from TDP-43$^{Q331K+/Q331K+}$ (A), wild-type (B) mice, followed by example images of the SVZ region from TDP-43$^{Q331K+/Q331K+}$ (C) and wild-type (D) mice. Images were taken by 10X objective lens. Representative of positive immunolabelled cells is shown by the arrows. Scale bar equals to 50μm. 103
Figure 3.6 2-week-old female TDP-43$^{Q331K+/Q331K+}$ mice show no reduction in immature neurone number. IHC-DAB was carried out for DCX on hippocampal sections from female TDP-43$^{Q331K+/Q331K+}$ and wild type mice. The number of DCX$^+$ cells were counted in the entire DG (A), DCX$^+$ cell immunoreactive area (B), rostral pole (C)(D), caudal pole (E)(F), SVZ region (G)(H). The experiments comprised of 2 groups. n=6 in each group. Unpaired t-test, ns = not significant. All data shown are mean ± SEM.....105
Figure 3.7 The expression of DCX$^+$ cells in the hippocampus of 6-month-old female TDP-43$^{Q331K/Q331K}$ mice. IHC-DAB was carried out for DCX on hippocampal sections from female TDP-43$^{Q331K+/Q331K+}$ and wild type mice. Above are example images of the DG region from TDP-43$^{Q331K+/Q331K+}$ (A), wild-type (B) mice, followed by example images of the SVZ region from TDP-43$^{Q331K+/Q331K+}$ (C) and wild-type (D) mice. Images were taken by 10X objective lens. Representative of positive immunolabelled cells is shown by the arrow. Scale bar = 50μm.....107
Figure 3.8 6-month-old female TDP-43$^{Q331K+/Q331K+}$ mice have a significantly reduced number of immature neurones in the DG. IHC-DAB for DCX$^+$ cells was performed on DG sections from 6-month-old female wild type and TDP-43$^{Q331K+/Q331K+}$ mice. The number of DCX$^+$ cells were counted per DG section (A), or DCX$^+$ cells were normalised per DG section area (B), or the number of DCX$^+$ cells were normalised per DG area (C). The number or area of DCX$^+$ cells were also quantified in either the rostral (D, F) or caudal (E, G) DG sections. The number (H) or area (I) of DCX$^+$ cells were also quantified in the SVZ. Wild type mice n=6, TDP-43$^{Q331K+/Q331K+}$ mice n=4. Statistical analysis was performed using Student's unpaired t-test (two tailed). ns = not significant, *P<0.05. All data shown are mean ± SEM. 110
Figure 3.9 The expression of DCX$^+$ cells in the hippocampus of 6-month-old male TDP-43$^{Q331K/Q331K}$ mice. IHC-DAB was performed for DCX on hippocampal sections from TDP-43$^{Q331K+/Q331K+}$ and wild type mice. Above are example images of the DG region from TDP-43$^{Q331K+/Q331K+}$ (A), wild-type (B) mice, followed by example images of the SVZ region from TDP-43$^{Q331K+/Q331K+}$ (C) and wild-type (D) mice. Images were taken by 10X objective lens. Representative of positive immunolabelled cells is shown by the arrow. Scale bar equals to 50μm.....112
Figure 3.10 TDP-43$^{Q331K/Q331K}$ mice have significantly reduced numbers of immature neurones in 6-month-old males. IHC-DAB was carried out for DCX on hippocampal sections from maleTDP-43$^{Q331K+/Q331K+}$ and wild type mice. The number of DCX$^+$ cells were counted in the entire DG (A), both rostral (B) and caudal (C) areas of the DG and the SVZ region (D). E represented the percentage of DCX$^+$ versus the area of the SVZ. Each group n=6. Statistical analysis was carried out using a student's unpaired t-test. ns = not significant, *P<0.05, **P<0.01, ***P<0.001. All data shown are mean ± SEM.....114
Figure 3.11 TDP-43$^{Q331K/Q331K}$ mice have significantly reduced numbers of immature neurones in DG in 6-month-old mice. IHC-DAB was carried out for DCX

on hippocampal sections for TDP-43$^{Q331K+/Q331K+}$ and wild type mice. The number of DCX^{+} cells were counted in the entire DG (A), both rostral (B) and caudal (C) areas of the DG, the cell number in SVZ region (D) and immunoreactive area in SVZ (E). WT group n=6, TDP-43$^{Q331K+/Q331K+}$ group n=10. Statistical analysis was carried out using a student's unpaired t-test. ns = not significant, *P<0.05, **P<0.01, ***P<0.001. All data shown are mean ± SEM.....117
Figure 3.12 The expression of DCX^{+} cells in the hippocampus of 24-month-old male TDP-43$^{Q331K/Q331K}$ mice. IHC-DAB was performed for DCX on hippocampal sections from TDP-43$^{Q331K+/Q331K+}$ and wild type mice. Above are example images of the DG region from TDP-43$^{Q331K+/Q331K+}$ (A), wild-type (B) mice, followed by example images of the SVZ region from TDP-43$^{Q331K+/Q331K+}$ (C) and wild-type (D) mice. Images were taken by 10X objective lens. Representative of positive immunolabelled cells is shown by the arrows. Scale bar equals to 50μm. 119
Figure 3.13 Twenty-four-month-old male TDP-43$^{Q331K/Q331K}$ mice do not have a significantly reduced number of immature neurones in the hippocampus. IHC-DAB was performed for DCX on hippocampal sections from male TDP-43$^{Q331K+/Q331K+}$ and wild type mice. The number of DCX^{+} cells were counted across the entire DG (A), rostral (B), caudal (C) poles and SVZ (D)(E). The experiments comprised of 2 groups. Each group n=6. Comparison was conducted by student's unpaired t-test. ns = not significant. All data shown are mean ± SEM.....121
Figure 3.14 The number of immature DCX^{+} neurones decrease between 6 - 24 months in both in TDP-43$^{Q331K+/Q331K+}$ and wild-type mice. IHC-DAB was performed for DCX on hippocampal sections from male TDP-43$^{Q331K+/Q331K+}$ and wild type mice. The number of DCX^{+} cells were counted across the entire DG in TDP-43$^{Q331K+/Q331+}$ mice and wild-type mice (A), SVZ in TDP-43$^{Q331K+/Q331+}$ and wild-type mice (B). For statistical comparison, ordinary two-way ANOVA was performed, followed by Tukey's post hoc comparison. ***P<0.001 vs control. All graph shows as mean ± SEM. n=6 for each group.....123
Figure 3.15 DCX^{+} cells in the hippocampus and SVZ of 6-month-old male and female TDP-43$^{Q331K/Q331K}$ and WT mice. IHC-DAB was performed for DCX on hippocampal and SVZ sections from TDP-43$^{Q331K+/Q331K+}$ and wild type mice of both sexes. Above are example images of the DG from TDP-43$^{Q331K+/Q331K+}$ (A), and wild-type (B) mice, followed by example images of the SVZ from TDP-43$^{Q331K+/Q331K+}$ (C) and wild-type (D) mice. Images were taken by 10X objective lens. Representative of positive immunolabelled cells is shown by the arrows. Scale bar equals to 50μm. 125
Figure 3.16 Wild type male mice generate more immature neurones compared to females at 6 months of age. IHC-DAB was performed for DCX on hippocampal sections from male and female TDP-43$^{Q331K+/Q331K+}$ and wild type mice. Graphs show DCX+ counts in the DG of wild type and TDP-43$^{Q331K/Q331K}$ mice (A), and in SVZ of wild type and TDP-43$^{Q331K/Q331K}$ mice (B). TDP-43$^{Q331K/Q331K}$ male mice, n=6, female mice, n=4. Male mice each generic type, n=6. Comparison was conducted by ordinary two-way ANOVA, followed by Tukey's post hoc comparison. ns = not significant, *P<0.05, **P<0.01, ***P<0.001. All data shown are mean ± SEM. 127
Figure 3.17 Categories of the different morphologies of DCX^{+} neurones according to their developmental stage. Adapted from (Plümpe *et al.*, 2006).....130

Figure 3.18 Analysis of DCX$^+$ cell morphology in the DG of six-month-old male TDP-43 $^{Q331K+/ Q331K+}$ and wild type mice. IHC-DAB for DCX was performed on hippocampal sections from TDP-43 $^{Q331K+/ Q331K+}$ and wild type mice. The morphology of the DCX$^+$ cells was assessed according to (Plümpe *et al.*, 2006). Image shows a hippocampal DG taken by 10X objective lens. The arrows indicate a representative of each morphology type from A to F. Scale bar equals to 100μm.....131
Figure 3.19 The distribution of the morphologies of DCX$^+$ cells in 6-month-old male TDP-43$^{Q331K+/Q331K+}$ and the wild type mice. The pie charts show the distribution of neurones according to their morphology, expressed as a population of the total number of DCX$^+$ cells. n=6 in each group.....132
Figure 3.20 6-month-old male TDP-43$^{Q331K+/Q331K+}$ mice show no difference in the morphology of their DCX$^+$ cells in comparison to wild-type mice. The DCX$^+$ cells were assessed and distributed according to their morphology as previously described by Plumpe et al 2006. The number of DCX$^+$ cells in each morphological category was counted in the DG (A), rostral DG (B), caudal DG (C), suprapyramidal (D), infrapyramidal (E), rostral suprapyramidal (F), rostral infrapyramidal (G), caudal suprapyramidal (H), caudal infrapyramidal (I). n=6. Comparison was conducted by ordinary tow-way ANOVA, followed by Tukey's post hoc comparison. ns = not significant, *P<0.05. All data shown are mean ± SEM. 136
Figure 3.21 The analysis of DCX$^+$ cell morphology in the DG. IHC-DAB for DCX was performed on hippocampal sections from TDP-43$^{Q331K+/ Q331K+}$ and wild type mice. The morphology of the DCX$^+$ cells was quantified according to Plumpe et al 2006. The representative image shows a hippocampal DG collected using a 10X objective lens. The arrows indicate a representative of each morphological types from A to F. Scale bar equals to 100μm. 138
Figure 3.22 The distribution of DCX$^+$ cell morphology in 6-month-old female TDP-43$^{Q331K+/Q331K+}$ and wild type mice. The pie charts show the distribution of neurones according to their morphology, expressed as a population of the total number of DCX$^+$ cells. Wild type mouse n=6, TDP-43$^{Q331K/Q331K}$ mice n=4. 139
Figure 3.23 The TDP-43$^{Q331K+/ Q331K+}$ mutation affects the morphology of DCX$^+$ cells in 6-month-old female mice. The DCX$^+$ cells were quantified according to their morphology as previously described by Plumpe et al 2006. The number of DCX$^+$ cells in each morphological category was counted in the DG (A), rostral DG (B), caudal DG (C), suprapyramidal (D), infrapyramidal (E), rostral suprapyramidal (F), rostral infrapyramidal (G), caudal suprapyramidal (H), caudal infrapyramidal (I). The experiments comprised of 2 groups. Wild type mice, n=6; TDP-43$^{Q331K/Q331K}$ mice, n=4. Statistical analysis was conducted by ordinary two-way ANOVA, followed by Tukey's post hoc comparison. ns = not significant, *P<0.05, **P<0.01, ***P<0.001. All data shown are mean ± SEM.....143
Figure 3.24 The distribution of DCX$^+$ cell morphology in 6-month-old TDP-43$^{Q331K+/Q331K+}$ and wild type mice. The pie charts show the distribution of neurones according to their morphology, expressed as a population of the total number of DCX$^+$ cells. Wild type mouse n=12, TDP-43$^{Q331K/Q331K}$ mice n=10. 145
Figure 3.25 The TDP-43$^{Q331K+/ Q331K+}$ mutation affects the morphology of DCX$^+$ cells in 6-month-old mice. The DCX$^+$ cells were quantified according to their morphology as previously described by Plumpe et al 2006. The number of DCX$^+$ cells

in each morphological category was counted in the DG (A), rostral DG (B), caudal DG (C), suprapyramidal (D), infrapyramidal (E), rostral suprapyramidal (F), rostral infrapyramidal (G), caudal suprapyramidal (H), caudal infrapyramidal (I). The experiments comprised of 2 groups. Wild type mice, n=12; TDP-43$^{Q331K/Q331K}$ mice, n=10. Statistical analysis was conducted by ordinary two-way ANOVA, followed by Tukey's post hoc comparison. ns = not significant, *P<0.05, **P<0.01, ***P<0.001. All data shown are mean ± SEM.....149

Figure 3.26 Analysis of DCX$^+$ cell morphology in the DG of 24-month-old male mice. IHC-DAB for DCX was performed on hippocampal sections from TDP-43$^{Q331K+/ Q331K+}$ and wild type mice. The morphology of the DCX$^+$ cells was then assessed and counted according to Plumpe et al 2006. Images include hippocampal DG captured using a 10X objective lens. The arrows indicate a representative cell of each morphology type from A to F. Scale bar equals to 50μm.....152

Figure 3.27 The distribution of DCX+ cell morphology in 24-month-old male TDP-43$^{Q331K+/Q331K+}$ and wild type mice. The pie charts show the distribution of neurones according to their morphology, expressed as a population of the total number of DCX$^+$ cells. Each group, n=6.....153

Figure 3.28 In male 24-month TDP-43$^{Q331K+/Q331K+}$ mice, the number of category A & B immature neurones is altered in comparison to wild-type mice. The DCX$^+$ cells were assessed and distributed according to their morphology as previously described by Plumpe et al 2006. The number of DCX$^+$ cells in each morphological category was counted in the DG (A), rostral DG (B), caudal DG (C), suprapyramidal (D), infrapyramidal (E), rostral suprapyramidal (F), rostral infrapyramidal (G), caudal suprapyramidal (H), caudal infrapyramidal (I). The experiments comprised of 2 groups, with n=6/group. Statistical analysis was conducted using ordinary two-way ANOVA, followed by Tukey's post hoc comparison. ns = not significant, *P<0.05, **P<0.01. All data shown are mean ± SEM. 157

Figure 3.29 PHF1-Tau and DCX cells in the DG in 6-month-old female mice. IHC-IF for PHF1-Tau and DCX was carried out on hippocampal sections from TDP-43$^{Q331K+/ Q331K+}$ and wild type mice. PHF1-Tau$^+$/DCX$^+$ cells (A), PHF1-Tau$^+$/DCX$^-$ cells (B), PHF1-Tau$^-$/DCX$^+$ cells (C) (PHF1-Tau, green channel; DCX, red channel). Images were taken using a 40X objective lens. Representative immunolabelled cells are shown by arrows. Scale bar = 50μm. 160

Figure 3.30 The TDP-43$^{Q331K/Q331K}$ regulates DCX and PHF1-Tau in the DG. Statistical analysis performed by unpaired Student's t-test. n = 4-6/group. ns = not significant, *P<0.05, **P<0.01. All data shown are mean ± SEM.....161

Figure 3.31 The TDP-43$^{Q331K/Q331K}$ mutation regulates PHF1-Tau$^+$ cell number in the infrapyramidal blade of the DG. Data analysis comprised of 4 groups. Wild type mouse, n=6; TDP-43$^{Q331K/Q331K}$ mice, n=4. Two-way ANOVA, followed by Tukey's post hoc comparison, ns = not significant, *P<0.05. All data shown are mean ± SEM. 162

Figure 3.32 The TDP-43$^{Q331K/Q331K}$ mutation predominantly reduces DCX$^+$ cell number in the suprapyramidal blade of the DG. The experiments comprised of 4 groups. Wild type mice, n=6; TDP-43$^{Q331K/Q331K}$ mice, n=4. Two-way ANOVA, followed by Tukey's post hoc comparison, ns = not significant, *P<0.05, ***P<0.001. All data shown are mean ± SEM.....163

Figure 3.33 The TDP-43$^{Q331K/Q331K}$ mutation reduces the DCX^{+}/PHF1-Tau^{+} cell number predominantly in the suprapyramidal blade of the DG IN 6-month-old female mice. The experiments comprised of 4 groups. wild type mice, n=6; TDP-43$^{Q331K/Q331K}$ mice, n=4. Two-way ANOVA, followed by Tukey's post hoc comparison, ns = not significant, *P<0.05, **P<0.01. All data shown are mean ± SEM. 164
Figure 4.1 Schematic of experimental timeline for 6-OHDA treated rats. .....**Error! Bookmark not defined.**
Figure 4.2 Schematic timeline of MPTP treated mice.**Error! Bookmark not defined.**

List OF TABLES

Table 1.1.....30
Table 2.1 CRISPR/Cas9 PAM sequences.....67
Table 2.2 TDP43 mutation.....67
Table 2.3 Primers Sequence.....68
Table 2.4 TDP-43 Sequence 68
Table 2.5 Primary antibodies used.....74
Table 2.6 Secondary antibodies used.....74
Table 2.7 Primary antibodies used.....79
Table 2.8 Secondary antibodies used.....79
Table 2.9 Antibodies used.....82
Table 3.1 Antobody used in IHC: 91
Table 3.2 Primary antibodies used in IF 91
Table 3.3 Secondary antibodies used in IF 92
Table 4.1 Primary antibodies used for 6-OHDA rat IHC 171
Table 4.2 Secondary antibodies used for 6-OHDA rat 171
Table 4.3 Antibodies used for MPTP mouse and human IHC.....171
Table 4.4 Multiple comparisons List of MPTP PD mice model... **Error! Bookmark not defined.**
Table 4.5.....181

PUBLICATIONS

MRI-guided histology of TDP-43 knock-in mice implicates parvalbumin interneuron loss, impaired neurogenesis and aberrant neurodevelopment in ALS-FTD, *Brain Communications,* DOI: 10.1101/2020.05.24.107177
https://www.biorxiv.org/content/10.1101/2020.05.24.107177v1

List OF CONFERENCES

2018 Swansea University Medical School Post Graduate Research Conference

2019 Swansea University Medical School Post Graduate Research Conference

2019 BNA conference in Dublin

ABBREVIATIONS

3H-Tdr	Tritiated thymidine
6-OHDA	6-hydroxy dopamine
ALS	Amyotrophic lateral sclerosis
ASO	Antisense oligonucleotide
ATP	Adenosine Triphosphate
BDNF	Brain-derived neurotrophic factor
BrdU	Bromodeoxyuridine
BvFTD	Behavioural variant FTD
CM	Conditioned media
CNS	Central nervous system
CREB	cAMP response element-binding protein
DAT	Dopamine transporter
DG	Dentate gyrus
EE	Environment elements
EGF	Epidermal growth factor
EMG	Electromyogram
ERK	Extracellular signal-regulated kinases
FGF-2	Fibroblast growth factor-2
FTD	Frontotemporal dementia
FUS	Fused in sarcoma
GCs	Granule cells
GFAP	Glial fibrillary acidic protein
GRN	Granulin precursor
IFN- γ	Interferon
IGFBP-6	Insulin like growth factor binding protein-6
IL-6	Interleukin-6
IP-10	Interferon-induced protein 10
IPCs	Intermediate progenitor cells
L-DOPA	Levodopa

LPS	Lipopolysaccharide
MAPK	Mitogen-activated protein kinase
MAPT	Microtubule associated protein Tau
MFB	Medial forebrain bundle
MND	Motor neurone disease
MPP	1-methyl-4-phenylpyridinium
MPTP	1-methyl-4-phenyl-1,2,3,6-tetrahydropyridine
MSK	Mitogen stress-activated kinase 1
MSK	Muscle-Specific Kinase
NADH	Nicotinamide adenine dinucleotide + hydrogen
NeuN	Neuronal Nuclei
nfvPPA	Nonfluent variant primary progressive aphasia
NFκB	Nuclear factor kappa-light-chain-enhancer of activated B cells
NGF	Nerve growth factor
NOS	Nitric oxide synthase
NSCs	Neural stem cells
OB	Olfactory bulb
PD	Parkinson’s disease
PHF1-Tau	PHD finger protein 1 Tau
PSP	Progressive supranuclear palsy
RGCs	Radial glia cells
ROS	Reactive oxygen species
SGZ	Subgranular zone
SNpc	Substantial nigra pars compacta
SRY	Sex determining region Y-box
SSRIs	Selective serotonin uptake inhibitors
svPPA	Semantic variant primary progressive aphasia
SVZ	Subventricular zone
TGF-β	Transforming growth factor-β
TH	Tyrosine hydroxylase
TNF-α	Tumour necrosis factor-α
TrkB	Tropomyosin receptor kinase B

VCAM-1	Vascular cell adhesion molecule-1
VEGF	Vascular endothelial growth factor
VENs	Von economou neurones
Wnt	Wingless and Int

1 Chapter 1
General Introduction

1.1 Frontotemporal dementia

Frontotemporal dementia (FTD) was first described in 1892, also described as Pick's disease initially. The most common feature of FTD is cell loss in the frontal and temporal lobes. The definition and criterion of FTD have been updated several times consistent with further research discoveries (Pick, 1892). The accelerated decline of language ability related to temporal lobe atrophy is classified as Semantic Variant Primary Progressive Aphasia (svPPA) (Gorno-Tempini *et al.*, 2011). The pathology of Pick's disease, initially analysed using silver stain, identified the argyrophilic cytoplasmic granules and proteinaceous inclusions representative of Pick's disease (Alzheimer, 1911). Until 1923, the frontal lobe together with temporal lobe atrophy was defined as 'Pick's atrophy (Thibodeau and Miller, 2013). The FTD spectrum was first named Pick's disease. FTD spectrum includes 3 disorders which cover motor movement and muscle syndromes. Pathologic changes occur in motor or muscle functions with or without language or behaviour problems which will be described in detail below (Lomen-Hoerth, Anderson and Miller, 2002)(Warren, Rohrer and Rossor, 2013)(Zarei *et al.*, 2015).

1.1.1 Epidemiology

Based on statistical records, for every 100,000 people, it is estimated that 1.61 to 4.1 cases of FTD will occur every year (Coyle-Gilchrist *et al.*, 2016)(Knopman and Roberts, 2011). For humans aged between 65 to 69 years old, the number of those diagnosed increases to 10.8 cases in every 100,000 people (Coyle-Gilchrist *et al.*, 2016). However, as many of the psychiatric symptoms of FTD overlap with many other psychiatric disorders it makes it difficult to determine the precise level of disease

prevalence. As a result, many consider the disease to be under-reported (Knopman and Roberts, 2011)(Lanata and Miller, 2016).

For the population under 65 years old, Alzheimer's disease is the most common dementia disorder, while FTD is the second most prevalent among all dementia diseases (Hodges *et al.*, 2003)(Knopman and Roberts, 2011)(Knopman and Roberts, 2011). The onset of FTD is normally reported in people between 45 to 65 years old, however, there are reports of this disease in people aged less than 30 years of age (Snowden, Neary and Mann, 2002). FTD appears to affect males and females similarly (Hogan *et al.*, 2016). FTD cases can be divided into two broad groups, Behavioural variant FTD (BvFTD) and other various deficient groups such as primary progressive aphasia (PPA), for which, the former accounts for 60% of all the cases, while the latter contains the other 40% (Onyike and Diehl-Schmid, 2013).

1.1.2 Behavioural syndrome (BvFTD)

BvFTD is mainly related to the pathologic changes in personality, emotion, behaviour and executive control (Rascovsky *et al.*, 2011). Several FTD-related syndromes overlap with other psychiatric diseases such as new compulsions, disinhibition, dietary behaviour changes, decreased empathy and apathy (Woolley *et al.*, 2011). Currently, in the diagnostic clinics, 6 criteria have been used to strengthen the accuracy of the diagnosis of FTD, which include, disinhibition, apathy, lack of empathy, compulsions, hyperorality and dysfunction of execution. If at least 3 symptoms are present, it will be considered to be FTD (Rascovsky *et al.*, 2011). Orbital frontal, medial frontal, anterior cingulate and front insular cortices are normally referred to as the paralimbic areas, relating mostly to the behavioural symptom (Rosen *et al.*, 2005)(Seeley *et al.*, 2008).

Compared with the left hemisphere, behaviour symptoms seem to be more related to right hemisphere atrophy (Rosen *et al.*, 2005). Around the pregenual anterior cingulate cortex, orbital frontal, and front insular cortex, it is common to find Von Economou Neurones (VENs), which are present in great apes and humans (Seeley *et al.*, 2006) (Seeley *et al.*, 2008). The areas which contain VENs, are believed to occupy have a certain vulnerability that may lead to susceptibility to bvFTD pathology, and the same

areas have also been reported to become the first pathologically associated locations (Schroeter *et al.*, 2008)(Seeley *et al.*, 2007)(Seeley, Zhou and Kim, 2012). Some scholars support the theory that during progressive neurodegeneration, toxic protein aggregates are passed from one cell to another, consistent with a prion-like behaviour syndrome (Kfoury *et al.*, 2012)(Wu *et al.*, 2013).

Based on different brain locations which correlate with pathologic changes, bvFTD patients showed heterogeneous clinical phenotypes. When the dorsolateral prefrontal cortex starts to show a pathological decline, it is common to observe patients reporting symptoms involving the loss of executive control, since that region can interact with bilateral parietal lobes (Kramer *et al.*, 2003)(Seeley *et al.*, 2007). Behaviours that are deemed inappropriate including getting too familiar with strangers, over-touching, and invading personal space are defined as disinhibition. The symptoms also include careless and compulsive behaviours and actions such as theft, gambling and making decisions without thinking about the outcomes. In this case, the degeneration of the right orbital frontal cortex is likely to be associated with disinhibition in BvFTD (Tekin and Cummings, 2002)(Tranel, Bechara and Denburg, 2002). From statistical records, 37%-54% of patients who have been diagnosed with bvFTD exhibit new criminal actions (Liljegren *et al.*, 2015). Some of the most reported symptoms are patients using rude language and lacking a sense of embarrassment (Rankin *et al.*, 2005). Also, different forms of apathy have been noted (Chow *et al.*, 2009). 'Affective apathy' is linked with not caring and indifference, while 'motor apathy' is linked with decreased drive and less overall movement. 'Cognitive apathy' manifests as reduced engagement with reaching specific goals in different activities (Merrilees *et al.*, 2009) (Chow *et al.*, 2009). Some other apathy phenomena such as a tendency to cancel family involvement, individual hobbies and work engagement may also occur. Under such circumstances, extra reminders and encouragement are frequently required in order to keep conversations going, finish chores or even move.

1.1.3 Motor syndrome

Frequent ritualistic activity which contains consistency, compulsion and stereotype elements becomes common in bvFTD (Ames *et al.*, 1994)(Josephs, Whitwell and Jack,

2008)(Perry *et al.*, 2012)(Rosso *et al.*, 2001). Some of the most reported repetitive motor behaviours are clapping, tapping, picking, rubbing, and lip-smacking. Other progressive behaviours include counting rituals, collecting small things, walking in a fixed pattern and altered speech patterns. All these compulsive and stereotypical activities can be associated with several brain regions. For example, the right dorsal anterior cingulate cortex and left premotor cortex atrophy are linked with aberrant motor behaviour (Rosen *et al.*, 2005). Atrophy of the striatum can cause stereotypical symptoms including rocking and tapping, while asymmetric temporal lobe atrophy leads to complex compulsion (Josephs, Whitwell and Jack, 2008)(Rosso *et al.*, 2001). Furthermore, in the globus pallidus (bilateral), left putamen and lateral temporal pole, grey matter loss is widely related to compulsive obsession behaviour in bvFTD (Perry *et al.*, 2012).

1.1.4 Primary Progressive Aphasias (PPA)

Primary progressive aphasias are one of the characteristics of FTD, which shows language impairment within the first 2 years of diagnosis (Mesulam, 1987)(Mesulam, 1982). It is a disorder that involves focal degeneration of brain areas that are involved in governing language (Grossman, 2010)(Mesulam *et al.*, 2014). However, in the clinic, it is difficult for even experienced clinicians to diagnose language-led dementia. The possible reason for this is that it is uncommon, with the prevalence rate being about 3 per 100,000 cases (Magnin *et al.*, 2016)(Coyle-Gilchrist *et al.*, 2016). The understanding of PPA has also been changed as pathogenic proteins can selectively cause brain network degeneration such as Tau which is described in detail below (Warren *et al.*, 2013). There are 3 main forms of PPA: nonfluent agrammatic variant (nfvPPA), semantic variant (svPPA) and logopenic variant (lvPPA). They comprise the consensus diagnostic criteria (Gorno-Tempini *et al.*, 2011). Each type of PPA is associated with a specific linguistic or cognitive deficit and represents the most probable anatomical pathological features (Montembeault *et al.*, 2018).

1.1.5 Frontotemporal Dementia with Motor Neurone Disease

Motor neurone disease (MND), dementia and parkinsonism were first summarised by Guamanian Chamorros in 1874 as Amyotrophic Lateral Sclerosis-parkinsonism dementia complex (ALS) (Betz, 1874). Similar symptoms can be observed for about 15% of FTD patients and 30% of MND patients (Lomen-Hoerth, 2011). Even in the neurological disease clinic, it is difficult to recognize those diseases as distinct because of the overlap of coexisting characteristics (Lomen-Hoerth, 2011). Indeed, approximately 90% of patients who have been diagnosed with MND are mixed with ALS. So at the clinic, MND and ALS are mostly used to describe the same disease (OUH, 2022).

In the clinical diagnosis criterion, upper and lower motor neurone damage is identified following a physical body examination and electromyogram (EMG) to confirm it is MND for an FTD patient (Geevasinga *et al.*, 2016). It is worth emphasizing that EMG can help enable the early diagnosis of MND in FTD patients (Al-Chalabi, 2017)(Brooks, 1994) (Carvalho and Swash, 2009) (Geevasinga *et al.*, 2016). Previous studies have suggested that if FTD patients start to present with muscle weakness, fasciculations, difficulty in swallowing, spastic tone, pathological crying and laughing, further MND exanimation is recommended. Notably, more practice in neuro-muscular activities can attenuate the symptoms (Olney *et al.*, 2005).

1.1.6 FTD and ALS

Amyotrophic Lateral Sclerosis (ALS), which is normally described as a pathologic phenomenon of upper and lower motor neurone loss, is 1 of the 5 motor neurone diseases (Lomen-Hoerth, Anderson and Miller, 2002)(Warren, Rohrer and Rossor, 2013). It has been reported that 19% of FTD patients will advance to ALS (Talbot, 2009). ALS is characterised by the loss of specific groups of motor neurones, upper neurones in the primary motor cortex and lower neurones in the brain stem and spinal cord (Ingre *et al.*, 2015). Symptoms normally include muscle atrophy and weakness, which advance into muscle paralysis. Ultimately the respiratory muscles will be involved and cause difficulties in breathing (Ingre *et al.*, 2015). Of all ALS patients, 3-5% will eventually be diagnosed with FTD by post-mortem as ALS and FTD share numerous clinical (Fallini *et al.*, 2020) and pathological characteristics (Rakowicz and Hodges, 1998).

1.1.7 FTLD (Frontotemporal lobar degeneration) -Tau

Tau protein was discovered as an important protein in assembling microtubules in 1975 (Weingarten *et al.*, 1975). Indeed, cellular transport and cell structure stabilization rely widely on the Tau protein (Weingarten *et al.*, 1975). Subsequent work has identified the importance of the Tau protein for its role in regulating cellular signalling pathways (Jenkins and Johnson, 1998)(Leugers and Lee, 2010)(Morris *et al.*, 2011). This polypeptide contains a microtubule-binding domain which allows to binding of some heterodimers with microtubule lattice (Avila *et al.*, 2016). The gene encoding the Tau protein, Microtubule Associated Protein Tau (MAPT), located on chromosome 17q21, is associated with the FTD-Tau pathology (Clark *et al.*, 1998)(Hutton *et al.*, 1998)(Mandelkow and Mandelkow, 2012)(Poorkaj *et al.*, 1998)(Spillantini, Murrell JR, *et al.*, 1998)(Wilhelmsen *et al.*, 1994). Six different sub-forms of Tau protein can be created by alternative splicing of the MAPT gene shown below. In FTD patients, 4R Tau and 3R Tau (seen in Figure 1.1) are predominantly generated by this alternative splicing (Mandelkow and Mandelkow, 2012). Hyperphosphorylation of Tau protein can result in insoluble aggregates leading to neurodegeneration (Šimić *et al.*, 2016). In Alzheimer's disease, it has been considered that both 4R Tau and 3R Tau's hyperphosphorylation promotes the formation of neurofibrillary tangles (O'Neill *et al.*, 2001). In FTD, 3R Tau plays a key role in the pathological changes (Brunden, Trojanowski and Lee, 2008), while in other dementia diseases, 4R Tau is implicated in disease pathology (Van Swieten and Spillantini, 2007).

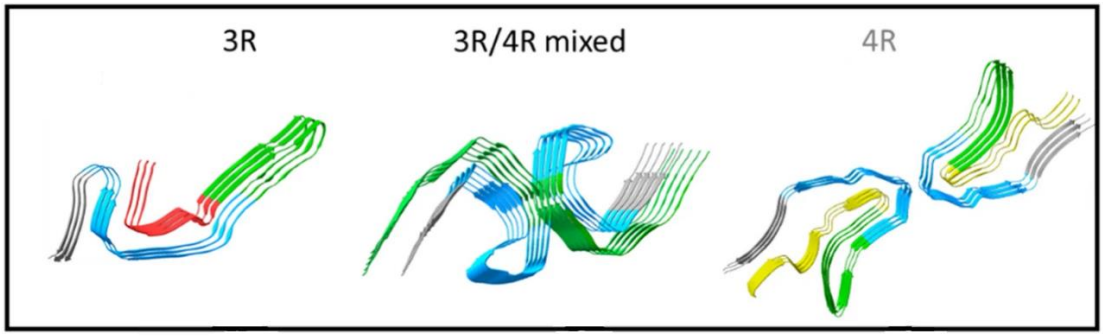

Figure 1.1 The structure of 3R-Tau and 4R-Tau.

The figure depicts 3 different types of Tau proteins: 3R-Tau, 3R/4R mixed Tau and 4R-Tau. Different colours represent different tau substrates. In this polypeptide, there are 4 binding region: Red – R1; Yellow – R2; Green – R3; Blue – R4 (Metrick *et al.*, 2020)

1.1.8 Pick's Disease (3R Tau)

Pick cells, which refer to ballooned-shaped neurones, are a typical cell morphology in FTD. Another neurochemical characteristic of FTD cells is Pick bodies, which is a structure containing argyrophilic neurone cytoplasm with a spherical shape. In most reports (Yoshida, 2006), Pick bodies are immunopositive for 3R Tau, although occasionally 4R Tau can be produced in some cell types (Zhukareva *et al.*, 2002). More specifically, the autopsy recorded 23% of Nonfluent Variant Primary Progressive Aphasia (nfvPPA) and 9% of Semantic Variant Primary Progressive Aphasia (svPPA) as being positive for 3R tau. FTD, originally known as Pick's disease, now mainly refers to a clinical syndrome and a group of brain disorders.

1.1.9 Progressive supranuclear palsy (PSP) (4R Tau)

Tufted astrocytes, spherical neurofibrillary tangles and thorny astrocyte formation in subcortical nuclei are characteristic of progressive supranuclear palsy (PSP) pathology (Dickson *et al.*, 2002)(Josephs *et al.*, 2011)(Josephs *et al.*, 2006)(Litvan *et al.*, 1996). This pathology type normally shows symptoms such as loss balance during walking and inability to aim eyes (Golbe, 2014). Typical pathological features include coiled bodies in the white matter of the subcortex and cortex which contain oligodendroglial

cytoplasm (Dickson and Inc, 2011). In these coiled bodies, 4R Tau is the predominant protein, and this phenomenon can also be observed in the brainstem (Lee, Goedert and Trojanowski, 2001). Cortical pathological formation normally relates to the frontal eye field and primary motor cortex causing deteriorated cognition performance (Bigio, Brown and White, 1999).

1.1.10 FTLD-TDP (Frontotemporal lobar degeneration)

FTD and ALS share certain features. For example, TAR DNA-binding protein 43 (TDP-43, transactive response DNA binding protein 43 kDa) plays a very important role in both FTD and ALS (Amyotrophic lateral sclerosis) pathology (Arai *et al.*, 2006)(MacKenzie *et al.*, 2011)(Neumann *et al.*, 2006). TDP-43 is responsible for micro-RNA production, stabilization, transport and translation (Fiesel and Kahle, 2011). It is deemed a part of the heterogeneous cell nuclear ribonucleoproteins (Baralle, Buratti and Baralle, 2013). The mechanism connecting TDP-43 to FTD pathology is still unclear, but scholars report thousands of mRNA functions associated with it (Polymenidou *et al.*, 2011). In FTD, cytoplasmic aggregates of TDP-43 have been observed and are thought to be related to altered ubiquitination and phosphorylation (Scotter, Chen and Shaw, 2015). In 2011, FTD-TDP pathology was introduced as a key hallmark of FTD research, which in most cases can only be diagnosed post-mortem (Mackenzie and Neumann, 2012).

1.1.11 Fused in sarcoma (FUS)

The Fused in sarcoma (FUS) gene was discovered in 2009, and its mutation is linked with MND, with post-mortem studies revealing the accumulation of FUS proteins in the cytoplasm of pathologic motor neurones (Kwiatkowski *et al.*, 2009)(Neumann *et al.*, 2011)(Vance *et al.*, 2009). The FUS proteins which normally remain in an insoluble form, are mostly expressed in adult differentiated neurones and their overexpression can reduce lifespan (Miguel *et al.*, 2012). Although FUS's molecular function is still poorly understood, it is known to have DNA/RNA binding properties,

similar to TDP-43 (Baloh, 2012)(Mackenzie and Neumann, 2012)(Birsa, Bentham and Fratta, 2020).

1.1.12 Genetics

Currently, records show that at least 50% of FTD cases are characterised as sporadic, meaning that they have no known cause. Approximately 40% of patients have a family history of dementia and they are likely to share a genetic cause, which is called familial FTD (fFTD). The motor symptoms stay at a similar distribution as 40% of them have a family history. The autosomal dominant pattern is reported in 10% of familial FTD cases (Chow *et al.*, 1999) (Goldman *et al.*, 2005)(Capozzo *et al.*, 2017).

Three genes have been reported to have a strong association with FTD, including C9ORF72, MAPT and GRN (Granulin precursor). Other genes linked to FTD include TARDBP, FUS, VCP, CHMP2B, EXT2 and AQATM1 (Borghero *et al.*, 2011) (Kovacs *et al.*, 2009)(Mosca *et al.*, 2012). CHMP2B (Skibinski *et al.*, 2005) TBK1 (Freischmidt *et al.*, 2015) (Pottier *et al.*, 2015) OPTN (Pottier *et al.*, 2015)(Pottier *et al.*, 2016) SQMSTM1 (Fecto, 2011) (Pottier *et al.*, 2016) UBQLN2 (Deng *et al.*, 2011) and EXT-2 (Narvid *et al.*, 2009)

Table 1.1

Gene Name	Abbreviation	Reference	GWAS Records
Chromosome 9 open reading frame 72	C9ORF72	(Babić Leko *et al.*, 2019)	Yes
Microtubule-associated protein tau	MAPT	(Rademakers, Cruts and van Broeckhoven, 2004)	Yes
Granulin precursor	GRN	(van Swieten and Heutink, 2008)	Yes
TAR DNA-binding protein	TARDBP	(Bourbouli *et al.*, 2017)	Yes
FUS RNA binding protein	FUS	(Seelaar *et al.*, 2011)	No
Valosin-containing protein	VCP	(Kimonis *et al.*, 2008)	Yes
Charged multivesicular body protein 2B	CHMP2B	(M Isaacs *et al.*, 2011)	Yes
Exostosin glycosyltransferase 2	EXT2	(Puangmalai *et al.*, 2020)	Yes
TANK-binding kinase 1	TBK1	(Abreha *et al.*, 2021)	Yes

According to published data, in all the genetic cases, 63% of the cases were caused by C9ORF72 mutations, 26% of the cases were related to GRN and only 11% of the cases were associated with MAPT (Steele *et al.*, 2018). However, investigations are still undergoing investigating the effect of C9ORF72 as this gene mutation is only present in about 40% of familial FTD (Friedland *et al.*, 2012).

1.1.13 Neurogenesis and FTD

In order to study the connection between adult hippocampal (AHN) neurogenesis and FTD, researchers have used post-mortem brain samples. AHN is a process where new adult-born neurones are continuously generated in the hippocampus throughout life and contribute to episodic memory function. This paradigm is described in more detail in section 1.3 below. Adult-born dentate granular cells from post-mortem FTD patients show an abnormal morphology (Thompson *et al.*, 2008). Indeed, based on the expression of different biomarkers of immature neurones, the morphology is abnormal and the ratio of quiescent and proliferating hippocampal stem cells is altered (Adusumilli *et al.*, 2021). More specifically, these data suggest neurogenesis was impaired. During FTD, the reduced activity of microglia strengthens the capability of astrogliosis (Heneka, Kummer and Latz, 2014).

1.1.14 Treatments

Currently, for FTD, there is no effective treatment, but behavioural therapy can contribute to attenuating the symptoms of FTD. Though many similarities have been noted between FTD and Alzheimer's disease (Coppola *et al.*, 2012), the treatment, which is effective for alleviating cognitive decline in Alzheimer's disease such as Acetylcholinesterase (AChE) inhibitors, does not change FTD pathology or those syndromes (Noufi *et al.*, 2019).

Some published research suggests that selective serotonin uptake inhibitors (SSRIs) can improve FTD patient symptoms by helping to control overeating and compulsive behaviours (Herrmann *et al.*, 2012)(Ikeda *et al.*, 2004)(Mendez, Shapira and Miller, 2005)(Swartz *et al.*, 1997). With extra caution, atypical antipsychotics can be prescribed to FTD patients, but they have the potential to cause extrapyramidal syndrome side effects such as acute dyskinesias and dystonic reactions. For elderly people (Pijnenburg *et al.*, 2003). When SSRIs do not show efficacy in patients, antipsychotics can decrease the severity of challenging behaviours which may put the patient at risk of self-harm (*Frontotemporal dementia - Treatment - NHS*, 2022).

Behavioural education as well as adopting physical and environmental techniques can provide support to reduce inappropriate behaviours (Merrilees, 2007). Physical exercise has also been commonly recommended to FTD patients as it delays cognitive decline and is considered safe for elderly and vulnerable populations (Cheng *et al.*, 2014). For patients whose symptoms present mainly with language dysfunction such as nfvPPA and svPPA, speech therapy will be a front-line treatment (Kortte and Rogalski, 2013).

Although there are no FDA-approved treatments for FTD, this is a hopeful time for their development. There is a currently active clinical trial targeting specific FTD mechanisms and pathologies (ClinicalTrials.gov Identifier: NCT04408625). Further trials targeted at tau pathology with therapeutics aimed at preventing tau aggregation, tau microtubule stabilization and removal of tau with tau-targeted antibodies are also ongoing / have also been performed (Karakaya *et al.*, 2012)(Schneider and Mandelkow, 2008)(Tsai and Boxer, 2016). There are trials currently targeting the haploinsufficiency in Granulin Precursor (GRN) gene expression by using different methods of increasing progranulin (Boxer *et al.*, 2013)(Lagier-Tourenne *et al.*, 2013). Antisense oligonucleotide (ASO) therapies are being developed to target the toxic gain of function associated with *C9orf72* genetic mutation (Lagier-Tourenne *et al.*, 2013). The possibility of evidence-based treatments targeting molecularly defined targets for FTD is closer than they have ever been. During a report in the American Neurological Association annual meeting, Washington University, the School of Medicine reported a negative result for their phase 3 trial which involved an antisense therapy for FTD-ALS which suggested this therapy was not effective. These important clinical studies draw great interest in exploring the mechanisms of neurodegenerative diseases.

1.1.15 Frontotemporal Dementia TDP-43 animal model

Due to the reported toxicity of the insoluble TDP-43 different pre-clinical experimental models have been generated in order to explore the mechanisms of FTD-ALS. For example, drosophila and zebrafish have been used to test the TDP-43 function (Loganathan *et al.*, 2020)(Ash *et al.*, 2010) (Hanson *et al.*, 2010)(Kabashi *et*

al., 2009)(Yoshida and Ihara, 1993). In these models, TDP-43 aggregates have been discovered in glia and muscle cells which causes FTD and ALS-like effects in the form of age-related motor deficits and premature lethality (Diaper *et al.*, 2013)(Liachko, Guthrie and Kraemer, 2010)(Minami *et al.*, 2014). These studies suggested that TDP-43 aggregation was observed in motor neurone axons, similar to that seen in human FTD-ALS (Hanson *et al.*, 2010)(Kabashi *et al.*, 2009). Mouse models with a reduced expression of TDP-43 revealed low muscle strength when testing forelimb grip (Kraemer *et al.*, 2010). TDP-43 knockout mice also displayed an age-dependent progressive motor neurone degeneration (Iguchi *et al.*, 2013). Also, in an animal TDP43 pF-wt model, according to a research group in Trieste, Italy, TDP-43 protein can regulate its mRNA in a negative feedback manner (Ayala *et al.*, 2011). Another mouse model that injected a human TDP-43 cDNA into hybrid eggs showed that it can be regulated by heterologous promotors to increase the expression in disease-relevant cells such as central nervous system (CNS) neurones (Stallings *et al.*, 2010)(Da Cruz and Cleveland, 2011). TARDBP is the gene that encodes TDP-43 and the discovery of TARDBP mutations in humans with ALS led to the generation of specific TDP-43 knock-in models to express the mutated form of the gene such as TDP-43^{A315T} and TDP-43^{G348C} (Kabashi *et al.*, 2008). Using a modified murine promoter to create an amplified human TARDBP cDNA that was microinjected into a mouse pronuclear oocyte resulted in offspring that were crossbred and validated to overexpress hTDP-43. The overexpression was reported to cause a dose-dependent disease phenotype that included motor dysfunction, gliosis, TDP-43 phosphorylation and neurodegeneration (Janssens *et al.*, 2013).

So far, numerous TARDBP mutations have been published (http://www.molgen.ua.ac.be/FTDMutations/) and now TARDBP is recognised as one of the causes of ALS familial type (Gendron, Rademakers and Petrucelli, 2013). Each of these mouse models presents some aspects of the disease, including motor neurone degeneration and cognitive impairment, and they suggest that Tau's function has changed leading to instability of microtubules (Trinczek *et al.*, 1995)(Gu *et al.*, 2017)(Kabashi *et al.*, 2008). It has been reported that in TDP-43^{A315T} and TDP-43^{G348C} models the mutations led to Tau mRNA instability (Gu *et al.*, 2017). By exploring Tau exon 10 (Figure 1.2) and the 3R:4R Tau ratio, different isoforms can also be detected in FTD-ALS (Gu *et al.*, 2017). The increase of 4R to 3R tau is reported in FTD and

some other neurodegenerative diseases, while the 2:1 on 4R:3R ratio was described in Alzheimer's disease. (Ginsberg *et al.*, 2006)(Conrad *et al.*, 2007)(Hutton *et al.*, 1998)

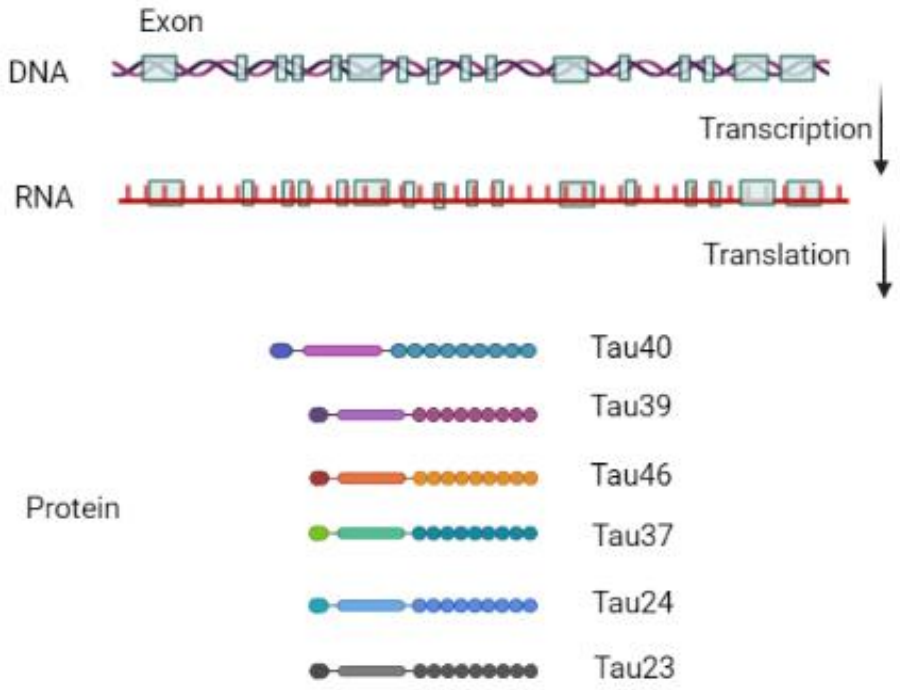

Figure 1.1.2 Schematic of the TARDBP gene and 6 different isoforms of Tau caused by alternate splicing.

The alternate splicing of exons 2 and 3 can lead to either 1 or 2 N-terminal inserts. When exon 10 is spliced, it leads to 3 microtubule binding domains. When included it, it leads to 4 microtubule binding domains. When the amino acids length ranges from 352-441, it can lead to 6 different isoforms, shown above. (Liu and Gong, 2008)

As mentioned above, a number of TDP-43 models have been generated. Several of these include the overexpression of transgenes such as the TDP43^{A315T} mice (Estes *et al.*, 2011). To improve the validity of disease models efforts are being made to generate mice that harbour disease-causing mutations with physiological expression levels. For example, the TDP-43^{Q331K} knock-in mouse model with a human equivalent mutation in TARDBP - glutamine to lysine substitution at position 331 (White, Kim, Duffy, Adalbert, Phillips, Peters, Stephenson, Yang, Massenzio, Lin, Andrews, Segonds-Pichon, Metterville, Saksida, Mead, Ribchester, Barhomi, Serre, Coleman, J. R. Fallon, *et al.*, 2018) (Watkins *et al.*, 2021). In particular, the TDP-43^{Q331K} mice did not show an increased expression of human TDP-43 in comparison to the murine form (White, Kim, Duffy, Adalbert, Phillips, Peters, Stephenson, Yang, Massenzio, Lin, Andrews, Segonds-Pichon, Metterville, Saksida, Mead, Ribchester, Barhomi, Serre, Coleman, J. R. Fallon, *et al.*, 2018). Indeed, the TDP-43^{Q331K} gene knock-in model seems to replicate the behavioural and some pathologic changes associated with human FTD (White, Kim, Duffy, Adalbert, Phillips, Peters, Stephenson, Yang, Massenzio, Lin, Andrews, Segonds-Pichon, Metterville, Saksida, Mead, Ribchester, Barhomi, Serre, Coleman, J. R. Fallon, *et al.*, 2018). While this model has a dose-dependent influence on TARDBP gene expression, no significant neuromuscular phenotypes have been reported (Arnold *et al.*, 2013)(White, Kim, Duffy, Adalbert, Phillips, Peters, Stephenson, Yang, Massenzio, Lin, Andrews, Segonds-Pichon, Metterville, Saksida, Mead, Ribchester, Barhomi, Serre, Coleman, J. R. Fallon, *et al.*, 2018). However, significant spatial learning and memory impairments were reported with this model (White, Kim, Duffy, Adalbert, Phillips, Peters, Stephenson, Yang, Massenzio, Lin, Andrews, Segonds-Pichon, Metterville, Saksida, Mead, Ribchester, Barhomi, Serre, Coleman, J. R. Fallon, *et al.*, 2018). Therefore, it will be important to explore the cellular and molecular mechanisms mediating these changes in this model.

Notably, TDP-43 is the major protein sub-unit of the ubiquitinated inclusions which are found in FTD/ALS (Ratti and Buratti, 2016). Furthermore, researchers have shown that the Q331K mutation can trigger the progressive age-dependent degeneration of motor axons in mice (Mitchell *et al.*, 2015). It can also cause motor neurone death in mice (Mitchell *et al.*, 2015). This recapitulates the possibility of losing nuclear function during disease pathogenesis. Thus, the TDP-43 Q331K mouse model of FTD/ALS represents a novel tool to further characterise the neurochemistry

underpinning the disease spectrum and provides a new opportunity to study hippocampal neurogenesis.

1.2 Parkinson's disease (PD)

Dr James Parkinson was the first to publish details of this disease in 1817, in 'An Essay on the Shaking Palsy', which included the key characteristics of Parkinson's disease (PD) such as tremors, stiffness and impaired balance (Shulman, De Jager and Feany, 2011)(Donaldson, 2015)(National Institute on Aging., 2016). A general term for neurological disorders that involve impaired movement is Parkinsonism. The most common form of Parkinsonism is PD (Kharkar, 2013)(Schrag, 2008). In the clinic, Parkinsonism, also known as atypical PD, does not include tremors. Parkinsonism typically affects both sides of the body, while PD is generally associated with one side being more affected than the other (Elbaz *et al.*, 2002)(*Parkinsonism vs. Parkinson's Disease: What's The Difference?*, 2022).

1.2.1 Epidemiology of PD

Parkinson's disease is an age-related neurodegenerative disease that normally occurs in individuals over 60 years old, within which about 1% of the population will be affected (Lotharius and Brundin, 2002a)(Jones Jr *et al.*, 2013). World-wide it is thought about 1 in 500 people will have PD. Most people who have PD start to develop symptoms after 60 years old and above (*Parkinson's disease - NHS*, 2022). In the UK, about 145,000 people live with PD (PARKINSON UK, 2020) with a male-to-female diagnosis rate of about 3:2 (Kalia and Lang, 2015). When patients start showing matched criteria of PD syndromes and receive a diagnosis in the clinic, their average life expectancy ranges from about 7 to 14 years (Sveinbjornsdottir, 2016)(Mosley, 2009). There is no doubt that the PD patient's quality of life will be significantly affected, and social care support will be required (Bosboom, Stoffers and Wolters, 2004)(Jankovic, 2008).

1.2.2 Syndrome of PD

Rigidity, slow movement, tremor and walking difficulties are commonly present at the earliest stages of the disease (Nithianantharajah and Hannan, 2006). However, the most outstanding feature of PD is the resting tremor, which normalises during movement or deep sleep. Often one hand starts to show this phenomenon which is then followed by both hands as the pathology progresses (Jankovic, 2008). Some patients with PD syndrome report visuospatial difficulties which can be identified using tests of line orientation and memory for spatial position and mental rotation (Caproni *et al.*, 2014). Visuospatial difficulties correlate with the degradation of behaviour, cognition, mood and thought (Blochberger and Jones, 2011). At a very early stage, PD patients can have cognitive difficulties, which will deteriorate during the progression of PD (Blochberger and Jones, 2011)(Bosboom, Stoffers and Wolters, 2004). One of the most common signs is executive dysfunction such as planning difficulties, cognitive flexibility, summarizing thinking, understanding rules, lack of embarrassment, career memory and difficulties in concentration. Notably, the cognitive decline is different between PD and AD. PD normally declines faster than AD in the visuospatial domain whilst memory is more impaired in AD. Also, language function declines more rapidly in AD compared to PD (Smirnov *et al.*, 2020).

Pathological changes in motor function, especially in fine movement, are also included in parkinsonism or parkinsonian syndrome (Kalia and Lang, 2015)(Jones Jr *et al.*, 2013). The motor system is one of the systems which are heavily impaired because of the degradation of the motor neurones which are controlled by basal ganglia circuits in the CNS at a slow progressing rate. Indeed, the importance of dopamine to movement, motivation and mood is notable and its reduction is a consequence of the death of the dopamine-producing neurons in the brain (Mor, Daniels and Ischiropoulos, 2019)).

Other behavioural features may also be present including, apathy, agitation, hypersexuality, stereotypic movements, pathological gambling and abuse of antiparkinsonian drugs (Trojano and Papagno, 2018) (Bosboom, Stoffers and Wolters, 2004). Other non-motor features also present in some patients, which include constipation, impaired GI motility, cognitive deficits and REM-sleep disorders (Sveinbjornsdottir, 2016)(Schapira, Chaudhuri and Jenner, 2017). With the

progression of PD, dementia also develops as a common characteristic for a large proportion of those diagnosed (Jankovic, 2008). In addition, about 30% of PD patients will also suffer from depression and anxiety, which may be observed years after diagnosis (Sveinbjornsdottir, 2016).

Less common symptoms of PD include sleeping difficulties, sensory dysfunction and emotional disorders (Sveinbjornsdottir, 2016). This normally indicates the slow initiation of involuntary movement which becomes progressively worse. Repetitive activities such as finger tapping can occur and normally combines with at least 1 of the 3 main physical signs; muscular rigidity, postural instability and resting tremor (Ling *et al.*, 2012)(Thomas and Beal, 2017). Motor-related symptoms present a clear diagnostic criterion for clinicians to diagnose PD. Indeed, WHO has documented 4 main motor syndromes to consider as PD, including slow movement, postural instability, rigidity and tremor. Non-motor features, including neuropsychiatric problems, sensory changes, sleeping difficulties and autonomic dysfunction can also aid in diagnosing PD. Neuropsychiatric problems can include alterations in mood, behaviour, cognition and thinking changes. Sensory changes are particularly linked to olfactory changes which is difficult to test during diagnosis. However, it is still a challenge for the clinician to provide an accurate diagnosis as only some of these symptoms may be present in patients (Deuschl *et al.*, 2006). In addition to the motor and non—motor diagnostic symptoms described above, the diagnosis of PD can be aided by the use of neuroimaging tests such as positron emission tomography (PET) and single photon emission computed tomography (SPECT)(Hughes *et al.*, 1992) to quantify levels of dopamine or related proteins such as the dopamine transporter within the CNS.

1.2.3 Treatment of PD

Currently, there is no cure for PD, but in alleviating the symptoms, progress has been achieved (Kharkar, 2013). Levodopa (L-DOPA) in the clinic is the first recommended treatment for PD. L-DOPA is a precursor to dopamine and can act as a dopamine replacement (see figure 1.3). L-dopa therapy has been shown to increase dopamine levels in the striatum and the DA transporter of nerve terminals (Dorszewska *et al.*,

2014). For about 50% of patients, levodopa reduces abnormal movements (such as gait, and resting tremor). The possible mechanism is still not clear. However, chronic use often results in L-DOPA-induced dyskinesias (LIDS) – a debilitating movement disorder characterised by pronounced involuntary muscle contractions (Pandey and Srivanitchapoom, 2017).

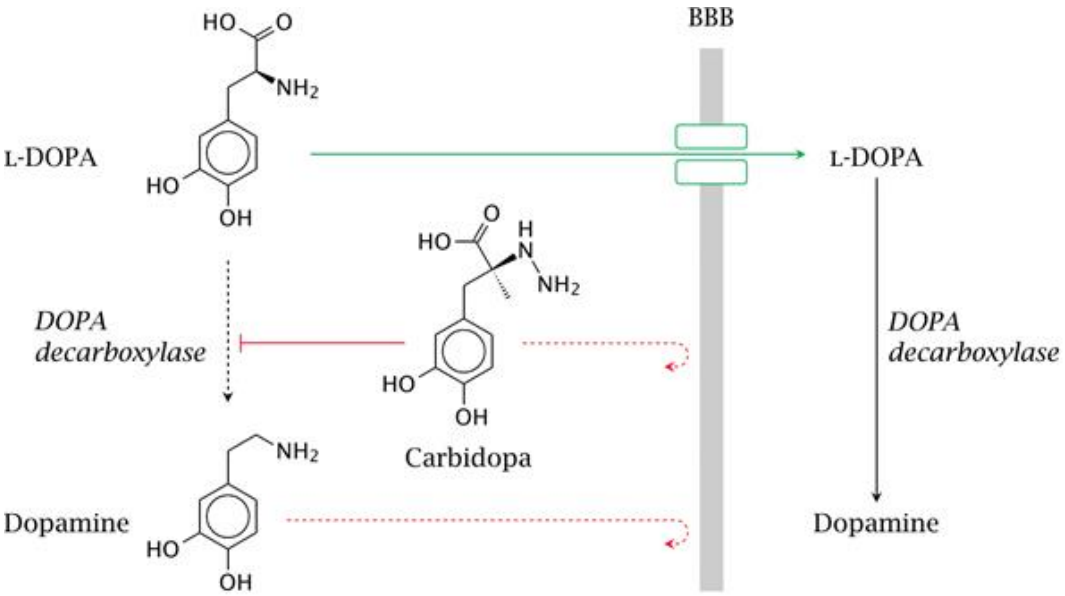

Figure 1.1.3 L-Dopa and dopamine pathway.

Image shows the pathway from L-dopa to dopamine and their structure alteration. Carbidopa is also depicted as a DOPA decarboxylase inhibitor that does not cross the BBB. Its use results in reduced peripheral side effects as less dopamine is generated outside of the CNS.

Dopamine agonists are another group of drugs that have been widely used to attenuate the symptoms of PD. These include Bromocriptine, Cabergoline and Apomorphine. Dopamine agonists work by stimulating bothD1 and D2 dopamine receptors in brain regions such as the striatum and hippocampus and are believed to activate similar chemical pathways as dopamine and thus mimic its actions (Brooks, 2000). However, as PD progresses there is a progressive loss of dopaminergic neurones, meaning that the effectiveness of these treatments decreases. For early PD treatment, especially for people less than 60 years old, this treatment is often effective. Furthermore, this therapy is associated with an undesired side effect of involuntary writing movements (Sveinbjornsdottir, 2016).

Since 1993, deep brain stimulation (DBS) has been widely used to treat PD. This involves surgically inserting a microelectronic stimulator into the subthalamic nucleus in the thalamus. Although this treatment option is less common because of the invasive brain surgery involved, the therapy often results in an astonishing improvement in attenuating the motor symptoms of PD and improves the patient's quality of life. This method normally shows a certain effect for a range of Parkinson's syndromes and is regarded as the next option if earlier drug treatments have a positive effect (Deuschl *et al.*, 2006). Notably, DBS of the sub-thalamic nucleus has been reported to stimulate AHN in rodents, leading to the suggestion that it may be effective in slowing cognitive decline (Rubchinsky, Park and Worth, 2012).

Other methods which attenuate sleeping disturbances and emotional interference are also effective therapies, and they address different kinds of non-movement-related symptoms of PD (Kalia and Lang, 2015). According to published research, patients who have sleeping disorders might benefit from procedures that alter the sleeping environment or help to build patterns in sleep behaviour. If there is no improvement in symptoms, some medicines can be prescribed to help according to the different types of sleeping disorders. For example, Clonazepam can be used for rapid eye movement (REM) sleeping disorders (Roychowdhury and Forsyth, 2012). Moreover, REM sleeping disorders are also considered the prodrome of PD (Postuma, 2014).

1.2.4 Cause of PD

Both genetic and environmental factors are thought to contribute to PD, however, the underlying pathogenic mechanisms are not fully understood (Kalia and Lang, 2015). Epidemiological research suggested that people with a history of prolonged contact with certain agricultural pesticides had an increased risk of developing this disease (Berry, La Vecchia and Nicotera, 2010). Further work revealed that patients who had central neurological injuries, including traumatic brain injury and spinal cord injury, had a higher probability of being diagnosed with PD later in life (Bazarian *et al.*, 2009). Interestingly, populations who have a culture of smoking tobacco, and drinking tea and coffee had a lower incidence rate of PD (Kalia and Lang, 2015) (Quintana *et al.*, 2009).

1.2.5 Pathology of PD

The key histopathological hallmark of PD is the loss of dopaminergic cells in the substantia nigra pars compacta region of the adult brain. Another highlighted pathological phenomenon is the accumulation of proteins forming Lewy bodies in mature neurones (Kalia and Lang, 2015). The current clinic guidelines normally indicate risk factors such as infection, toxins, inflammation, medical side effects, injuries, metabolic diseases and other brain diseases (Kharkar, 2013)(Nuytemans *et al.*, 2010).

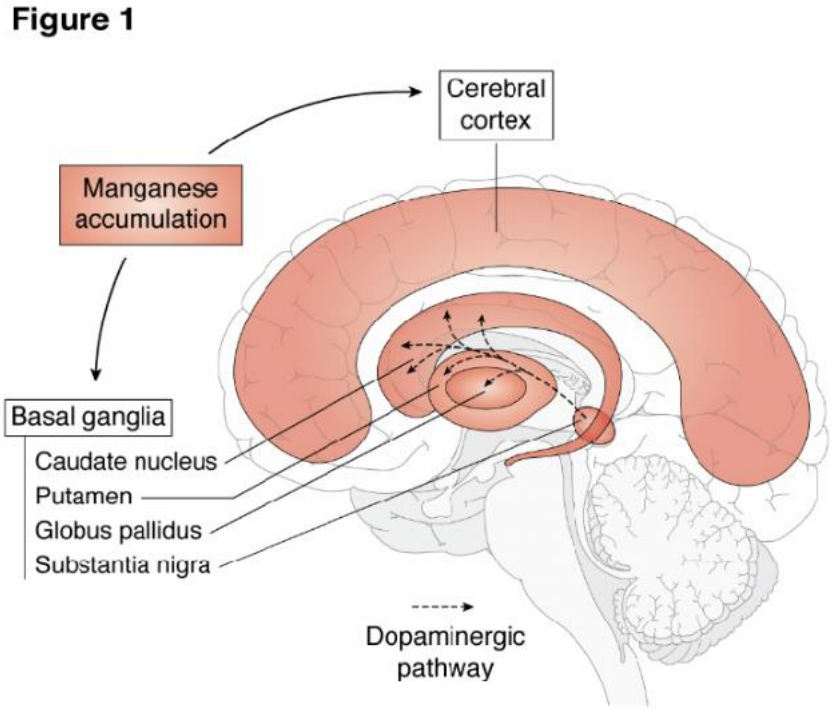

Figure 1.1.4 Substantia nigra pars compacta region of the adult brain.

Image shows the location of Substantia Nigra in Adult human brain, dopaminergic pathway and manganese accumulation.

Whilst memory loss is the main characteristic of Alzheimer's disease, PD is primarily a syndrome of slowness, stiffness, tremor, rigidity and postural instability (Aarsland, Zaccai and Brayne, 2005). However, cognitive impairment is also a possible factor in

PD, with ~70% of PD cases eventually succumbing to PD dementia (Watson and Leverenz, 2010). PD patients have a 2-6 times greater risk of developing dementia compared to healthy subjects (Jankovic, 2008)(Bosboom, Stoffers and Wolters, 2004). Notably, those diagnosed with cognitive problems within 12 months of a PD diagnosis are re-diagnosed as having Dementia with Lewy Body disease (Kane *et al.*, 2018)(Stephen N. Gomperts, 2016)(Stephen N Gomperts, 2016).

Due to the degeneration of dopaminergic neurones in the midbrain, striatal dopamine depletion quickly occurs (Bernheimer *et al.*, 1973). More specifically, cell death within the substantia nigra results in depleted dopamine release from neuronal terminals within the striatum that cause the motor symptoms in PD (Fearnley, Julian M., 1991). Neurodegenerative disease is also often associated with misfolded proteins such as Tau in Alzheimer's disease and FTD. However, in PD and PD dementia, Lewy bodies are apparent which are made up of proteinaceous inclusions of insoluble ubiquitin and aggregates of misfolded alpha-synuclein protein. The disease is therefore known as synucleinopathy (Galpern and Lang, 2006), a group of neurodegenerative diseases in which alpha-synuclein abnormally accumulates and creates aggregates in cells' bodies or axons. Synucleinopathies include PD, dementia with Lewy bodies and multiple system atrophy (Jellinger, 2010). The symptoms of PD caused as a result of the pathological changes and cell loss in the brain are regarded as irreversible.

1.2.6 Immune system and PD

The immune system plays a very important role in PD. In particular, neuroimaging of post-mortem brain samples showed that the immune system was active in PD patients (Brooks, 2004). Functional MRI depicts alter activation of blood flow and reduced metabolism (Lenka *et al.*, 2015). In-vivo at the early stage of PD, microglia activation as assessed by Schapansky's group, is caused by the toxic level of alpha-synuclein formation and neuronal dysfunction (Schapansky, Nardozzi and LaVoie, 2015). The early stage of PD normally refers to little facial expression and no swing arms during a walk (Perlmutter, 2009). Microglia's activation was assessed by the cell morphology changes (Ransohoff and Cardona, 2010). Generally, microglia are important in

removing the misfolded proteins such as alpha-synuclein aggregates observed in PD, but their chronic activation resulting in the production of reactive oxygen species and pro-inflammatory cytokines may trigger signals for apoptosis (Lee *et al.*, 2010) or other forms of programmed cell death. Peripheral signals can also influence microglial activation and neuronal death during adulthood (Matcovitch-Natan *et al.*, 2016). Indeed, neuronal health and plasticity are highly associated with microglia function (Weinhard *et al.*, 2018). Furthermore, in a chronic microglial activation environment, researchers report that alpha-synuclein can lead to neuronal dysfunction without causing cell death in rodents (Phan *et al.*, 2017).

Chemokines which are produced by microglia can also increase the migration of peripheral immune cells like macrophages into the CNS (Tansey and Romero-Ramos, 2019). Leukocyte antigen is also increased in the Substantia nigra of PD patients which suggests increased immune reaction in PD (Hurtgen *et al.*, 2016). The Tumour Necrosis Factor -α (TNF -α) expression is also increased in the SN in PD patients (Boka et al., 1994). Apart from the brain, pro-inflammatory cytokines also increase in cerebrospinal fluid (CSF) in PD patients (Mogi et al., 1995). Interestingly, an epidemiological study in humans revealed that long-term non-steroidal anti-inflammation drugs (NSAIDs) in mid-age may decrease the incidence of PD, providing further evidence that the inflammatory response plays a role in the pathology of PD (Gagne and Power, 2010)(Gao et al., 2011).

In addition to microglia, humoral peripheral immune pathways, such as the adaptive immune system, can also contribute to the pathological reaction of PD (Tansey and Romero-Ramos, 2019).

1.2.7 Genetics of PD

Although most cases of PD are not the result of genetically inherited mutations, there are still some genetic factors that can contribute to an increased risk of PD. These genes are mostly associated with immune cells. For example, a mutation in Leucine-rich repeat kinase-2 (LRRK2), which is widely expressed in immune cells such as neutrophils, B cells, T Cells, and $CD16^{+}/CD14^{-}$ non-classical monocytes, has been linked to causes of familial PD (Hakimi *et al.*, 2011). LRRK2 mutation can impair the structure of synapses which causes reduced mitochondrial transport and affects

normal protein production (Bae and Lee, 2015). Indeed, about 1% of sporadic PD is reported to include a mutation in this gene (Hernandez, Reed and Singleton, 2016). Compared with age-matched controls, the expression of LRRK2 is higher in the peripheral blood of PD patients (Cook *et al.*, 2017). Based on this, researchers concluded that LRRK2 is associated with an increased risk of PD (Cook *et al.*, 2017)(Dzamko, Geczy and Halliday, 2015).

Furthermore, specific single nucleotide polymorphism (SNPs) nucleotide in the TNF gene is also reported to contribute to an increased incidence of PD (Chu, Zhou and Luo, 2012). It produces part of the major histocompatibility complex (MHC) class II. In PD patients who were tested to have mutated SNP gene, it maybe forms the augmented antigen capacity in peripheral immune cells (Kannarkat *et al.*, 2015)(Tansey and Romero-Ramos, 2019). Other genes such as SNCA and PINK are also the reasons for familial PD (Nuytemans *et al.*, 2010).

1.2.8 NSPCs and neurogenesis in PD

Neural stem/progenitor cell (NSPC) morphogenesis is known to be regulated by dopamine (Nakanishi *et al.*, 2007). During the early periods of ontogenesis such as the embryonic stage, dopamine, via the dopamine receptors D1 and D2, plays an important role in signalling and regulating cell proliferation in the embryonic germinal area (Lidow and Rakic, 1995)(Diaz *et al.*, 1997)(Ohtani *et al.*, 2003). Published data suggest that dopamine signalling continues to regulate NSPC function throughout adulthood (Annenkov, 2014). The depletion of dopamine in PD is therefore considered to have a detrimental effect on NSPC populations within the adult brain and subsequent neurogenesis. Indeed, in 2004 experiments revealed that under both in-vitro and in-vivo conditions, adult neurogenesis is regulated directly by dopamine (Höglinger *et al.*, 2004). The dopaminergic neurones of the SNpc also innervate NSPC populations in the sub-granular zone of the hippocampal dentate gyrus (Darwish *et al.*, 2019). Depleted innervation in models of PD resulted in reduced adult hippocampal neurogenesis. In their experiments, MPTP was used to generate a PD mice model. Not only were the dopamine cells destroyed, but the fibres of dopamine cells were also destroyed (Park and Enikolopov, 2010). Interestingly, after 14 days of MPTP

treatment, the cell proliferation in DG increased (Park and Enikolopov, 2010). For PD patients, there is evidence that the reduction in dopamine correlates with impairments in adult hippocampal neurogenesis (Höglinger *et al.*, 2004).

In the adult mammalian subventricular zone (SVZ), neural stem/progenitor cells (NSPCs) exist which contribute to SVZ neurogenesis (Reynolds and Weiss, 1992) (Luskin, 1993)(Morshead *et al.*, 1994)(Doetsch *et al.*, 1999). Dopaminergic cells in the SVZ are required for NSPC proliferation. Their loss in PD can be attenuated by introducing extra EGF, not FGF (O'Keeffe *et al.*, 2009). The afferent neurites from substantia nigra to the SVZ have been confirmed to be dopaminergic, and they are mainly located very close to the striatum (Höglinger et al., 2004). The effect of SNpc dopamine nerve cell depletion is being more widely explored in neurogenic regions, such as the SVZ and the hippocampus. A number of studies show reduced AHN in models of PD. In particular, a mouse model of induced PD using the neurotoxin MPTP (Ahuja *et al.*, 2021) and a rat model using the neurotoxin 6-OHDA (Silva *et al.*, 2018) show reduced AHN. Furthermore, a PD mouse model ~~with Alpha-synuclein A53T~~ which expresses human A53T alpha-synuclein also shows impairments in AHN (Seo *et al.*, 2019)(Guerreiro *et al.*, 2017).

1.2.9 MPTP

MPTP (1-methyl-4-phenyl-1,2,3,6-tetrahydropyridine) is a neurotoxic agent (Langston and Irwin, 1986)(Heikkila *et al.*, 1989; Tsuchiya *et al.*, 2001). In mammals, its toxicity results in neurodegeneration, bearing similar hallmarks to that of PD (Kopin and Markey, 1988)(Burrow, 1993)(Jenner, Schapira and Marsden, 1992). For example, motor deficits can be observed as a result of MPTP in humans and nonhuman primates similar to those seen in Parkinson's disease (Langston and Irwin, 1986)(Heikkila *et al.*, 1989; Tsuchiya *et al.*, 2001). Furthermore, MPTP causes pathological changes in the nigrostriatal dopaminergic pathway in monkeys and mice (Langston and Irwin, 1986)(Heikkila *et al.*, 1989; Tsuchiya *et al.*, 2001), which is shown by the decreased number of striatal dopamine cells (Langston and Irwin,

1986)(Heikkila *et al.*, 1989; Tsuchiya *et al.*, 2001). A similar effect has been found in substantial nigra pars compacta (SNpc) in mice (Jackson-Lewis *et al.*, 1995). . The eosinophilic Lewy body is also called the brainstem-type Lewy body, which contains intracytoplasmic inclusion with an eosinophilic core (Spillantini, Crowther, *et al.*, 1998). One of the effects caused by MPTP is the generation of superoxide radicals. Indeed, in mice superoxide radicals were the key factor in a destructive cascade caused by MPTP, which eventually led to the death of dopaminergic neurones in the SNpc (Przedborski *et al.*, 1992). In an *in-vitro* experiment, the generation of superoxide radicals has also been shown following incubation of neurones with MPTP (Hasegawa *et al.*, 1990). Furthermore, the damaging effects of MPTP on the activity of striatal dopamine can be prevented by using nitric oxide synthase (NOS) (Beckman *et al.*, 1990). However, the effect of superoxide is still controversial as it is considered a weak reactive radical which does not inflict serious direct damage (Parke, 1991)(Valko, Morris and Cronin, 2005).

Astrocytes can also process MPTP to 1-methyl-4-phenylpyridinium (MPP+) (Ransom *et al.*, 1987)(Shen *et al.*, 1985). During this process selected dopaminergic neurones were killed whilst astrocytes remained undamaged. One possible mechanistic explanation is the selective uptake of MPP+ by DA neurones (Shen *et al.*, 1985). After being sequestered by the DA neurones, the MPP+ locates in the mitochondria which go on to inhibit the mitochondrial respiratory chain (Ramsay *et al.*, 1986)(Ramsay, Salach and Singer, 1986)(Ramsay *et al.*, 1987) and therefore decreases the formation of Adenosine Triphosphate (ATP) (Chan *et al.*, 1991), resulting in cell death. It has also been reported that MPTP administered to non-human primates such as rhesus-monkey can decrease the amount of dopamine stored in cells (Chen *et al.*, 2008). This is similar to what has been seen in PD patients. (Lotharius and Brundin, 2002b).

Other molecules like nicotinamide adenine dinucleotide (NAD) + hydrogen (NADH) are reported to correlate with mitochondrial dysfunction in PD, which has led to increased interest in the association between PD and the mitochondria (Schapira, Cooper, *et al.*, 1990)(Schapira, Mann, *et al.*, 1990)(Bindoff *et al.*, 1991).

Tyrosine Hydroxylase (TH) is the enzyme which catalyses the amino acid L-tyrosine to L-DOPA. TH has been confirmed to exist in subependymal zone neurone radial glial fibres, showing these neurites are dopaminergic (Höglinger *et al.*, 2004). 5-

Bromo-2'-deoxyuridine (BrdU) is a thymidine analogue which is incorporated into cellular DNA during the S-phase of cell division. Interestingly, 80% of the $BrdU^+$ cells in the subependymal zone have close contact with dopaminergic fibres which validates the close connection between dopamine and SVZ (Höglinger *et al.*, 2004). The MPTP model continues to be an important tool in exploring neurodegeneration associated with PD (Haas *et al.*, 1995)(Schapira, Holt, *et al.*, 1990)(Di Monte, 1991).

1.2.10 6-OHDA

In addition to MPTP, the neurotoxin 6-hydroxydopamine (6-OHDA) can mimic the mechanisms of parkinsonian symptoms because it directly leads to pathological changes in the basal ganglia and causes neurone death in the SNpc (Costall, Naylor and Pycock, 1976)(Maneuf *et al.*, 1994)(Robertson and Robertson, 1989)(Ungerstedt and Arbuthnott, 1970). However, the underlying mechanism of the cellular and molecular changes induced by 6-OHDA remains unclear.

In mice treated with 6-OHDA, some studies reported changes in synaptic plasticity (Hutchison *et al.*, 1994)(Pan, Penney and Young, 1985). However, this report only focused on juvenile mice (4 weeks old), where deficits in neurogenesis are not prominent. It has been reported about the toxic effect of 6-OHDA on adult mice. The administration of 6-OHDA unilaterally into the medial forebrain bundle（MFB）which is a neural pathway that includes fibres projecting to the brainstem region, ventral area and nigrostriatal pathway, but the results demonstrated a very high mortality rate, where only 14% of adults mice survived the surgery for at least 21 days (Pan and Walters, 1988)(Iancu *et al.*, 2005). Whilst this model has been used to explore potential neuroprotective agents, the current literature suggests that the use of 6-OHDA in mice does not generate a model of PD with stable symptoms. Indeed, researchers often found it failed to generate similar motor deficits and showed a variable extent of the unilateral lesion (Lundblad *et al.*, 2004)(Grealish *et al.*, 2010)(Dauer and Przedborski, 2003b)(Francardo *et al.*, 2011).

6-OHDA cannot cross the blood-brain barrier, and thus, in order to have an effect on the CNS, it has to be directly administered to the location of interest by injection during surgery. DAT recognises 6-OHDA and takes it up into cells (Chotibut *et al.*,

2012). This has been confirmed using a knock-out mouse model where DAT was inactivated resulting in decreased 6-OHDA-related neurotoxicity (Luthman *et al.*, 1989)(Van Kampen, McGeer and Stoessl, 2000). Results from other research groups suggest that the main form of damage caused by 6-OHDA on neurones is the result of oxidative stress (Asanuma, Hirata and Cadet, 1998)(Blum *et al.*, 2001). It has been suggested that the oxidative toxicity of 6-OHDA can be through both enzymatic and nonenzymatic mechanisms. For example, 6-OHDA administration can lead to the production of hydrogen peroxide (H_2O_2), which is a highly toxic agent and can also trigger the production of more oxygen radicals (Cadet and Brannock, 1998) (Choi *et al.*, 1999)(Lotharius, Dugan and O'Malley, 1999). Furthermore, 6-OHDA can undergo an auto-oxidative process leading to the generation of reactive oxygen species (ROS). In this case, H_2O_2 and ROS have been explored to have a negative effect on nucleophilic groups (Padiglia *et al.*, 1997)(Palumbo *et al.*, 1999). At the same time, they may be capable of rapidly damaging/inactivating the anti-oxidant enzymes, which eventually leads to damaged cell structure and impaired metabolism. (Blum *et al.*, 2001). Studies using 6-OHDA in rats have suggested that the use of antioxidant agents may attenuate the damage incurred to neurones (Cadet and Brannock, 1998)(Perumal *et al.*, 1989)(Soto-Otero *et al.*, 2000)(Zbarsky *et al.*, 2005). This synthetic neurotoxin then selectively destroys dopaminergic and noradrenergic neurones in the brain. Mitochondrial activity may also be exacerbated in the rat model of 6-OHDA (Glinka and Youdim, 1995). However, this effect seems to be independent of oxidative stress, as it revealed no sensitivity to anti-oxidants (Glinka, Tipton and Youdim, 1996). Further exploration about its mechanism would be very interesting to explore.

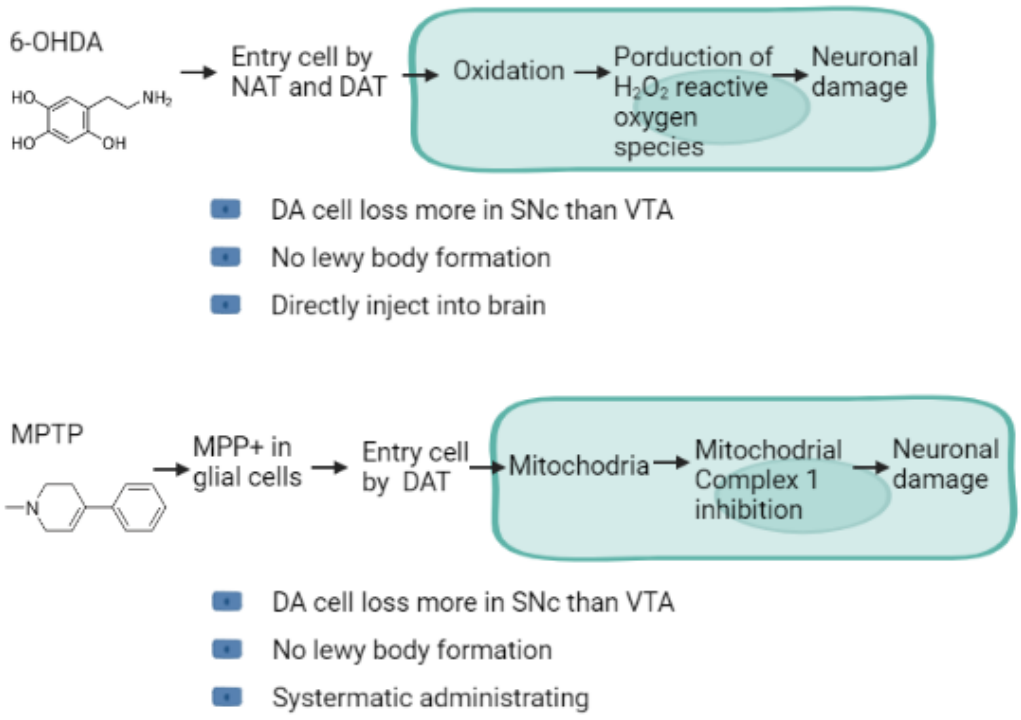

Figure 1.5 PD disease animal model comparison.

The figure lists two different types of PD model for research, which include 6-OHDA and MPTP. The mechanisms, advantages and disadvantages are listed (Jagmag *et al.*, 2016). N-acetyltransferase (NAT), dopamine transporter (DAT), substantia nigra pars compacta (SNc), ventral tegmental area (VTA).

1.3 Neurogenesis

Neurogenesis is defined as the birth of new neurones throughout life. Within the past 20 years, researchers have made significant achievements in the study of adult neurogenesis (Deng, Aimone and Gage, 2010), (Gage, 2000) (Gould and Gross, 2002), (Zhao, Deng and Gage, 2008). Whilst the initial studies identifying cell division in the adult rat brain date from the 1950s, it has taken considerable effort for most scholars to agree that immature neurones are generated from progenitor cells in the adult mammalian brain (ALTMAN and DAS, 1967)(Gross, 2000), (Kaplan, 2001). Starting from the late 1990s, the development of new techniques accelerated our understanding of neurogenesis. In particular, the coupling of fluorescence immunohistochemistry and confocal laser scanning microscopy (CLSM) to identify new adult-born hippocampal neurones was key. Using antibodies raised against bromodeoxyuridine (BrdU), that is incorporated into replicating cells, and NeuN to identify mature neurones, in post-mortem adult brain tissue sections allowed the identification of new neurones via three dimensional (z-plane) CLSM (Eriksson *et al.*, 1998). Early studies demonstrated that physical activity and the home-cage environment have a big influence on cell division, immature neurones (neuroblasts) and maturation into new adult born neurones in rodents.

Pattern separation, the ability to differentiate between similar experiences, is regarded as a key characteristic of new adult-born neurones in rodents. This process has been hypothesized to need the hippocampus as the hippocampus is related to storing memories, retrieving memories from cues and applying stored memories to new situations. Pattern separation is a mechanism that allows the formation of new distinct memories that have overlapping features. The ability to recall these events as distinct non-overlapping memories termed pattern completion, can be tested empirically in rodents and humans. In humans with dementia, reduced pattern separation becomes one of the first key elements to show cognition and memory decline (Yassa and Stark, 2011).

Clelland et al. used a low volume of X-irradiation to fully destroy the dividing hippocampal cells in 8-week-old (adult) female mice, while the SVZ was left free (Clelland *et al.*, 2009). Their IHC results showed there was no significant difference in the morphology of microglial cells, but they showed a significant reduction in both

immature and proliferating neurones. They concluded that this method ablated hippocampal neurogenesis. Behaviour tests using this model showed a significant impairment in both the spatial navigation arm maze and touch screen task. Based on these findings they suggested that new adult-born neurones may be essential for pattern separation in the DG of adult mice (Clelland *et al.*, 2009).

Subsequently, a research group at Columbia University used a genetically modified mouse model with enhanced survival of recently divided hippocampal cells - resulting in increased neurogenesis - to show a significantly faster learning capability when it came to pattern separation (Sahay *et al.*, 2011). Furthermore, adult hippocampal neurogenesis (AHN) stimulation resulted in increased exploratory behaviour (Sahay *et al.*, 2011).

.—According to research using post-mortem human brain samples, thousands of immature neurones were identified in the DG in previously neurologically healthy humans up to 90 years old (Moreno-Jiménez *et al.*, 2019). These data suggest that AHN is an active process that exists throughout life in the healthy aged brain.

In brain sections studied from different animals, neurogenesis has been observed to occur within the sub-granular zone (SGZ) of the dentate gyrus (DG) region of the hippocampus, and within the sub-ventricular zone (SVZ) lining the lateral ventricles (Brus, Keller and Lévy, 2013). However, there remains some controversy about whether neurogenesis occurs in other regions, especially in the neocortex and hypothalamus (Cameron and Dayer, 2008)(Gould, 2007)(Gould *et al.*, 1999) (Kokoeva, 2005)(Rakic, 2002). Neurogenesis in the olfactory bulb (OB) normally refers to neural stem/progenitor cells (NSPCs) that migrate from the subventricular zone (SVZ) along the rostral migratory stream to the OB where neurones mature and integrate with the olfactory circuit (Yamashita *et al.*, 2006). The relevance of this phenomenon to human physiology is again controversial as after adolescence in humans this phenomenon disappears (Bergmann *et al.*, 2012)(Curtis *et al.*, 2007)(Sanai *et al.*, 2004). Neurogenesis in the human DG was demonstrated in cancer patients that had been treated with BrdU by intravenous infusion to label cell division. Brain tissue was collected post-mortem, after full consent from each patient, and IHC was performed to label new adult-born neurones (Eriksson *et al.*, 1998). Researchers at the Karolinska Institute took advantage of the release of ^{14}C into the atmosphere in

the 1950-60s (due to atomic bomb testing) to quantify the ^{14}C:^{12}C in neurone DNA to investigate the age of brain cells collected at post-mortem from adult humans (Spalding *et al.*, 2013). They reported that ~700 new neurones appeared in the hippocampus every day. However, this phenomenon declined with ageing. This research led to the conclusion that AHN contributes to human brain function throughout life (Spalding *et al.*, 2013). The potential for enhancing adult brain plasticity has drawn the attention of scientists from different backgrounds including, molecular biology, genetics, computational neuroscience and animal behaviour to characterize the potential physiological role of these cells. Indeed, these efforts have revealed the positive effect of physical activity and environmental enrichment on hippocampal neurogenesis and its important role in learning and memory.

1.3.1 Characterization of Neurogenesis

The analysis of neurogenesis in the adult brain relies heavily on using different cell labelling methods to differentiate between dividing and mature cells. Characterizing a replicating cell involves labelling DNA synthesis as direct evidence for measuring mitosis. Tritiated thymidine (^{3}H) has been used to radiographically trace replicating cells. However, more recently bromodeoxyuridine (BrdU), a thymidine analogue that is incorporated into the S-phase of mitosis, has been used to label cell division using immunohistochemistry as it is retained within the cell nucleus with each generation of new cells. Importantly, this advancement enabled the identification of more than one protein target within the same tissue section – an ability that is crucial for confirming cell age and cell type. For example, the injection of BrdU into a mouse leads to its incorporation into dividing cells. These cells can be allowed to mature for a set length of time (e.g 4-weeks) before the tissue can be collected for IHC analysis. Cells that are immunopositive for BrdU and the mature neurone marker, NeuN, can be considered 4-week-old neurones. This approach, known as BrdU-pulse chase, can be used to birth date a variety of cell types in adult mammals in-vivo and in cells grown in culture (in-vitro). Although experimental consideration of BrdU dosage is required to avoid potential cellular toxicity (Kuhn and Cooper-Kuhn, 2007). Additionally, antibodies raised against endogenous proteins are also routinely used to identify specific cell types that are critical to neurogenesis. For example, Ki67 is valued for

marking proliferating cells. Ki67 is a nuclear protein encoded by the Marker Of Proliferation Ki-67 (MKI67) gene, which is generally expressed during interphase in the cell cycle, which includes G1, S, and G2 phases. It can be detected exclusively in the cell nucleus. In addition, sex-determining region Y (SRY)-box 2 (Sox-2) has been widely used together with Nestin as markers of neural stem/progenitor cells.

1.3.2 Neurogenesis in Humans

In contrast to rodents, neurogenesis in humans is very difficult to detect and has led to the question of whether adult hippocampal neurogenesis even exists in humans. As discussed, with the use of BrdU to monitor tumour cell progression in humans undergoing cancer treatment, hippocampal neurogenesis was investigated in their post-mortem brain (Eriksson *et al.,* 1998). Their results supported the theory that the adult human hippocampus retains the ability to generate neurones throughout life, however other scholars questioned whether the tissue sample number was sufficient for a complete quantification (Eriksson *et al.*, 1998)(Seress, 2007)(Seress *et al.*, 2001). These reports infer that in the adult human hippocampus, hundreds of new neurones are born in the DG every day, while some researchers hold a different view. For example, one study showed that in the first year of human life, there is a sharp decrease in the number of proliferating progenitor cells and young neurones in the DG (Sorrells *et al.*, 2018). At the age of 7 and 13 years, only a few young neurones can be observed. Furthermore, in the adult DG, no young neurones were discovered in the human DG. All these data were generated by post-mortem human samples or samples after surgery (Sorrells *et al.*, 2018).

A method for the detection of new adult-born cells was developed by quantifying the ratio of radioactive carbon (^{14}C:^{12}C) in dissociated human cells. This was made possible due to above-ground nuclear bomb testing that took place in the 1950s which led to an increase in atmospheric ^{14}C. With an accurate measurement of the rate of decay from ^{14}C to ^{12}C, scientists were able to determine the age range of the distinct cells collected from the adult brain. This approach suggested that new adult-born neurones are generated in the brain throughout development and across adulthood, resulting in ~700 new neurones being generated every day on each side of the

hippocampus (Spalding *et al.*, 2013). Some scholars questioned whether the immunoprecipitation of $NeuN^+$ cells accurately isolated a pure population of neurones.

Similar to [^{3}H] thymidine, ^{14}C can be quantified as it is incorporated into the DNA, which can then be used to determine the rate of neurogenesis. However, the restrictions of this method meant that the formation of newborn neurones could not be detected in some areas of the brain such as the OB. On the contrary, the Frisen team detected the presence of immature neurones in the human striatum (Ernst et al., 2014). Further evidence has indicated that AHN continues in humans until the 10th decade of life (Moreno-Jiménez *et al.*, 2019). However, in AD patients, there was an observable reduction in AHN (Song *et al.*, 2021).

Suitable sample preparation is key to these forms of investigations. However currently, for most brain banks, it is difficult to achieve a consistent reproducible standard (Moreno-Jiménez *et al.*, 2021). Flor-García *et al* suggest a 7-day protocol with strictly controlled conditions which is suitable for downstream IHC (Flor-García *et al.*, 2020) (Moreno-Jiménez *et al.*, 2019). Current methods measuring parameters of human neurogenesis lack the ability to quantify cellular plasticity and the effect of these cells on behaviour. More recent techniques, such as single-cell RNA sequencing, may supply more directly quantifiable information that is comparable with rodent AHN (Kempermann *et al.*, 2018).

1.3.3 NSCs

Neural stem/progenitor cells (NSPCs) have a limited capability of differentiating into different types of cells such as astrocytes, oligodendrocytes and neurones, in the adult brain. Understanding the mechanisms regulating this process is critical for the development of potential therapeutic strategies for age-related cognitive decline and neurodegenerative diseases. It is generally accepted that in the human brain, neurogenesis continues throughout life mainly in 2 areas, the sub-granular zone (SGZ) of the hippocampal dentate gyrus (DG). In the sub-ventricular zone (SVZ), neurogenesis persists until 14 years old and then decreases quickly.

In these regions, NSPCs are capable of proliferating into NSPCs - to maintain the stem cell pool - and can differentiate into neurones and glial cell types, including astrocytes and oligodendrocytes (Gage, 2000). During differentiation, the cells migrate a short distance, from the SGZ into the granular cell layer of the dentate gyrus. Here, the immature neurones develop and integrate into the existing hippocampal circuitry where they play an important role in pattern separation memory function. (Bonaguidi *et al.*, 2012)).

It has been demonstrated that the radial glial cells (RGCs), also known as type 1 stem/progenitor cells, can stimulate the proliferation of non-radial glial cells, usually called type-2 stem/progenitor cells, while it is still unclear if RGC replication is asymmetric or symmetrical (Bonaguidi *et al.*, 2012)). Asymmetric cell division normally creates 2 cells that show different cellular fates, while symmetrical division produces 2 cells with the same cellular fate (Morrison and Kimble, 2006). It was also reported that the cell mutation rate in symmetrically divided cells was significantly lower than that of asymmetrically divided cells (Shahriyari and Komarova, 2013).

Type 2 stem cells are known to have the potential to turn into intermediate progenitor cells (IPCs), often described as type 3 stem cells, in which the transcription of T-box brain protein 2 (Tbr2) is characterised. (Hodge *et al.*, 2008)). Tbr2 and DCX expression may concentrate in the SGZ 7 days post-birth (Nicola, Fabel and Kempermann, 2015). These proteins can be found in IPC, neuroblasts and immature neurones (Ghosh, 2019). The OB also was found to contain a few IPCs which suggest a certain level of neurogenesis (Cárdenas *et al.*, 2018). In the DG area, IPCs still maintain a proliferative activity, but this process highly relies on the function of the mitochondria. However, mitochondrial-derived ROS generated as a result of this process was reported as being fatal to IPCs in the DG (Gillotin *et al.*, 2021).

NSPCs can self-renew and have the capacity to differentiate into different cell types, but with limited potential to differentiate into glia and neurones. When quantifying neurogenesis, researchers tend to describe three key features, cell proliferation, differentiation and maturation. Some studies have evidenced that ageing can contribute to reducing the proliferation of NSPCs which suggests exhaustion of the NSPC pool (Boldrini *et al.*, 2018)(Schouten *et al.*, 2020)(Encinas *et al.*, 2011). Under epilepsy conditions, the radial neural stem cells (rNSCs) will perform symmetrical

division, but both mother and daughter cells can differentiate into functioning astrocytes. This suggests impaired neurogenesis as a result of stem cell exhaustion (Sierra *et al.*, 2015).

It is documented that away from the SVZ and DG neurogenic areas, NSPCs can commit to self-proliferating in the adult brain, but it is uncommon to find them differentiating into neurones. On the contrary, they tend to go on to become astrocytes and oligodendrocytes (Xapelli *et al.*, 2020). Alternatively, NPC cells in the adult brain are likely to self-replicate and become neurones in the presence of the fibroblast growth factor-2 (FGF-2), especially if the NPCs originate from the cortex and optic nerve (Palmer *et al.*, 1999)). Based on this phenomenon, FGF2 is regarded as a neurogenic factor for proliferation and differentiation (Woodbury and Ikezu, 2014).

It has been reported that NPC replication and neurone differentiation is decreased in the aged brain, resulting in fewer immature neurones when compared with younger brains (Bondolfi *et al.*, 2004)(Heine *et al.*, 2004))(Kuhn, Dickinson-Anson and Gage, 1996)). It seems NPC proliferation is regulated by astrocytes through the Wnt pathway (Miranda *et al.*, 2012).

1.3.4 Microglia and neurogenesis

Microglia that function as the brain immune cells are also called resident macrophages and are essential for healthy brain function. M1 and M2 stage microglia continually search for the presence of non-self-factors across all the cells of the adult brain, including neurones, astrocytes, and endothelial cells. (Nimmerjahn, 2005)). The M1 microglia are characterised by chronic activation and the secretion of harmful cytokines which causes cell damage/death, whilst M2 microglia show homeostatic function - playing a more inflammatory resolving role (Al-Shaheeb, 2019).

In adult DG, the molecular layer contains most of the microglia cells (Wirenfeldt, Dalmau and Finsen, 2003)) and these have been linked to the process of neurogenesis. Interestingly, in DG the majority of new adult-born immature neurones do not survive beyond the first week (Kempermann *et al.*, 2003)(Sierra *et al.*, 2010)); However, once these cells survive past the first 3-4 weeks they become more stable (Kempermann *et al.*, 2003)(Sierra *et al.*, 2010)(Tashiro *et al.*, 2006)). Studies of this transition revealed

that microglia are involved with the removal of new adult-born cells during the first week mainly through apoptosis, (Sierra *et al.*, 2010)) and the regulation of dendritic development via a process termed trogocytosis (Bettadapur, Miller and Ralston, 2020).

Depending on the secretion of specific cytokines and chemokines, microglia can vary from anti-inflammatory to pro-inflammatory signalling, which is critical to creating a supportive or hostile environment for neurogenesis (Battista *et al.*, 2006)(Butovsky *et al.*, 2006)(Carpentier and Palmer, 2009)). For example, the secretion of Tumour Necrosis Factor-α (TNF-α) and interleukin-6 (IL-6) causes inflammation (Carpentier and Palmer, 2009). This phenomenon is especially seen in aged brains (Lucin and Wyss-Coray, 2009)(Njie *et al.*, 2012)). TNF-α and IL-6, the main pro-inflammatory cytokines produced by M2 microglia, can block NSCs from differentiating into mature neurones, with the assistance of astrocytes (Carpentier and Palmer, 2009)). Astrocytes can act to regulate the development of the vasculature scaffold (Bozoyan, Khlghatyan and Saghatelyan, 2012) and help to modulate vasculature through cytokines such as TNF-α and IL-6. They can also supply nutrients and regulate blood flow which is considered important for the integration and survival of new neurones. Another cytokine, Transforming Growth Factor-β (TGF-β), which is secreted by M1 microglia, can contribute to both anti-inflammatory and pro-inflammatory signalling to stimulate and inhibit neurogenesis (Battista *et al.*, 2006))(Buckwalter *et al.*, 2006)).

Lipopolysaccharide (LPS) can trigger the activation of microglia *in-vitro*, which can speed up M1 morphology diversification and produce more cytokines and nitric oxide (Beutler, 2004)(Nakamura, Si and Kataoka, 1999)). When using LPS-activated microglia media or similar conditioned media (CM), NPCs have a significant reduction in neurone differentiation (Butovsky *et al.*, 2006)(Monje, 2003)). On the contrary, interferon (IFN)-γ and IL-4 can seemingly upregulate NPC differentiation, which is evidence of neurogenic support (Butovsky *et al.*, 2006)).

1.3.5 Astrocytes and neurogenesis

Astrocytes, star-shaped cells that are a type of neuroglia, play a very important role in regulating neurogenesis. Notably, astrocytes co-cultured with NPCs lead to the differentiation of NPCs (Barkho *et al.*, 2006). During co-culturing, IL-6 and IL-1β

accelerated NPCs differentiation (Barkho *et al.*, 2006))(Song, Stevens and Gage, 2002). Glial fibrillary acidic protein (GFAP) and vimentin have also been reported to play an important role in regulating co-cultured astrocytes and neurospheres (Wilhelmsson *et al.*, 2012). GFAP and vimentin inhibited the rate of neuronal differentiation *in-vitro* (Wilhelmsson *et al.*, 2012). Without GFAP and vimentin, the expression of Jagged1 and Notch mRNA is reduced in astrocytes which suggests low neurogenesis (Wilhelmsson *et al.*, 2012). These results suggest that IL-1β and IL-6 are expressed by astrocytes, that increase inflammation, and upregulate the differentiation of NPCs, together with other factors, such as interferon-induced protein 10 (IP-10) and vascular cell adhesion molecule-1 (VCAM-1) (Barkho *et al.*, 2006). Alternatively, Insulin-like growth factors secreted by astrocytes originating from the spinal cord contain the insulin-like growth factor binding protein-6 (IGFBP-6), enkephalin and decorin, which downregulate neurogenesis (Barkho *et al.*, 2006).

NPC function can be directly affected by astrocytes. Because stabilized β-catenin cannot start the differentiation of NPCs and blockade Wnt3a, which is created by astrocytes, can inhibit the NPC differentiation (Lie *et al.*, 2005). In both *in-vivo* and *in-vitro* studies, NPC differentiation and proliferation are regulated by Wnt, Wingless and Int-1, signal communication (Kuwabara *et al.*, 2009)(Lie *et al.*, 2005)(Wexler *et al.*, 2009). During the differentiation of NPC cells, the transcription factor Neuro D1 is activated by Wnt which suggests increasing neurogenesis (Kuwabara *et al.*, 2009). The secretion of an important retrotransposon by astrocytes, long interspersed nuclear elements – 1 (LINE-1), which prevents NPCs from dying, is triggered by Wnt to support neurogenesis (Kuwabara *et al.*, 2009).

In addition, ATP can pass from astrocyte to NPC to increase proliferation (Cao, Li, Qin, *et al.*, 2013). Interestingly, depression-related behaviour can be attenuated by ATP-producing astrocytes (Ariyannur *et al.*, 2021) and promote AHN (Cao, Li, Wang, *et al.*, 2013)(Sahay, Drew and Hen, 2007).

Astrocytes secrete Brain-derived Neurotrophic Factor (BDNF) in the hippocampus (Rudge *et al.*, 1992)(Rudge *et al.*, 1995). BDNF is reported to enhance adult hippocampal neurogenesis (Li *et al.*, 2008)(Palmer, Takahashi and Gage, 1997) and its receptor, Tropomyosin receptor kinase B (TrkB), is expressed in NPCs (Li *et al.*, 2008)(Katoh-Semba *et al.*, 2002). In the DG, BDNF expression is most prevalent in

the granule cell nuclei, which shows no deficiency with ageing (Katoh-Semba *et al.*, 2002)(Bimonte, 2003)(Katoh-Semba *et al.*, 1998)(Lapchak *et al.*, 1993)). Published work suggests that reduced endogenous BDNF can impair vesicular glutamate release (Brigadski and Leßmann, 2014). In BDNF knock-out mice, oligodendrocytes can significantly exacerbate this effect.

However, the negative consequences of reduced BDNF can be attenuated by a BDNF agonist. Thus, oligodendrocyte production of BDNF in the hippocampus may assist memory performance (Jang *et al.*, 2019). In contrast, its receptor, TrkB, is decreased in the aged rat hippocampus (Croll *et al.*, 1998)(Silhol *et al.*, 2005). Interestingly, hippocampal volume and memory performance correlate with serum BDNF levels in humans, with elderly humans showing increased memory loss and hippocampal shrinkage alongside a reduction in serum BDNF (Erickson *et al.*, 2010). However, the function of astrocytes in regulating the rate of differentiation varies when considering which part of the brain the astrocytes are isolated from. For example, astrocytes from the hippocampus can support the NPCs changing into mature neurones, while spinal cord astrocytes cannot support the same function *in-vitro* (Song, Stevens and Gage, 2002).

1.3.6 Ghrelin

Ghrelin is a gastrointestinal peptide hormone first discovered by Kojima et al. in 1999 and binds to the Growth hormone secretagogue receptor (GHSR) 1a. The anterior pituitary head releases growth hormone (GH) following stimulation of GHSR1a (Kojima *et al.*, 1999). Ghrelin is often referred to as the 'Hunger hormone' as it can regulate body weight and food intake. Modulating glucose metabolism is another characteristic of ghrelin (Tschop, Smiley and Heiman, 2000). In this process, the activation of orexigenic neural circuits in the hypothalamus is important for ghrelin function (Cowley *et al.*, 2003)(Nakazato *et al.*, 2001). Furthermore, sleep regulation, reward-seeking behaviour, adaptation to stress and anxiety, and attenuating muscle atrophy are also reported (Tolle *et al.*, 2002)(Cai *et al.*, 2013)(Lutter *et al.*, 2008)(Filigheddu *et al.*, 2007). The stomach oxyntic cells mainly produce ghrelin, whilst other organs such as the kidney, pancreas and placenta can produce ghrelin in

lower amounts (Date *et al.*, 2000)(Mori *et al.*, 2000)(Gualillo *et al.*, 2001). Ghrelin mediates its central effects by penetrating the blood-brain barrier (BBB) and binding its receptor in the brain (Banks *et al.*, 2002)(Diano *et al.*, 2006).

Ghrelin is post-translationally modified by the addition of an acyl group to the 3rd amino acid, resulting in acyl-ghrelin (AG). The AG form of ghrelin can increase AHN in mice and rats. In adult rat hippocampal progenitor cells, AG increases neurone proliferation (Johansson *et al.*, 2008). The intraperitoneal administration of acyl-ghrelin for 8 days increased the number of hippocampal $BrdU^+$ cells in mice (Moon, S. Kim, *et al.*, 2009). Interestingly, the neurogenic effect was demonstrated following administration of a lower, physiological, dose of AG (Kent *et al.*, 2015). This effect was accompanied by a significant improvement in spatial pattern separation performance (Kent et al.2015). A similar function of Ghrelin was also observed in other studies (Elabi *et al.*, 2018)(Zhao *et al.*, 2014)(Li *et al.*, 2013). Notably, mild calorie restriction was shown to increase AHN in a ghrelin-receptor-dependent manner (Hornsby et al.2016). These data suggest that reducing caloric intake stimulates acyl-ghrelin secretion to promote AHN and associated memory function. Hippocampal neurogenesis is reduced in Alzheimer's disease (AD) which also shows cognitive impairment (Moon, Cha and Mook-Jung, 2014). Choi et al used mouse model confirmed AHN deficits and cognitive impairment (Moon, Cha and Mook-Jung, 2014). Acyl-ghrelin was introduced by i.p. for 30 days (Moon, Cha and Mook-Jung, 2014). Results showed the number of immature neurones increased by using DCX and calretinin markers (Moon, Cha and Mook-Jung, 2014). This is evidence suggesting that peripheral acyl-ghrelin elevation can improve AHN in AD mouse model (Moon, Cha and Mook-Jung, 2014).

1.3.7 Environmental Enrichment (EE) and exercise on neurogenesis

As discussed, ageing and calorie intake modulate AHN, however, environmental enrichment (EE) also influences this process. These EE elements include social connection, activity, and stimulating the senses, as researchers used toys, huts, tunnels, and running wheels to provide enrichment. Interestingly, 10-month-old mice contain significantly more newborn immature neurones as a result of EE (Kempermann, Gast

and Gage, 2002). In 4-week-old mice, the number of new BrdU labelled immature neurones was increased due to EE (Tanti *et al.*, 2013). More specifically, the total granule cell number was significantly increased in the hippocampus, however, the rate of cell proliferation showed no statistical difference, suggesting that EE influences mechanisms that support new neurone survival, maturation and/or integration (Kempermann, Kuhn and Gage, 1997). In rats exposed to 4 weeks of EE, vascular endothelial growth factor (VEGF) mRNA expression was increased (Cao *et al.*, 2004). Furthermore, the effects of EE disappear when VEGF is knocked out in the hippocampus (Cao *et al.*, 2004). This suggests that EE can regulate rat neurogenesis via VEGF. In mice exposed to 4 weeks of EE, epidermal growth factor (EGF) and VEGF mRNA expression were unchanged, however, BDNF mRNA expression was increased (Kuzumaki *et al.*, 2011). This phenomenon correlated with increased trimethylation of histone H3K4 and decreased trimethylation of H3K9 at the BDNF promoter which indicates age-dependent effects on DCX. BDNF plays a very important role in phosphorylating mitogen stress-activated kinase 1 (MSK1) (Simon *et al.*, 2004), which can be triggered by extracellular signal-regulated kinases (ERK1/2) or Mitogen-activated protein kinase (MAPK) (Rakhit *et al.*, 2005)(Kuzumaki *et al.*, 2010). Muscle-Specific Kinase (MSK) has also been linked to altering neurogenesis either directly or indirectly. For example, MSK can accelerate the phosphorylation of cAMP response element-binding protein (CREB) and H3, activate nuclear factor kappa-light-chain-enhancer of activated B cells (NFkB) signalling (Arthur C., 2008)). MSK1 also correlates with synaptic plasticity and adult neurogenesis in the hippocampus, which was assisted by EE (Corrêa *et al.*, 2012), (Karelina *et al.*, 2012). Notably, MSK1 knock-out mice have fewer new adult-born neurones and reduced cell proliferation in the DG compared to wild-type littermates (Karelina *et al.*, 2012). EE for 40 days significantly increased CREB phosphorylation and cell proliferation in wild-type mice, but not in $MSK1^{-/-}$ mice, leading to the notion that EE-induced neurogenesis depends on the MSK1 pathway function (Karelina *et al.*, 2012).

Exercise has also been associated with regulating neurogenesis. Remarkably, brain cell survival and neurone differentiation was improved in 18-month-old mice when equipped with access to a running wheel for 45 days (van Praag *et al.*, 2005).

1.3.8 Ageing and neurogenesis

The ageing process is accompanied by a decline in cell proliferation, differentiation, and survival of new adult-born hippocampal neurones. In the DG, reduced proliferation is detected from 6 months of age (McDonald and Wojtowicz, 2005). Importantly, in rats, there was a ~80% reduction in the number of new adult-born immature neurones between 12 – 27 months, which suggests that ageing is an important factor in neurogenesis (Kuhn, Dickinson-Anson and Gage, 1996). In a different experiment, the size of the DG in mice was quantified to show that between 2-6 weeks, the DG continued to increase in size, but then remained unchanged until 24 months old age (Restivo *et al.*, 2015). In the rat, cell proliferation started to decline from 6 weeks of age, at 12 months of age there is an accelerated reduction in the rate of cell proliferation (Heine *et al.*, 2004). In aged humans, angiogenesis and neuroplasticity were reduced. In the DG, a smaller pool of quiescent progenitor cells was observed in older humans. (Heine *et al.*, 2004).

In mice, a similar effect was reported for cell proliferation in the hippocampus. A reduction in cell proliferation started from 1-2 months of age, and then accelerated at 18 months old. However, after that, no significant reduction in cell proliferation was reported (Bondolfi *et al.*, 2004)). Similarly in mice, new adult-born mature neurones (labelled using NeuN and BrdU) also decreased in number with age – with significant decreases reported at 6 months of age (Kuhn, Dickinson-Anson and Gage, 1996)(van Praag *et al.*, 2005).

The expression of the transcription factor, Sox2, which is a biomarker of stemness, remained consistent during ageing while cell proliferation decreased (Encinas and Sierra, 2012). This finding suggests that the reduction in hippocampal neurogenesis during ageing is due to the decline of NSC activity rather than a reduction in the number of NPCs (Hattiangady and Shetty, 2008).

1.3.9 Diet

Diet has also been associated with altering neurogenesis. Indeed, the removal of essential vitamins and minerals such as Vitamin E and Zinc from the diet leads to a decline in AHN and impaired learning and memory performance in mice and rats (Stangl and Thuret, 2009)(Bonnet *et al.*, 2008)(Corniola *et al.*, 2008). However, supplementation with omega-3 fatty acids, a calorie-restricted diet, blueberry, and polyphenols are reported to increase aspects of hippocampal neurogenesis (Kawakita, Hashimoto and Shido, 2006)(Lee *et al.*, 2000)(An *et al.*, 2008)(Casadesus *et al.*, 2004). Flavonoids are another dietary factor that has been reported to help in promoting memory and increasing cell proliferation (An *et al.*, 2008) In particular, cognitive performance was improved in 70 – 74-year-old humans with the regular consumption of wine, tea, and chocolate, which contain higher levels of flavonoids (Nurk *et al.*, 2009). Furthermore, following a 10-year diet study, 65-year-old humans with increased intake of flavonoids were reported to have improved performance in a cognitive function test. (Letenneur *et al.*, 2007). Calorie Restriction (CR) is another way to increase AHN (Mattison *et al.*, 2017). CR is reduced food intake without malnutrition (Mattison *et al.*, 2017). Lifespan has been prolonged by CR which suggests its effect is against ageing (Di Francesco *et al.*, 2018). Interestingly, neurodegeneration is ameliorated by CR in rodents (Maswood *et al.*, 2004)(Gräff *et al.*, 2013) whilst cognitive decline can also be attenuated by CR (Halagappa *et al.*, 2007). In monkeys, CR reduces brain atrophy (Mattison *et al.*, 2017)(Colman *et al.*, 2009) and improves verbal memory performance in humans (Witte *et al.*, 2009). As mentioned in section 1.3.6, the pro-neurogenic effect of CR appears to be mediated, at least in part, by acyl-ghrelin signalling via GHS-R1a.

1.4 Aim and hypothesis

My doctoral thesis will explore AHN in a novel model of FTD and ALS, specifically, in TDP43$^{Q331k+/Q331k+}$ mice. I also explore the effect of the neurotoxins, 6-OHDA and MPTP, that are associated with PD, on AHN in adult mice. I also study whether their effects can be attenuated by acyl-ghrelin.

More specifically, the thesis aims to:

1. Characterize the effect of TDP43 Q331K knock-in mutation on NSPC proliferation, immature neurone number and morphology in the neurogenic niches of the adult mouse brain at different ages.
2. Quantify PHF1-Tau expression in immature neurons of TDP43$^{Q331k+/Q331k+}$ mice.
3. Determine whether 6-OHDA and MPTP neurotoxins impair AHN in adult rodents.
4. Determine whether acyl-ghrelin can protect or even enhance AHN in neurotoxin-based rodent models of PD.

2 Chapter 2 Materials & Methods

2.1 Animal studies

All the animals used in this project comply with UK Home Office ASPA 1986 and Swansea University Medical School animal experiment regulations.

2.2 FTD mice model

2.2.1 Generation of an FTD mouse model using CRISPR/Cas9

To explore the underlying mechanisms of FTD, a transgenic mouse model of FTD was developed by Dr Jemeen Sreedharan at Kings College London, the animal experiment was designed by Dr Jemeen Sreedharan, who was responsible for raising the mice. The widely used CRISPR/cas9 method was adopted for the mutagenesis by splicing a mutation for the TDP protein (TAR DNA-binding protein) at Q331k, which according to the report can cause a high level of DNA strand breaks. To validate the CRISPR work, a GFP reporter plasmid was inserted to show the performance of the mutation. The mid area of the mutation was the 121-bp length fragment which was in the single-strand DNA oligonucleotide which was called the repair template. The 270 C57BL/6J single-cell embryo was selected to receive the injection of the donor oligonucleotide and the capped cas9 mRNA. For off-target prediction, the Kings research team used crisprseek. (White et al., 2018)

Table 2.1 CRISPR/Cas9 PAM sequences

CRISPR/Cas9 PAM sequences	
Name	target site (spacer+PAM)
gRNAf5_msTDP43_ptmutStart66End88	aggcagcgttgcagagc|agttgg
gRNAf6_msTDP43_ptmutStart67End89	ggcagcgttgcagagca|gttggg
gRNAf7_msTDP43_ptmutStart68End90	gcagcgttgcagagcag|ttgggg

Table 2.2 TDP43 mutation

Single-stranded DNA (ssDNA) oligonucleotide	
ssDNA donor oligonucleotide_ TDP43msPtmut1(mutation highlighted in red)	atgaactttggtgcttttagcattaacccagcgatgatggctg cggctcaggcagcgttgAagagcagttggggtatgatgggcatgttagccag ccagcagaaccagtcgggcccatctg

2.2.2 Preparation of DNA for genotyping

DNA extraction was performed with ear biopsies at 10 days of age using QuickExtract (Epicentre).

Table 2.3 Primers Sequence

Genotyping primers	
Name	Sequence
Forward	TTGTTCAGCAGATTGCCACC
Reverse	CAGCAGTTCACTTTCACCCA

Table 2.4 TDP-43 Sequence

Gene	Forward	Reverse
Sqstm1 (TDP-43 Q331Kvariant)	ACCCATCTACAGGCTGATCC	GTCTGTAGGAGCCTGGTGAG

2.2.3 Breeding of mice

At King's College London, Dr Jemeen bred the wild-type C57BL/6J mice, by performing crossbreeding of the f4 heterozygotes （TDP-$43^{Q331k/+}$） mice and the viability of the homozygous animals were witnessed, for which the normal juveniles were observed. The breeding process was located in UK and USA. An Automated continuous behavioural monitoring (Acbm) was carried out to assess the rodent neurodevelopment behaviour. The testing was carried out at a testing facility at Brown University (USA). The behaviour test, e. g. touched screen analysis, marble burying, and RNA sequencing was carried out in the UK. All experiments processed in the UK were in accordance with the United Kingdom Animal (scientific procedures) Act (1986), and the United Kingdom Animals (scientific procedures) Act (1986) amendment regulations 2012. Each cage accommodated a maximum of 5 animals, and the environment was managed by using 12h light and dark cycles every 24 hours. The mice were culled by Cervical vertebrae dislocation, complying with the animal experiment regulation from Kings College London. There were 6 male and 6 female mice in 1 experiment, which contain 3 wild-types (TDP-$43^{+/+}$) and 3 mutated (TDP-$43^{Q331k/Q331k}$) mice.

Wild-type C57BL/6J mice were used to crossbreed with number 52 mouse founder to acquire the f3 mixed generation. Then wild-type C57BL/6J mice again were used to outcross with 3 f3 male cohorts. The next-generation f4 was labelled as f4 TDP-$43^{q331k/+}$ mutants, with which intercross was performed to create animals for further research.

2.2.4 Mice feeding

During the experiments, 1 cage housed 2 or 3 mice of the same genotype. Every Monday morning, 400g of food was offered for each cage. Also, every Monday, any food remnants, including any food crisps in the cage were cleared out and weighed to keep a record. The animals feeding records began at 12 months of age. All the tests were performed based on a blinded genotype and randomized principle.

2.2.5 Brain exposure and preparation

All the mice brains were fixed by immersing in 4% paraformaldehyde (PFA) at 4 ^{o}C for 24 hours and then were transported from Kings College London to Swansea University Medical School, in PBS-0.01% sodium azide. One hemisphere was used by King's College London for molecular analyses requiring frozen tissue, which meant that only one hemisphere underwent immersion fixation for subsequent IHC. Due to this reason, all the FTD mice brain were immersion fixed instead of perfusion fixation. After arrival, the brain tissue would be examined and checked for wholeness, mould, or other contamination, all the brain trunks were washed thoroughly with PBS to remove any attached animal furs and other bone fragments. To reduce the expansion of tissue in frozen water, the brain trunks were immersed in 30% sucrose, followed by a sectioning process at 30 µm thickness along the corona plane by microtome (microm, Thermo scientific) by holding the brain trunk on the frozen-stage with snap-frozen ECL. Each brain section was allocated sequentially to 12 wells to create 1 in 12 ratios in each well for future calculation. To reduce the affecting on microbiology, PBS-0.01% azide was immersed in all the sections at 4 ^{o}C until needed.

2.2.6 DCX DAB Immunohistochemistry

All the tissue sections were kept in 0.01% Azide in PBS. Twice 10 minutes washes in PBS were carried out in a new plate with the selected tissue sections, then followed by 1 PBS-T wash for 10 minutes at room temperature on a shaker. 1.5% H_2O_2 prepared in PBS was used to inactivate the endogenous peroxidase activity. Another twice 10-minute PBS wash and 10 minutes PBS-T wash were then followed. The blocking buffer was Normal donkey serum (NDS) diluted in 0.1M PBS-T at a 5% ratio for 1-hour incubation at room temperature on a shaker at 30 rounds per minute. Goat anti-DCX was mixed at 1 in 750 dilution in PBS-T with 2% NDS for overnight primary antibody treatment at 4^{o}C. Goat anti-DCX was confirmed as a immature neurones marker (Masui *et al.*, 2008). Positive control and negative control were used in this project to confirm the specificity furthermore. In this PhD project, DCX was used to explore the morphology of immature neurones. Based on the shape of the DCX^{+} cells, different stages of cell maturation can be observed. This is another important validation for DCX antibody specificity. Method optimization selected 2 different DCX concentrations, 1:500, 1:750. The the lower concentration optimally stained the immature neurones and was therefore selected as the final concentration. 10 minute PBS wash was carried out twice followed by a 10-minute PBS-T wash to decrease the background immunoactivities. Biotinylated Donkey anti-Goat was used at 1 in 400 in PBS-T for 1-hour secondary antibody binding at room temperature covered away from light. 2 washes using PBS for 20 minutes totally were operated followed by 10 minutes PBS-T wash. After 30 minutes of mixing preparation of 0.4% agent A and 0.4% agent in PBS-T, it was added to the tissue sections for 90 minutes of signal amplification. 10 minutes of PBS washes were contributed twice along with 10 minutes of sodium acetate wash. In a weighting boat, all the tissue sections were transferred carefully with a brush for DAB virtualisation with which 500ml nickel-DAB and 30µl glucose oxidase were presented freshly. Under the inspection for every minute, proper colour sliding process time was selected, which normally lasted around 5 minutes to 10 minutes. To attenuate the toxicity of the DAB agent. Washing was conducted twice with PBS for a totally of 20 minutes. Immersed with TBS-T, all the tissue sections were mounted on super frost glass slides. To prevent any detachment, drying at room temperature overnight was fitted to the protocols. Based on 3 minutes period, tissue stabilization processes were practised by sinking all the slides in 70% ethanol, 90%

ethanol, twice 100% ethanol and twice histoclear. For long-term storage, all the sections were protected by Entellan sealing with a cover slip. Room temperature exposure on a bench was to reach the cover agent coagulation to get ready for microscope imaging.

2.2.7 Immunofluorescence co-localization IHC for DCX and PHF1 (PHD finger protein 1) -Tau

3 rostral and 3 caudal sections were removed into DD-water (Double distilled water) in a petri-dish for considering saving antibodies by using the entire well of tissue. 1x PBS was used to rinse the sections three times for 10 minutes. A 5-minute permeabilization step was carried out in methanol, followed by another three 10 minutes in PBS. The tissue sections were then incubated with 20% normal donkey serum diluted in PBS-T to block any non-specific antigen binding by the donkey antibody. Next, the tissue sections were incubated with the first primary antibody, goat anti-DCX (diluted 1 in 200 in 2% NDS), overnight at 4^{o}C. The next day, after three 10 minutes washes in PBS, the sections were incubated with donkey anti-goat (568) diluted 1 in 500 in PBS-T for 1 hour. The sections were then incubated with 20% normal goat serum in PBS-T for 1 hour followed by another 3 10 minutes of washes in PBS. Next, a mouse anti-phf1-tau antibody (diluted 1 in 200 in 2% NGS in PBS-T) was added to the tissue and incubated overnight at 4^{o}C. The tissue was then washed three times for 10 minutes then incubated with a biotinylated goat anti-mouse, diluted 1 in 400 in PBS-T, for 1 hour at room temperature. Finally, streptavidin 488, diluted 1 in 500 in PBS-T, was applied to the tissue for 1 hour. The tissue was then washed three times for 10 minutes with PBS, during the final wash, Hoechst at 1 in 10,000 was added as a counterstain, and then the sections were mounted onto Super Frost glass slides before applying ~50 to 70µl Prolong Gold solution (Thermofisher) with a coverslip. Incubation at room temperature overnight (in the dark) can accelerate the sealing of Prolong Gold. All slides were stored at 4°C in a dark plastic box to keep the section humidity and stain signal stable.

IF-IHC analysis of slides was carried out using Carl Zeiss Fluorescence microscope and images were taken using a fluorescence camera with a 40 X objective len.

2.2.8 Ki67 DAB Immunohistochemistry

Tissue sections were gently transferred to a fresh 24-well plate and washed twice for 10 minutes in 0. 1M PBS followed by once in PBS-T. The tissue was then treated with 1.5% H_2O_2 diluted in PBS was used to inactivate endogenous peroxidases. This was followed by 2 10-minute washes in PBS, followed by one 10-minute wash in PBS-T. Next, an antigen retrieval step was carried out, which involved incubating the tissue in 0.1M sodium citrate (pH6, in 0.05% Tween-20) for 1 hour in a 70 ^{o}C dry oven. The sections were then blocked for 1 hour with 5% normal goat serum which was diluted in 0.1M PBS-T and then incubated with a ki67 antibody diluted 1 in 500 in 2% NGS in PBS-T. Positive and negative controls were included to show Ki67 specificity. A 1 in 500 concentration was selected after method optimisation. Ki67 was confirmed to label proliferating cell which are in S and G1 stage of the cell cycle. We demonstrated that Ki67^{+} cells were restricted in neurogenic zones. The tissue sections were then incubated overnight at 4 ^{o}C. The next day, the sections underwent twice 10-minute wash in PBS followed by one 10-minute wash in PBS-T (0.03% triton-x in 0. 1M PBS). A biotinylated goat anti-rabbit diluted 1:400 in 2% NGS in 0. 1M PBS-T was added to the tissue and incubated for 70 minutes at room temperature, protected from the light. Two 10-minute washes in PBS and one wash in PBS-T were carried out, followed by an antibody signal amplification step. An avidin-biotin complex ABC kit was used where solutions A and B were diluted to 0. 4% in PBS-T and then incubated with the tissue for 90 minutes at room temperature, protected from light. 2 more 10-minute washes with PBS were then followed by a 10-minute wash in sodium acetate (pH 6). To visualize the cell staining the cells were treated with DAB. Briefly, the tissue sections were carefully transferred into a weighing boat which contained 500µl nickel-DAB, 30µl glucose oxidase was added and mixed with the DAB solution, and the tissue was incubated for 3 to 15 minutes to enable the development of the stain. The tissue was then washed twice for 10 minutes in PBS. The sections were then mounted onto super frost glass slides and left at room temperature overnight to ensure a firm attachment onto the surface and this process would stop any air-related pollution from contaminating the sections. Haematoxylin is a water-based cell nuclear staining reagent and based on this property was used as a counterstain. The slides were gently

immersed in Haematoxylin solution for 30 seconds to 50 seconds, then rinsed with tap water to stop the continuation of the staining.

The slides then went through a dehydration procedure which contained 6 consecutive 3-minute immersions in the following solutions: 70% ethanol, 95% ethanol, 2 x 100% ethanol, and then 2 x histoclear immersions. 4 to 8 drops of Entellan were applied to each slide using a Pasteur pipette then a coverslip was applied to protect and seal the sections. Each slide was left to dry on a flat surface before being imaged on a light field microscope using x10 objectives.

Table 2.5 Primary antibodies used

Primary antibody name	anti-DCX	anti-PHF1-Tau	anti-Ki67
Concentration	1:200	1:200	1:500
Species raised in	Goat	Mouse	Rabbit
Catalogue number	Sc-8066		Abcam (Ab16667)
Company	Santa Cruz		Abcam

Table 2.6 Secondary antibodies used

Secondary antibody & antibody labelling names	anti-Goat (Alexa Fluor 568 IgG)	anti-mouse (Biotin, IgG)	Streptavidin Alexa Fluor 488
Concentration	1:500	1:400	1:500
Species raised in	Donkey	Goat	na
Catalogue number	AB175474	BA-9200-1.5	AB272187
Company	Abcam	Vector Lab	Abcam

2.3 A rat model of PD using 6-hydroxydopamine (6-OHDA)

This experiment was performed according to the Animal Scientific Procedures Act, 1986 (UK) and the ARRIVE guidelines and performed at the School of Biosciences, Cardiff University. It was approved by the Cardiff University Animal Welfare Ethical Review Body. The method for this study has been described in Rees et al.2021 BioRxiv (Rees *et al.*, 2022).

6-OHDA (Oxidopamine) can selectively destroy dopaminergic and noradrenergic neurons in the brain by entering the cells via dopamine reuptake transporters. In substantial nigra pars compacta (SNpc), it can create lesions to dopaminergic neurons

by producing superoxide radicals. To explore whether the neurotoxin 6-OHDA has a Parkinson-like pathologic effect on neurogenesis and whether acyl-ghrelin can increase immature neurones number to accelerate neurogenesis, we used this PD model on rats. From some researchers' outcomes, the neurotoxin 6-OHDA has been shown to have a PD-like effect in rats (Deumens, Blokland and Prickaerts, 2002). This generates a good PD model to investigate the cellular pathways that underlie PD-related motor dysfunction and its biochemistry. After SNpc dopaminergic neurones are destroyed, there is a deficit of dopamine in the hippocampus leading to the PD phenotype. This can also be called neurotoxin-induced neurodegeneration. My studies will investigate the effect of 6-OHDA on neurogenesis and whether this could be altered by treatment with acyl-ghrelin. Males SD (Sprague–Dawley) rats were supplied by Charles River (Margate, UK).

2.3.1 Housing Conditions and 6-OHDA treatment

All rats were housed under the conditions of 12 hours light / 12 hours dark, with the light on at 6 am in Cardiff University by Tim Wells' group. Male SD rat were supplied by Charles River (Margate, UK). All the rat weigh from 194g to 241g. All animals were fed a crushed diet (SDS 801066 RM3(E); 3.64kcal/g) and water ad libitum in the School of Bioscience. For each rat, daily records were kept for food intake and body weight. The Procedure timetable was as follows: On day1, Osmotic minipumps were used to deliver acyl-Ghrelin. A single unilateral medial forebrain bundle (MFB) injection was applied on day 8 to deliver 6-OHDA (prepared in 0.2mg/ml ascorbic acid in 0.9% sterile saline, PH5.0) or Vehicle (saline). On days 12 and 18, rats received an i.p. injection of BrdU. On the last day, day 35, rats were culled, and the brain tissue was removed and either immediately frozen and kept at -80C or underwent transcranial perfusion of 1.5% paraformaldehyde (PFA) (Sigma-Aldrich, P6148-1KG). After perfusion, the brain was removed and post-fixed by immersing in 1.5% PFA in 0.1M PBS at 4^{o}C overnight. 30% of sucrose then was applied at 4^{o}C until further process.

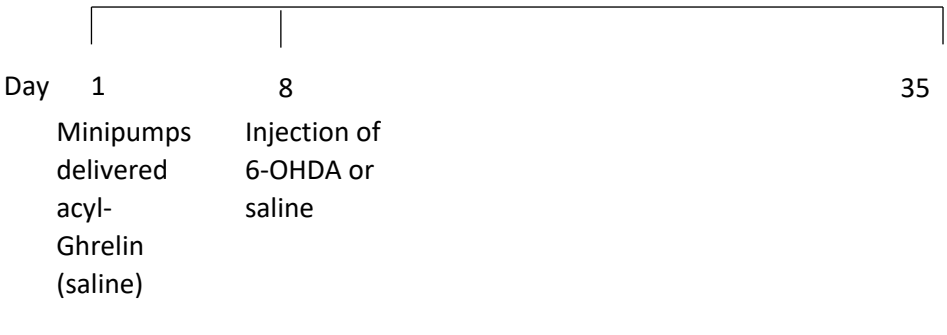

Figure 2.1 Schematic of 6-OHDA rats experimental timeline.

Experimental paradigm of 6-OHDA rats. Ghrelin or saline were given on day 1. 6-OHDA (0.2mg/ml) or saline were injected on day 8 at unilateral brain. Rats were culled on day 35.

2.3.2 Group Information

In this experiment, the rats were randomly assigned into 3 groups. Group 1 were the blank control, which received saline treatment only, containing 8 rats. Group 2, containing 9 rats, comprised the 'lesion group', in which the unilateral side of the brain received the injection of 6-OHDA and i.p. vehicle solution. Group 3, containing 8 rats, received both unilateral 6-OHDA injection and i.p acyl-ghrelin treatment.

2.3.3 Brain sectioning

After the brain tissues were cut to a thickness of 30um along the coronal axis, PBS with 0.01% Azide was used to store the tissue sections – and prevent fungal contamination – at 4^{o}C. Normally for 1 mouse brain, we allocated each consecutive section into 12 consecutive wells of either 24 wells plates, 48 wells plates or 96 well plates. This means each well contains a 1 in 12 representation of the whole brain. This method helps us efficiently and accurately estimate whole-brain immunoreactivity without having to process all sections of an entire brain. We adopted this method when analysing cell numbers, cell types and cell morphology. All tissue sections were immersed in PBS Azide; within sterile multi-well plates, sealed by parafilm (to

prevent potential water evaporation) and stored at 4℃, so the cell structure, protein, and peptides could be preserved for subsequent immunohistochemistry assays.

For each rat, we collected 1 whole well of sections (1:12 representation of the entire caudal axis of the brain tissue that was sectioned) for immunohistochemistry work. This allowed us to calculate the average number of immunopositive cells across the entire brain region. During the IHC protocol, each section was carefully handled using a fine paintbrush. Every care was taken to prevent tissue damage to allow for accurate cell counting.

2.3.4 Immunofluorescence co-localization IHC for TH (Tyrosine hydroxylase) and Doublecortin (DCX) (free-floating method)

Tissue sections were gently removed from storage (PBS-T/0.003% azide at 4^{o}C) into a new well-containing 300µl. Subsequently, three 5-minute PBS washes at room temperature on a shaker (30 rotations per minute) were carried out (note, all incubations and washes were carried out with shaking). To permeabilize the brain sections, we immersed tissue in methanol at -20℃ for 2 minutes. Three further 5-minute PBS washes were performed followed by incubation with 5% Normal Donkey Serum (NDS) (diluted in 0.1M PBS-Triton X-100 (PBS-T) for 20 minutes at room temperature. PBS-T was used to dilute Primary Rabbit Antibody for TH 1:500 and Primary Goat antibody for DCX 1:200, which were incubated with the tissue sections overnight at 4℃. DCX antibody validation was described above. TH antibody was purchased from Abcam, which was validated by the company in staining dopamine cells. In this project, after incubation with TH antibody, only VTA and SNpc areas showed immune-positive stain as these areas contain a high proportion of the dopamine cells. This immune reactivity provides further validation for the specificity of TH antibody used. The next day, three 5-minute PBS washes were carried out then the tissue sections were incubated for 60 minutes in a dark with Donkey anti-Rabbit (AF568 1:500) and Donkey anti-Goat (AF488 1:500) (for TH and DCX procedures respectively) which were diluted in 0.1M PBS-T. This was followed by another three 5-minute washes with PBS. Normally, During the last wash included Hoechst (diluted 1:10,000), a counterstain for cell nuclei. Tissue sections were then mounted onto Super Frost glass slides before applying ~50 to 70µl Prolong Gold solution (Thermofisher)

with a coverslip. Incubation at room temperature overnight (in the dark) can accelerate the sealing of Prolong Gold. All slides were stored at 4℃ in a dark plastic box to keep the section humidity and stain signal stable.

Table 2.7 Primary antibodies used

Primary antibody name	anti-DCX	anti-TH
Concentration	1:200	1:500
Species raised in	Goat	Rabbit
Catalogue number	Sc-8066	Ab122
Company	Santa Cruz	Abcam

Table 2.8 Secondary antibodies used

secondary antibody name	anti-Goat (Alexa Fluor 488 IgG)	anti-rabbit (Fluor 568 IgG)
Concentration	1:500	1:500
Species raised in	Donkey	Donkey
Catalogue number	Ab150129	Ab175470
Company	Abcam	Abcam

2.4 Generating a mouse model of PD using N-methyl-4-phenyl-1, 2, 3, 6-tetrahydropyridine (MPTP)

This experiment was performed at Monash University, Australia. It was approved by the Monash University Animal Welfare Ethical Review Committee. The method for this study has been described in Bayliss et al.2016.

To determine whether acyl-ghrelin promotes adult hippocampal neurogenesis in a model of PD we used a mouse neurotoxin-based model of SNpc neurodegeneration. The generation of the AMPK KO and AMPK WT mice used in this study are described in Bayliss et al.2016. (Dat-Cre; Ampk $\beta1^{fl/fl}$; Ampk $\beta2^{fl/fl}$ designated AMPK KO & Ampk $\beta1^{fl/fl}$; Ampk $\beta2^{fl/fl}$ designated AMPK WT) Briefly, DAT^{IRES}cre knock-in mice were created in the Jackson Laboratory. (Stock No. 006660; B6.SJL-Slc6a3< tm1.1(cre)bkmn > /j) The resultant offspring, AMPK KO and AMPK WT mice were selected as experimental subjects. (O'Neill et al., 2011).

AMPK, 5' AMP-activated protein kinase or 5' adenosine monophosphate-activated protein kinase is an enzyme (EC 2.7.11.31) that plays a role in cellular energy homeostasis. It consists of three proteins (subunits) that together make a functional

enzyme which plays an important role in cellular energy homeostasis. It can increase glucose uptake and oxidation during a low level of energy. The human brain contains AMPK to bind AMP (Adenosine monophosphate) and ADP (Adenosine diphosphate). It also activates autophagy, increases mitochondrial biogenesis and affects human physical excise which suggests it may play an important role in the mechanism of PD.

2.4.1 The generation of Dopamine transporter (DAT) knock-in mice

DAT^{IRES}cre knock-in mice have Cre recombinase expression directed to dopaminergic neurones, without disrupting endogenous dopamine transporter expression. These mice will be useful for studying gene function in dopaminergic neurones, such as drug addiction, Parkinson's disease, and Attention Deficit-Hyperactivity Disorder (ADHD).

TdTomato is an exceptionally bright red fluorescent protein here to show the DAT expressing neurones.

Briefly, to knock out the β1 and β2 subunits of AMPK in only the DAT-expressing dopamine neurons in mice, Dat-Cre knock-in mice obtained from The Jackson Laboratory were crossed with Ampk β1 subunit (β1) and β2 sub-unit (β2) floxed mice. The offspring (Dat-Cre;Ampk $\beta1^{fl/fl}$; Ampk $\beta2^{fl/fl}$ refers to AMPK knockout (KO) or Ampk $\beta1^{fl/fl}$; Ampk $\beta2^{fl/fl}$ represents AMPK wild type (WT)). To validate this model, the created offspring, AMPK WT and AMPK KO mice were also bred with cre-dependent loxSTOPlox tdTOMATO reporter mice. The offspring Dat-Cre;tdTomato or Dat-Cre;Ampk $\beta1^{fl/fl}$; Ampk $\beta2^{fl/fl}$; tdTomato mice helped tdTomato visualization of DAT-expressing neurons that have undergone cre recombination. The Dat-Cre; tdTomato were used as AMPK WT mice. The Dat-Cre; Ampk $\beta1^{fl/fl}$; Ampk $\beta2^{fl/fl}$; tdTomaro mice were used as AMPK KO mice which is described in Bayliss et al.2016.

2.4.2 Housing Conditions and MPTP treatment

Mice (8 –10 weeks old) were maintained under standard laboratory conditions with ad libitum access to food and water at 21°C with a 12 h light/dark cycle unless otherwise stated. MPTP, a mild neurotoxin was discovered to have the ability to destroy dopaminergic neurones. It results in striatal dopamine loss, nigral cell loss and

behavioural dysfunction. This model has been widely used to explore the mechanisms of PD and the potential therapeutic treatments.

The procedure timetable was as follows: During the raising stage, days 1-13, mice have administrated Ghrelin (1 mg/kg) or saline daily according to the group code. On days 7 and 8, mice were injected by i.p. with saline or MPTP (30mg/kg diluted in saline) according to the experiment design. Finally, on day 14, mice were culled and perfused by 1.5% PFA. Immersion in 1.5% PFA overnight at 4^{o}C made the brain ready for sectioning and immunohistochemical analysis.

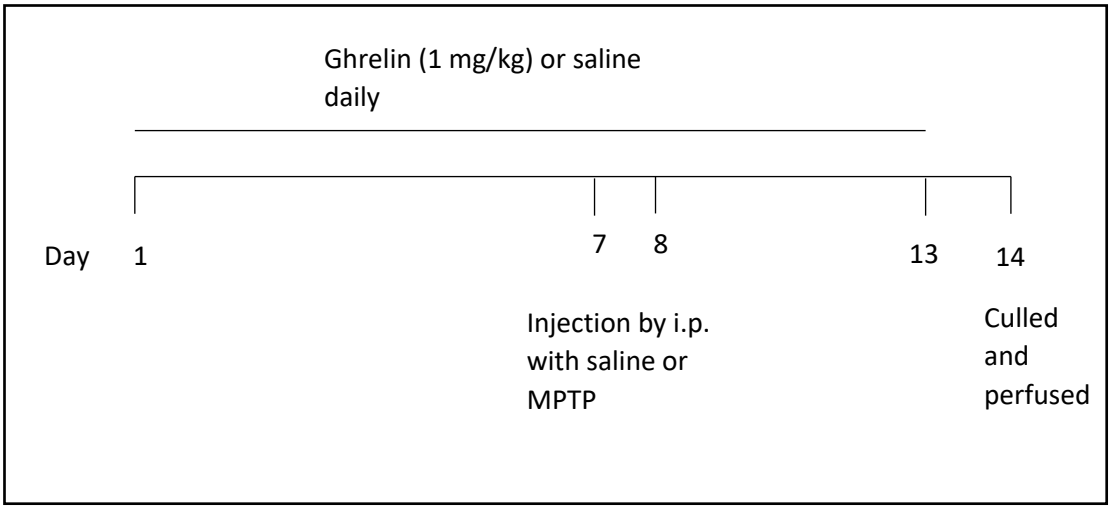

Figure 2.2 Schematic of AMPK KO mice experimental timeline.

Experimental paradigm of AMPK KO mice. Ghrelin (1 mg/kg) or saline were given from day 1-13. MPTP (30mg/kg) or saline were injected by i.p. on day 7 and 8. Mice were culled on day 14.

2.4.3 Group information

AMPK WT and AMPK KO mice were randomised and allocated into 4 groups. Group 1 received saline/saline treatment. Group 2 was treated with saline, and Ghrelin treatment. Group 3 was given MPTP, saline treatment. Group 4 was treated with MPTP, Ghrelin.

2.4.4 DCX DAB Immunohistochemistry

The DCX DAB immunohistochemistry method is the same as shown in 2.2.7, only with DCX diluted at 1 in 500 in PBS-T.

Table 2.9 Antibodies used

Table: Antibody used	Primary antibody	Secondary antibody
Antibody name	Goat anti-DCX	Donkey anti-Goat (Biotinylated IgG)
Concentration	1:750	1:400
Species raised in	Goat	Donkey
Blocking serum	2% NDS	2% NDS
Treatment duration	Overnight	Room Temperature
Catalogue number	Sc-8066	BA-1000-1.5
Company	Santa Cruz	Vector Laboratories

2.5 Analysis of IHC images using ImageJ

The ImageJ version of 1. 52p was used, from the national institutes of health, USA, based on java 1. 8. 0_66 (32-bit) in windows7 and windows10 operating system environment.

Firstly, the image selected was dragged to the software to open it. On the panel, the straight function could be used to draw a line on the scale of the image, based on the analysis menu, in set-scale, set distance in pixels as 159, known distance as 100, pixel aspect ratio as 1.0, unit of length as um, ticking the global option. To change the property of the image we chose the 8-bit typed from the image in the menu bar. To make the picture resolution clearer we set the radius as 10. 0 pixels and mask weight (0. 1-0. 9) as 0. 6 in the unsharp mask function from the process (filters) menu bar. At the image (adjust) menu, we set the bottom bar of the value as 115, so the percentage showed around 1% when compared to the whole image spectrum. In the process menu, the binary function could help the image to convert to mask and watershed the big blocks in the image. Polygon could perfectly help to circle a line between the DG and

GCL in which the background stains would be excluded. In analyse menu, the analyse particles function could design the size (pixel2) as 22- infinity, circularity as 0. 00-1. 00, showing outlines, ticking cleared results and summarising. The results shown up by a graph were copied on an excel sheet for further calculation. Similarly, from the analyse menu, the measured choice could calculate the area data and it was transferred on the same excel sheet as the raw data of the experiment.

After counting the DCX positive cell number, similarly, the original image was opened again, and a polygon was chosen to draw a line precisely only including the DG area. In analyse menu, by clicking the measure function, the software could calculate the chosen area, and the results were copied to the excel sheet as the DG area data for future comparisons.

2.6 ImageJ coding lists

2.6.1 FTD disease model, (2 weeks old) DG images, Macro Coding records

The Macro code for the DG section:

```
run("8-bit");

run("Unsharp Mask...", "radius=10 mask=0.60");

setAutoThreshold("Default");

//run("Threshold...");

setThreshold(0, 28);

setOption("BlackBackground", false);

run("Convert to Mask");

run("Watershed");
```

2.6.2 FTD disease model, (2 weeks old), SVZ images, Macro Coding records

The Macro code for the SVZ section:

```
run("8-bit");

run("Unsharp Mask...", "radius=10 mask=0.60");

setAutoThreshold("Default");

//run("Threshold...");

setThreshold(0, 121);

setOption("BlackBackground", false);

run("Convert to Mask");
```

2.7 Data calculation & Statistical analysis

Microsoft Office 365, excel software was used to collect all the counting data based on each tissue section. Based on Excel formulas, all the counting from the images of 1 tissue section was processed by the 'sum' function, then followed by used the 'average' function to operate the average counting number of all the tissue sections from 1 animal. GraphPad. Prism. 9. 0. 0. 121 was used to continue all the data analysis and plotting all the graphs. Facing 2 groups comparison about 1 variation element, an unpaired student's t-test was adopted to calculate if there was statistical significance or not. In this project, when the statistical test result $P \leqslant 0.05$, the null hypothesis was rejected, and the test result is significant. Based on population data, normality distribution was tested before using parametric test. For grouped data which includes more than 2 variations, ANOVA was selected. On the GraphPad software, after choosing the 'data tables', the 'analyze' function is directed to the options panel. For 'experiment design', 'unpaired, 'yes, used parametric test', 'unpaired t-test, assumed both populations had the same sd' were selected. About the 'option', 'two-tailed', '95%' confidence levels complied before processing the p-value calculation.

2.8 Human PD brain

The post-mortem human brain tissue used in this study was donated to the UK Parkinson's Disease Society Tissue Bank at Imperial College London with ethical approval (07/MRE09/72). Fixed frozen hippocampal sections (6-8um thick) were placed onto Superfrost^{+} glass slides and shipped to the Davies lab on dry ice. The control slides were donated by individuals with no evidence of degenerative disease or cognitive decline. The tissue used in this preliminary study was from a male, aged 35 years, with a post-mortem interval of 22 hours.

Brain and tissue samples were removed by a trained neuropathologist. Weight and PH were recorded from the fresh brain. Hippocampus was selected for a specific research purpose. Formalin was used to fix the tissue for a later histological process.

Hippocampus was sectioned at 20 µm thickness and directly placed on glass slides. Tissue samples were grouped according to Brain Bank code and then stored at -80^{o}C.

After the tissue slides arrived at Swansea University, code and tissue quality were recorded for further exploration. Carefully, the slides sections were taken out from the -80 ^{o}C freezer and placed on the bench for 1-3 minutes to let them dry at room temperature. Tissue was used to wiping away any moisture around and beneath the glass sides and a hydrophobic pen was used to draw a circle around the tissue on the glass slide. The drawing location needed to be precise in order not to touch and affect any of the human brain samples. 150µl of 10% NBF (Neutral buffered formalin) was used to immerse and fix all of the tissue for 1 hour at room temperature, which was followed by 2 1minute washes with 150µl PBS. Next, an antigen retrieval step was carried out, 0.5% sodium borohydride freshly prepared in PBS was added to the tissue for 30 minutes at room temperature. PBS-T-BSA (Bovine serum albumin) was used to wash the sections 5 times for 30 seconds. To inactivate endogenous peroxidases, H_2O_2 (1%) diluted in PBS was added for 8 minutes at room temperature, then followed by two 1-minute washes with PBS.

Antigen retrieval was carried out using three different methods in order to compare their effectiveness. For the first method, the sections were incubated for 1 hour in sodium citrate at 95 ^{o}C in a Milli Q purified water-based steamer. For the second method, the sections were immersed for 1 hour in sodium citrate in the Hybez oven at 70 ^{o}C. For the third method, the sections were incubated for 1 hour with sodium citrate at room temperature.

A blocking buffer was prepared to contain 2% BSA and 10% NDS in PBS-T. The slides were incubated in the solution for 20 minutes at room temperature. A primary antibody, goat anti-DCX (1 in 200 diluted in 1% BSA in PBS-T) was added to the sections for 24 hours of treatment in the cold room at 4 ^{o}C.

The second-day procedure started with two 10 minutes washes in PBS. Biotinylated secondary antibody Donkey anti-goat (diluted1 in 500 in 1% BSA in PBS-T) was added to the sections for 1 hour at room temperature. After twice 1-minute washes with PBS, ABC solution was used to amplify the antigen signal. This was prepared 30 minutes prior to use by preparing 0.4% of solutions A and B in PBS-T, the sections were incubated with the ABC solution protected from light at room temperature for 1

hour. Next, two 1-minute washes in PBS were carried out. The presence of the signal was visualised using Impact DAB. With a 1:1 ratio, 100µl of reagent A and reagent B were mixed in a small tube, and then quickly applied to the tissue section for 8 minutes. During the Impact DAB treatment, the slide needed to be placed on the microscope stage in order to observe the colour change of the stain. To stop the DAB reaction, the slides were immersed in tap water at room temperature. The slides were then treated for 30 seconds with the counterstain haematoxylin, followed by rinsing in tap water to stop any further reaction. Next, a dehydrating process was carried out, the slides were immersed for 3 minutes each in 70% ethanol then 2 x 100% ethanol, followed by two 1minute immersions in histoclear. 4 to 8 drops of Entellan were applied to each slide using a Pasteur pipette then a coverslip was applied to protect and seal the sections. Each slide was left to dry on a flat surface, long-term, the slides were stored at 4 ^{o}C. Analysis of the slides was carried out using a bright field microscope using x4 and x10 objectives lens then followed by taking images.

3 Chapter 3 - Characterisation of adult hippocampal neurogenesis in a novel mouse model of Frontotemporal Dementia (FTD)

3.1 Introduction

3.1.1 FTD

The loss of multiple cognitive functions is the main characteristic of FTD, which shows progressive degenerative atrophy of the frontal and temporal lobes (Chapman *et al.*, 2006). Three main subgroups of FTD are described to show more detailed symptoms of FTD, which include frontal-variant or behavioural-variant FTD (fvFTD), progressive non-fluent aphasia (PNFA) and semantic dementia (SD). Apart from those 3 groups, other motor syndromes: cortical basal degeneration (CBD), progressive supranuclear palsy (PSP) and motor neurone disease (also known as Amyotrophic Lateral Sclerosis) are also classified in the spectrum of FTD, because of the similar pathology (Graff-Radford and Woodruff, 2007)(Knibb, Kipps and Hodges, 2006).

In contrast to other neurodegenerative diseases, FTD is pathologically characterised by neurone loss, gliosis accumulation, and superficial spongiform degeneration. As described in the name, these changes mainly occur in the frontal-temporal lobes (Lomen-Hoerth, Anderson and Miller, 2002)(Kertesz and Munoz, 2002). Standard histology reveals that due to the severe loss of neurones, the outer cortical laminae depict microvacuolation (dementia without showing diagnostic histological features)(Neary, Snowden and Mann, 2005).

The phenomenon of Tau protein aggregation is widely accepted. Tau has been confirmed to correlate with fvFTD, CBD and PSP. Due to the high number of Tau-related FTD cases, some researchers suggest that this neurodegenerative disease can be divided into Tau-positive and Tau-negative variations, and could segregate with the different clinical treatment strategies (Sydow *et al.*, 2011) (Sha *et al.*, 2006)(Kertesz, 2005). It has been regarded as essential to quantify Tau abnormalities in the evaluation of the FTD pathological report. Some researchers also suggest that the presence of

ubiquitin can be included to provide more detailed information as ubiquitin 2 inclusions cause sporadic FTD (Zhang *et al.*, 2014) (McKhann *et al.*, 2001).

Risk factors for the onset of FTD have been explored by different research groups. The main two include head trauma and genetic inheritance. In the investigation of head trauma as a risk factor, 80 cases of sporadic FTD were analysed in a case-control study and suggested a significant correlation with brain trauma (Chapman *et al.*, 2006). Family history has also been widely accepted as an important risk factor for FTD, with several gene mutations associated with FTD. For example, mutation of the TDP-43 gene is known to mainly affect ALS-FTD. The heterozygous missense mutation P106L has been reported to contribute to bvFTD, whilst the N267S mutation causes the CBS type of FTD (Huey *et al.*, 2012). Q331K mutation is also reported to contribute to an FTD behaviour syndrome (Kim *et al.*, 2020). Most FTD cases can be identified with pathology, including TDP-43, which is located in the nucleus. It can cause nuclear TDP-43 mislocalization and cytoplasmic inclusions (Riku *et al.*, 2021). Researchers found that the TDP-43^{Q331K} knock-in mouse demonstrates typical FTD cognitive syndromes, e.g., memory loss and inattention (Sreedharan *et al.*, 2015). Moreover, altered splicing of the Tau gene, which associates with FTD, was also found in this genetic model. This 'face validity' suggests that this model may represent better research value than other genetic models in exploring FTD (Hutton *et al.*, 1998). A mouse model containing the Q331K human mutation is the first mouse model to contain physical symptoms which are more consistent with the human form of FTD (White, Kim, Duffy, Adalbert, Phillips, Peters, Stephenson, Yang, Massenzio, Lin, Andrews, Segonds-Pichon, Metterville, Saksida, Mead, Ribchester, Barhomi, Serre, Coleman, J. R. Fallon, *et al.*, 2018).

Chromosome-17 has also been reported to show a strong correlation with familial FTD, especially with the mutation of Microtubule-associated protein tau (MAPT) (Neary, Snowden and Mann, 2005). In humans, there are 6 isoforms of Tau. 3 isoforms depict three microtubule-binding regions, named 3R Tau, while others show 4 repeated regions, known as 4R Tau, shown in figure 1.1.2 in Chapter1. The dysregulation of any Tau protein isoform production or degradation can cause the instability of microtubules and its dysfunction, which can eventually prevent regular cellular function (Neary, Snowden and Mann, 2005). Thus, there is a growing need for the assessment of Tau abnormalities during the pathological report of human FTD cases.

As described in chapter 1, Tau can also be phosphorylated, forming PHD Finger Protein 1 (PHF1-Tau). Tau protein is also regarded as one of the most complicated proteins as it has multiple phosphorylation sites (Kimura *et al.*, 2018). Some studies show phosphorylated Tau can change its release from neurones (Noble *et al.*, 2013).

Mouse experiments also reveal $Tau^{-/-}$ mice depicts can decrease newborn granule neurones maturation (Pallas-Bazarra *et al.*, 2016). Tau hyperphosphorylation may become the negative influence of stress on cognition impairment (Sotiropoulos *et al.*, 2011). However, the mechanism of its role in neurogenesis is currently not known. By focusing on these isoforms, it will be important to see if phosphorylation has any relation to AHN.

3.1.2 Chapter aims

The primary aim of this chapter is to quantify neurogenesis in the hippocampus of the novel $TDP43^{Q331K}$ mouse model of ALS/FTD. A secondary aim involves quantifying phosphorylated Tau immunopositive neurones in the hippocampal niche of the same mice.

3.2 Materials

All generic protocols used are described in chapter 2. E.g., image j.

Table 3.1 Antibody used in IHC:

	Primary antibody	Secondary antibody
Antibody name	Goat anti-DCX	Donkey anti-Goat (Biotinylated IgG)
Concentration	1:750	1:400
Species raised in	Goat	Donkey
Blocking serum	2% NDS	2% NDS
Treatment duration	Overnight	Room Temperature
Catalogue number	Sc-8066	BA-1000-1.5
Company	Santa Cruz	Vector Laboratories

Table 3.2 Primary antibodies used in IF

Primary antibody name	anti-DCX	anti-PHF1-Tau	anti-Ki67
Dilution	1:200	1:200	1:500
Species raised in	Goat	Mouse	Rabbit
Catalogue number	Sc-8066	Supplied by Dr Peter Davies, Albert Einstein College of Medicine, New York	Ab16667
Company	Santa Cruz	Albert Einstein College of Medicine	Abcam

Table 3.3 Secondary antibodies used in IF

Secondary antibody & antibody labelling names	anti-Goat (Alexa Fluor 568 IgG)	anti-mouse (Biotin, IgG)	Streptavidin Alexa Fluor 488
Dilution	1:500	1:400	1:500
Species raised in	Donkey	Goat	na
Catalogue number	AB175474	BA-9200-1.5	AB272187
Company	Abcam	Vector Lab	Abcam

3.3 Results

3.3.1 Cell proliferation is not altered in two-week-old female TDP-43$^{Q331K+/Q331K+}$ and wild-type mice.

To compare the level of cell proliferation between wild-type and TDP-43$^{Q331K+/Q331K+}$ mice, two rostral brain sections and two caudal brain sections underwent IHC-DAB for Ki67. The number of Ki67^{+} cells was unchanged in both the DG and the SVZ of wild-type mice and TDP-43$^{Q331K+/Q331K+}$ mice when expressed as either the cell number per section or as immunoreactive area per DG or SVZ (Figure 3.14). The results suggest that the Q331K/Q331K mutation may have no effect on cell proliferation in the neurogenic niches of 2-week-old mice.

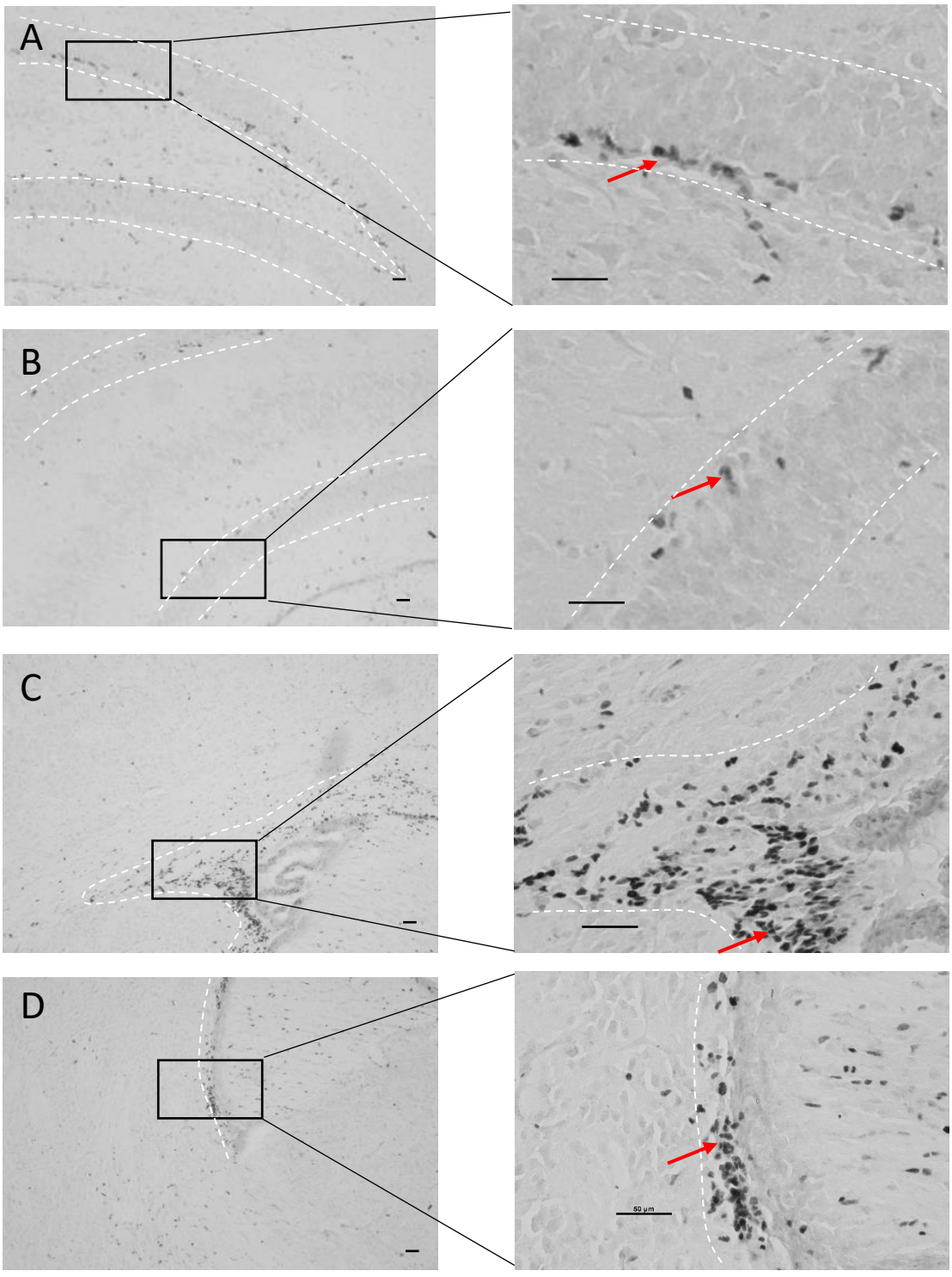

Figure 3.1 Ki67^{+} cells in the hippocampus and SVZ of 2-week-old TDP-43$^{Q331K/Q331K}$ and WT mice. IHC-DAB was performed for Ki67 on brain tissue sections from TDP-43$^{Q331K+/Q331K+}$ and wild type mice. Above are example images of the DG from TDP-43$^{Q331K+/Q331K+}$ (A), wild-type (B) mice, followed by example images of the SVZ from TDP-43$^{Q331K+/Q331K+}$ (C) and wild-type (D) mice. Images were taken by 10X objective lens. Representative of positive immunolabelled cells is shown by the arrows. Scale bar equals to 50µm.

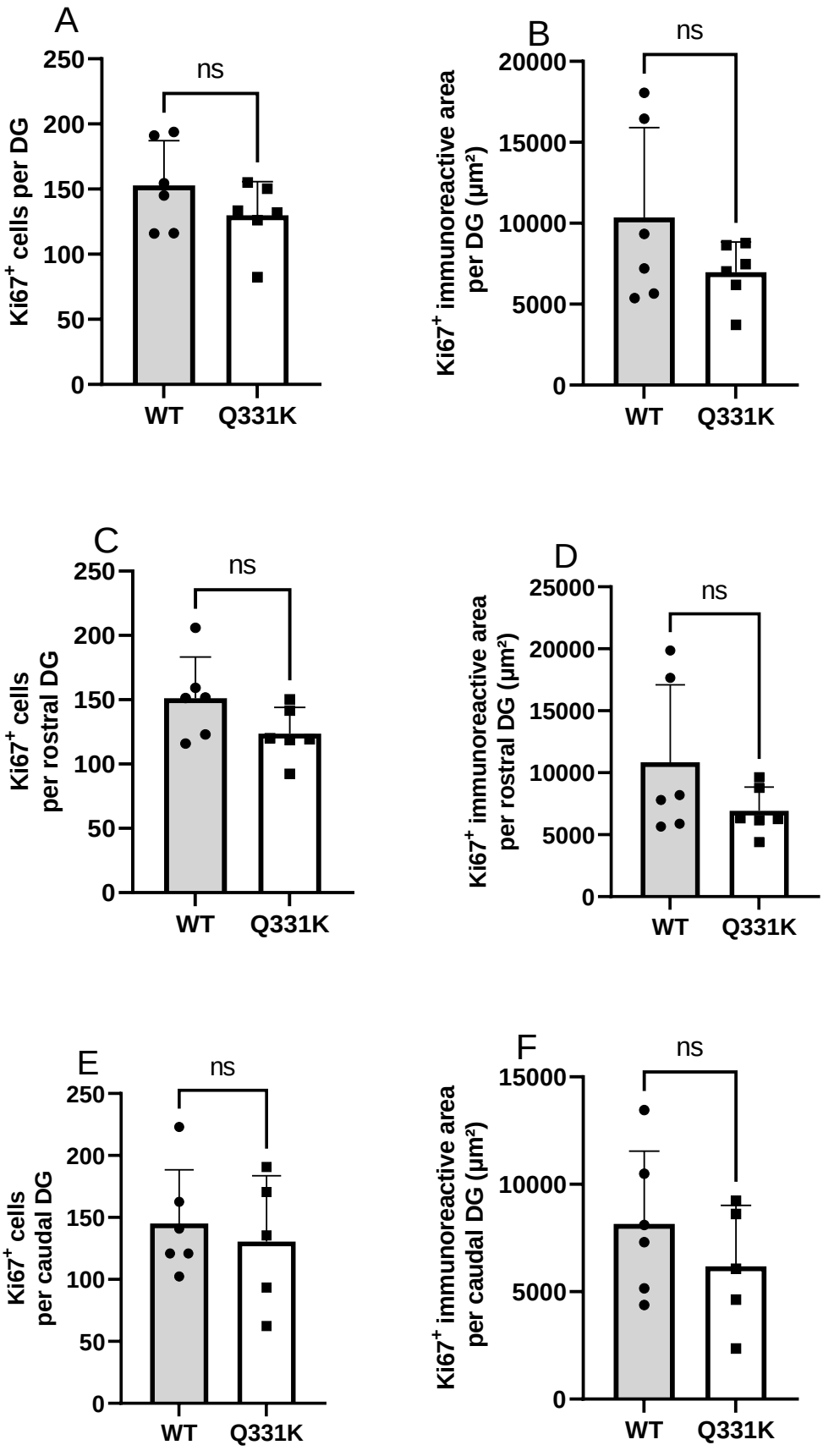
A
ns
Ki67+ cells per DG
250
200
150
100
50
0
WT
Q331K
B
ns
Ki67+ immunoreactive area per DG (µm²)
20000
15000
10000
5000
0
WT
Q331K
C
ns
Ki67+ cells per rostral DG
250
200
150
100
50
0
WT
Q331K
D
ns
Ki67+ immunoreactive area per rostral DG (µm²)
25000
20000
15000
10000
5000
0
WT
Q331K
E
ns
Ki67+ cells per caudal DG
250
200
150
100
50
0
WT
Q331K
F
ns
Ki67+ immunoreactive area per caudal DG (µm²)
15000
10000
5000
0
WT
Q331K

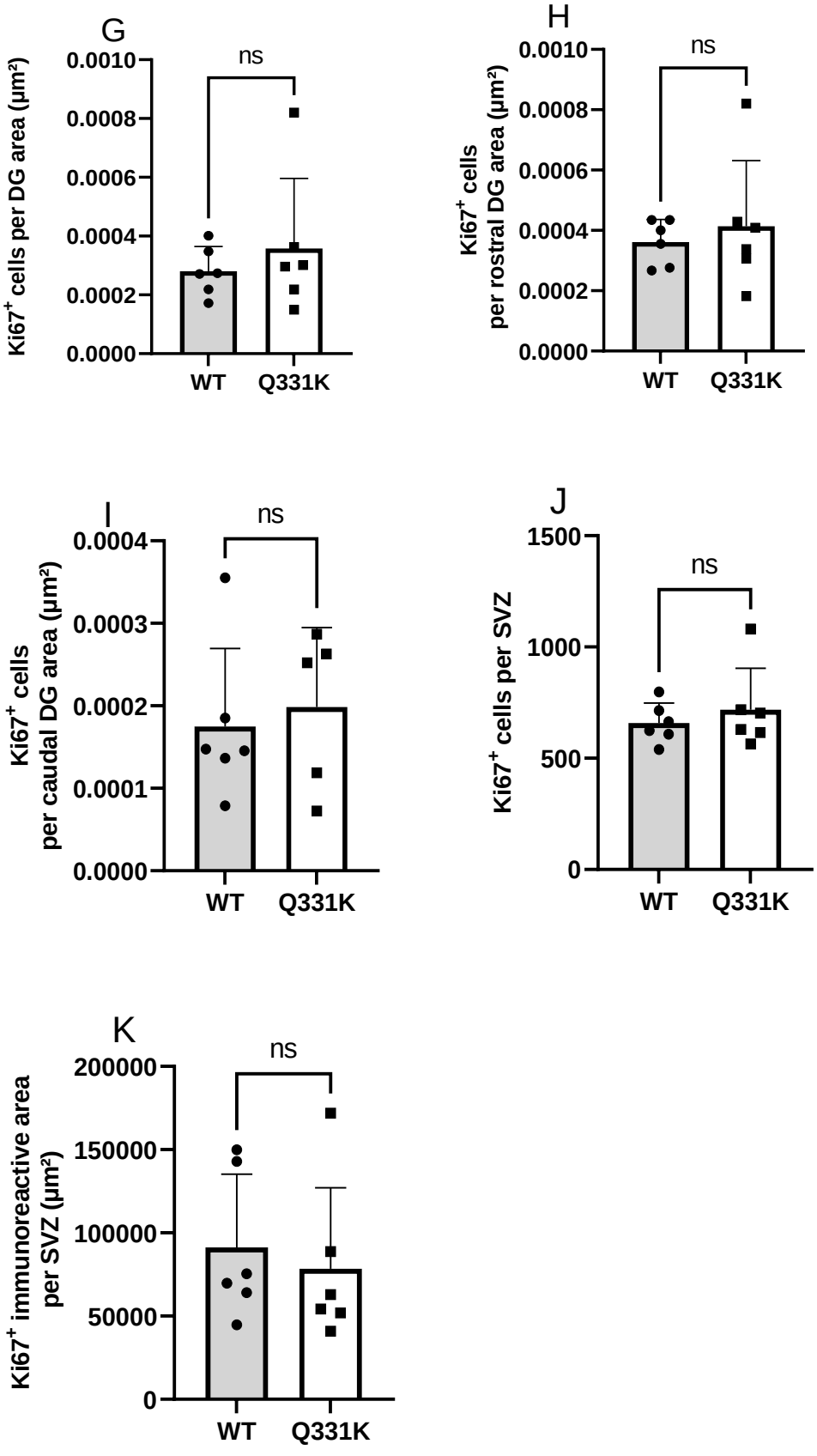

(Legend showed on next page due to content size)

Figure 3.2 Cell proliferation is similar in 2-week-old TDP-43$^{Q331K+/Q331K+}$ and wild type mice. IHC-DAB was performed for Ki67 on brain sections from male TDP-43$^{Q331K+/Q331K+}$ and wild type mice. The number of Ki67^{+} cells (A), Ki67^{+} immunoreactive area (B), rostral DG (C)(D), caudal DG (E)(F). Ki67^{+} cell number / average DG area (G)(H)(I). SVZ region (J)(K). The experiments comprised of 2 groups. Each Group n=6. Comparison was conducted by student's unpaired t-test. ns = not significant. All data shown are mean ± SEM.

3.3.2 The immunoreactive area of Ki67^{+} cells was increased in 6-month-old female TDP-43$^{Q331K+/Q331+}$ mice compared to wild-type mice.

Whilst investigating the number of DCX^{+} cells can indicate the development of newborn immature neurones, the Ki67 protein gives an indication of cell division. Cell division within the sub-granular zone of the DG can be used as a marker of stem cell proliferation. A Ki67 antibody used to immunolabel the replicating cells demonstrated that there was no change in the number of Ki67^{+} cells in either the DG or the SVZ in wild-type and TDP-43$^{Q331K+/Q331K+}$ mice (Figure 3.16 A), whilst there was a significant increase in the area covered by the Ki67^{+} cells in TDP-43$^{Q331K+/D331+}$ mice across the entire DG (Figure 3.16 B, P= 0.0073, Mean±SEM: WT 237.2±40.0, Q331K 497.6±67.03) and in the caudal pole of the DG (Figure 3.16 F, p=0.0308, Mean±SEM: WT 302.0±53.49, Q331K 750.5±199.6). The results suggest that in 6-month-old mice, the Q331K mutation increase cell proliferation in the DG.

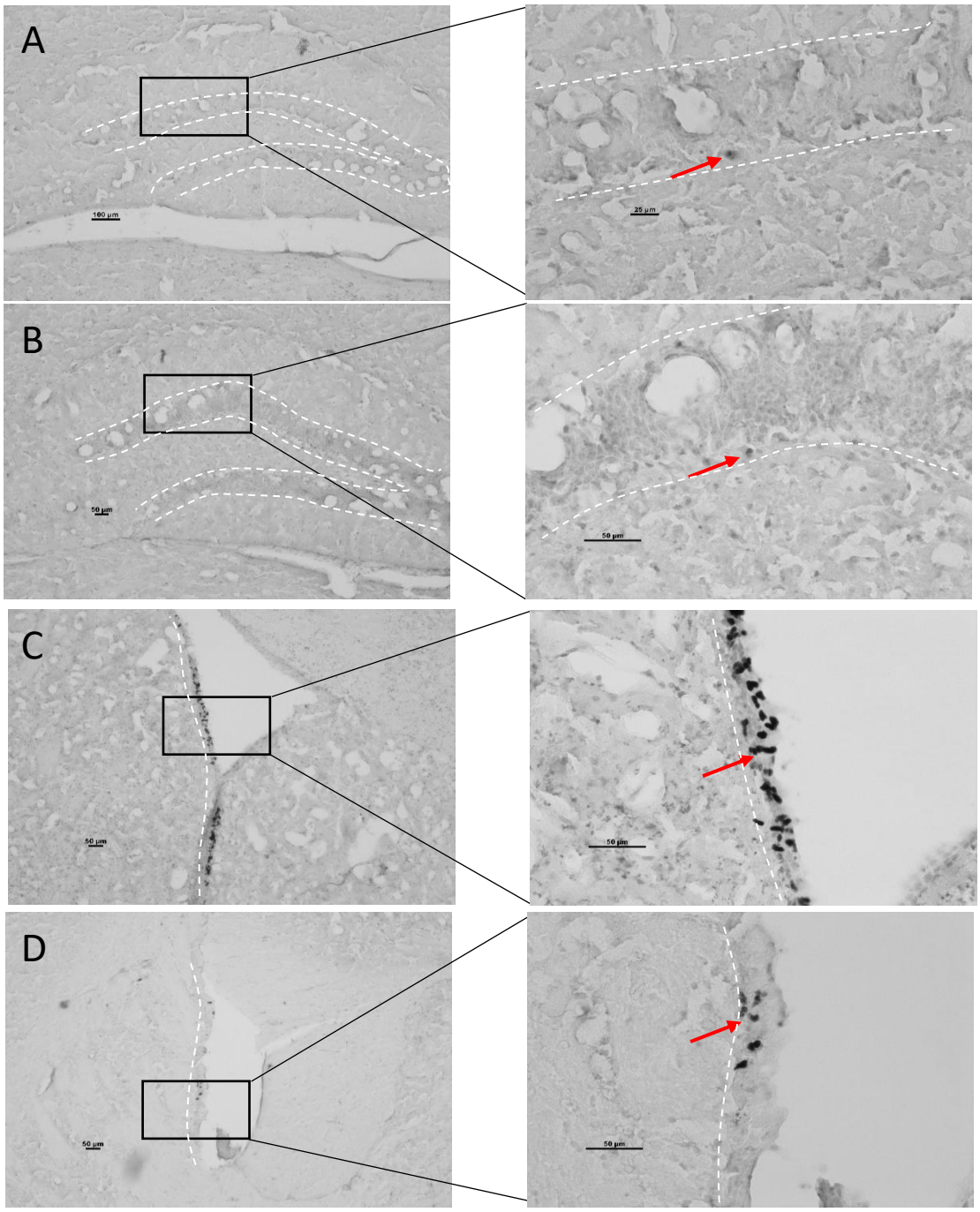

Figure 3.3 Ki67^{+} cells in the hippocampus and SVZ of 6-month-old female TDP-43$^{Q331K/Q331K}$ mice and wild type mice. IHC-DAB was performed for Ki67 on hippocampal and SVZ sections from TDP-43$^{Q331K+/Q331K+}$ and wild type mice. Above are example images of the DG region from TDP-43$^{Q331K+/Q331K+}$ (A), wild-type (B) mice, followed by example images of the SVZ from TDP-43$^{Q331K+/Q331K+}$ (C) and wild-type (D) mice. Images were taken by 10X objective lens. Representative of positive immunolabelled cells is shown by the arrows. Scale bar equals to 50µm.

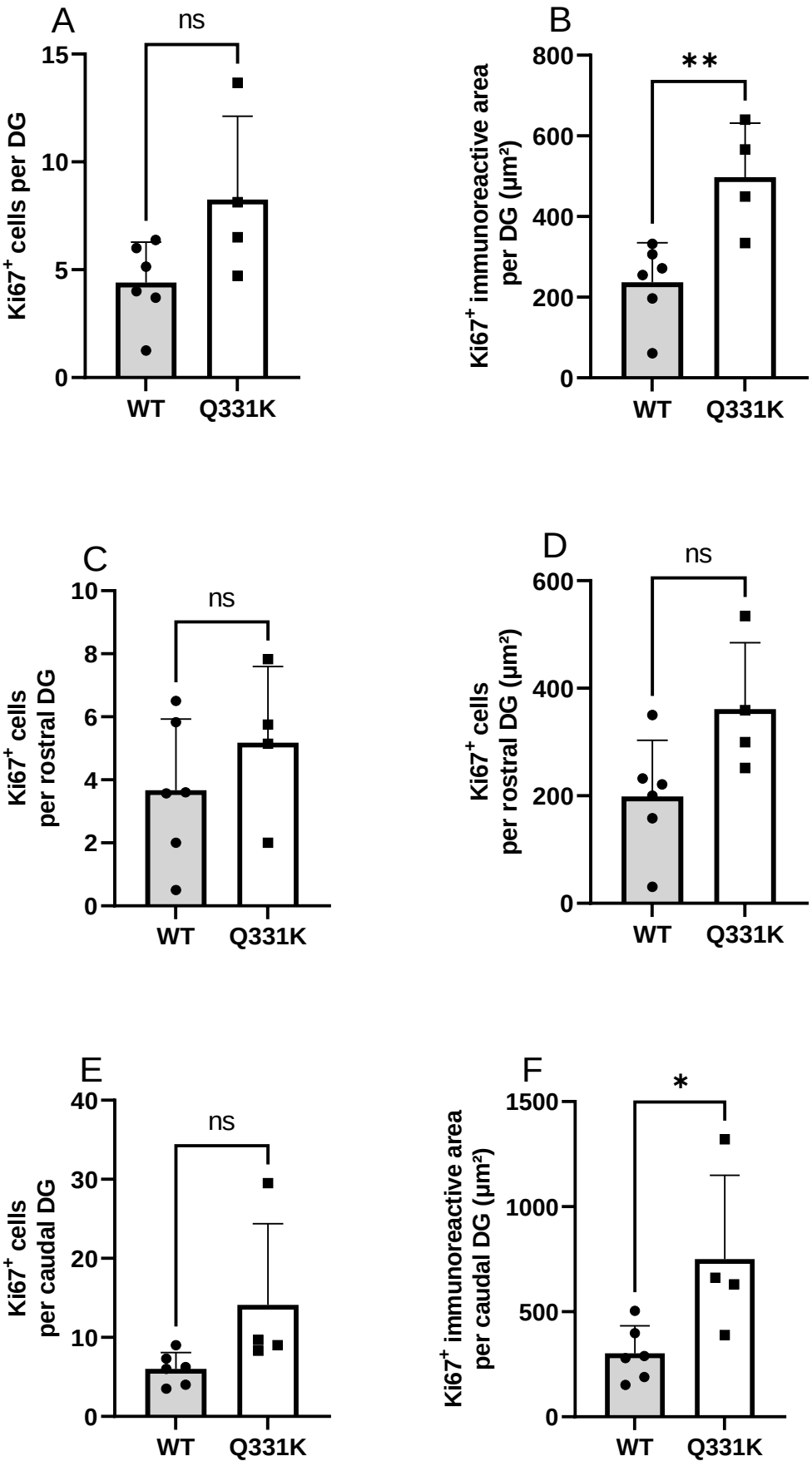
A
ns
Ki67+ cells per DG
15
10
5
0
WT
Q331K
B
**
Ki67+ immunoreactive area per DG (µm²)
800
600
400
200
0
WT
Q331K
C
ns
Ki67+ cells per rostral DG
10
8
6
4
2
0
WT
Q331K
D
ns
Ki67+ cells per rostral DG (µm²)
600
400
200
0
WT
Q331K
E
ns
Ki67+ cells per caudal DG
40
30
20
10
0
WT
Q331K
F
*
Ki67+ immunoreactive area per caudal DG (µm²)
1500
1000
500
0
WT
Q331K

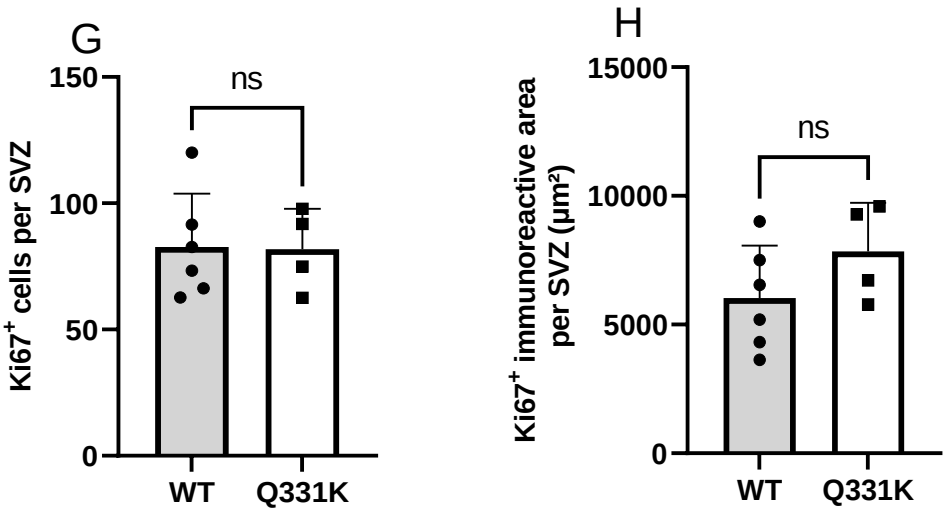

Figure 3.4 The area of Ki67+ cells increased in 6-month-old female TDP-43$^{Q331K+/Q331+}$ mice. IHC-DAB was performed for Ki67^{+} on hippocampal and SVZ sections from male TDP-43$^{Q331K+/Q331K+}$ and wild type mice. The number of Ki67^{+} cells were counted across the entire DG (A) immune positive cell area (B), Rostral DGs (C)(D), Caudal DGs (E), immuno positive cell area (F), SVZ (G)(H). The experiments comprised of 2 groups. Wild type mouse n=6, TDP-43$^{Q331K/Q331K}$ mice n=4. Comparison was conducted by student's unpaired t-test. ns = not significant, *P<0.05, **P<0.01. All data shown are mean ± SEM.

3.3.3 2-week-old female TDP-43$^{Q331K+/Q331K+}$ mice show no reduction in immature neurone numbers

To determine whether TDP-43$^{Q331K/Q331K}$ has an effect on neurogenesis in 2-week-old female mice, immature neurones were quantified in the hippocampal GCL. Brain tissue sections were stained for DCX using Nickel-DAB IHC and the number of DCX^{+} cells was counted. The data was analysed across the entire rostro-caudal extent of the hippocampus. However, both the rostral pole and caudal pole data were also calculated separately to determine the effect of the Q331K knock-in mutation on both poles.

Firstly, the analysis suggested that the average DCX^{+} cell number in wild-type mice was not significantly different from TDP-43$^{Q331K/Q331K}$ mice, shown in Figure 3.5, p=0.75. With regard to the average DCX^{+} immunostained cell area in each section, wild-type mice were not significantly different from TDP-43$^{Q331K/Q331K}$ mice, Figure 3.5B, p=0.84. The rostral pole of the hippocampus is associated with different functions compared to the caudal pole. For the rostral hippocampus, there was no significant change between the 2 groups in DCX^{+} cell number, p=0.82. Regarding the DCX^{+} cell immunoreactive area in the rostral hippocampus, similar results were observed as the two groups showed no significant differences, p=0.80. From the analysis, the causal sections' average DCX^{+} cells number is not significant compared to the other group, p=0.36. Similarly, the DCX^{+} immunoreactive cell area in the caudal hippocampus was not significantly different in the TDP-43$^{Q331K/Q331K}$ and wild-type mice, Figure3.5F p=0.71.

In addition to analysing the newborn immature neurones in the DG area, the SVZ was included for further exploration. With the same statistical analysis methods, for DCX^{+} cells average number, no significant difference was observed between 2 groups, shown as in Figure 3.5, p=0.67. With the comparison for DCX^{+} cells average area, wild-type mouse keeps up a no significant different result from TDP-43$^{Q331K/Q331K}$ mice, Figure 3.5H p=0.77.

Altogether, these results suggest that the TDP43^{Q331K} mutation may have no influence on AHN in 2-week-old female mice.

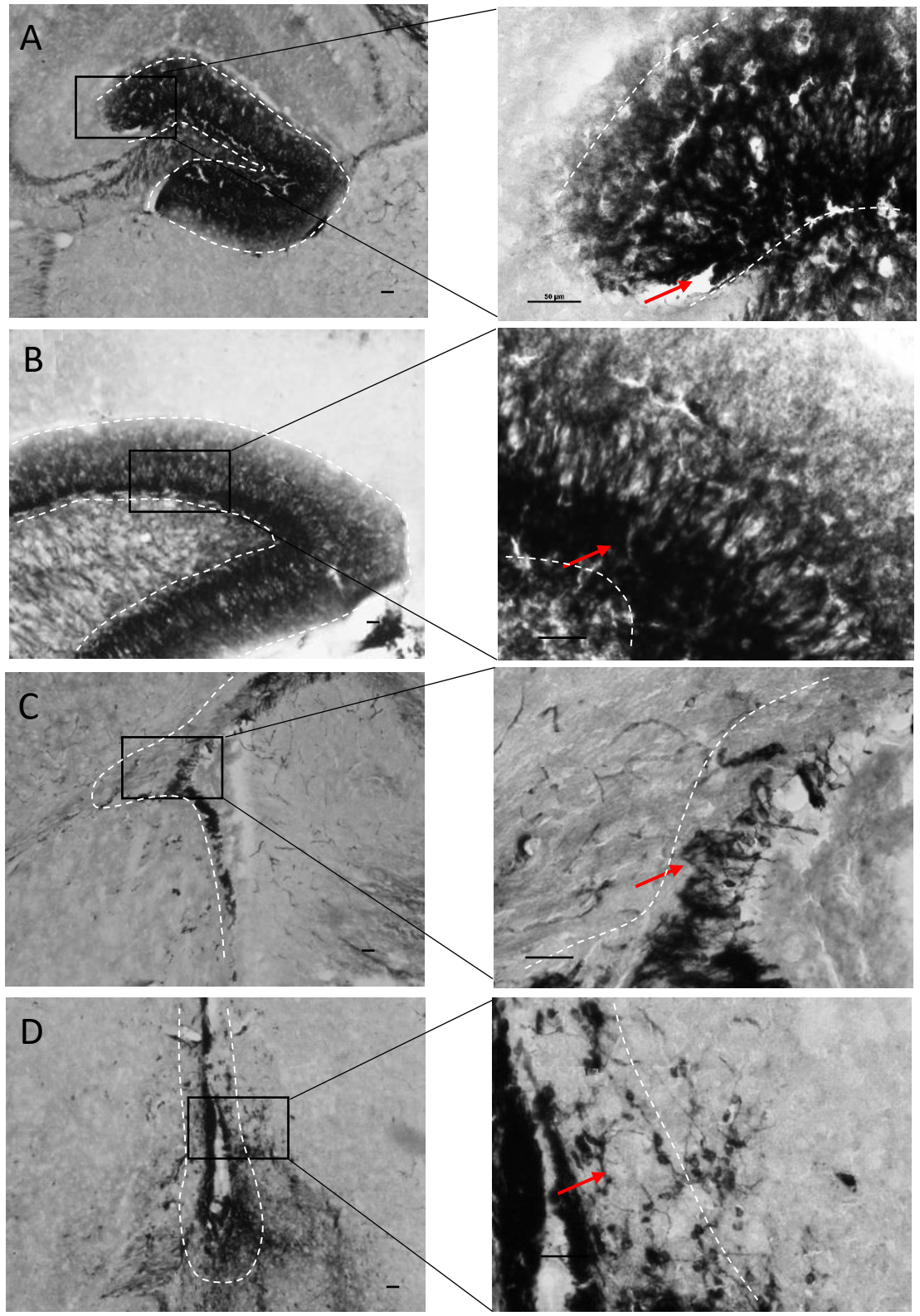

Figure 3.5 The expression of DCX^{+} cells in the hippocampus of 2-week-old female TDP-43$^{Q331K/Q331K}$ mice. IHC-DAB was carried out for DCX on hippocampal sections from TDP-43$^{Q331K+/Q331K+}$ and wild type mice. Above are example images of the DG region from TDP-43$^{Q331K+/Q331K+}$ (A), wild-type (B) mice, followed by example images of the SVZ region from TDP-43$^{Q331K+/Q331K+}$ (C) and wild-type (D) mice. Images were taken by 10X objective lens. Representative of positive immunolabelled cells is shown by the arrows. Scale

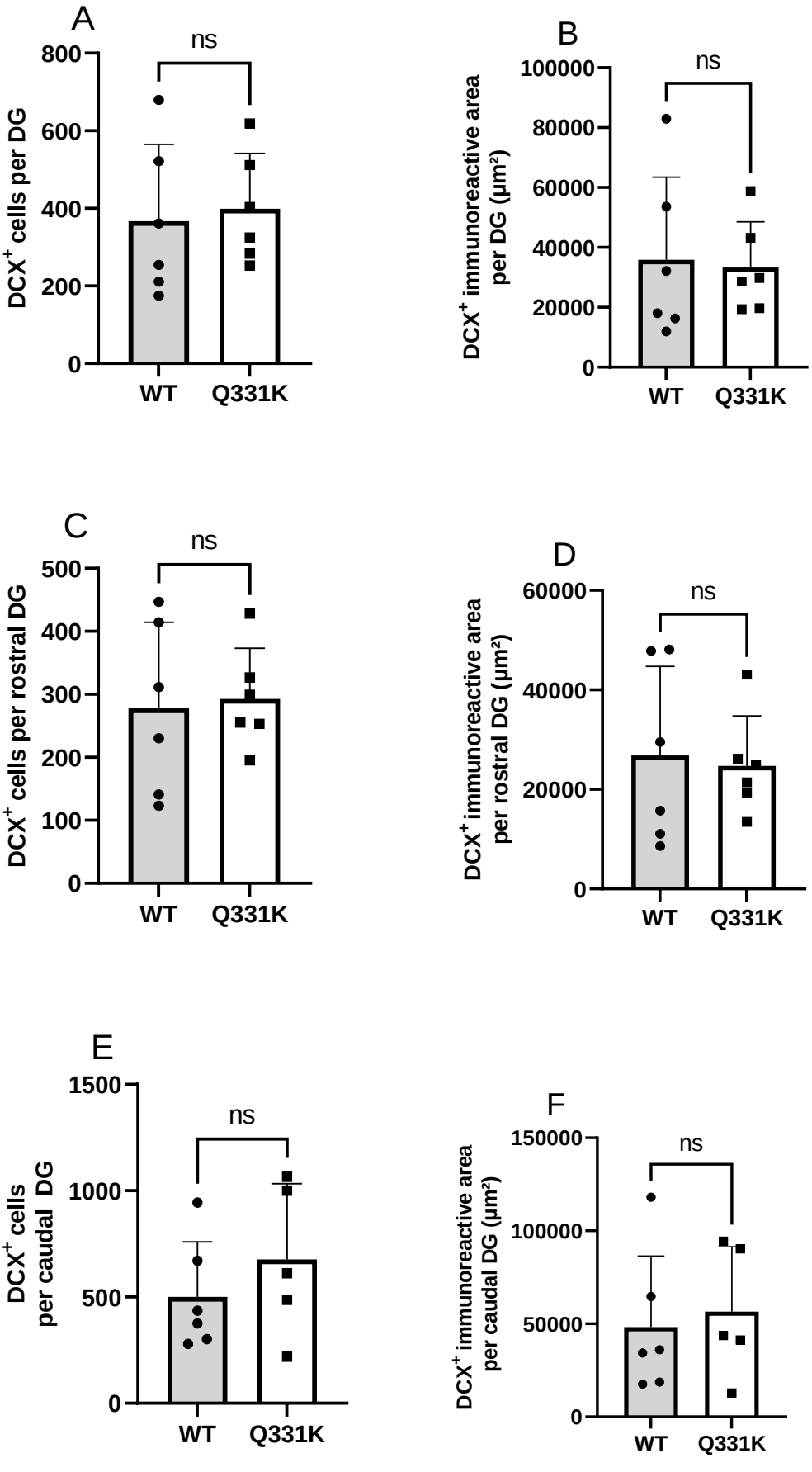
A
ns
800
600
400
200
0
DCX+ cells per DG
WT
Q331K
B
ns
100000
80000
60000
40000
20000
0
DCX+ immunoreactive area per DG (µm²)
WT
Q331K
C
ns
500
400
300
200
100
0
DCX+ cells per rostral DG
WT
Q331K
D
ns
60000
40000
20000
0
DCX+ immunoreactive area per rostral DG (µm²)
WT
Q331K
E
ns
1500
1000
500
0
DCX+ cells per caudal DG
WT
Q331K
F
ns
150000
100000
50000
0
DCX+ immunoreactive area per caudal DG (µm²)
WT
Q331K

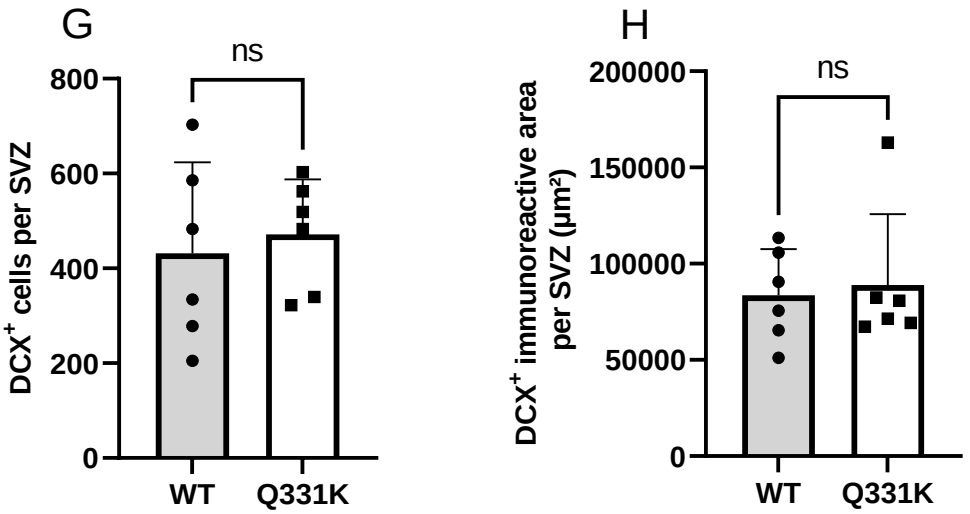

Figure 3.6 2-week-old female TDP-43$^{Q331K+/Q331K+}$ mice show no reduction in immature neurone number. IHC-DAB was carried out for DCX on hippocampal sections from female TDP-43$^{Q331K+/Q331K+}$ and wild type mice. The number of DCX$^+$ cells were counted in the entire DG (A), DCX$^+$ cell immunoreactive area (B), rostral pole (C)(D), caudal pole (E)(F), SVZ region (G)(H). The experiments comprised of 2 groups. n=6 in each group. Unpaired t-test, ns = not significant. All data shown are mean ± SEM.

3.3.4 Six-month-old TDP-43$^{Q331K/Q331K}$ female mice have significantly reduced numbers of immature neurones in the hippocampus.

To determine whether there were any differences in the number of new adult-born immature neurones in 6-month-old female TDP-43$^{Q331K/Q331K}$ mice, DCX IHC (see Figure 3.3) was used to quantify these cells as described in section 3.2.1. No significant differences were observed in the number of DCX^{+} cells present in the neurogenic niche of the DG between the wild-type group and the TDP-43$^{Q331K+/Q331K+}$ group (Figure 3.4A). There was also no significant change in the area covered by the DCX^{+} cells (Figure 3.4B). However, the number of DCX^{+} cells was significantly reduced in female TDP-43$^{Q331K+/Q331K+}$ mice when normalised to the total area of the DG (Figure 3.4C; p=0.0159). Interestingly, the number of DCX^{+} cells was reduced in the rostral pole of the DG but not the caudal pole, when expressed either as a total number of DCX^{+} cells per section (Figure 3.4D; p=0.0191; Mean±SEM: WT 7.803±9.087, Q331K 2.748±1.531) or as the area covered by the DCX cells (Figure 3.4E; p=0.18). There was also no significant difference in the number or the area of DCX^{+} cells in the SVZ (Figure 3.4H; p=0.28). Overall, the results suggest that in 6-month-old female TDP-43$^{Q331K+/Q331K+}$ mice, neurogenesis is specifically affected in the rostral pole of the DG.

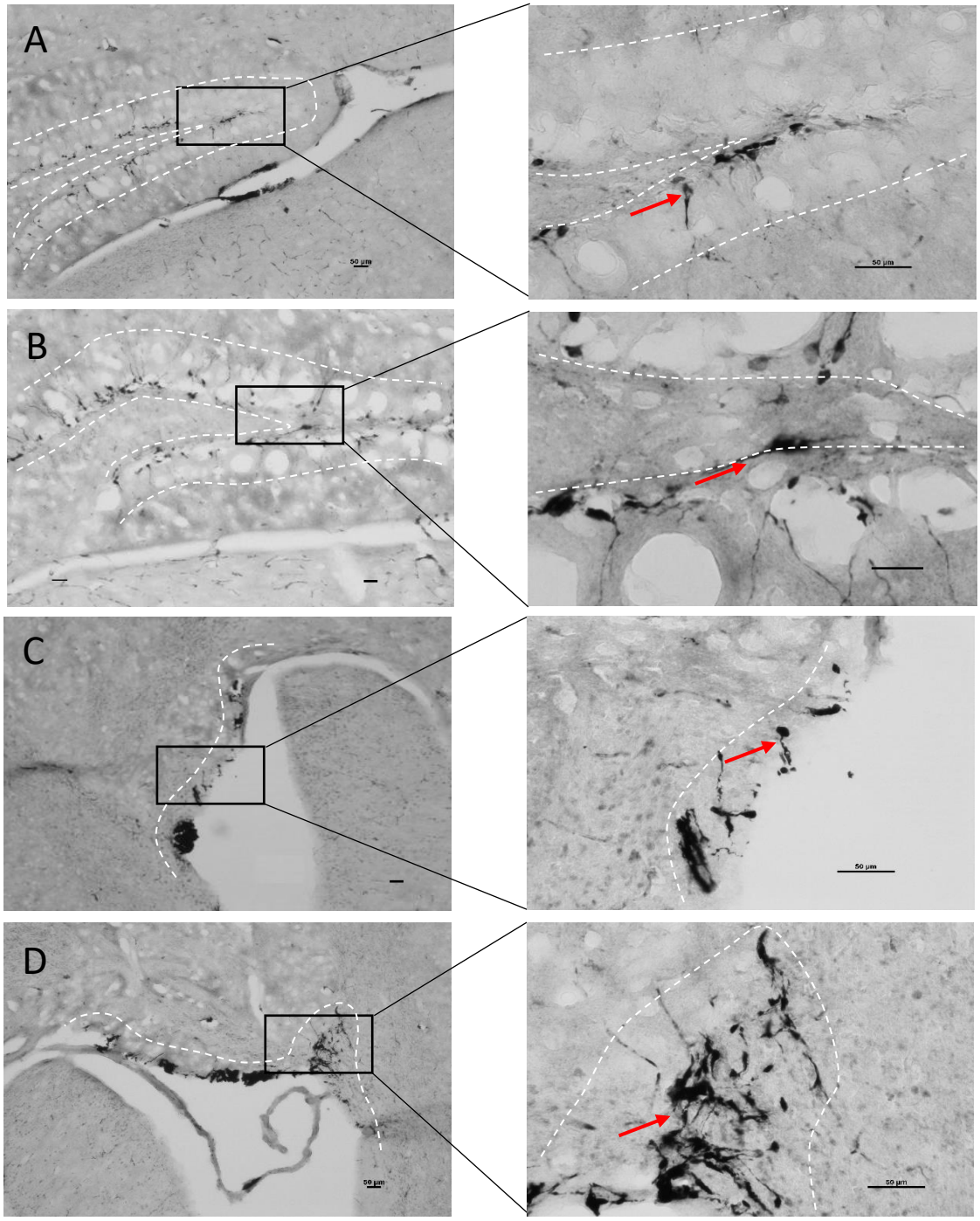

Figure 3.7 The expression of DCX^{+} cells in the hippocampus of 6-month-old female TDP-43$^{Q331K/Q331K}$ mice. IHC-DAB was carried out for DCX on hippocampal sections from female TDP-43$^{Q331K+/Q331K+}$ and wild type mice. Above are example images of the DG region from TDP-43$^{Q331K+/Q331K+}$ (A), wild-type (B) mice, followed by example images of the SVZ region from TDP-43$^{Q331K+/Q331K+}$ (C) and wild-type (D) mice. Images were taken by 10X objective lens. Representative of positive immunolabelled cells is shown by the arrow. Scale bar = 50µm.

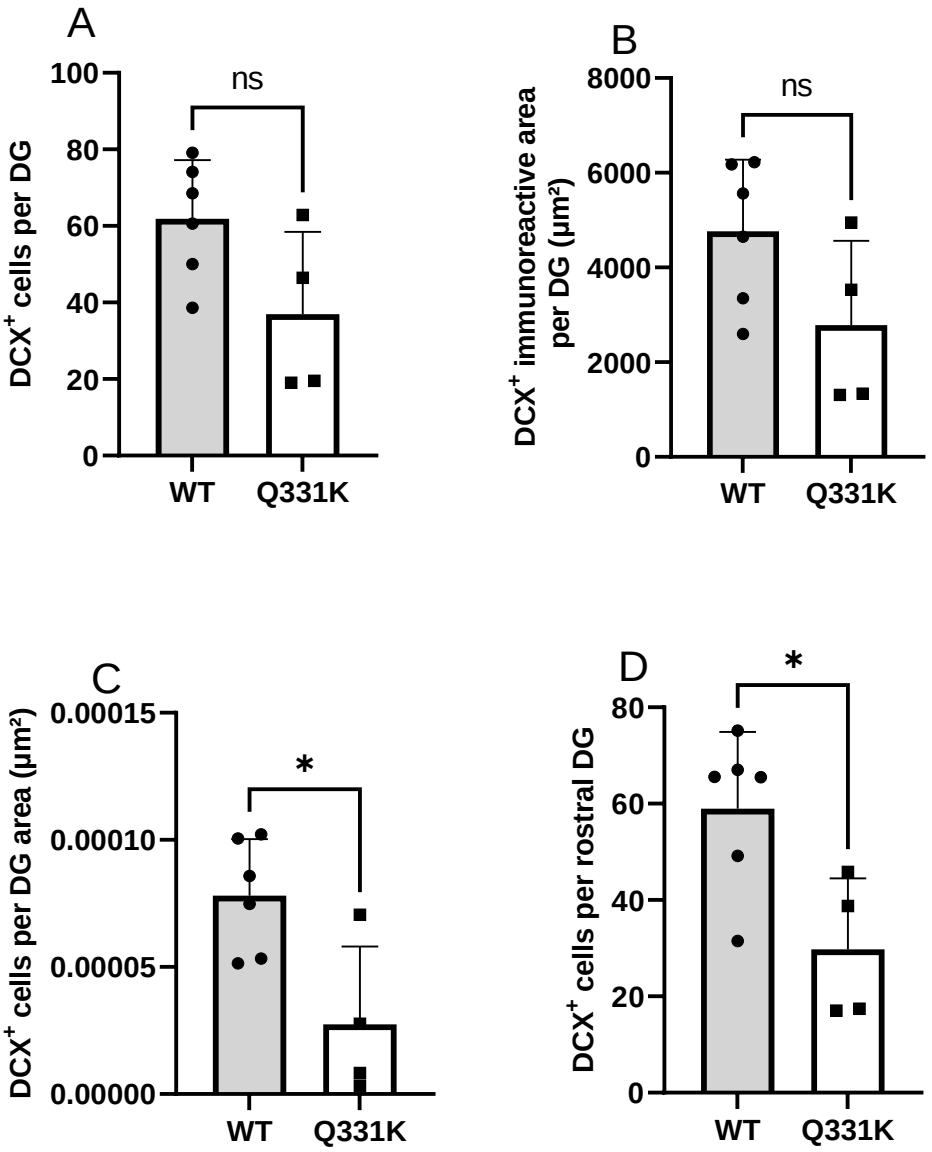
A
ns
100
80
60
40
20
0
DCX+ cells per DG
WT
Q331K
B
ns
8000
6000
4000
2000
0
DCX+ immunoreactive area per DG (µm²)
WT
Q331K
C
*
0.00015
0.00010
0.00005
0.00000
DCX+ cells per DG area (µm²)
WT
Q331K
D
*
80
60
40
20
0
DCX+ cells per rostral DG
WT
Q331K

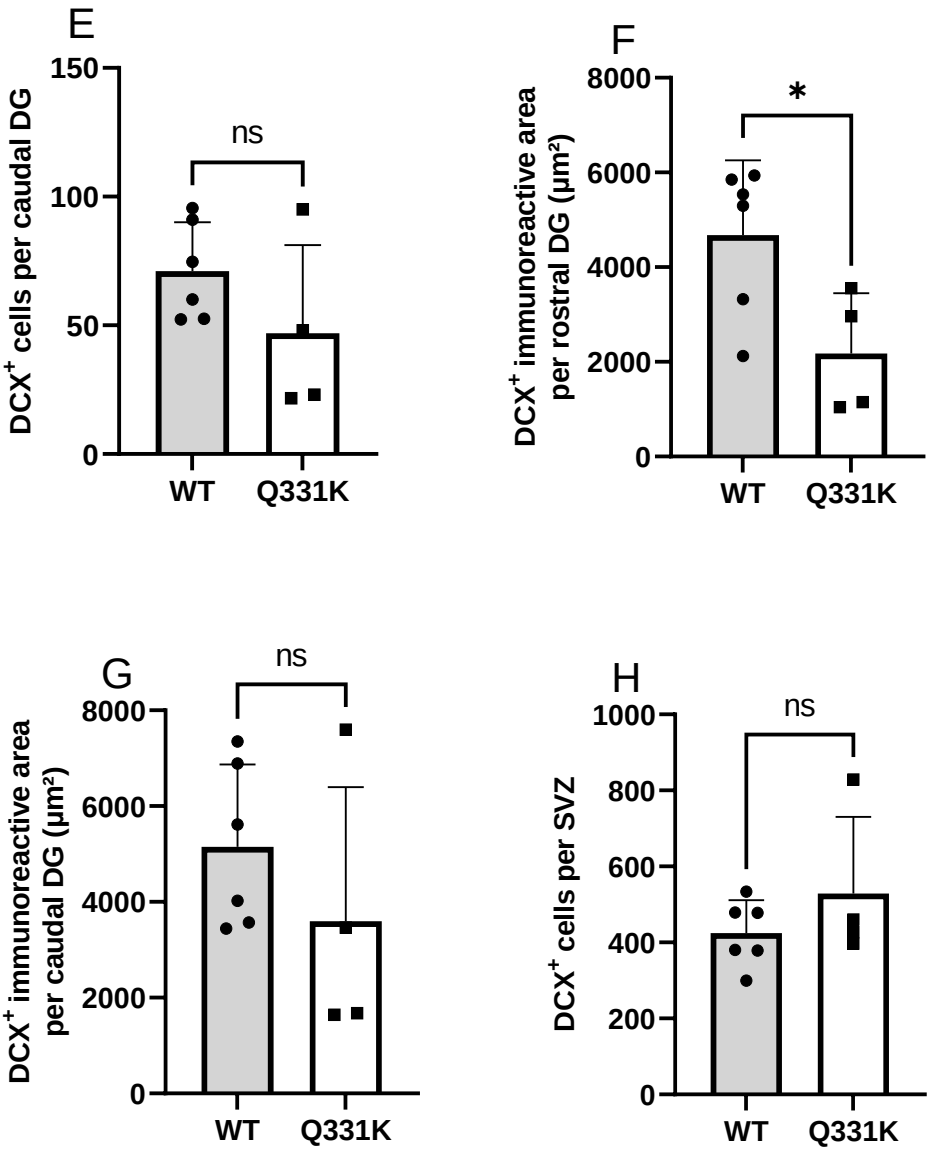

(Legend showed on next page due to content size)

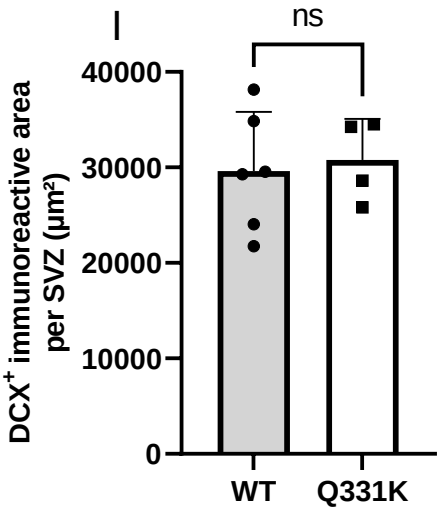

Figure 3.8 6-month-old female TDP-43$^{Q331K+/Q331K+}$ mice have a significantly reduced number of immature neurones in the DG. IHC-DAB for DCX^{+} cells was performed on DG sections from 6-month-old female wild type and TDP-43$^{Q331K+/Q331K+}$ mice. The number of DCX^{+} cells were counted per DG section (A), or DCX^{+} cells were normalised per DG section area (B), or the number of DCX^{+} cells were normalised per DG area (C). The number or area of DCX^{+} cells were also quantified in either the rostral (D, F) or caudal (E, G) DG sections. The number (H) or area (I) of DCX^{+} cells were also quantified in the SVZ. Wild type mice n=6, TDP-43$^{Q331K+/Q331K+}$ mice n=4. Statistical analysis was performed using Student's unpaired t-test (two tailed). ns = not significant, *P<0.05. All data shown are mean ± SEM.

3.3.5 Six-month-old TDP-43$^{Q331K/Q331K}$ male mice have significantly reduced numbers of immature neurones in the hippocampus.

To determine whether TDP-43$^{Q331K/Q331K}$ has an effect on neurogenesis, immature neurones were counted in the hippocampal GCL of male mice. Brain tissue sections were stained for DCX using Nickel-DAB IHC and the number of DCX^{+} cells was counted. The data was analysed across the entire rostro-caudal extent of the hippocampus. However, both the rostral pole and caudal pole data were also calculated separately to determine the effect of the Q331K knock-in mutation on both individual poles.

Firstly, the analysis suggested a significant decrease in the number of DCX^{+} cells per dentate gyrus in TDP-43$^{Q331K/Q331K}$ mice when compared with the wild-type mice (Figure 3.6 A, p=0.0335, Mean±SEM: WT 82.56±5.919, Q331K 48.24±4.08. Subsequent analysis of rostral pole and caudal pole sections demonstrated that there was a significant reduction in the number of DCX^{+} cells in TDP-43$^{Q331K/Q331K}$ mice in both poles of the hippocampus (Figure 3.6 B, rostral, p=0.0017, Mean±SEM: WT 80.5±3.037, Q331K 51.31±6.179) (Figure 3.6 C, caudal, p=0.0013, Mean±SEM: WT 92.78±9.009, Q331K 46.69±5.157).

When DCX^{+} cells were quantified in the SVZ, no significant differences were discovered between TDP-43$^{Q331K/Q331K}$ and wild-type mice (Figure 3.6 D, p=0.17).

In addition to analysing the number of DCX^{+} cells in the SVZ, I also investigated whether expressing the number of DCX^{+} cells as a percentage of the SVZ area had an impact on the result. The ImageJ polygon tool function was used to encircle the SVZ area before calculating the DCX^{+} cells as a percentage of the SVZ area. However, no differences were reported between TDP-43$^{Q331K/Q331K}$ and wild-type mice, as shown in Figure 3.6E, p=0.71. Altogether, these results suggest that neurogenesis may be impaired in the DG but not in the SVZ of male mice.

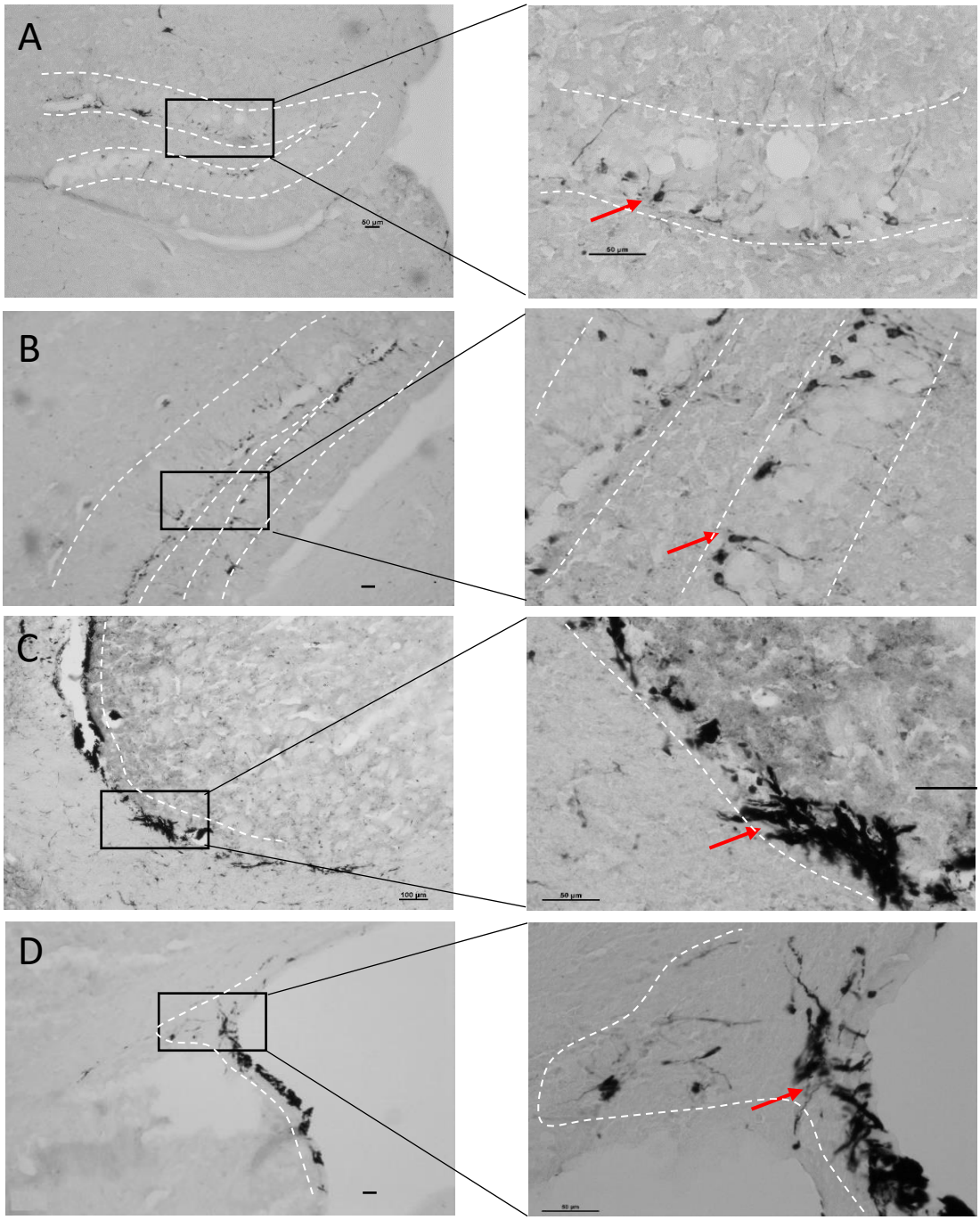

Figure 3.9 The expression of DCX^{+} cells in the hippocampus of 6-month-old male TDP-43$^{Q331K/Q331K}$ mice. IHC-DAB was performed for DCX on hippocampal sections from TDP-43$^{Q331K+/Q331K+}$ and wild type mice. Above are example images of the DG region from TDP-43$^{Q331K+/Q331K+}$ (A), wild-type (B) mice, followed by example images of the SVZ region from TDP-43$^{Q331K+/Q331K+}$ (C) and wild-type (D) mice. Images were taken by 10X objective lens. Representative of positive immunolabelled cells is shown by the arrow. Scale bar equals to 50µm.

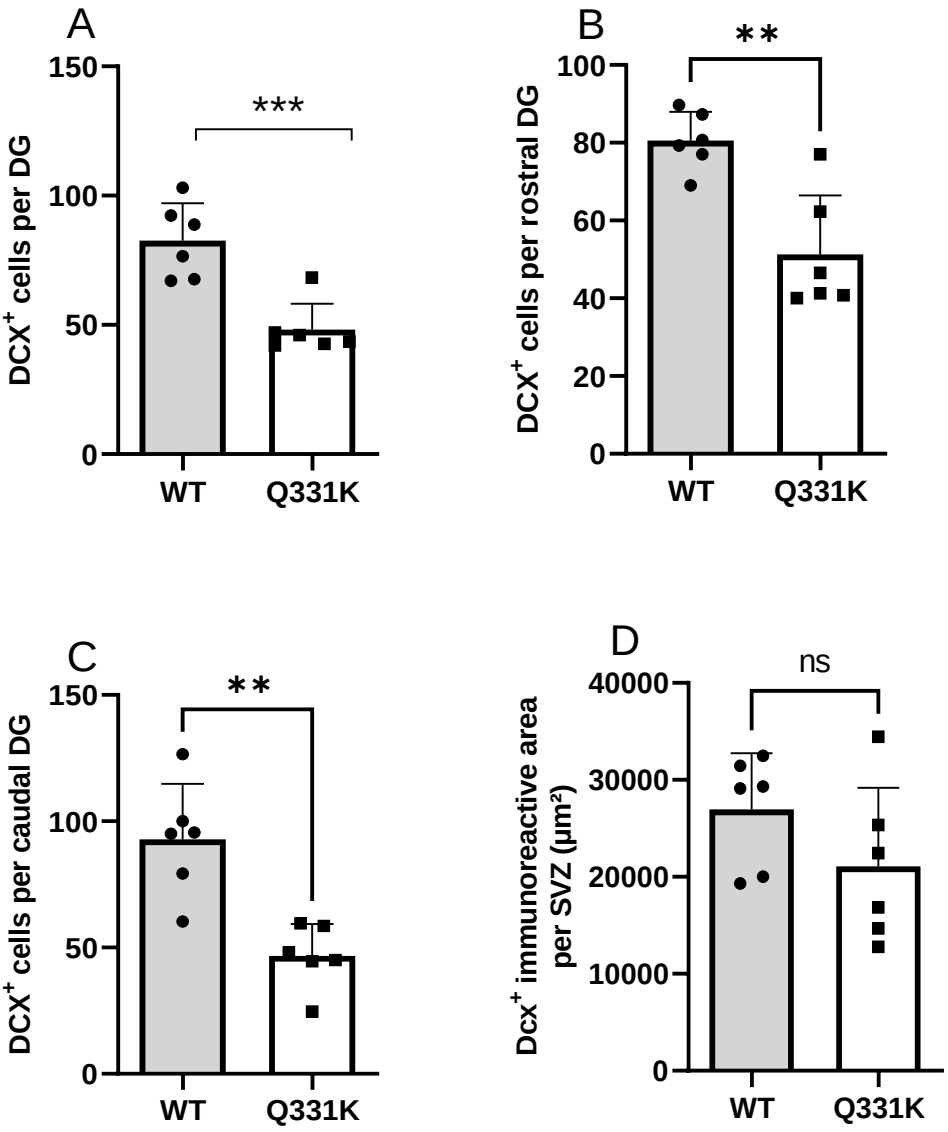

(Legend showed on next page due to content size)

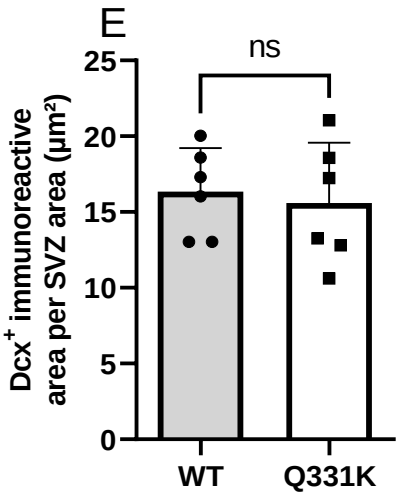

Figure 3.10 TDP-43$^{Q331K/Q331K}$ mice have significantly reduced numbers of immature neurones in 6-month-old males. IHC-DAB was carried out for DCX on hippocampal sections from maleTDP-43$^{Q331K+/Q331K+}$ and wild type mice. The number of DCX^{+} cells were counted in the entire DG (A), both rostral (B) and caudal (C) areas of the DG and the SVZ region (D). E represented the percentage of DCX^{+} versus the area of the SVZ. Each group n=6. Statistical analysis was carried out using a student's unpaired t-test. ns = not significant, *P<0.05, **P<0.01, ***P<0.001. All data shown are mean ± SEM.

3.3.6 Six-month-old TDP-43$^{Q331K/Q331K}$ mice have significantly reduced numbers of immature neurones in the hippocampus.

To determine whether TDP-43$^{Q331K/Q331K}$ has an effect on neurogenesis, immature neurones were counted in the hippocampal GCL of all the 6-month-old mice which includes both male and female mice. Brain tissue sections were stained for DCX using Nickel-DAB IHC and the number of DCX^{+} cells was counted. The data was analysed across the entire rostro-caudal extent of the hippocampus. Both the rostral pole and caudal pole data were also calculated separately to determine the effect of the Q331K knock-in mutation on both individual poles. IHC stain is shown above in Figure 3.7 and Figure 3.9.

Firstly, the analysis suggested a significant decrease in the number of DCX^{+} cells per dentate gyrus in TDP-43$^{Q331K/Q331K}$ mice when compared with the wild-type mice (Figure 3.13 A, p=0.0008, Mean±SEM: WT 72.20±5.159, Q331K 43.73±4.932). Subsequent analysis of rostral pole and caudal pole sections demonstrated that there was a significant reduction in the number of DCX^{+} cells in TDP-43$^{Q331K/Q331K}$ mice in both poles of the hippocampus (Figure 3.13 B, rostral, p=0.0014, Mean±SEM: WT 69.74±4.71, Q331K 42.68±5.691) (Figure 3.13 C, caudal, p=0.0015, Mean±SEM: WT 81.89±6.562, Q331K 46.78±6.929).

When DCX^{+} cells were quantified in the SVZ, no significant differences were discovered between TDP-43$^{Q331K/Q331K}$ and wild-type mice (Figure 3.13 D, p=0.88). With regard to the DCX^{+} immunoreactive area, no differences were reported between TDP-43$^{Q331K/Q331K}$ and wild-type mice, as shown in Figure 3.6E, p=0.28. Altogether, these results suggest that neurogenesis may be impaired in the DG but not in the SVZ of 6-month-old mice.

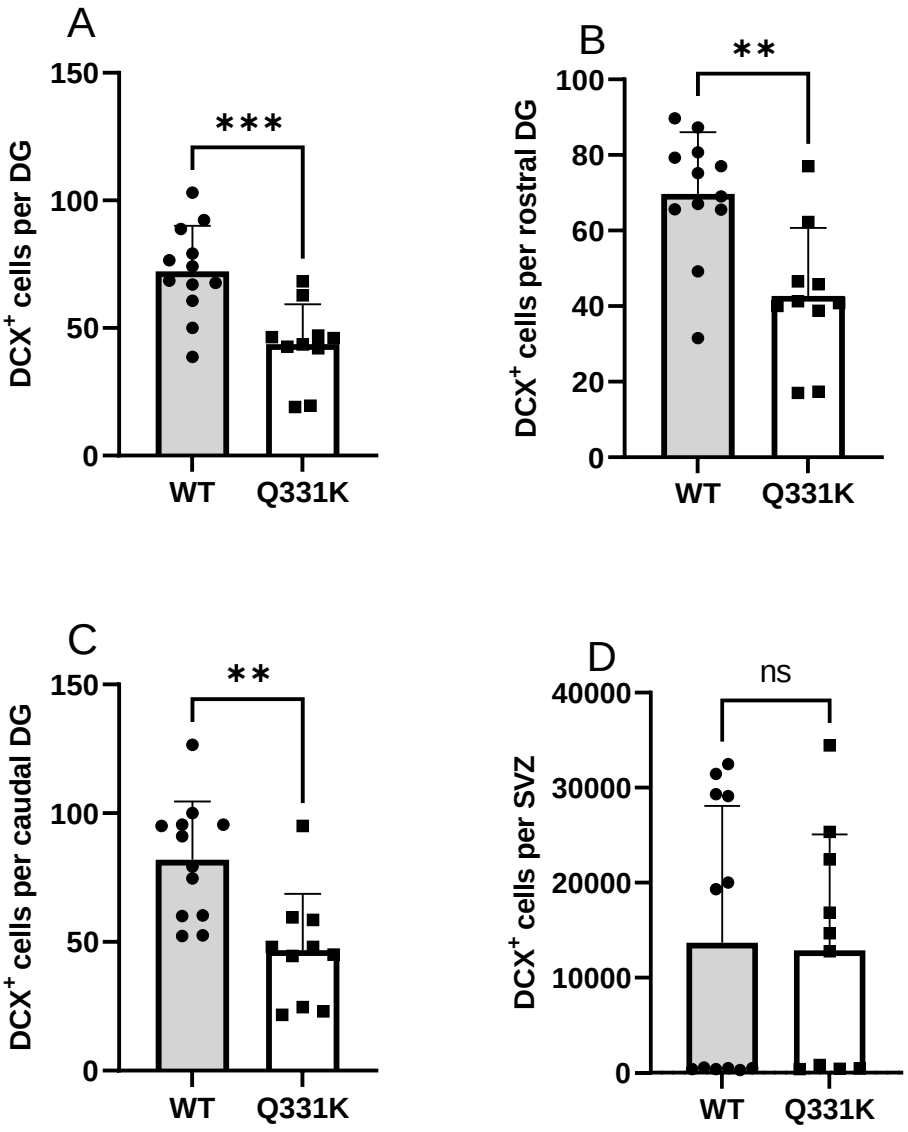

(Legend showed on next page due to content size)

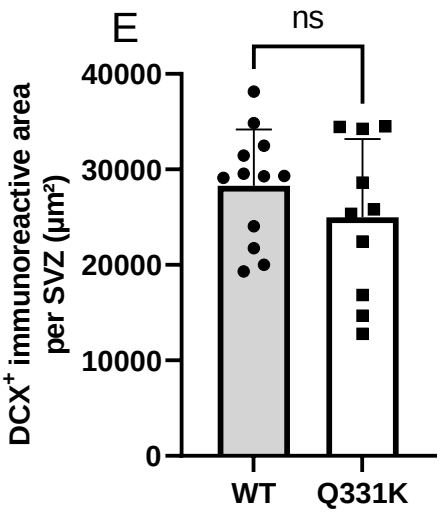

Figure 3.11 TDP-43$^{Q331K/Q331K}$ mice have significantly reduced numbers of immature neurones in DG in 6-month-old mice. IHC-DAB was carried out for DCX on hippocampal sections for TDP-43$^{Q331K+/Q331K+}$ and wild type mice. The number of DCX^{+} cells were counted in the entire DG (A), both rostral (B) and caudal (C) areas of the DG, the cell number in SVZ region (D) and immunoreactive area in SVZ (E). WT group n=6, TDP-43$^{Q331K+/Q331K+}$ group n=10. Statistical analysis was carried out using a student's unpaired t-test. ns = not significant, *P<0.05, **P<0.01, ***P<0.001. All data shown are mean ± SEM.

3.3.7 Twenty-four-month-old male TDP-43$^{Q331K/Q331K}$ mice do not have a significantly reduced number of immature neurones in the hippocampus.

As ageing plays an important role in several neurodegenerative diseases, I investigated the impact of age on neurogenesis in TDP-43$^{Q331K+/Q331K+}$ mice. IHC-DAB for DCX was used to label newborn immature neurones in 24-month-old TDP-43$^{Q331K+/Q331K+}$ mice and wild-type littermates.

The number of DCX^{+} cells was counted in DG and SVZ sections, however, there was no significant difference between wild type and the TDP-43$^{Q331K+/Q331K+}$mice in both DG and SVZ (Figure 3.8 A D, p=0.26).

No significant differences were found between wild-type and TDP-43$^{Q331K+/Q331K+}$ mice when the number of DCX^{+} cells was counted across the entire rostro-caudal axis of the hippocampus (Figure 3.8 A, p=0.26), in the rostral (Figure 3.8 B, p=0.08) or caudal DG (Figure 3.8 C, p=0.98), or in the SVZ when expressed either as the number of DCX^{+} cells (Figure 3.8 D, p=0.60) or area of DCX^{+} cells per section (Figure 3.8 E, p=0.73).

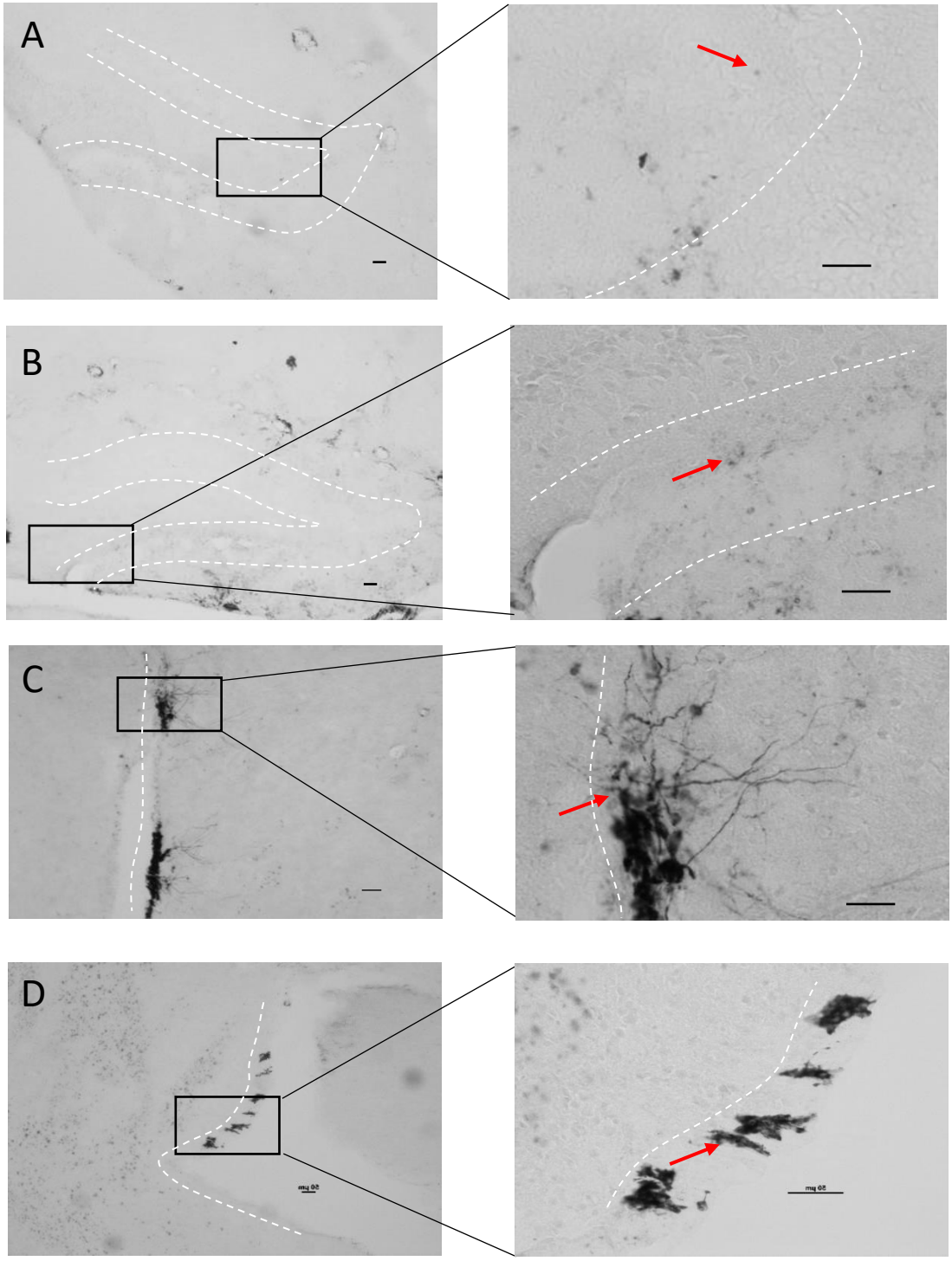

Figure 3.12 The expression of DCX^{+} cells in the hippocampus of 24-month-old male TDP-43$^{Q331K/Q331K}$ mice. IHC-DAB was performed for DCX on hippocampal sections from TDP-43$^{Q331K+/Q331K+}$ and wild type mice. Above are example images of the DG region from TDP-43$^{Q331K+/Q331K+}$ (A), wild-type (B) mice, followed by example images of the SVZ region from TDP-43$^{Q331K+/Q331K+}$ (C) and wild-type (D) mice. Images were taken by 10X objective lens. Representative of positive immunolabelled cells is shown by the arrows. Scale bar equals to 50µm.

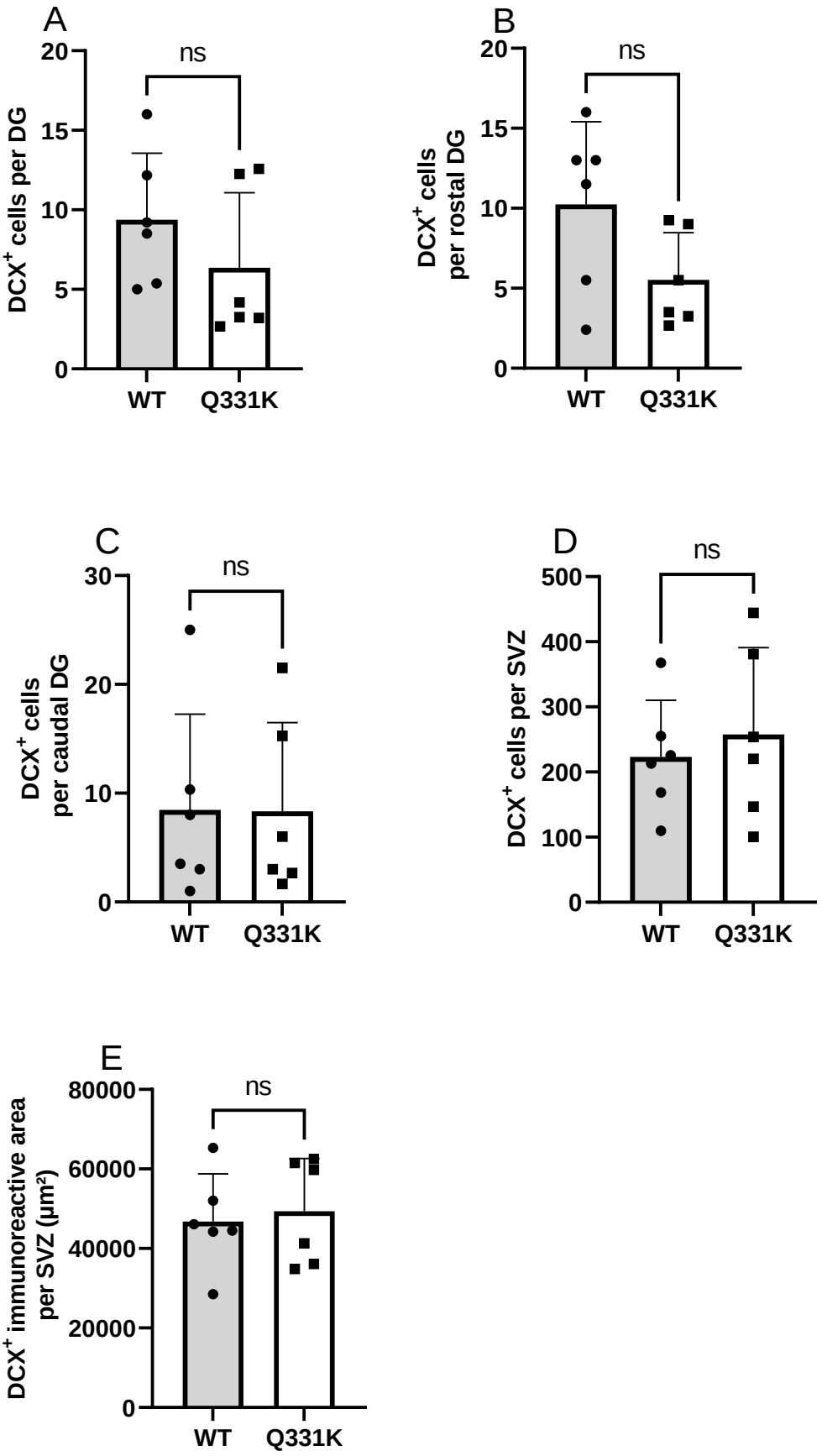

(Legend showed on next page due to size)

Figure 3.13 Twenty-four-month-old male TDP-43$^{Q331K/Q331K}$ mice do not have a significantly reduced number of immature neurones in the hippocampus. IHC-DAB was performed for DCX on hippocampal sections from male TDP-43$^{Q331K+/Q331K+}$ and wild type mice. The number of DCX^{+} cells were counted across the entire DG (A), rostral (B), caudal (C) poles and SVZ (D)(E). The experiments comprised of 2 groups. Each group n=6. Comparison was conducted by student's unpaired t-test. ns = not significant. All data shown are mean ± SEM.

3.3.8 The number of immature neurones decreases between 6 - 24 months in both TDP-43$^{Q331K+/Q331+}$ and wild-type male mice.

To identify the impact of ageing in TDP-43$^{Q331K+/Q331K+}$ and wild-type mice, the number of DCX^{+} cells was compared between the TDP-43$^{Q331K+/Q331K+}$ and wild-type mice at both 6 and 24 months of age. IHC images are shown in Figure 3.5, and Figure 3.7. For wild-type mice, the number of DCX^{+} cells per DG section significantly decreased in 24 months old male mice compared to 6-month-old male mice, (Figure 3.10 A, $p<0.0001$). Similarly, the age-related decrease in DCX^{+} cells was apparent in 24-month-old TDP-43$^{Q331K/Q331K}$ male mice compared to 6-month-old TDP-43$^{Q331K/Q331K}$ male mice ((Figure 3.10 A, $p<0.0001$). With regard to the SVZ, the same age-related decline in DCX^{+} cells were observed for both wild-type and TDP-43$^{Q331K/Q331K}$ mice (Figure 3.10 B, $p<0.0001$). Mean and SEM information can be found in the appendix.

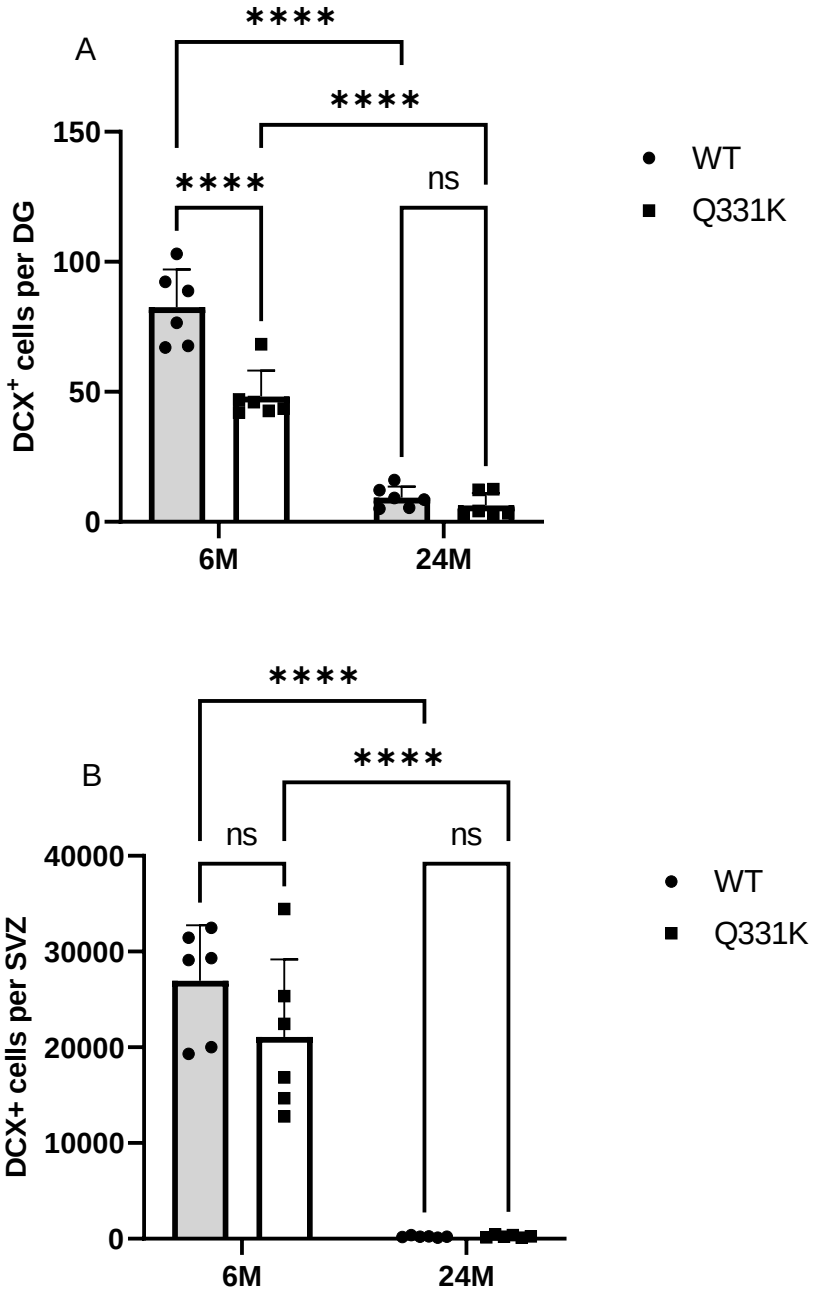

Figure 3.14 The number of immature DCX$^+$ neurones decrease between 6 - 24 months in both in TDP-43$^{Q331K+/Q331K+}$ and wild-type mice. IHC-DAB was performed for DCX on hippocampal sections from male TDP-43$^{Q331K+/Q331K+}$ and wild type mice. The number of DCX$^+$ cells were counted across the entire DG in TDP-43$^{Q331K+/Q331+}$ mice and wild-type mice (A), SVZ in TDP-43$^{Q331K+/Q331+}$ and wild-type mice (B). For statistical comparison, ordinary two-way ANOVA was performed, followed by Tukey's post hoc comparison. ***P<0.001 vs control. All graph shows as mean ± SEM. n=6 for each group.

3.3.9 Wild-type male mice generate more immature neurones in SVZ compared to females at 6 months of age.

To explore whether there were any differences in the number of immature neurones as a result of sex, all the data collected for 6-month-old male and female mice of both genotypes were compared. This will contribute to understanding gender differences in the formation of newborn immature neurones. At 6 months old, the number of DCX^+ cells in the DG of female mice shows no statistical difference in comparison to male mice in wild type group only (Figure 3.12 A). Whilst there was a significant reduction in the number of DCX^+ cells in the SVZ of female mice both in wild type and TDP43 $^{Q331K+/Q331K+}$ type (Figure 3.12 B, $p<0.0001$). The results suggest that female-related hormones may be having a negative effect on the generation of newborn neurons. Mean and SEM information can be found in the appendix.

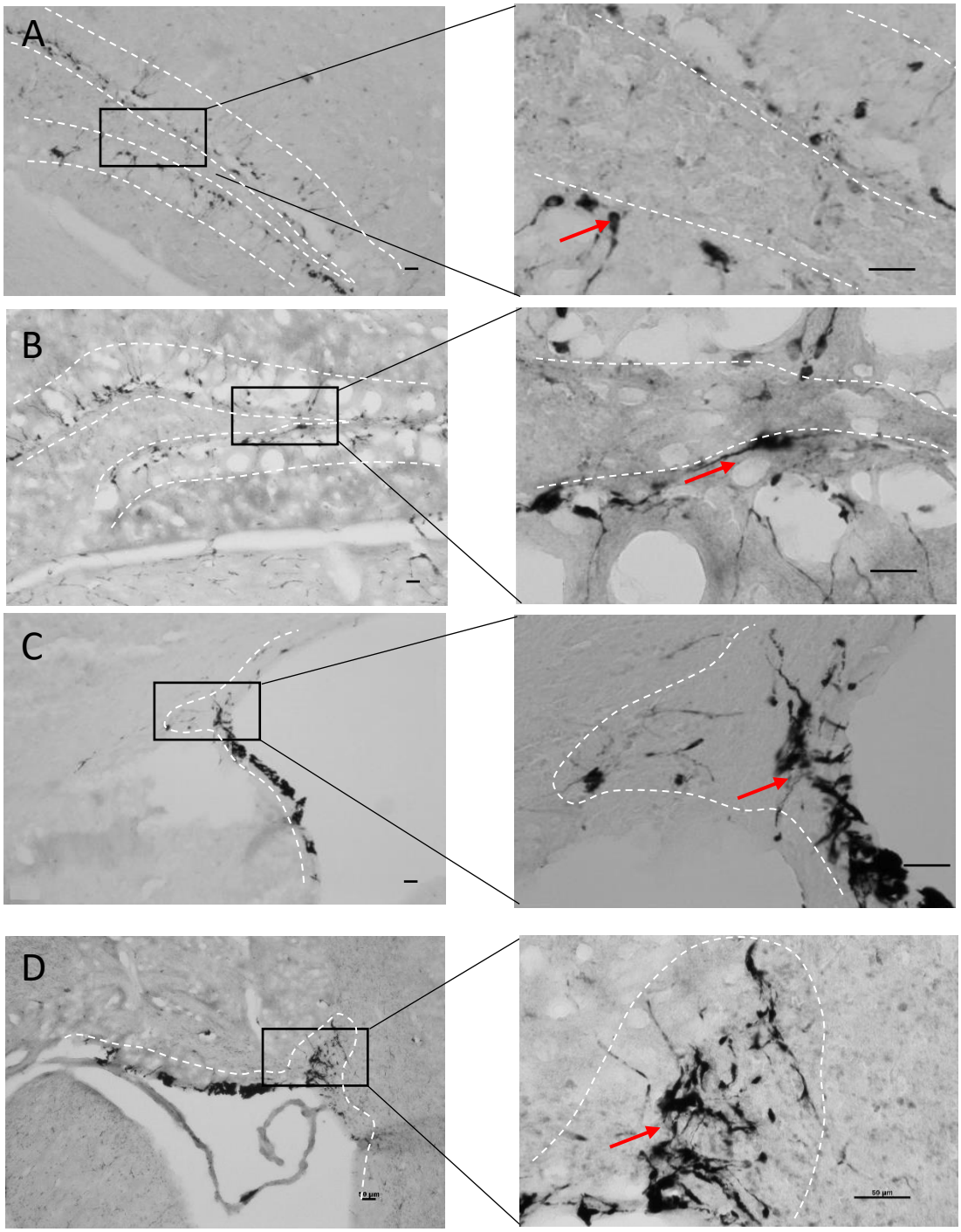

Figure 3.15 DCX^{+} cells in the hippocampus and SVZ of 6-month-old male and female TDP-43$^{Q331K/Q331K}$ and WT mice. IHC-DAB was performed for DCX on hippocampal and SVZ sections from TDP-43$^{Q331K+/Q331K+}$ and wild type mice of both sexes. Above are example images of the DG from TDP-43$^{Q331K+/Q331K+}$ (A), and wild-type (B) mice, followed by example images of the SVZ from TDP-43$^{Q331K+/Q331K+}$ (C) and wild-type (D) mice. Images were taken by 10X objective lens. Representative of positive immunolabelled cells is shown by the arrows. Scale bar equals to 50μm.

A

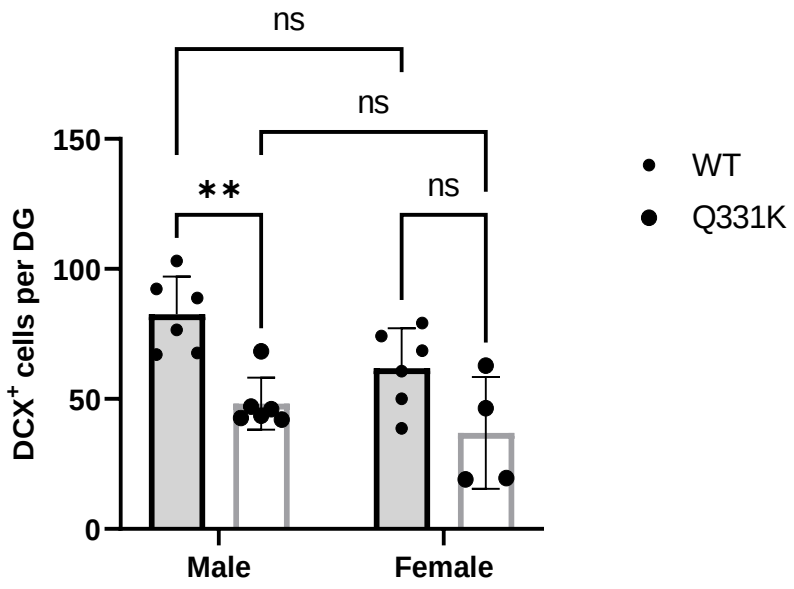
ns
ns
150
**
ns
100
50
0
DCX+ cells per DG
Male
Female
WT
Q331K

B

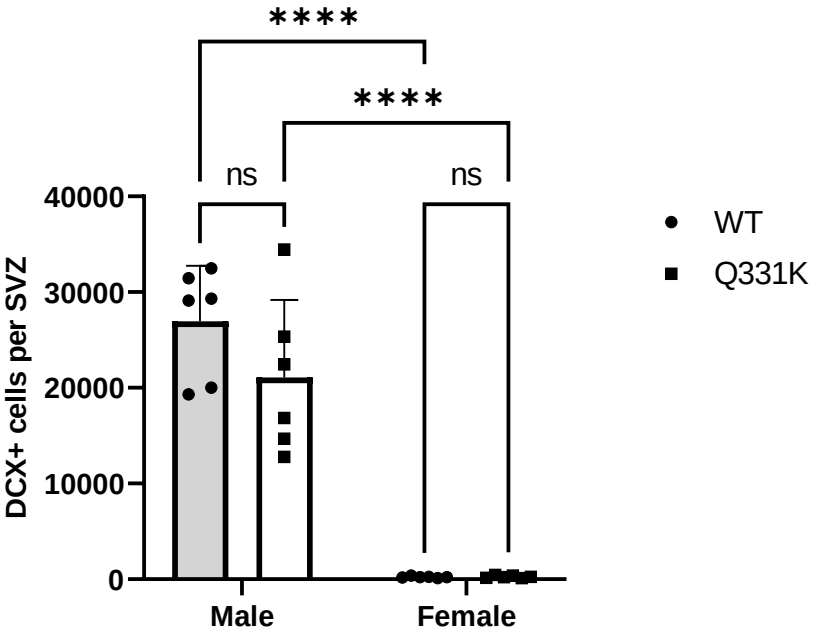
****
****
ns
ns
40000
30000
20000
10000
0
DCX+ cells per SVZ
Male
Female
WT
Q331K

Figure 3.16 Wild type male mice generate more immature neurones compared to females at 6 months of age. IHC-DAB was performed for DCX on hippocampal sections from male and female TDP-43$^{Q331K+/Q331K+}$ and wild type mice. Graphs show DCX+ counts in the DG of wild type and TDP-43$^{Q331K/Q331K}$ mice (A), and in SVZ of wild type and TDP-43$^{Q331K/Q331K}$ mice (B). TDP-43$^{Q331K/Q331K}$ male mice, n=6, female mice, n=4. Male mice each generic type, n=6. Comparison was conducted by ordinary two-way ANOVA, followed by Tukey's post hoc comparison. ns = not significant, *P<0.05, **P<0.01, ***P<0.001. All data shown are mean ± SEM.

3.3.10 DCX^+ cells from 6-month-old TDP-$43^{Q331K+/Q331K+}$ male mice show no difference in morphology in comparison to wild-type mice.

In the adult hippocampus, the early formation of dendrites can be observed during the post-mitotic stages. Dendrites on DCX^+ cells can be identified using the 40X magnifying lens based on the presence and the shape of the apical dendrites. They can be classified into 6 categories, Category A is cells with no visible process, with a round structure (Plümpe *et al.,* 2006). Category B contains cells with very small processes, the length of which are within the size of the cell, less than one nucleus-wide (< 10 µm). As the process length is small, the direction can be random. For Category C, cell processes are longer than Category B and greater than the width of the cell but have not reached the molecular layer. Conversely, the processes of Category D cells extend towards and reach the molecular layer. Category E and F cells both have processes that are longer than those of category D, and also include branches. Category E cells mainly have 1 branch or 1 strong process, while for Category F, cells will show at least 2 main processes and several branches. Based on the length of the process, Category A and B cells represent very young immature neurones, while Category E and F cells are more similar in structure to mature neurones. With regard to Categories C and D cells - they are more mature than A and B, but less mature than E and F (Plümpe *et al.*, 2006).

Next, I assessed the effect of the TDP-$43^{Q331K+/Q331K+}$ mutation on the development of immature neurones (Figure 3.19), by analysing the morphology of DCX^+ cells from 6-month-old male mice. In the DG, DCX^+ cells were counted and grouped into different categories as previously described by Plumpe et al 2006. For wild-type mice, most of the DCX^+ cells (37%) were in category B, followed by category A (19%) and E (18%). 10% of the DCX^+ cells were in either category C or F whilst 6% were in category D. Similarly, in TDP-$43^{Q331K+/Q331K+}$ mice, 44% of the DCX^+ cells were in category B, 22% were in category A, 12% and 11% in categories E and C respectively, followed by 6% and 5% in categories D and F, respectively. Statistical analysis showed that the groups were not significantly different (analysed by 2-way ANOVA). Next, the morphology of the DCX^+ cells was compared in the caudal and rostral regions of the DG. This was followed by the analysis of the suprapyramidal and

infrapyramidal blades of the entire DG and within the caudal and rostral poles (Figure 3.20). These analyses report no significant differences, apart from a significant increase observed in the number of category B DCX^{+} cells in the rostral infrapyramidal blade of TDP-$43^{Q331K+/Q331K+}$ mice (Figure 3.20 G, p=0.0256, Mean 3.564 / 5.128). These results suggest that the TDP-$43^{Q331K+/Q331K+}$ mutation does not alter the gross morphology of DCX cells, but it may do so in specific cell subpopulations within the neurogenic niche.

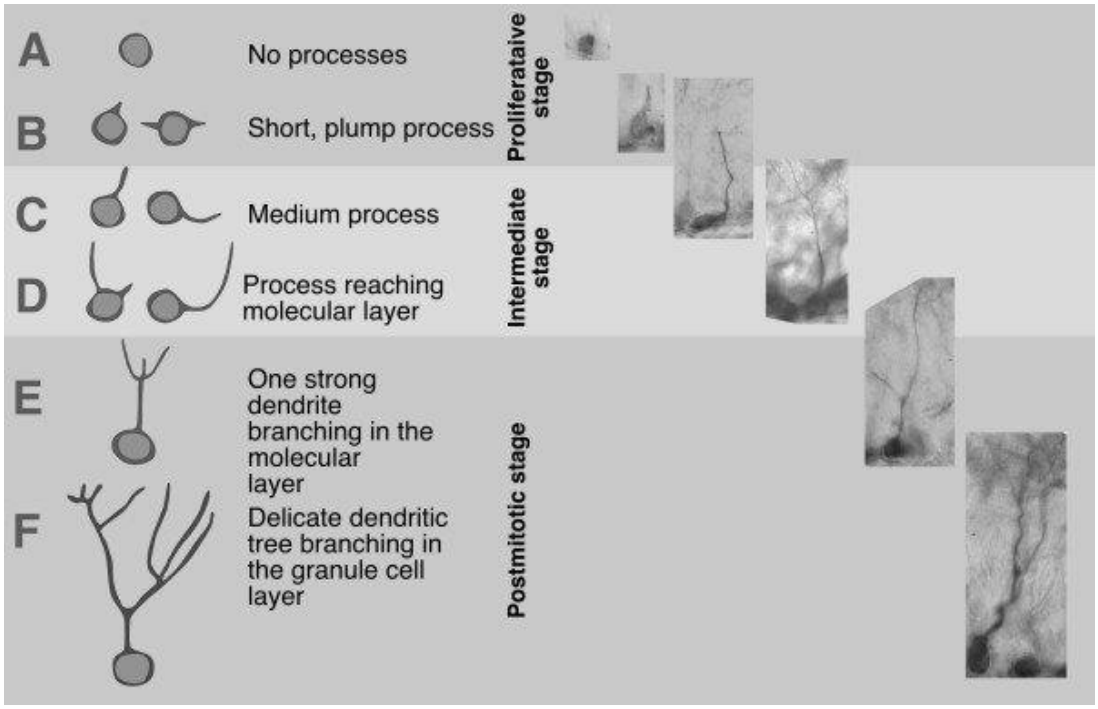

Figure 3.17 Categories of the different morphologies of DCX$^+$ neurones according to their developmental stage. Adapted from (Plümpe *et al.*, 2006).

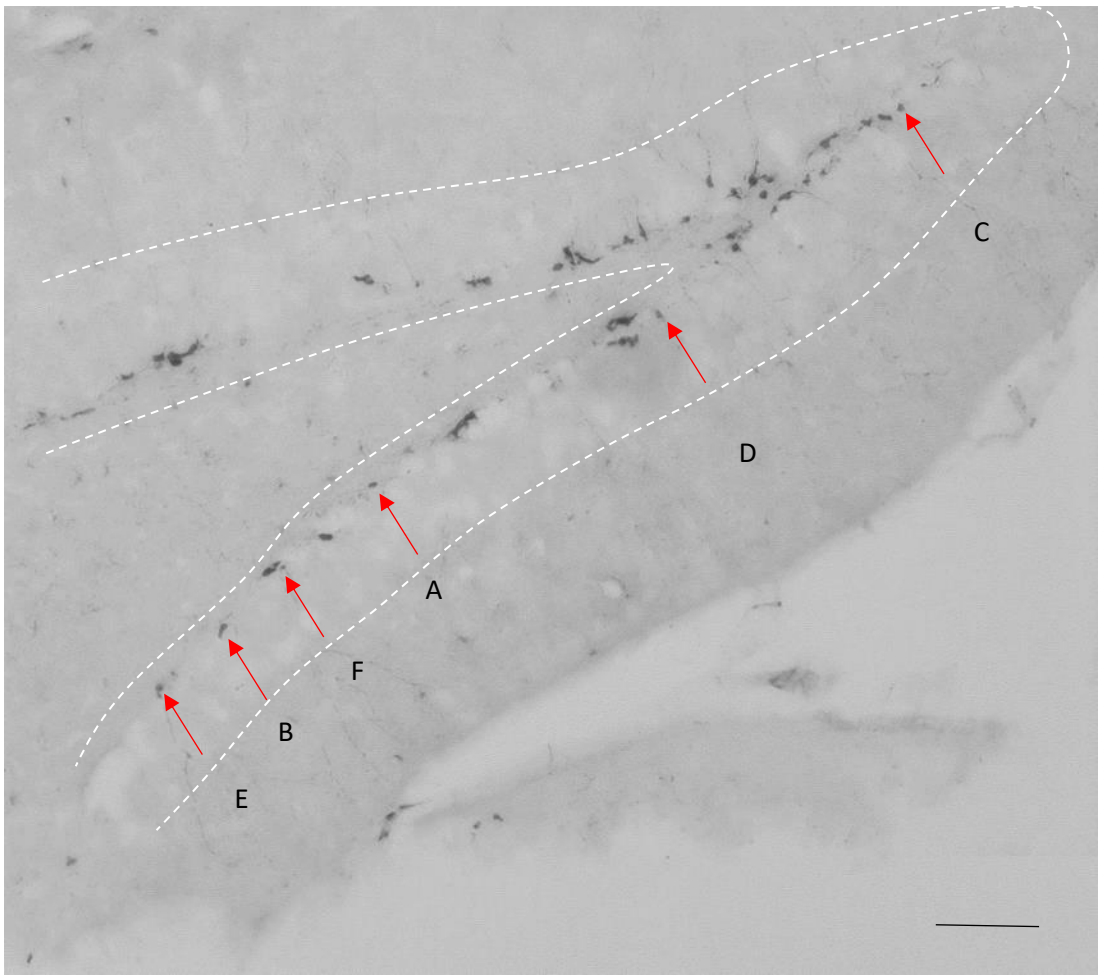

Figure 3.18 Analysis of DCX$^+$ cell morphology in the DG of six-month-old male TDP-43 $^{Q331K+/ Q331K+}$ and wild type mice. IHC-DAB for DCX was performed on hippocampal sections from TDP-43 $^{Q331K+/ Q331K+}$ and wild type mice. The morphology of the DCX$^+$ cells was assessed according to (Plümpe *et al.*, 2006). Image shows a hippocampal DG taken by 10X objective lens. The arrows indicate a representative of each morphology type from A to F. Scale bar equals to 100μm.

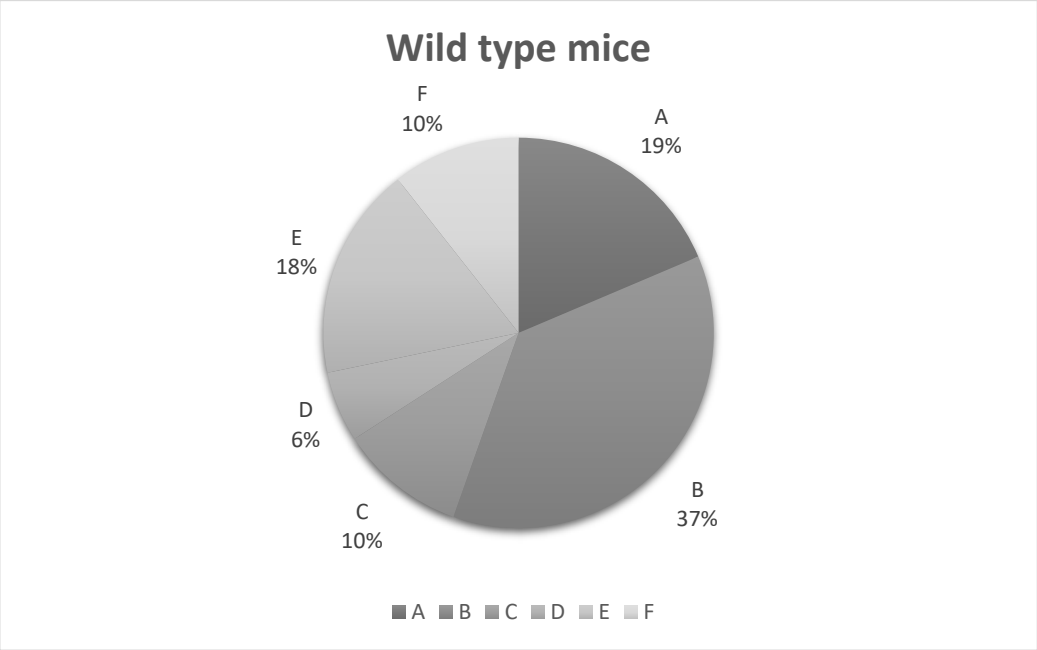

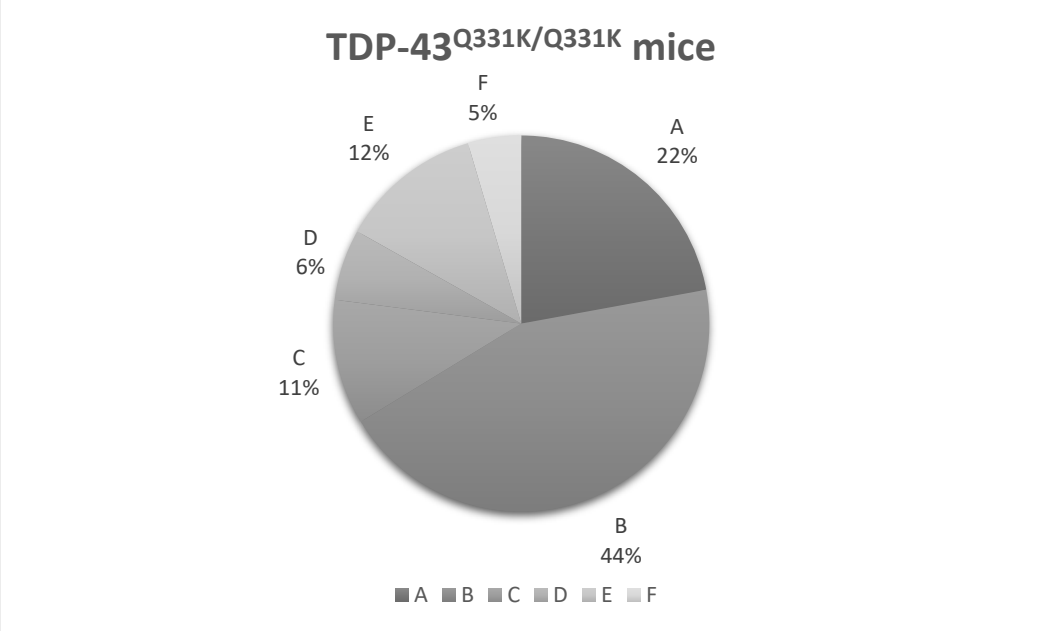

Figure 3.19 The distribution of the morphologies of DCX$^+$ cells in 6-month-old male TDP-43$^{Q331K+/Q331K+}$ and the wild type mice. The pie charts show the distribution of neurones according to their morphology, expressed as a population of the total number of DCX$^+$ cells. n=6 in each group.

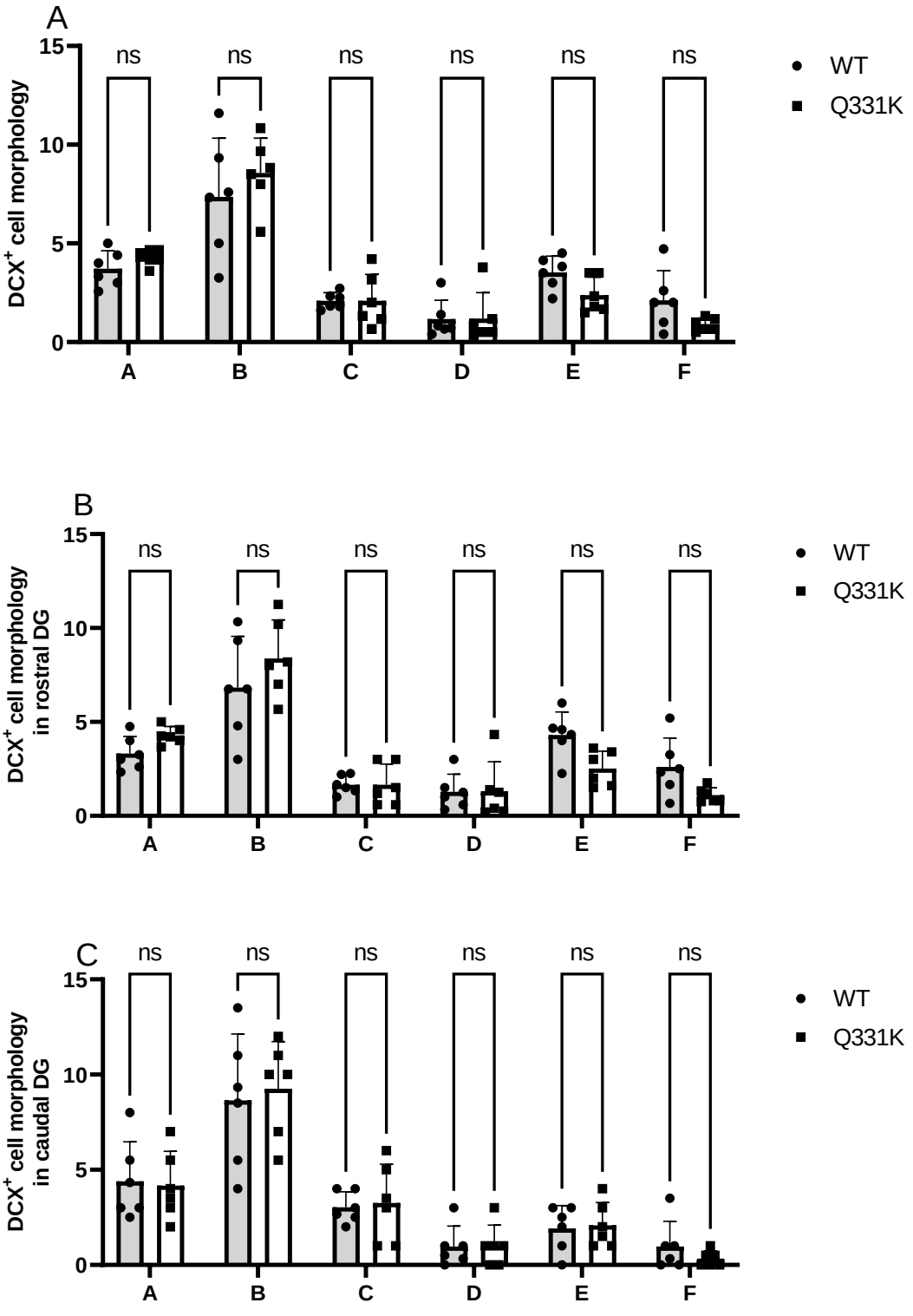

(Legend showed on next page due to content size)

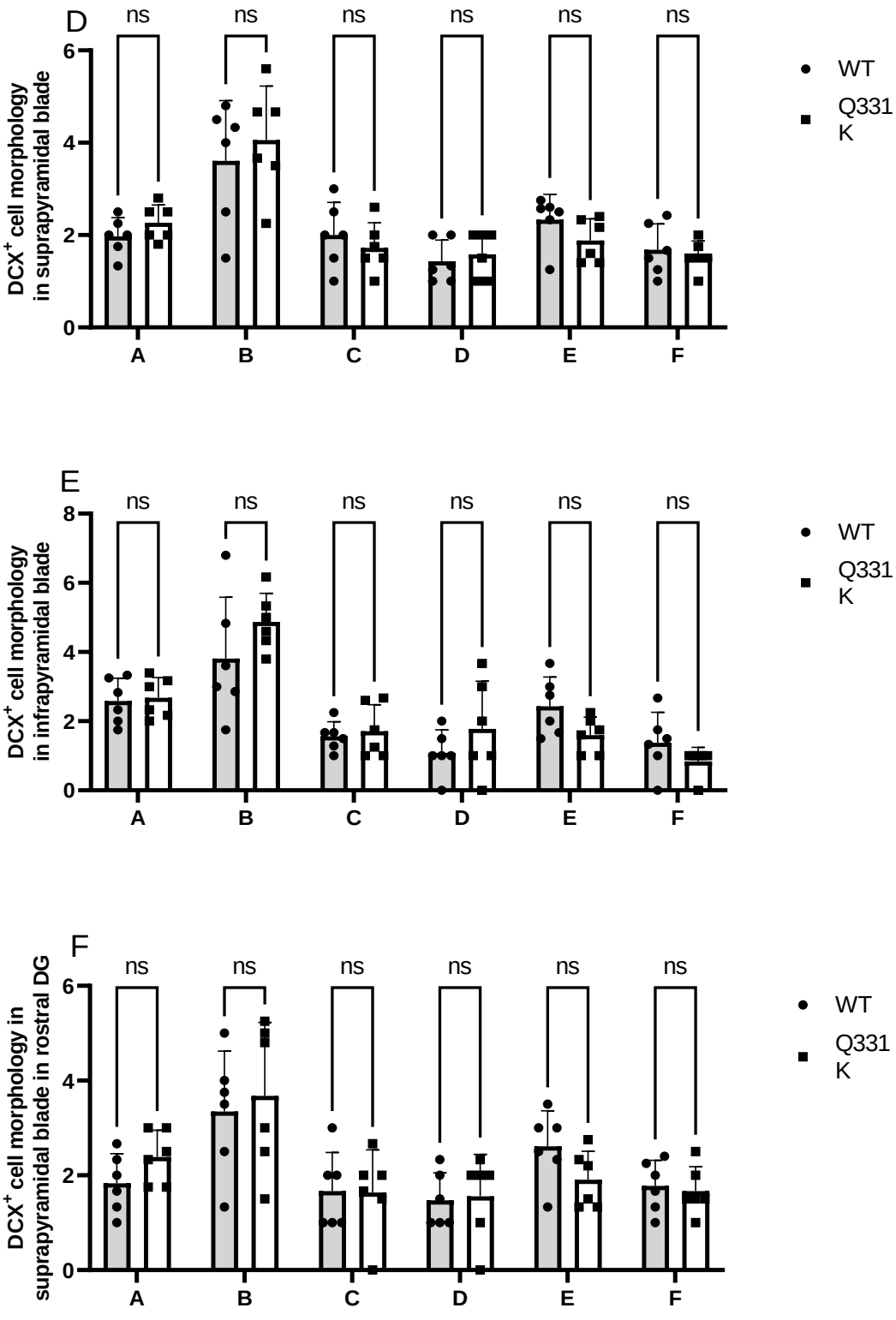

(Legend showed on next page due to content size)

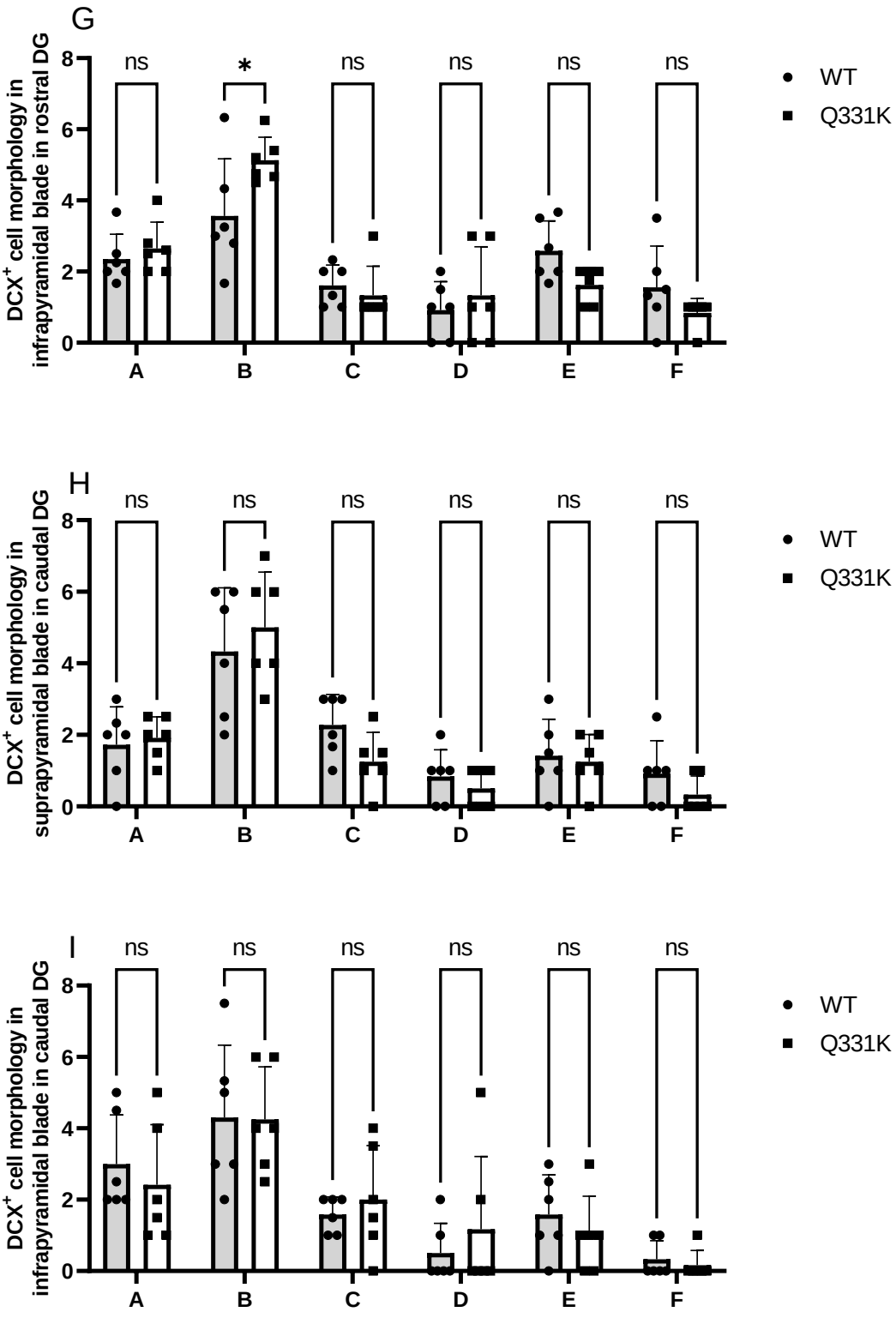

(Legend showed on next page due to content size)

Figure 3.20 6-month-old male TDP-43$^{Q331K+/Q331K+}$ mice show no difference in the morphology of their DCX^{+} cells in comparison to wild-type mice. The DCX^{+} cells were assessed and distributed according to their morphology as previously described by Plumpe et al 2006. The number of DCX^{+} cells in each morphological category was counted in the DG (A), rostral DG (B), caudal DG (C), suprapyramidal (D), infrapyramidal (E), rostral suprapyramidal (F), rostral infrapyramidal (G), caudal suprapyramidal (H), caudal infrapyramidal (I). n=6. Comparison was conducted by ordinary tow-way ANOVA, followed by Tukey's post hoc comparison. ns = not significant, *P<0.05. All data shown are mean ± SEM.

3.3.11 The TDP-43$^{Q331K+/\ Q331K+}$ mutation affects the morphology of the DCX^{+} cells in 6-month-old female mice.

Next, the morphology of DCX^{+} cells was assessed in 6-month-old female TDP-43$^{Q331K+/\ Q331K+}$ and wild-type mice. The distribution of DCX^{+} cells by distinct morphologies was performed as above and according to Plumpe et al 2006. For wild-type mice, 36% of cells were category B, 17% of cells were category A, 17% were category E, 14% were category C and 12% were category D. Only 4% of the cells were category F. For the TDP-43$^{Q331K/Q331K}$ mice, 50% of cells were category B, 18% of cells were category C, 14% were category A, 14% were category C, whilst the other 7%, 6% and 5% were in categories E, D and F, respectively (Figure 3.22). Analysis of the data using a 2-way ANOVA reported a significant increase in the number of cells in category B across the entire DG (Fig 3.23 A, $p<0.0001$, Mean: WT 7.173, Q331K 9.937), rostral DG (Fig 3.23 B, $p=0.0028$, Mean: WT 6.586, Q331K 9.171), caudal DG (Fig 3.23 C, $p= 0.0188$, Mean: WT 8.444, Q331K 11.08), for the entire DG, suprapyramidal blade (Fig 3.23 D, $p= 0.0117$, Mean: WT 3.449, Q331K 4.939), infrapyramidal blade (Fig 3.23 E, $p= 0.0326$, Mean: WT 3.995, Q331K 4.999). Combined, these data suggest that the TDP-43$^{Q331K+/\ Q331K+}$ mutation may increase the number of category B cells compared to WT mice.

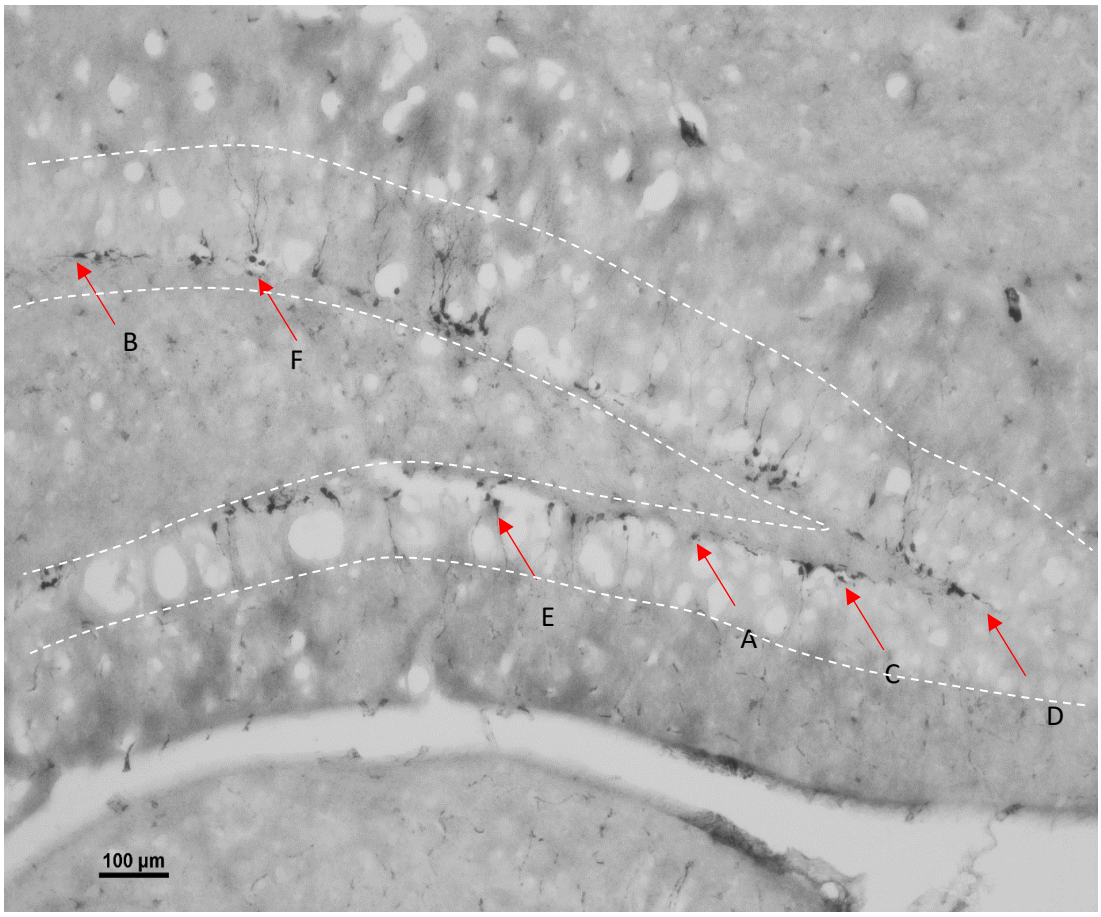

Figure 3.21 The analysis of DCX^{+} cell morphology in the DG. IHC-DAB for DCX was performed on hippocampal sections from TDP-43$^{Q331K+/\ Q331K+}$ and wild type mice. The morphology of the DCX^{+} cells was quantified according to Plumpe et al 2006. The representative image shows a hippocampal DG collected using a 10X objective lens. The arrows indicate a representative of each morphological types from A to F. Scale bar equals to 100µm.

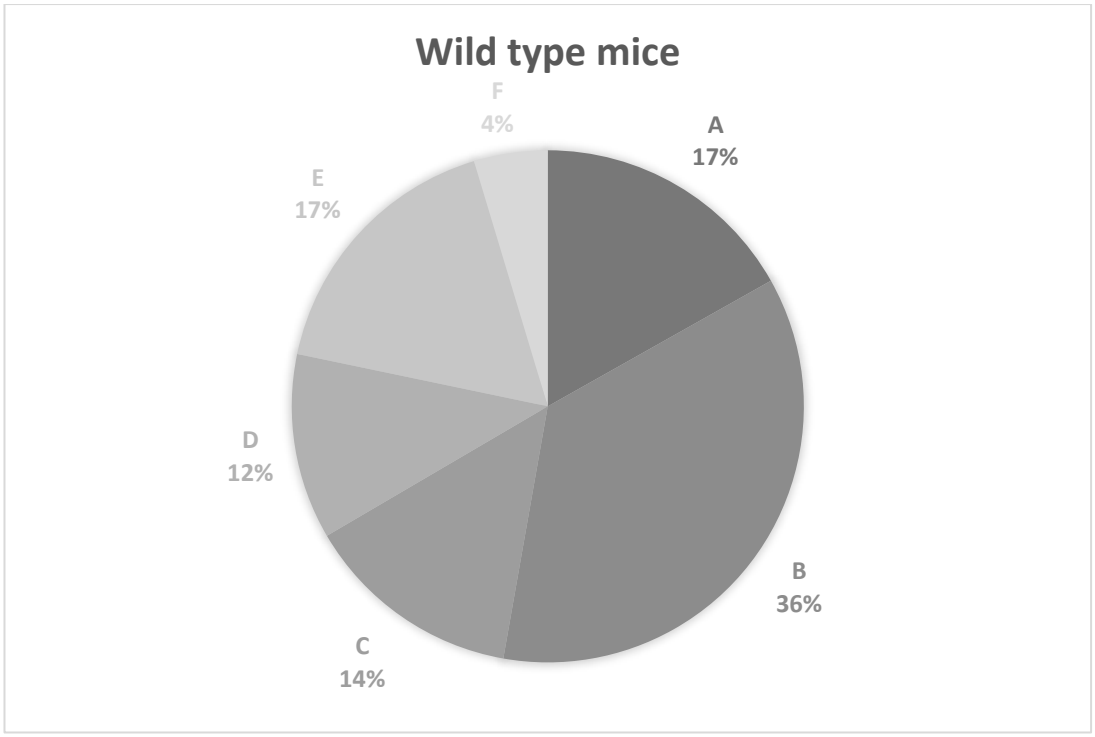

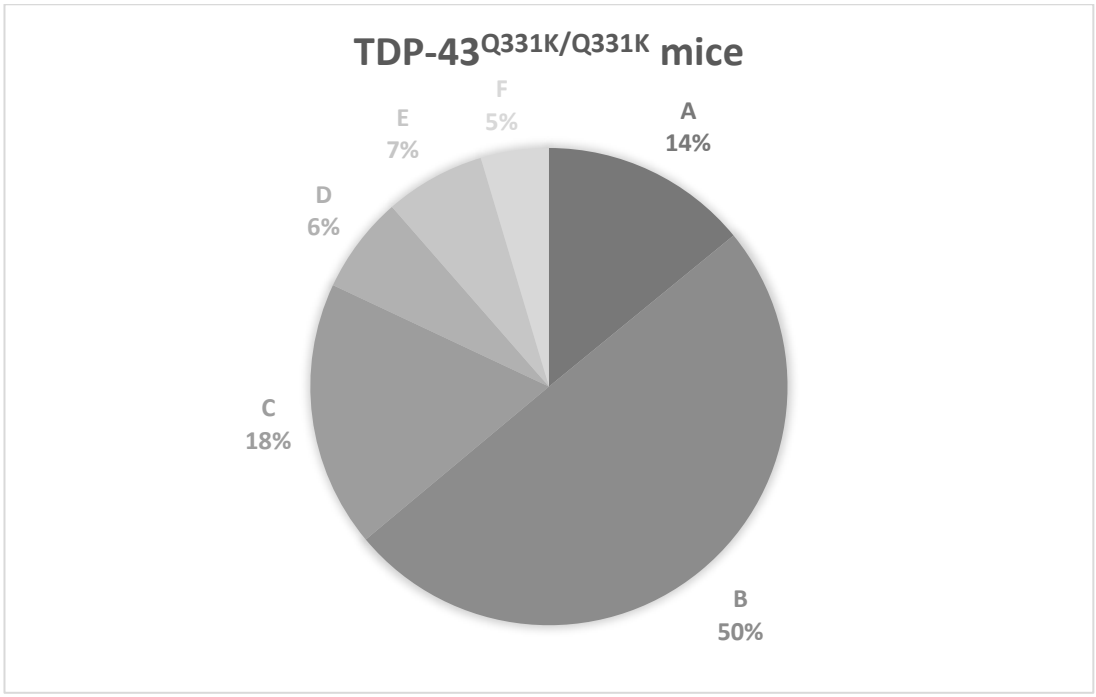

Figure 3.22 The distribution of DCX$^+$ cell morphology in 6-month-old female TDP-43$^{Q331K+/Q331K+}$ and wild type mice. The pie charts show the distribution of neurones according to their morphology, expressed as a population of the total number of DCX$^+$ cells. Wild type mouse n=6, TDP-43$^{Q331K/Q331K}$ mice n=4.

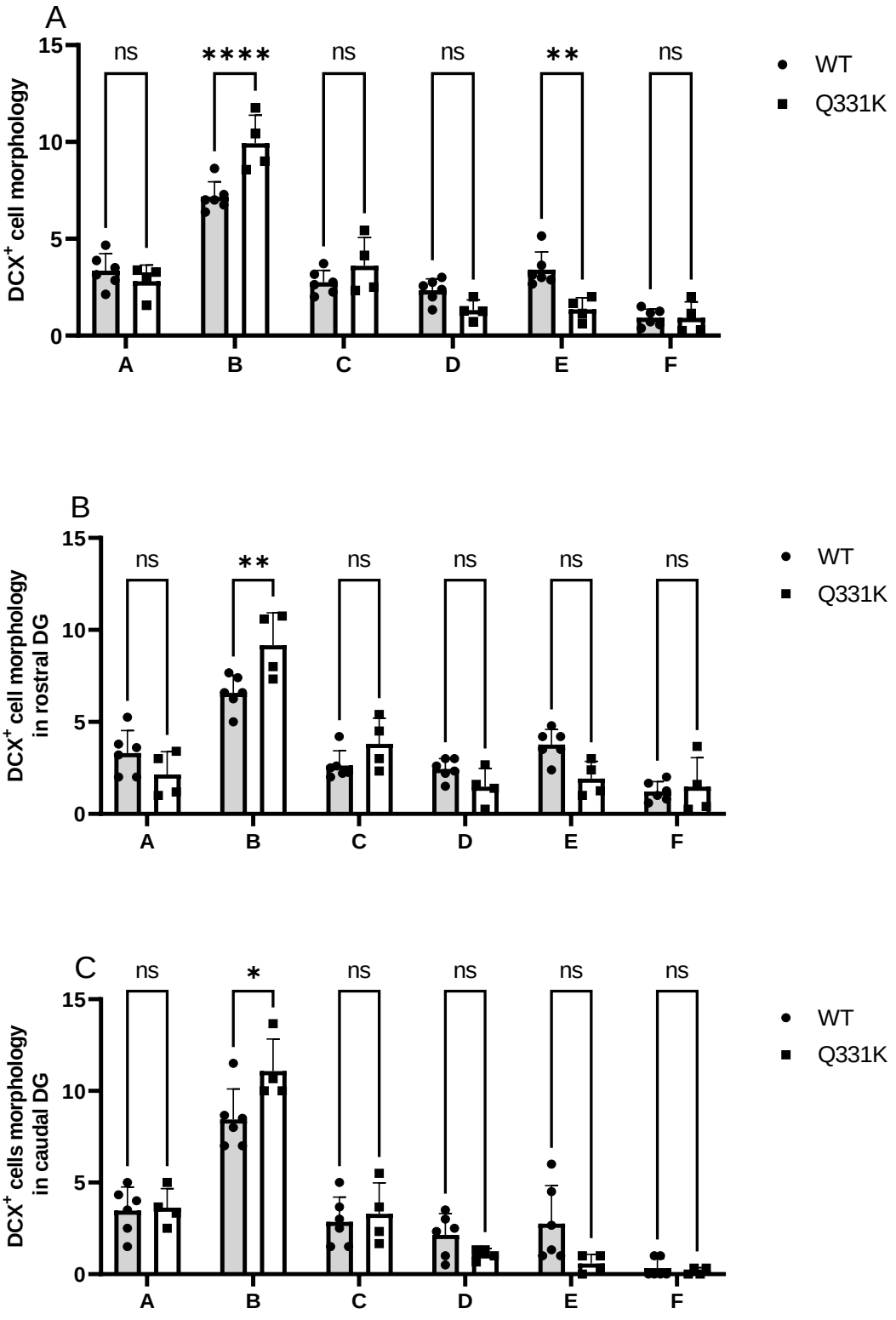

(Legend showed on next page due to content size)

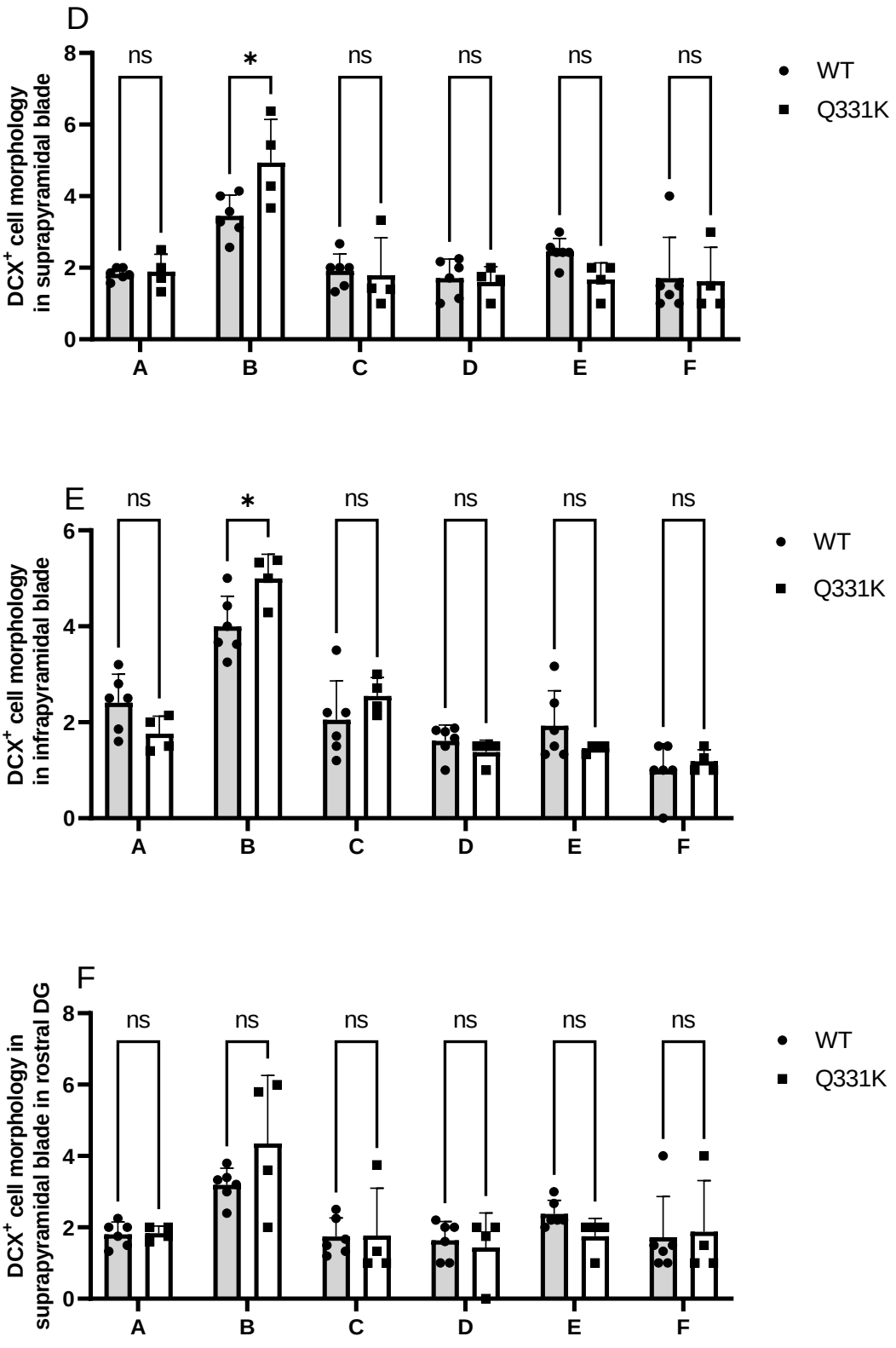

(Legend showed on next page due to content size)

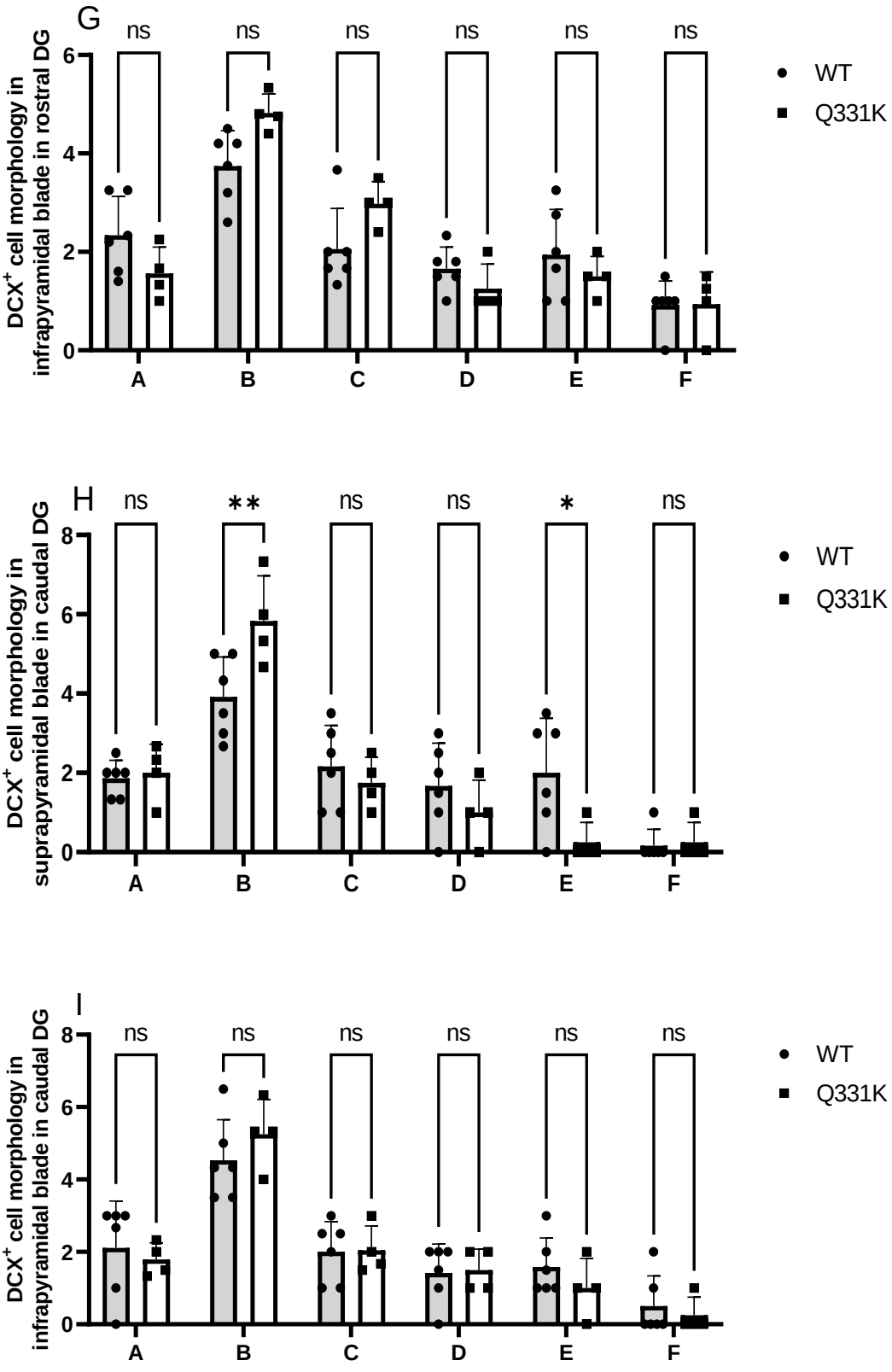

(Legend showed on next page due to content size)

Figure 3.23 The TDP-43$^{Q331K+/\ Q331K+}$ mutation affects the morphology of DCX^{+} cells in 6-month-old female mice. The DCX^{+} cells were quantified according to their morphology as previously described by Plumpe et al 2006. The number of DCX^{+} cells in each morphological category was counted in the DG (A), rostral DG (B), caudal DG (C), suprapyramidal (D), infrapyramidal (E), rostral suprapyramidal (F), rostral infrapyramidal (G), caudal suprapyramidal (H), caudal infrapyramidal (I). The experiments comprised of 2 groups. Wild type mice, n=6; TDP-43$^{Q331K/Q331K}$ mice, n=4. Statistical analysis was conducted by ordinary two-way ANOVA, followed by Tukey's post hoc comparison. ns = not significant, *P<0.05, **P<0.01, ***P<0.001. All data shown are mean ± SEM.

3.3.12 The TDP-43$^{Q331K+/ Q331K+}$ mutation affects the morphology of the DCX^{+} cells in 6-month-old mice.

Next, the morphology of DCX^{+} cells were assessed in all the 6-month-old TDP-43$^{Q331K+/ Q331K+}$ and wild-type mice, which include both male and female mice. The distribution of DCX^{+} cells by distinct morphologies was performed as above and according to Plumpe et al 2006. For wild-type mice, 36% of cells were category B, 18% of cells were category A, 17% were category E, 12% were category C and 9% were category D. Only 8% of the cells were category F. For the TDP-43$^{Q331K/Q331K}$ mice, 47% of cells were in category B, 18% of cells were in category A, 14% were in category C, 10% were in category E, whilst the other 6% and 5% were in categories D and F, respectively (Figure 3.22). Analysis of the data using a 2-way ANOVA reported a significant increase in the number of cells in category B across the entire DG (Fig 3.23 A, p=0.0024, Mean: WT 7.263, Q331K 9.118), category E (Fig 3.23 A, p=0.0239, Mean: WT 3.468, Q331K 1.973), rostral DG category B (Fig 3.23 B, p=0.0032, Mean: WT 6.707, Q331K 8.700). For the entire DG, suprapyramidal blade (Fig 3.23 D, p= 0.0163, Mean: WT 3.527, Q331K 4.411), infrapyramidal blade (Fig 3.23 E, p= 0.0128, Mean: WT 3.901, Q331K 4.923). Combined, these data suggest that the TDP-43$^{Q331K+/ Q331K+}$ mutation may increase the number of category B and E cells compared to WT mice.

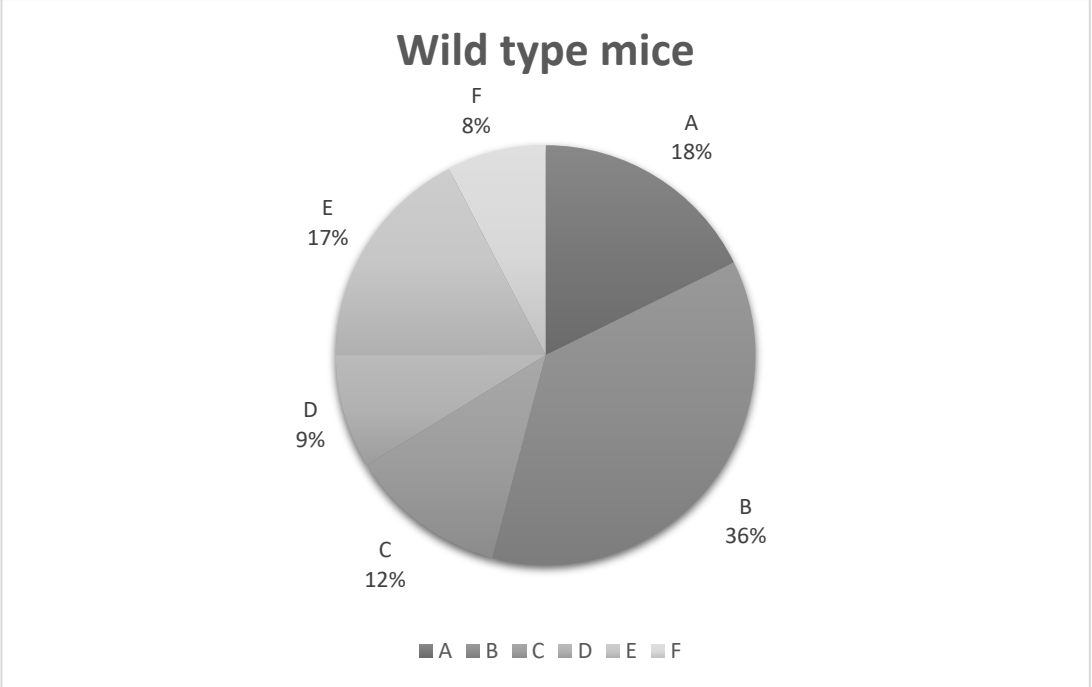

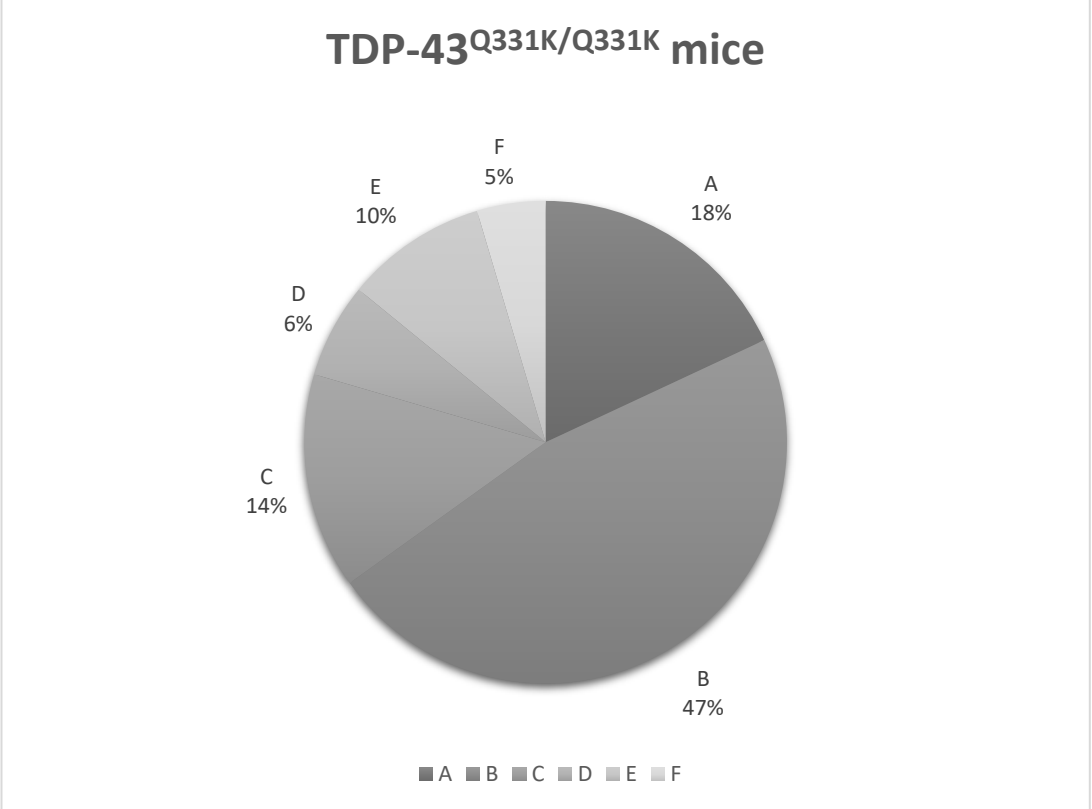

Figure 3.24 The distribution of DCX$^+$ cell morphology in 6-month-old TDP-43$^{Q331K+/Q331K+}$ and wild type mice. The pie charts show the distribution of neurones according to their morphology, expressed as a population of the total number of DCX$^+$ cells. Wild type mouse n=12, TDP-43$^{Q331K/Q331K}$ mice n=10.

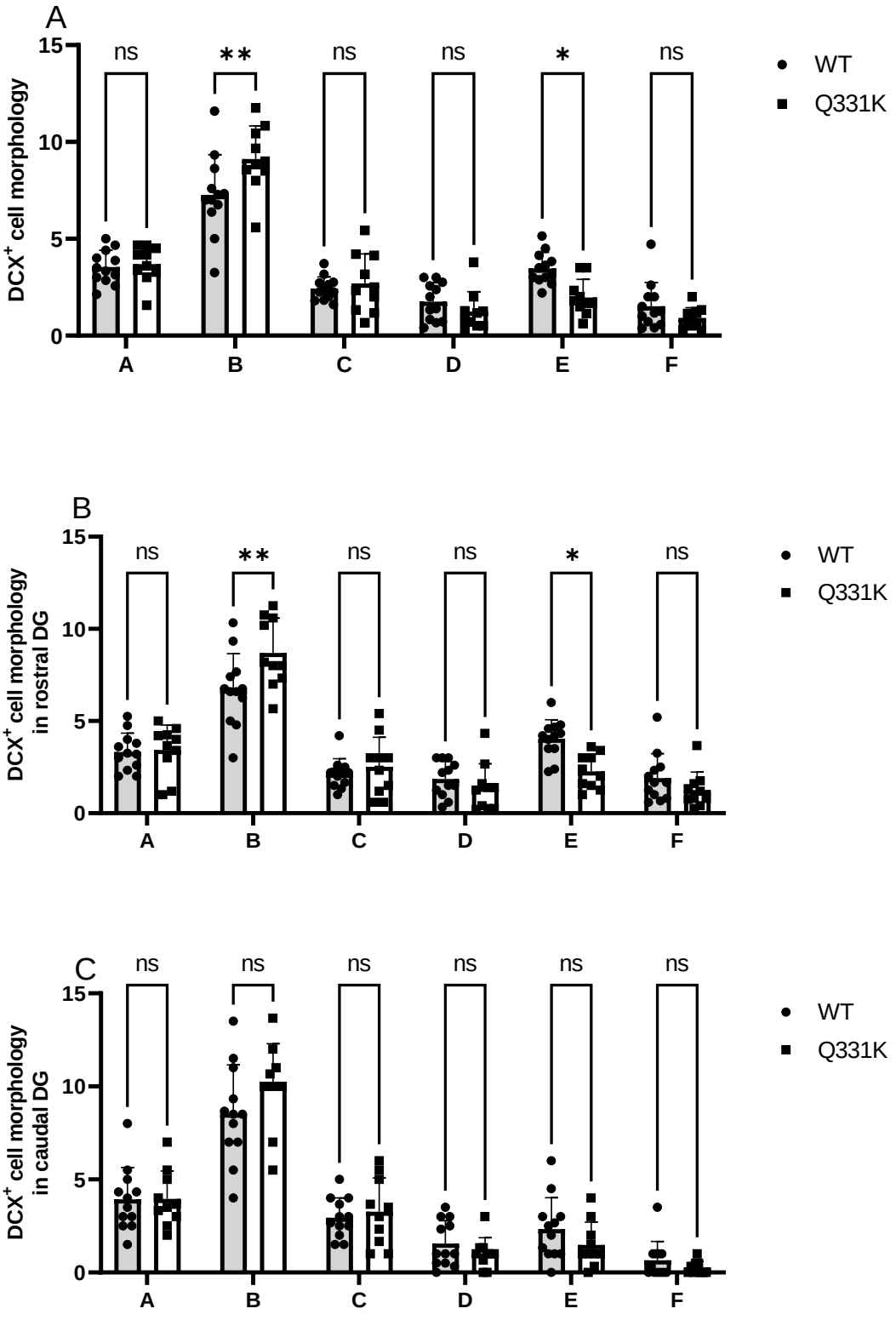

(Legend showed on next page due to content size)

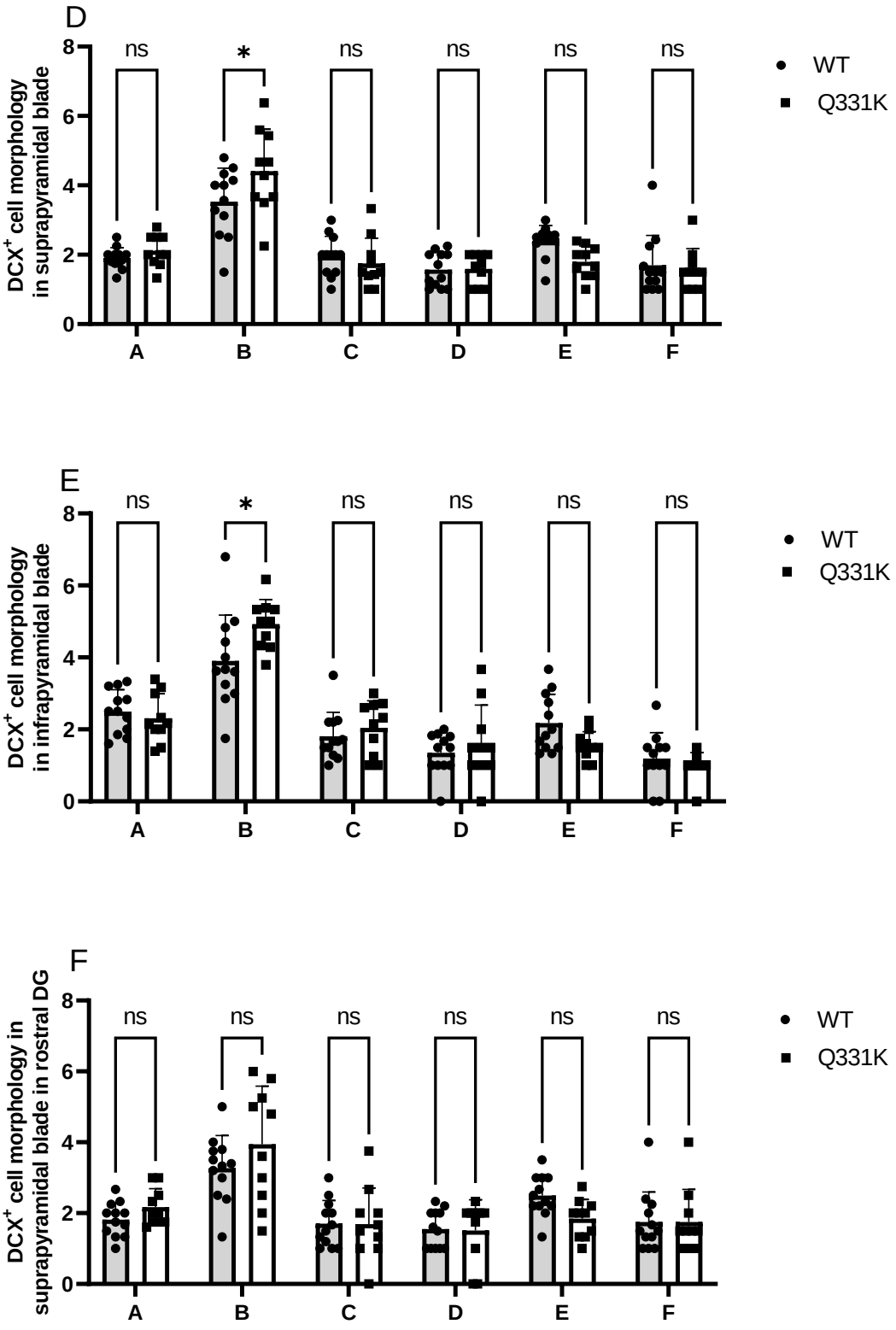

(Legend showed on next page due to content size)

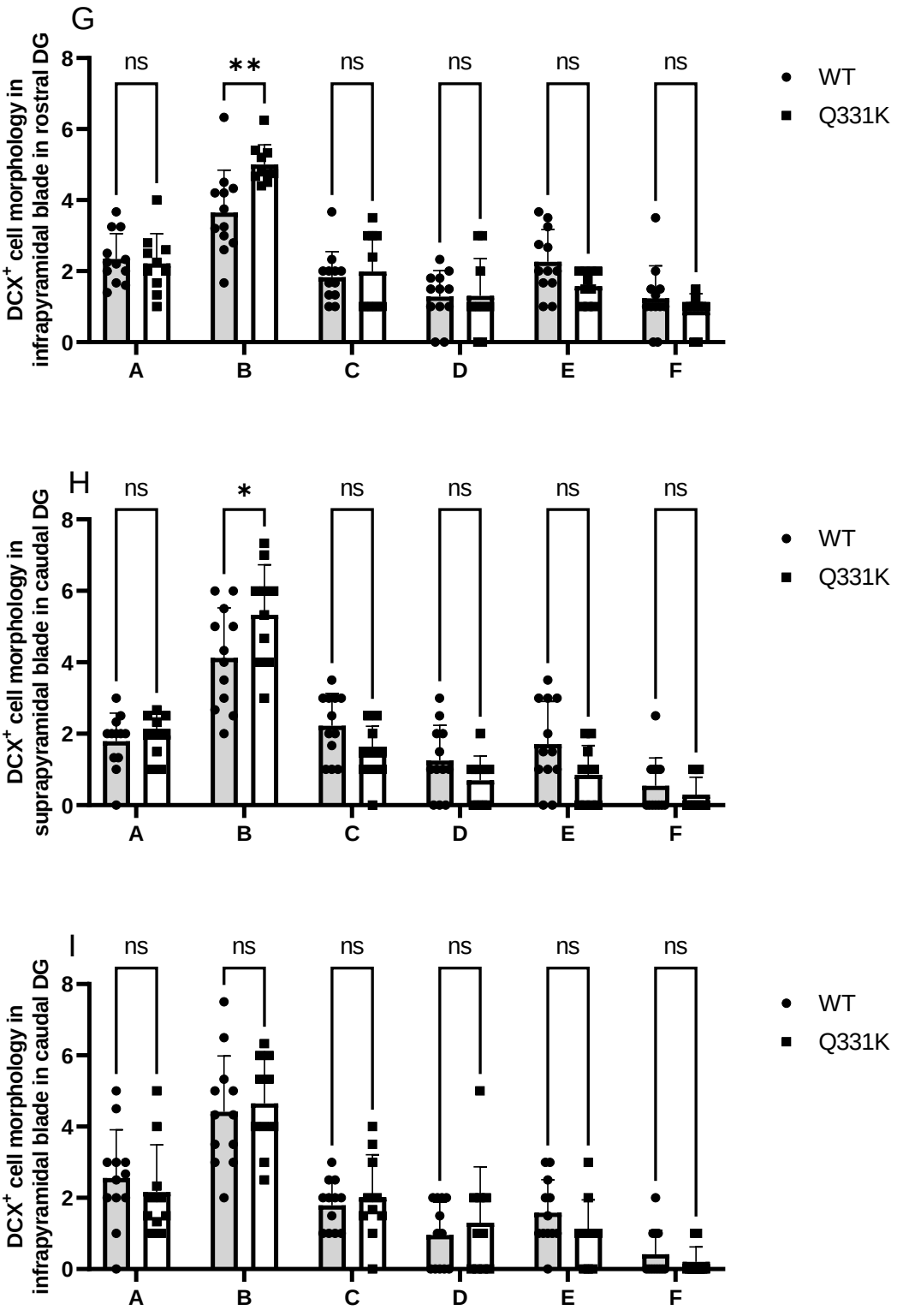

(Legend showed on next page due to content size)

Figure 3.25 The TDP-43$^{Q331K+/\ Q331K+}$ mutation affects the morphology of DCX$^+$ cells in 6-month-old mice. The DCX$^+$ cells were quantified according to their morphology as previously described by Plumpe et al 2006. The number of DCX$^+$ cells in each morphological category was counted in the DG (A), rostral DG (B), caudal DG (C), suprapyramidal (D), infrapyramidal (E), rostral suprapyramidal (F), rostral infrapyramidal (G), caudal suprapyramidal (H), caudal infrapyramidal (I). The experiments comprised of 2 groups. Wild type mice, n=12; TDP-43$^{Q331K/Q331K}$ mice, n=10. Statistical analysis was conducted by ordinary two-way ANOVA, followed by Tukey's post hoc comparison. ns = not significant, *P<0.05, **P<0.01, ***P<0.001. All data shown are mean ± SEM.

3.3.13 The number of category A & B immature neurones is altered in specific regions in male TDP-43$^{Q331K+/Q331K+}$ mice in comparison to male wild-type mice at 24 months of age.

To identify whether the Q331K mutation can impact the formation of immature DCX^{+} cells during ageing, the morphology of the DCX^{+} cells was also assessed in male 24-month-old TDP-43$^{Q331K+/Q331K+}$ and wild-type mice (example of which can be seen in Figure 3.24. For wild-type mice, 48% of cells were category B, 23% of cells were category A, 18% were category C, 7% were category E and 4% were category D. No cells were classified as category F (Figure 3.25). For the TDP-43$^{Q331K+/Q331K+}$ mice, 47% of cells were category B, 20% of cells were category A, 17% were category C, 3% were category E and 3% were category D. No cells were classified as category F. Analysis using a 2-way ANOVA showed no significant changes in any of the groups apart from a significant increase in the number of category B in the suprapyramidal blade of the caudal DG in TDP-43$^{Q331K+/Q331K+}$ mice (Figure 3.26 H, p= 0.0037, Mean: WT 0.750, Q331K 2.333). Furthermore, there was a significant increase in the number of categories A cells in the infrapyramidal blade of the rostral DG in TDP-43$^{Q331K+/Q331K+}$ mice (Figure 3.26 G, p= 0.0496, Mean: WT 0.6389, Q331K 1.778). The results suggest that the homozygous Q331K knock-in mutation may regulate the morphology of immature neurones in discrete niches of the DG.

A

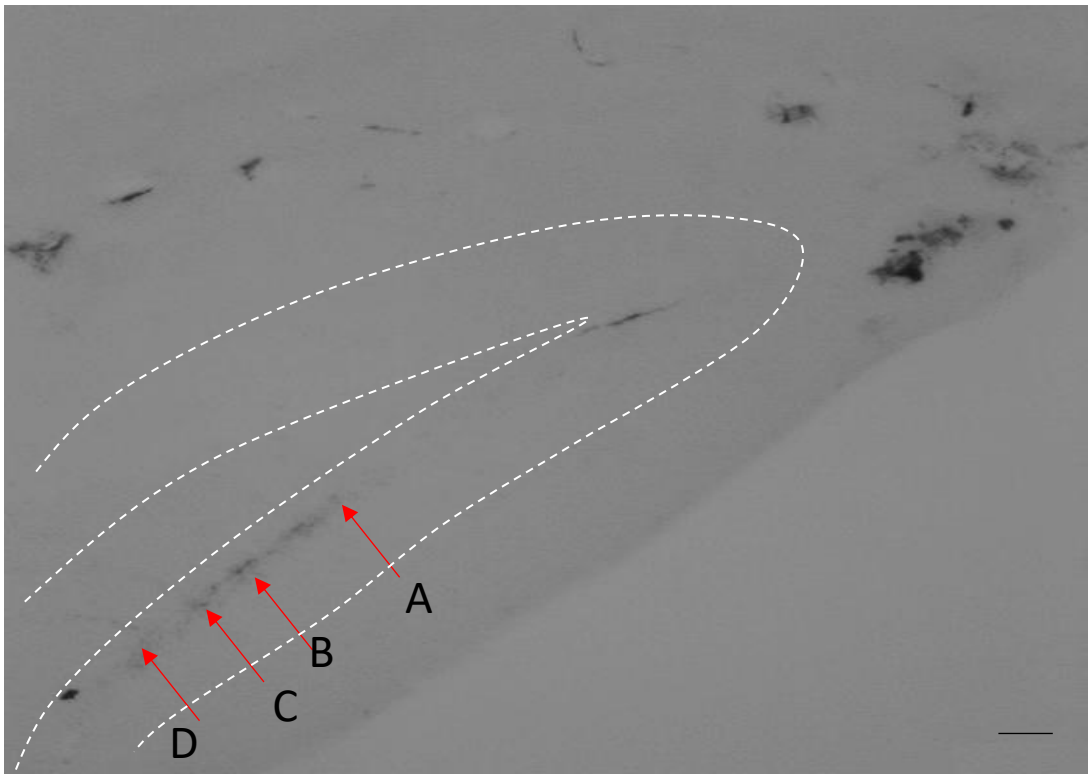

(Legend showed on next page due to content size)

B

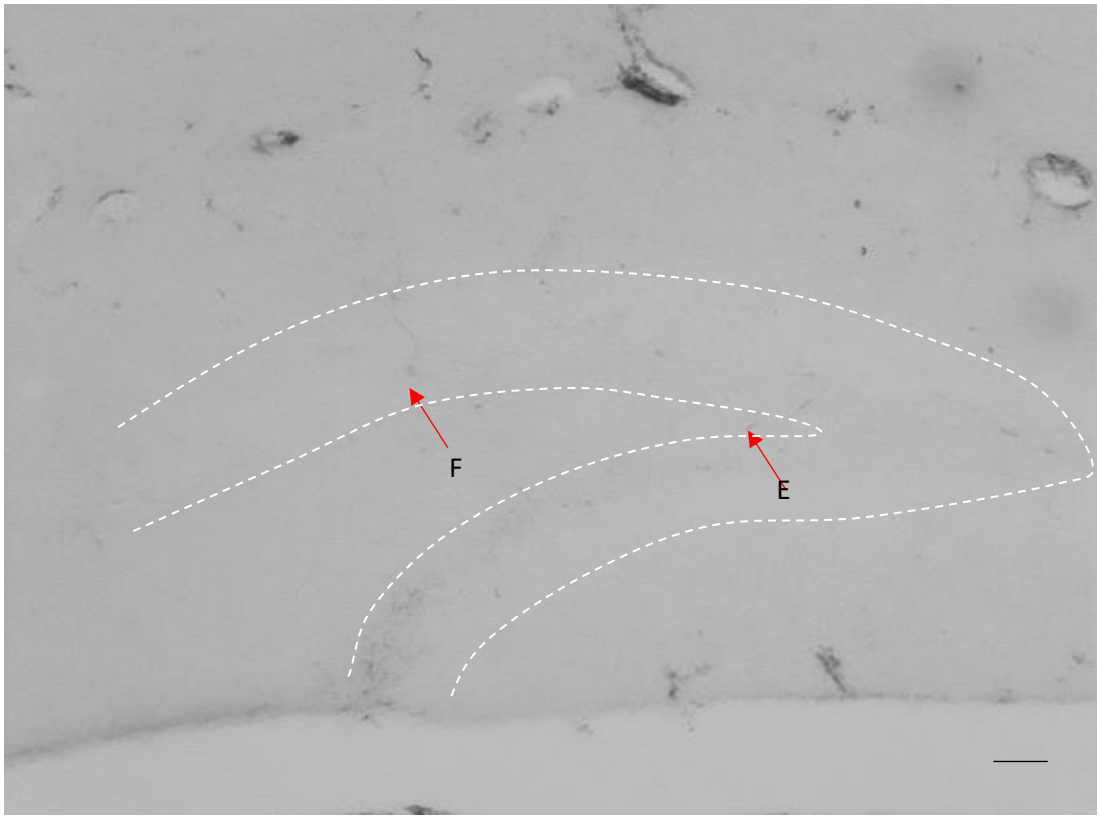

Figure 3.26 Analysis of DCX$^+$ cell morphology in the DG of 24-month-old male mice. IHC-DAB for DCX was performed on hippocampal sections from TDP-43$^{Q331K+/\ Q331K+}$ and wild type mice. The morphology of the DCX$^+$ cells was then assessed and counted according to Plumpe et al 2006. Images include hippocampal DG captured using a 10X objective lens. The arrows indicate a representative cell of each morphology type from A to F. Scale bar equals to 50µm.

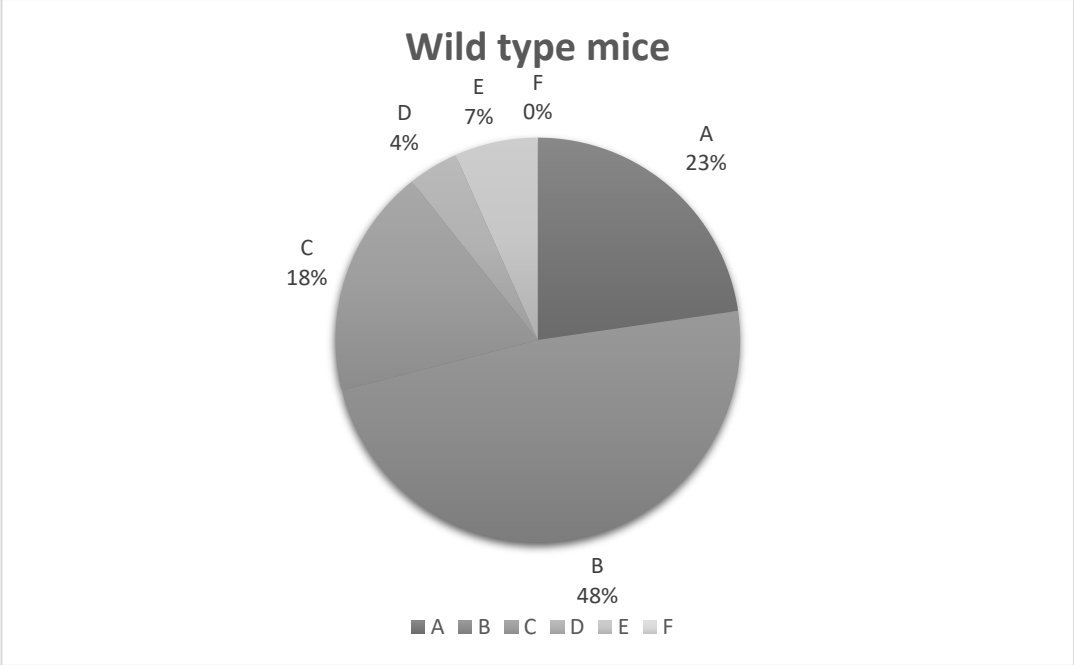

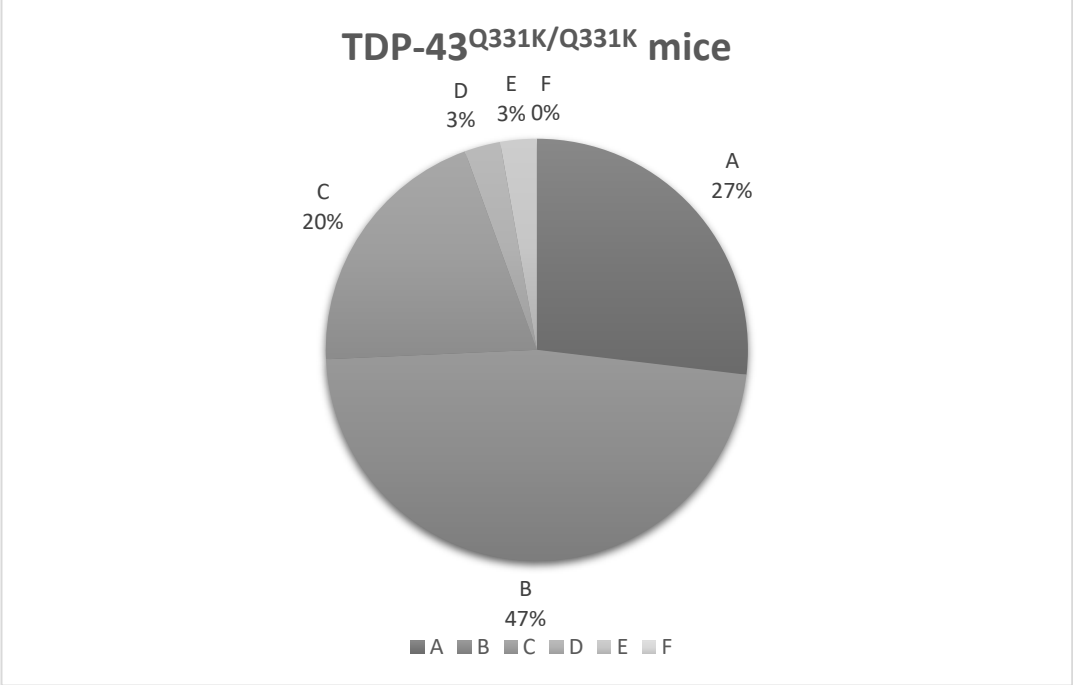

Figure 3.27 The distribution of DCX+ cell morphology in 24-month-old male TDP-43$^{Q331K+/Q331K+}$ and wild type mice. The pie charts show the distribution of neurones according to their morphology, expressed as a population of the total number of DCX^{+} cells. Each group, n=6.

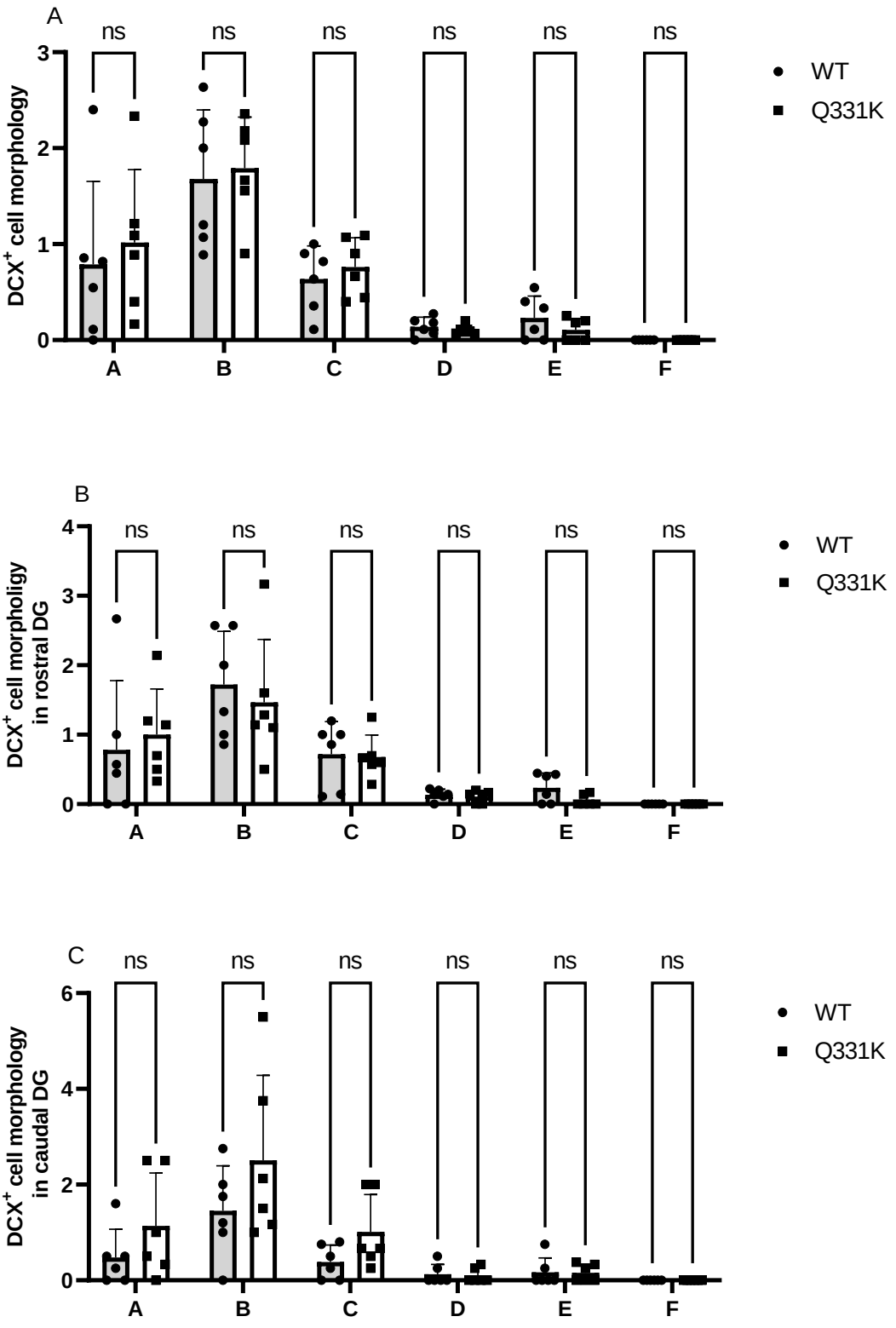

(Legend showed on next page due to content size)

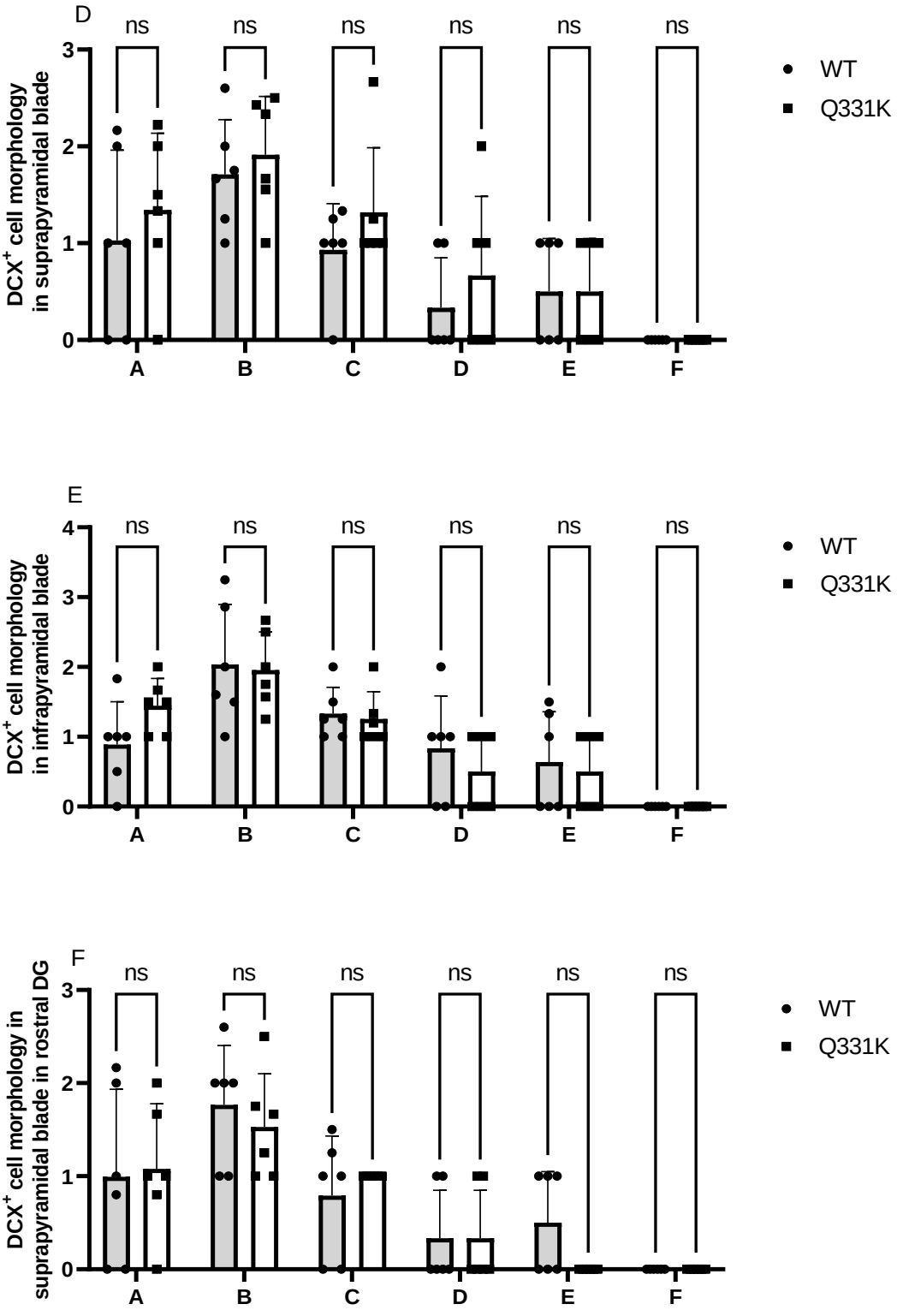

(Legend showed on next page due to content size)

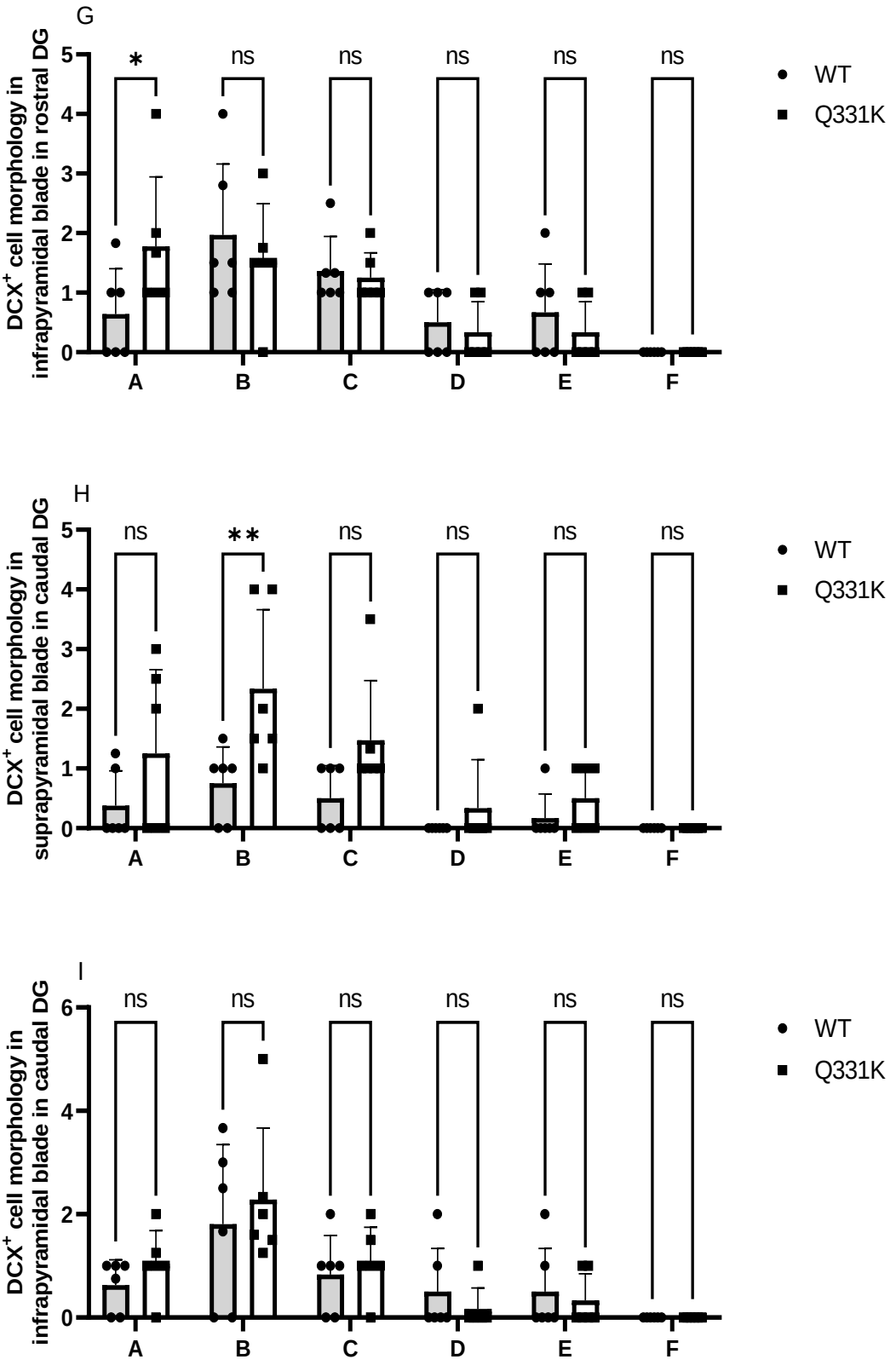

(Legend showed on next page due to content size)

Figure 3.28 In male 24-month TDP-43$^{Q331K+/Q331K+}$ mice, the number of category A & B immature neurones is altered in comparison to wild-type mice. The DCX^+ cells were assessed and distributed according to their morphology as previously described by Plumpe et al 2006. The number of DCX^+ cells in each morphological category was counted in the DG (A), rostral DG (B), caudal DG (C), suprapyramidal (D), infrapyramidal (E), rostral suprapyramidal (F), rostral infrapyramidal (G), caudal suprapyramidal (H), caudal infrapyramidal (I). The experiments comprised of 2 groups, with n=6/group. Statistical analysis was conducted using ordinary two-way ANOVA, followed by Tukey's post hoc comparison. ns = not significant, *P<0.05, **P<0.01. All data shown are mean ± SEM.

3.3.14 TDP-43$^{Q331K+/Q331K+}$ mice have impaired immature phospho-Tau^{+} neurones in 6-month-old female mice.

The TDP-43$^{Q331K/Q331K}$ mutation has been associated with the onset of Frontal temporal dementia (Kim *et al.*, 2020)(White et al., 2018). This mouse model gives us an opportunity to explore its role in the formation of new neurones in the adult DG. The synthesis of PHF1-Tau is important in the context of learning, creating and storing memories (Koren *et al.*, 2019). Thus, in this next experiment, I used IF-IHC to investigate whether the TDP-43$^{Q331K/Q331K}$ mutation can alter the expression of PHF1-Tau in DCX^{+} cells. The results show a significant decrease in the presence of PHF1-Tau^{+} / DCX^{+} cells of TDP-43$^{Q331K+/Q331K+}$ mice (Figure 3.28 A, p=0.012, Mean±SEM: WT 51.38±4.723, Q331K 33.44±4.510) as well as a decrease in the number of DCX^{+} / PHF1-Tau^{-} cells in TDP-43$^{Q331K+/Q331K+}$ mice (p=0.0087; Figure 3.30 B, Mean±SEM: WT 26.63±2.999, Q331K 12.25±2.289).

A: PHF1-Tau^{+}/DCX^{+}

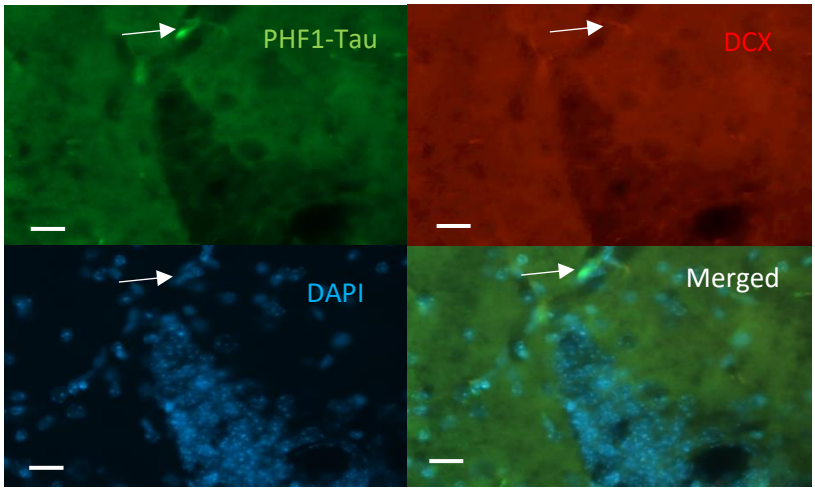

B: PHF1-Tau^{+}/DCX^{-}

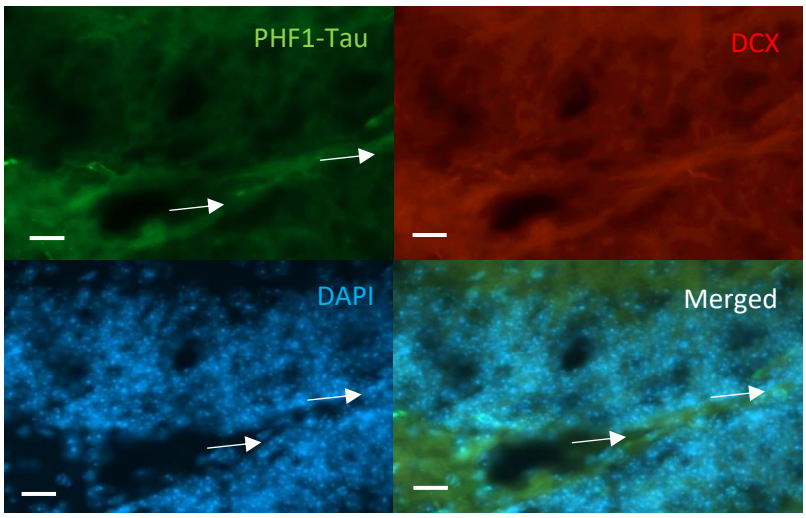

C: PHF1-Tau^{-}/DCX^{+}

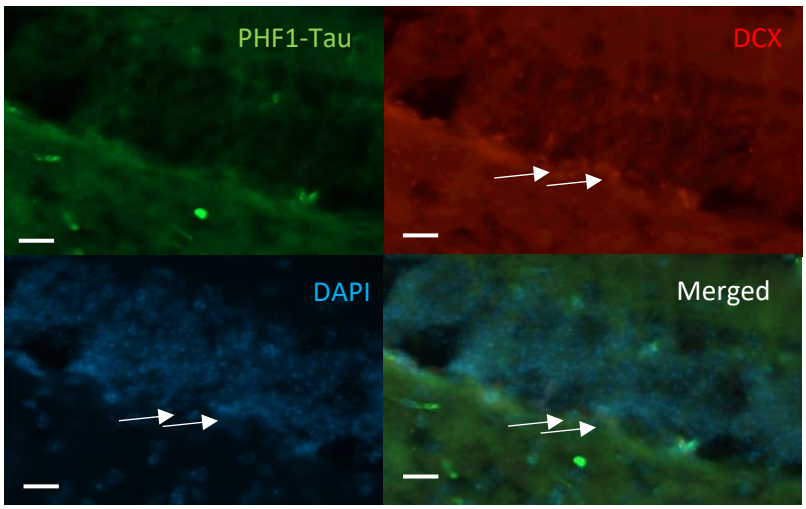

(Legend showed on next page due to content size)

Figure 3.29 PHF1-Tau and DCX cells in the DG in 6-month-old female mice. IHC-IF for PHF1-Tau and DCX was carried out on hippocampal sections from TDP-43$^{Q331K+/\ Q331K+}$ and wild type mice. PHF1-Tau^{+}/DCX^{+} cells (A), PHF1-Tau^{+}/DCX^{-} cells (B), PHF1-Tau^{-}/DCX^{+} cells (C) (PHF1-Tau, green channel; DCX, red channel). Images were taken using a 40X objective lens. Representative immunolabelled cells are shown by arrows. Scale bar = 50μm.

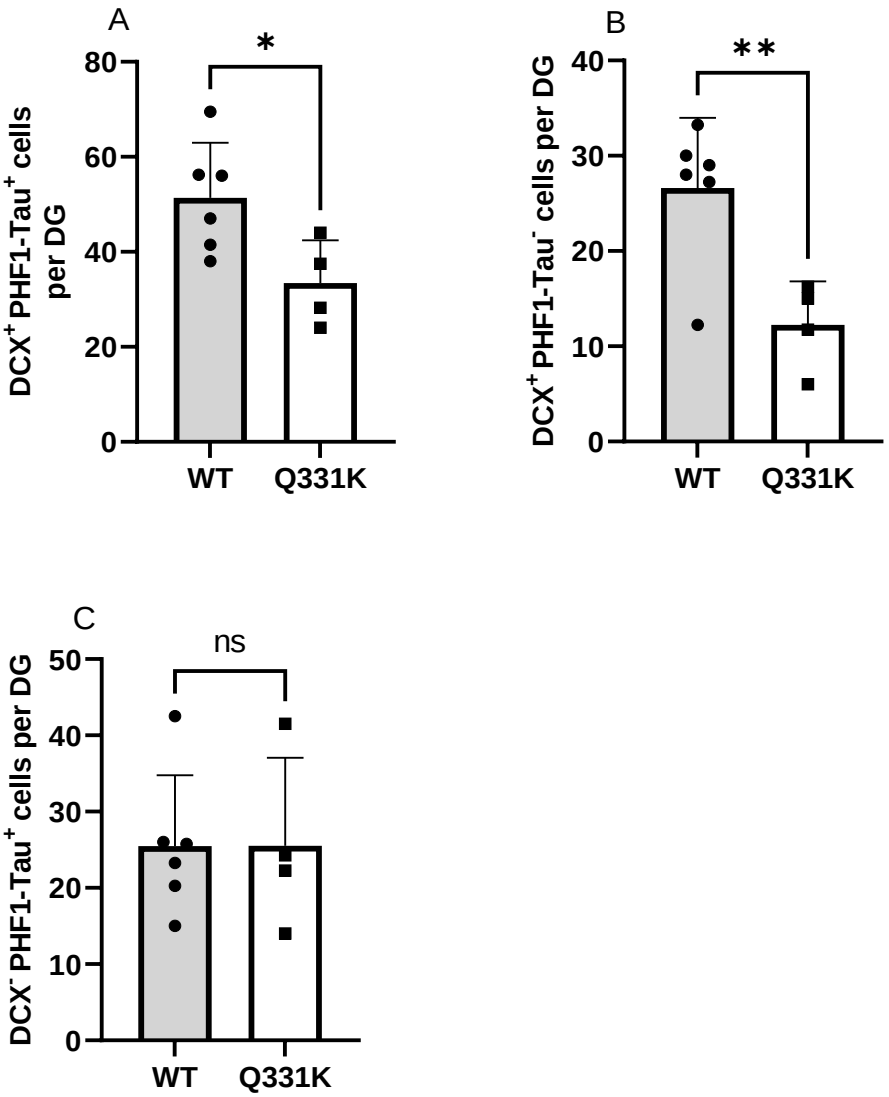

Figure 3.30 The TDP-43$^{Q331K/Q331K}$ regulates DCX and PHF1-Tau in the DG. Statistical analysis performed by unpaired Student's t-test. n = 4-6/group. ns = not significant, *P<0.05, **P<0.01. All data shown are mean ± SEM.

To determine whether the number of PHF1-Tau^{+} DCX$^{+/-}$ cells is altered in the infrapyramidal and suprapyramidal blades of the DG in TDP-43$^{Q331K+/Q331K+}$ and wild-type mice, the DG sections were analysed further. Results show that there is a significant decrease in the number of PHF1 Tau^{+} cells in the infrapyramidal blade compared to the suprapyramidal blade in TDP-43$^{Q331K+/ Q331K+}$ mice but not in wild-type mice (Figure 3.31, p=0.0201). Mean information is included in appendix.

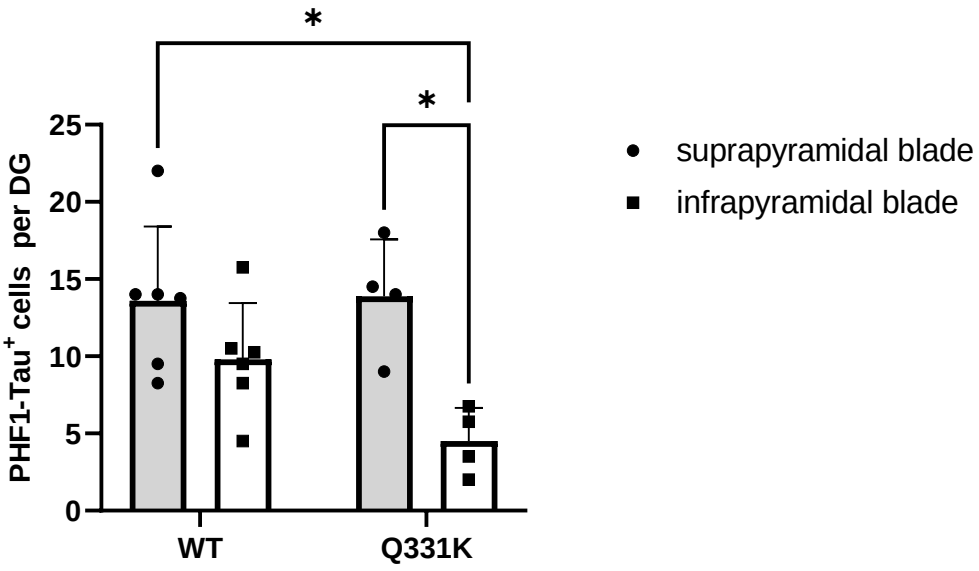

Figure 3.31 The TDP-43$^{Q331K/Q331K}$ mutation regulates PHF1-Tau^{+} cell number in the infrapyramidal blade of the DG. Data analysis comprised of 4 groups. Wild type mouse, n=6; TDP-43$^{Q331K/Q331K}$ mice, n=4. Two-way ANOVA, followed by Tukey's post hoc comparison, ns = not significant, *P<0.05. All data shown are mean ± SEM.

Analysis of wild-type mice revealed a significant reduction in the number of DCX^{+} cells in the infrapyramidal blade in comparison to the suprapyramidal blade (Figure 3.31, p=0.0323). There was also a significant reduction in the number of DCX^{+} cells in the suprapyramidal blade of TDP-43$^{Q331K+/Q331K+}$ mice in comparison to the suprapyramidal blade of wild-type mice (Figure 3.32, p=0.0125). Mean information is included in the appendix.

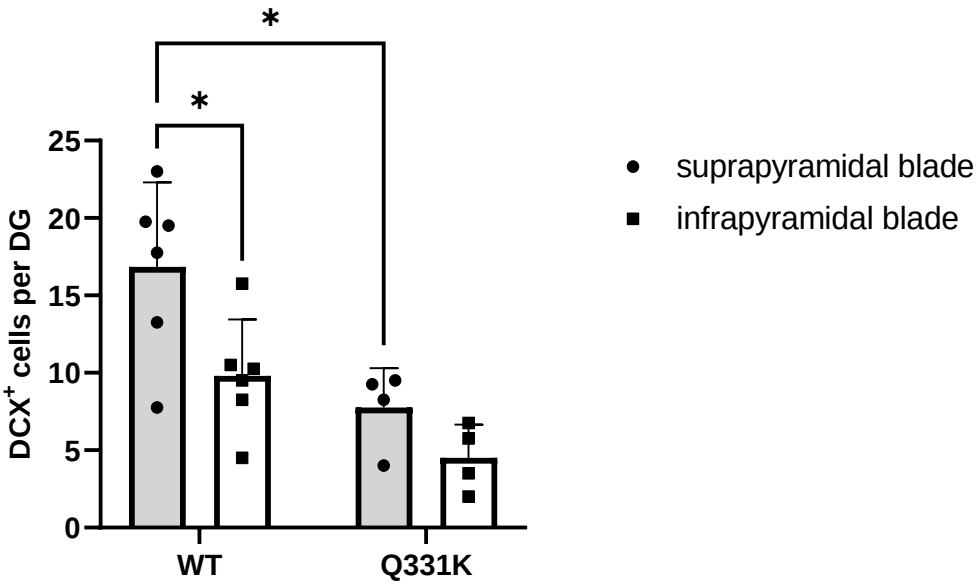

Figure 3.32 The TDP-43$^{Q331K/Q331K}$ mutation predominantly reduces DCX^{+} cell number in the suprapyramidal blade of the DG. The experiments comprised of 4 groups. Wild type mice, n=6; TDP-43$^{Q331K/Q331K}$ mice, n=4. Two-way ANOVA, followed by Tukey's post hoc comparison, ns = not significant, *P<0.05, ***P<0.001. All data shown are mean ± SEM.

Cells that co-express DCX and PHF1-Tau were also analysed for expression across both blades of the DG. The data show that there is a significant reduction in the number of $DCX^{+}PHF1\text{-}Tau^{+}$ cells in the suprapyramidal blade of TDP-$43^{Q331K+/Q331K+}$ mice in comparison to the suprapyramidal blade of wild type (Figure 3.33, p=0.0387). Overall, these results suggest that the TDP-$43^{Q331K/Q331K}$ mutation regulates new immature neurones predominantly within the suprapyramidal blade of the DG. Mean information is included in the appendix.

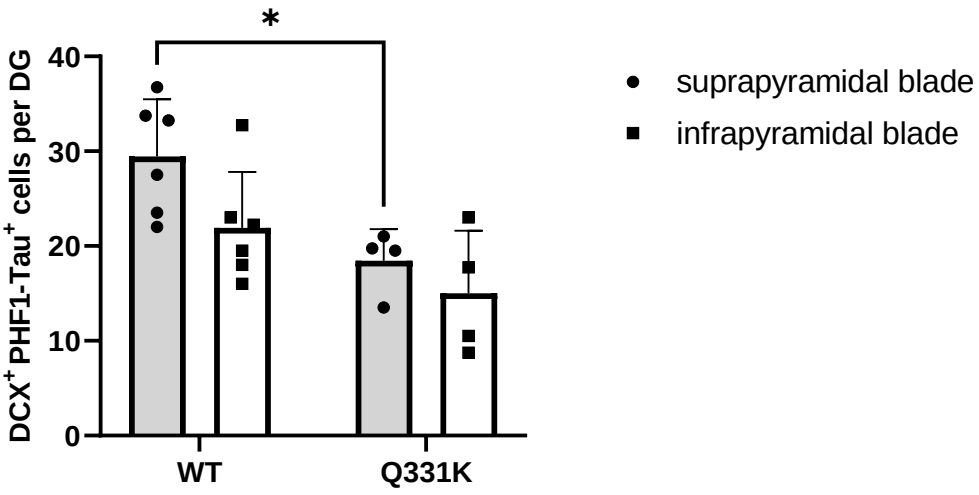

Figure 3.33 The TDP-$43^{Q331K/Q331K}$ mutation reduces the $DCX^{+}/PHF1\text{-}Tau^{+}$ cell number predominantly in the suprapyramidal blade of the DG IN 6-month-old female mice. The experiments comprised of 4 groups. wild type mice, n=6; TDP-$43^{Q331K/Q331K}$ mice, n=4. Two-way ANOVA, followed by Tukey's post hoc comparison, ns = not significant, *P<0.05, **P<0.01. All data shown are mean ± SEM.

3.4 Conclusion

To conclude, TDP-43$^{Q331K+/Q331K+}$ mice show deficits in immature neurone numbers and their development within the hippocampal neurogenic niche. The immature neurone number and morphology were not associated with either the supra- or infra-pyramidal blade of the DG. However, no deficits were reported in the SVZ neurogenic niche, suggesting that the process of generating new adult-born neurones in the hippocampus is particularly susceptible to the TDP-43$^{Q331K+/Q331K+}$ knock-in mutation. These data support the theory that AHN is currently understudied in FTD and ALS and suggest that further studies into the functional implications of impaired neurogenesis are warranted.

4 Chapter 4 Study of adult hippocampal neurogenesis in Parkinson's disease

4.1 Introduction

4.1.1 PD

Parkinson's disease (PD), which includes motor and non-motor system impairment, is defined as an idiopathic disease. It is a chronic, progressive degenerative disorder of the nervous system. Elderly people are more vulnerable to it, with diagnoses usually made in those aged over 60 years old. It is relatively uncommon to see the disease at a young age, however, early-onset PD has been reported. It is rare to see PD passed from parent to child. However, some researchers report that early-onset PD patients are more likely to inherit it from their parents (Gasser, 2001)(Hardy *et al.*, 2006)(Belin and Westerlund, 2008). In the clinic, it is regarded as the second most common neurodegenerative disease in the world. (Sherer *et al.*, 2012). Common features of idiopathic PD are also found in other neurodegenerative disorders, e.g. Dementia with Lewy Bodies (DLB), Corticobasal Degeneration (CBD), Multiple System Atrophy and Progressive Supranuclear Palsy (PSP) (Sherer *et al.*, 2012). A feature of PD includes abnormal intracellular aggregates called Lewy bodies, these are comprised of different proteins, e.g. alpha-synuclein and ubiquitin, which can cause neurone function impairment (Yao, Hart and Terzella, 2013). Lewy bodies are clumps of protein in the brain, they can be located in areas of the brain associated with memory, thinking and movement. The accumulation of Lewy bodies can impair neurone function (McNaught *et al.*, 2002) which can eventually cause neuronal death (Meredith *et al.*, 2002)(Mahul-Mellier *et al.*, 2018).

Typical PD patients have a significant loss of dopaminergic neurones. This loss of dopamine-generating nerve cells occurs in the substantial nigra pars compacta (SNpc) region. The SNpc receives nerve impulses from the caudate and putamen of the striatum. These projections synapse with two distinct dopaminergic neurone sub-types, the D1-family receptor neurones and D2 family receptor neurones. The D1-family

receptor neurones create inhibitory projections to the globus pallidus internus (GPi). This is called the direct pathway and involves the basal ganglia. The indirect pathway involves the D2-family neurones that project to the globus pallidus externus (HPe) to inhibit the stimulatory subthalamic nucleus (STN) (Sonne, Reddy and Beato, 2019). The hippocampus also receives D1 and D2 inputs (Lisman and Grace, 2005). The hippocampus is also vulnerable to neurodegeneration compared to other areas of the brain. The possible reason may be due to its high levels of neuroplasticity which is required for normal hippocampal function (Weerasinghe-Mudiyanselage *et al.*, 2022)(Marsh *et al.*, 2022).

With reduced dopamine levels, the motor neurone system starts to show impairment (Macphee and Stewart, 2001). Dopamine plays a messenger role in allowing neurotransmission between the substantia nigra and the corpus striatum, via the nigrostriatal pathway. As mentioned above, the basal ganglia which include the substantia nigra and corpus striatum are essential for operating body movement, therefore, low levels of dopamine lead to a dysfunction of this pathway. As a consequence, abnormal nerve firing patterns can be triggered, which results in problems with controlling movements such as resting tremors, postural instability and gait (Küppers *et al.*, 2000)(Purves *et al.*, 2001).

Several factors can contribute to the formation of PD. There is evidence that both environmental stress and ageing have a significant effect on disease susceptibility (Ceccatelli, 2013). In particular, environmental exposure to toxic chemicals has been associated with developing Parkinson-like disorders (Jones and Miller, 2008). For example, drug abuse (e.g heroin) has also been suggested to contribute to PD pathogenesis via chronic low-grade inflammation in the brain, resulting in neuronal cell senescence (Pajares *et al.*, 2020). However, in later research, it was noted that MPP+, a mitochondrial toxin, was present in the drugs that led to DA neurone death and the development of Parkinson-like symptoms (Dauer and Przedborski, 2003a). Notably, MPTP - a precursor to MPP+ - is widely used to induce PD-like phenotypes in rodents and other disease models (Chinta *et al.*, 2013)(Brown *et al.*, 2006)(Ceccatelli, 2013).

Pathologic examination of post-mortem brain tissue from PD patients revealed that nerve cell loss mainly happens in the SNpc (Bloch *et al.*, 2006). Gliosis is also

observed in the SNpc region of PD patients. Pathologic data shows motor features present when approximately 60-70% of the neurones in the SNpc area are already lost (Postuma, Gagnon and Montplaisir, 2010)(Jankovic, Hurtig and Dashe, 2014)(Dauer and Przedborski, 2003a). Some researchers consider that although PD pathology affects a variety of neurological systems, only a few cell types in the human nervous system are vulnerable to developing protein aggregations. The Lewy body is mostly located in the cortical and brainstem (Brion and Couck, 1995). For DLB, Lewy body accumulation occurs in the paralimbic and neocortical regions of the brain (Brion and Couck, 1995). Some neurone types, even those located beside the affected neurones, maintain their function and morphology. This suggests that the pathologic change of PD in the human brain is not random, but quite targeted (Braak *et al.,* 2003). However, the reason for this phenomenon is still not fully understood.

Parkinson's disease dementia (PDD) includes patients diagnosed with PD that subsequently develop impaired cognition, which impacts thinking and behaviour (Irwin, Lee and Trojanowski, 2013). In the early stages of PD, the parts of the brain responsible for movement are dysfunctional. Eventually, neuronal dysfunction can occur in parts of the brain processing learning and memory. Both PD and PDD cases are associated with increasing age and approximately 80% of PD patients eventually develop dementia (Postuma *et al.*, 2012). PDD patients may have memory problems and focus on tasks, depression, anxiety and irritability. Notably, if the cognitive decline is reported within one year of the PD diagnosis, the patient is considered to have Dementia with Lewy Bodies (DLB) rather than PDD. The movement disorder society (MDS) created a Task Force to diagnose PDD more accurately.

Researchers reported human hippocampal atrophy in PD and PDD compared to control patient groups. In this study, Magnetic Resonance Imaging (MRI), neurological examination and psychometric testing were used for exploring the hippocampal function (Camicioli *et al.*, 2003). Another research paper analysed 12 DLB patients, 16 PDD patients and 16 healthy control patients using MRI and neuropsychological assessment. They demonstrated that DLB patients had more hippocampal atrophy in the dentate gyrus in comparison to PDD and healthy controls and that the right hippocampus is correlated with visual memory deficits in the DLB group (Sanchez-Castaneda *et al.*, 2009).

Adult hippocampal neurogenesis (AHN) has been widely explored in the context of ageing and neurodegeneration. The subgranular zone in the granule cell layer of the hippocampal dentate gyrus hosts neural stem/progenitor cells that give rise to new granular cells throughout life (Yu, Marchetto and Gage, 2014). This process is associated with regulating spatial memory and anxiety-like behaviour in adult mammals such as mice, rats and humans (Revest *et al.*, 2009). In rat models of PD and human PD post-mortem brain tissues, AHN was impaired (Jasmin *et al.*, 2021). However, the detailed mechanisms are still yet to be fully understood (Marxreiter, Regensburger and Winkler, 2013).

Ghrelin is a gastric hormone which increases growth hormone (GH) secretion and food intake (Kojima *et al.*, 1999). It can adjust energy homeostasis and body weight in line with food consumption. Both acyl-ghrelin and unacylated ghrelin (UAG) can cross the blood-brain barrier (BBB) (Diano *et al.*, 2006) and acyl-ghrelin binds to the growth hormone secretagogue receptor 1a (GHS-R1a) to activate downstream signalling pathways (Kojima *et al.*, 1999)(Yin, Li and Zhang, 2014). GHS-R1a is expressed widely in the adult brain, with the highest expression reported in the olfactory bulb and the granule cell layer of the hippocampal dentate gyrus (Ratcliff *et al.*, 2016). Notably, ghrelin may regulate action potential firing, mitochondrial processing, immune signalling, neurone survival, and neural stem/progenitor cell (NSPC) differentiation in hippocampal granular cells (Diano *et al.*, 2006)(Bayliss *et al.*, 2016)(Beynon *et al.*, 2013)(Jiang *et al.*, 2008)(Elabi *et al.*, 2018). Ghrelin was also reported to enhance AHN. Johansson et al. (2008) reported that acyl-ghrelin can increase the proliferation of adult hippocampal progenitor cells in-vitro (Johansson *et al.*, 2008). Another experiment where mice received eight daily intraperitoneal (i.p) injections of acyl-ghrelin increased the number of new cells, quantified using BrdU, in the hippocampus (Moon, S. Kim, *et al.*, 2009). Acyl-ghrelin can improve brain performance in spatial pattern separation (Kent *et al.*, 2015). Moreover, acyl-ghrelin can increase immature neurone number in the DG of adult rats (Kent *et al.*, 2015). In a 6-OHDA rat model, acyl-ghrelin increases DCX^+ cell density in the DG (Elabi *et al.*, 2018). However, their motor task test showed no significant change (Elabi *et al.*, 2018). These studies suggest that ghrelin may have a beneficial effect on AHN and possibly in a model of PD.

Based on these published studies, work in this chapter will test the hypothesis that acyl-ghrelin protects against AHN decline in rodent models of PD.

4.1.2 Aim of the Chapter

The aims of this chapter include determining whether;

1. Mitochondrial toxins that induce PD-like phenotypes impact AHN,

2. Acyl-ghrelin modulates AHN in rodent toxin-based models of PD.

3. We have an additional exploratory aim to investigate evidence of AHN in human post-mortem brain tissue.

4.2 Materials

Protocols were described in above chaptor2.

Table 4.1 Primary antibodies used for 6-OHDA rat IHC

Primary antibody name	anti-DCX	anti-TH
Concentration	1:200	1:500
Species raised in	Goat	Rabbit
Catalogue number	Sc-8066	Ab122
Company	Santa Cruz	Abcam

Table 4.2 Secondary antibodies used for 6-OHDA rat

Secondary antibody name	anti-Goat (Alexa Fluor 488 IgG)	anti-rabbit (Fluor 568 IgG)
Concentration	1:500	1:500
Species raised in	Donkey	Donkey
Catalogue number	Ab150129	Ab175470
Company	Abcam	Abcam

Table 4.3 Antibodies used for MPTP mouse and human IHC

	Primary antibody	Secondary antibody
Antibody Name	Goat anti-DCX	Donkey anti-Goat (Biotinylated IgG)
Concentration	1:750	1:400
Species raised in	Goat	Donkey
Catalogue number	Sc-8066	BA-1000-1.5
Company	Santa Cruz	Vector Laboratories

4.3 Results

4.3.1 6-OHDA can generate a PD disease model by reducing immature neurone numbers.

The electron transport chain (ETC) inhibitor, 6-OHDA, often referred to as a mitochondrial toxin, has been widely used to generate rodent models that mimic features of PD. TH is a rate-limiting enzyme involved in the production of dopamine. When the dopamine cells are alive the dopamine-containing nerve cells will be identified by the TH staining - as shown in Figure 4.3. On the contrary, if the dopamine cells are no longer present the TH antibody cannot bind to neurones, as reflected by the lack of immuno-positive cells in the SNpc (Figure 4.4). This experimental model results in the death of dopamine neurones that under healthy conditions project from the SNpc to the striatum to control movement. Therefore, the lesion-induced phenotype involves impaired control of motor function – as reported in Rees et al.2022 (BioRxiv). It has been reported that synthesised dopamine can accelerate the formation of newborn immature neurones in the adult DG ((Park *et al.*, 2004)). The 6-OHDA rat model used in this study can imitate the GCL environment in the absence of dopamine innervation from the SNpc, allowing the study of AHN in the context of PD. As described in the materials and methods, the Lesion group rats received a 6-OHDA injection in one side of the brain. The rats in the acyl-ghrelin (AG) / Lesion group received the same unilateral 6-OHDA injection but also acyl-ghrelin supplied by the mini pump. With regard to the Sham group, saline was used for both the MFB injection and the mini pump in order to allow for appropriate control and reduce experimental bias.

Since only 1 side of the rat brain received a 6-OHDA or saline injection, while the other side did not, each rat brain was classified as either the lesion side or the intact side. Based on this, we used the TH^+ immunoreactivity to identify intact and lesioned hemispheres to allow quantification of the DCX^+ cell number by unpaired t-test to reveal that the 6-OHDA induced lesion reduced the number of new immature neurones in the hippocampus, $p=0.0351$ (Figure 4.5), Mean 9.565 / 7.503.

During the original removal of these brains from the rats, each brain was scored triangularly on the lesioned side of the brain in order to aid with the later identification of the lesioned side of the brain sections during IHC, because of the difficulties in recognising which hemisphere received injection (see Figure 4.6). However, during free floating IHC, whilst each brain tissue section can rotate, flip, and fold to aid with washes and antibody interactions, it also resulted in tissue damage, making it difficult to confidently identify the sections that originate from the lesioned side of the brain. However, as expected in the Saline (Sham)/Saline group, there was no significant difference in the number of TH^+ cells in either hemisphere meaning that I was unable to accurately identify the lesioned side of these control samples.

A DCX (GCL in an intact brain)

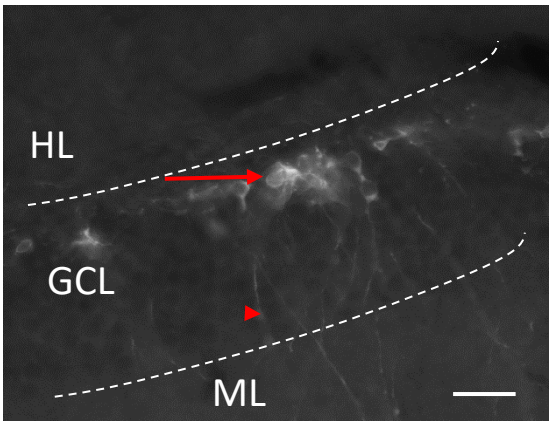

B DCX (GCL in a lesioned brain)

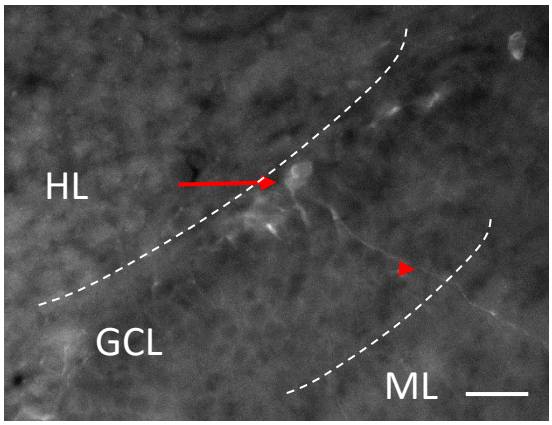

Figure 4.3 Example images of DCX$^+$ immunoreactivity in the lesioned brain. The hippocampal GCL of the intact brain (A) and lesioned brain (B) stained with anti-DCX. Images were taken by 40X objective lens. Representative immunolabelled cell bodies are shown by the arrow. Arrowhead indicates DCX$^+$ axon. Scale bar equals to 50μm. GCL = Granule Cell Layer. ML = Molecular layer. HL = hilus.

A TH (SNpc in an intact brain)

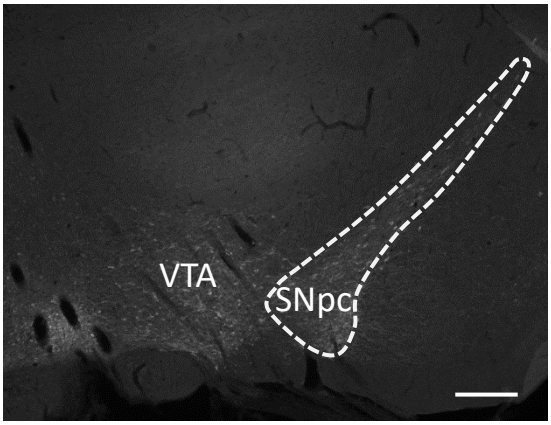

B TH (SNpc in a lesioned brain)

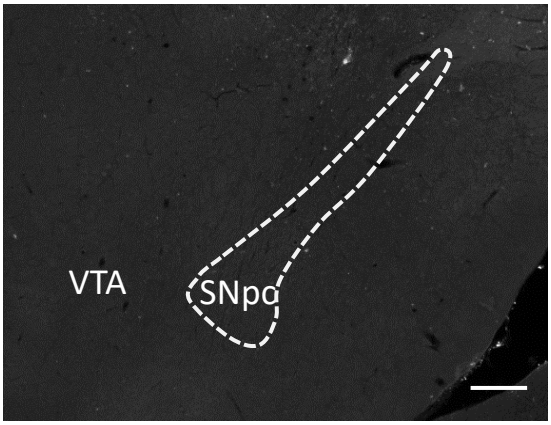

Figure 4.4 Example images of TH$^+$ immunoreactivity in the lesioned brain. The SNpc region of the intact brain (A) and lesioned brain (B) stained with anti-TH. Images were taken by 4X objective lens. VTA = ventral tegmental area. Scale bar equals to 200μm.

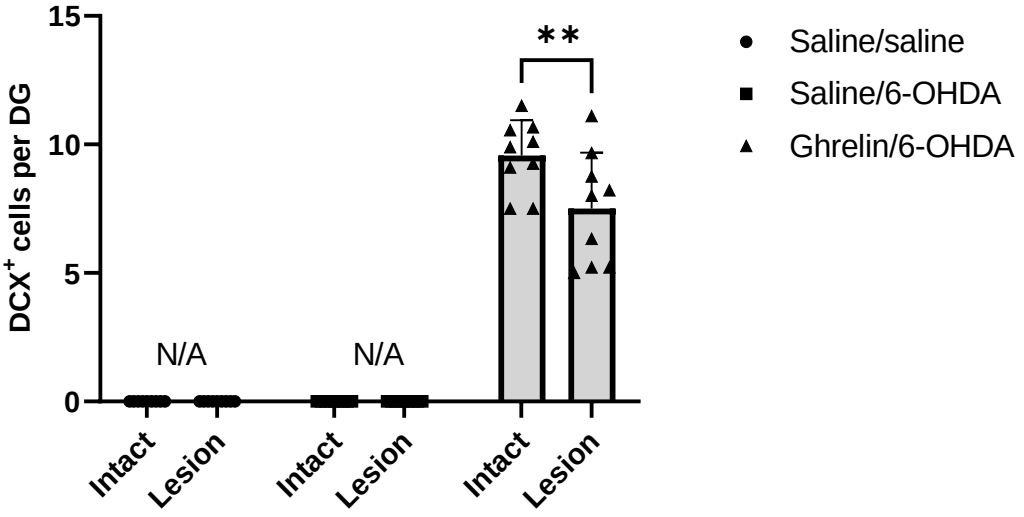

Figure 4.5 A 6-OHDA induced lesion causes a reduction in the number of immature neurones. IHC-IF was performed for anti-TH and anti-DCX on rat hippocampal sections. (A) Two-way ANOVA was performed the comparison. Saline/saline group and Saline/6-OHDA group data is not applicable due to technical problems. N=9. ns = not significant, *P<0.05, ** P<0.01. All data shown are mean ± SEM. N/A = not applicable.

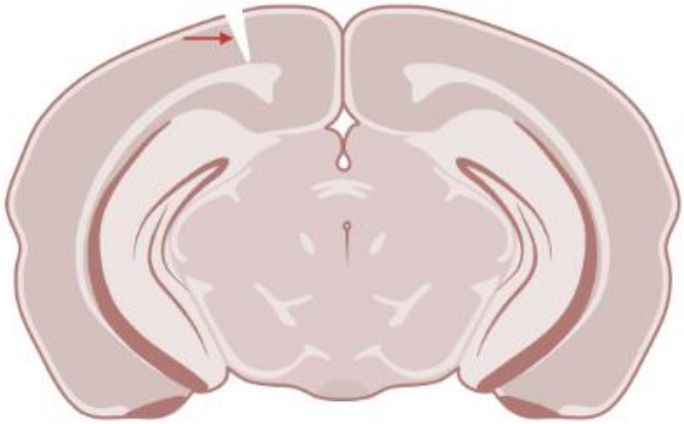

Figure 4.6 Schematic of coronal 6-OHDA rat brain tissue section. Red arrow points to the triangular incision made in the cortex to identify lesioned from intact hemisphere.

4.3.2 Acyl-ghrelin does not regulate adult hippocampal neurogenesis in a mouse MPTP-based model of PD

The mitochondrial toxin MPTP has been widely used to create a mouse PD model in neuroscience research. The intraperitoneal administration of MPTP results in the progressive degeneration of dopamine-containing neurones in the SNpc, with accompanying motor and non-motor deficits (Barata-Antunes *et al.*, 2020). A potential non-motor deficit includes the reduction of adult hippocampal neurogenesis in mice after treatment with MPTP (Agnihotri et al., 2019). The experiment described herein included wild-type (WT) mice and mice with the selective deletion of AMPK in dopamine transporter-containing neurones (AMPK-KO^{DAT}).

Two-way ANOVA analysis revealed that MPTP increased the number of new adult-born immature neurones significantly in acyl-ghrelin-treated WT mice when compared to the acyl-ghrelin / saline-treated group ($p=0.0074$, Figure 4.4, Mean 0.0003748 / 0.0006426). In the AMPK-KO^{DAT} group, MPTP did not have a significant effect on the number of cells expressing DCX in the DG ($p>0.99$). Notably, acyl-ghrelin did not increase the number of DCX^{+} cells in either WT or AMPK-KO^{DAT} mice, apart from in the MPTP-treated WT mice. For example, in WT mice, the acyl-ghrelin / saline group was not significantly changed compared to the saline/saline group ($p=0.94$). Similarly, the saline / saline group vs acyl-ghrelin / MPTP group ($p=0.51$), and the saline / saline group vs the saline / MPTP group, revealed no significant differences ($p>0.99$). These data suggest that acyl-ghrelin and MPTP had little effect on the number of DCX^{+} immature neurones in the adult mouse hippocampus of this experiment.

For AMPK-KO^{DAT} mice, acyl-ghrelin treatment did not show any statistically significant effect across any of the groups tested (see Table 4.1). Similarly, comparisons between the saline/saline group and the saline / MPTP group revealed no differences ($p>0.99$). MPTP neurotoxicity was confirmed using TH^{+} IHC within the SNpc (as described in Bayliss et al.2016), however, no significant decrease in hippocampal DCX^{+} cell number was reported here; saline/saline group vs saline / MPTP group ($p>0.99$); acyl-ghrelin / saline group and acyl-ghrelin / MPTP group ($p>0.99$), shown in Figure 4.8. Future work will include the exploration in SVZ.

These data suggest that;

- the removal of AMPK from DAT^{+} cells had no effect on immature neurone number in the hippocampus, as reported by DCX immunoreactivity
- the neurotoxin MPTP has no effect on the number of immature neurones in the adult mouse hippocampus, and that
- acyl-ghrelin was only pro-neurogenic when administered to WT mice receiving MPTP.

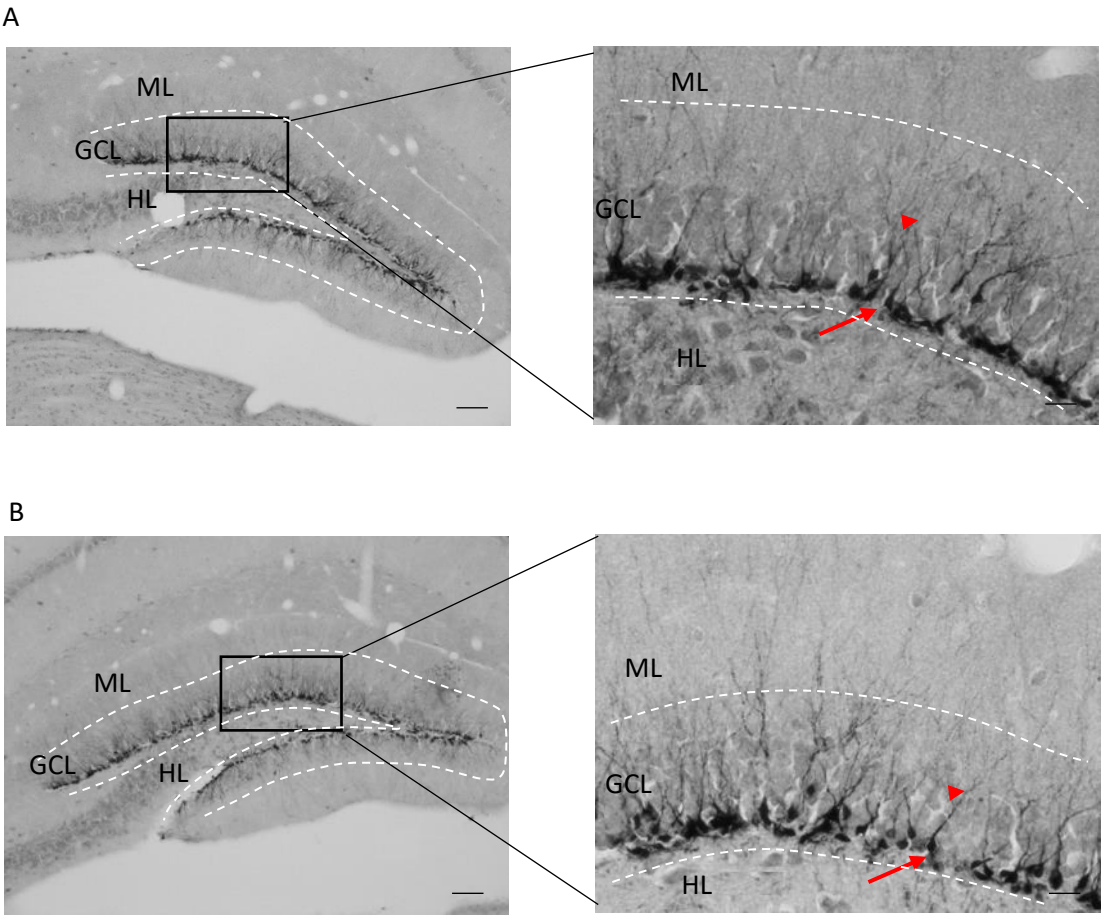

Figure 4.7 The expression of DCX^{+} cells in the hippocampus of AMPK-KO^{DAT} mice and WT mice. The DG region in AMPK-KO^{DAT} (A) and WT mice (B). ML, GCL HL mean molecular layer, granular cell layer and hillus. Images were taken by 10X and 40X objective lens. Representative immunolabelled cells are shown by the arrow and arrowhead indicates axons. Scale bar equals 50μm.

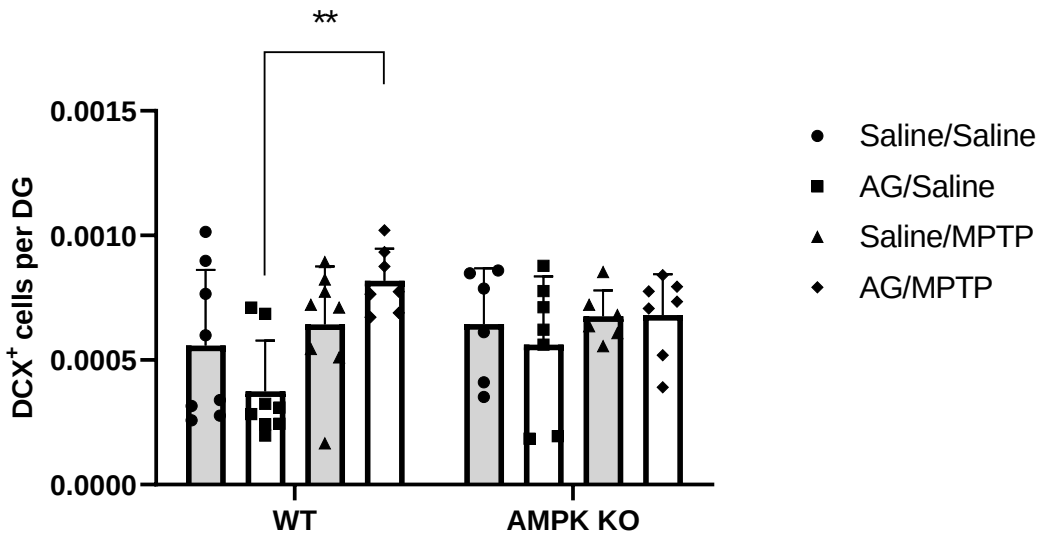

Figure 4.8 Acyl-ghrelin increases the number of Dcx$^+$ cells in the WT / MPTP treated mice. Hippocampal DCX$^+$ cell number was quantified in each experimental group. The wild-type mice included, saline/saline group (n=8), AG/saline group (n=8), saline/MPTP group (n=8), AG/MPTP group (n=7). The AMPK-KO^{DAT} mice also included saline/saline group (n=6), saline/MPTP group (n=6), AG/saline group (n=7), AG/MPTP group, (n=7). Ordinary two-way ANOVA with Sidak's post hoc comparison test was used to perform the comparison. ns = not significant, **P<0.01. All data shown are mean ± SEM.

4.3.3 There was no specific DCX immunostain observed in the post-mortem human hippocampus.

To determine whether the neurogenesis phenomenon is evident in the adult human brain, further experiments using anti-DCX were conducted. The post-mortem human brain tissue used in this study was donated to the UK Parkinson's Disease Society Tissue Bank at Imperial College London with ethical approval (07/MRE09/72). Fixed frozen hippocampal sections (6-8um thick) were placed onto Superfrost+ glass slides and shipped to the Davies lab on dry ice. The control slides were donated by individuals with no evidence of degenerative disease or cognitive decline. The tissue used in this preliminary study was from a male, aged 35 years, with a post-mortem interval of 22 hours.

After comparing different published protocols for assessing neurogenic factors in post-mortem human brain tissue (Table 4.5), an optimized method was adopted considering the properties of the brain tissue quality. Following the Boldrini group protocols (Boldrini *et al.*, 2018), we chose 0.5% sodium borohydride to retrieve the antigen. Another antigen retrieval reagent, sodium citrate was also added to the process to improve immunoreactivity. To decrease the background non-specific staining, NDS was changed from 2% to 10%. Similarly, the concentration of primary DCX antibody was also changed from 1 in 500 to 1 in 200 to enhance immunoreactivity. BSA, which also blocks non-specific binding, was added to the DCX antibody.

Table 4.4

	Boldrini et al.2018	Flor-Garcia et al.2019	Sorrells et al.2018
Antigen retrieval	0.5% sodium borohydride	1X Reveal Decloaker Buffer	10mM sodium citrate
Blocking buffer	20% normal goat serum	10% normal donkey serum	TNB solution (0.1M Tris-HCl, pH 7.5, 0.15M NaCl, 0.5% blocking reagent from PerkinElmer)
Antibody concentration	1 in 200	1 in 200 or 1 in 50	1 in 200
Post-mortem interval (PMI) (Hours)	26	43.55	2.5-10

When observing hippocampal tissue using a light microscope, brown immunoreactive cells were identified by ImmPACT DAB and were particularly concentrated in the DG area. The shape of these cells varied. Some cells presented with a round shape, whilst others had an angled elliptical soma or even an elongated somatic process (see Figure 4.9). Round-shaped cells resemble stem cells whilst elongated somatic cells more closely resemble mature cells (Terreros-Roncal *et al.*, 2022). With regards to comparing the anti-DCX treated tissue and the primary antibody blank treated tissue (negative control), there was no clear and obvious difference in the strength of the immune staining of the cells on treated tissues. Similarly, the observations of the density of the stained cells suggested no difference between the antibody-treated tissue and the negative control tissue, as shown in Figure 4.9. These data suggest that no immature neurones, as identified by DCX immunohistochemistry, were present in these adult human brain tissues.

A Anti-Dcx

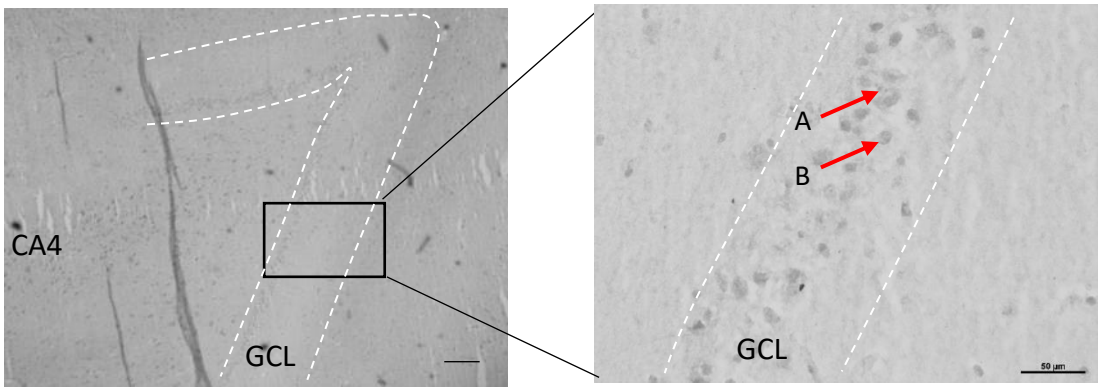

B Negative control

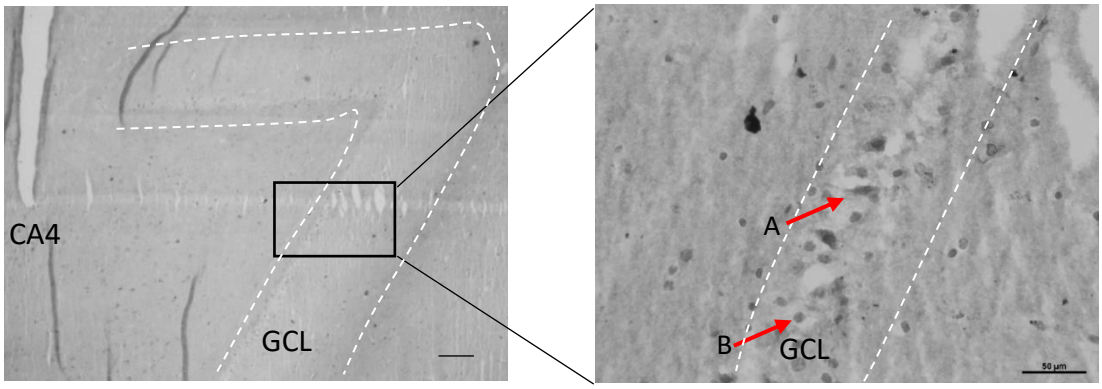

Figure 4.9 DCX⁺ **cells in the post-mortem human hippocampus.** The anti-DCX treated section (A) and negative control section (B). Images were taken by 4X and 40X objective lens. Representative immunolabelled cells are shown by arrows in (A). Arrow (A) shows elongated somatic process. Arrow (B) indicate round soma cells. However, negative control tissue sections (B) also contain cells with a similar appearance. Scale bar is 50µm GCL is granular cell layer.

4.4 Conclusion

In conclusion, for human IHC experiments, the published studies from the Llorens-Martin group suggest that brain tissue processing after death is critical for the successful identification of new adult-born cells in humans. My preliminary studies support this notion. In future work, fresh brain samples accompanied by optimal tissue fixation protocols are required for IHC studies in the adult human brain.

5 Chapter 5 Discussion

The overall aim of the experiments presented in this thesis was to increase our understanding of adult neurogenesis in models of FTD and PD. As a result, more evidence-based data is available that supports the hypothesis that neurogenic deficits occur in these chronic neurodegenerative disorders.

5.1 FTD

One part of my research was to quantify proliferating cells in DG to evaluate hippocampal neurogenesis. The cell proliferation marker, Ki67, was introduced to explore neurogenic mechanisms in these TDP-43$^{Q331K+/Q331K+}$ mice. To reduce sampling bias, ImageJ macro coding was applied to ensure consistent comparisons across all images.

For 2-week-old mice, the IHC resulted in a dense stain on all tissue sections. No significant differences were found through all the Ki67^{+} cell count analyses, with the data from both genotypes being highly similar. Therefore, the TDP-43$^{Q331K+/Q331K+}$ knock-in mutation does not appear to regulate cell proliferation as there was no difference compared to wild-type mice. This interpretation may be explained by the effect of age on neurogenesis. At 2 weeks of age, mice have been deemed neonates with high rates of brain plasticity. Their NSPCs are highly active and rates of neurogenesis remain high. Therefore, it can be argued that the neurogenic process during the neonatal period does not accurately reflect adult hippocampal neurogenesis.

In 6-month-old female mice, Ki67^{+} cell numbers in the DG of TDP-43$^{Q331K+/Q331K+}$ mice were unchanged compared to the WT mice. Whereas the immunoreactive area of Ki67^{+} cells were increased in TDP-43$^{Q331K+/Q331K+}$ mice. This suggests that 6-month-old female TDP-43$^{Q331K+/Q331K+}$ mice may have a slightly increased rate of cell division. This change may be predominantly caused by an alteration in signalling pathways in the caudal pole of the hippocampus.

Apart from using Ki67 to measure the cell proliferation in the DG, the DCX antibody was also used to quantify changes to the immature neurones in the DG. 2-week-old

mice had similar DCX^+ cell numbers between the 2 genotypes. This phenomenon may be due to the young age of the mice, with the Q331K mutation having little to no effect on neurogenesis. The average number of immature neurones per DG section was very high (about 120-150 cells per DG) when compared to 6-month-old animals. The high basal rate of hippocampal neurogenesis in young mice may dilute the impact of the TDP-$43^{Q331K/Q331K}$ mutation on this phenomenon. Interestingly, the DCX immunoreactivity in 2-week-old mice is considerably greater than that observed in the 6-month-old mice. However, it is difficult to accurately quantify the age-related differences due to the heavily expressed DCX shown in the IHC (Figure 3.1), making inter-group comparisons challenging.

For 6-month-old male mice, the average DCX^+ cell number was quantified for each mouse. The comparison shows a significant decline in TDP-$43^{Q331L+/Q331K+}$ mice compared to WT. Based on these analyses, it is evident that the Q331K mutation leads to a decline in neurogenesis. According to Professor Michael S.Fanselow's research, the rostral hippocampus plays a very important role in processing spatial memory while the caudal pole of the hippocampus is associated with processing information associated with mood and anxiety-like behaviour (Fanselow and Dong, 2010). With this in mind, the appropriate data were grouped into sections from either the rostral DG or the caudal DG. Both rostral DG and caudal DG in 6-month-old male TDP-$43^{Q331K+/Q331K+}$ mice demonstrate a reduction in the number of immature neurones, identified by DCX^+ cells when compared to the wild-type mice (Figure 3.6).

To have a better understanding of the effect of the homozygous knock-in Q331K mutation on AHN, I normalised cell counts based on the area of the granule cell layer (GCL) within the DG. In particular, this was important as the GCL area differed between sections, and caudal (ventral) hippocampus sections often required two 10x objective lens fields of view to capture the appropriate area. These analyses demonstrate that TDP-$43^{Q331K+/Q331+}$ knock-in mice have a clear deficit in the number of immature hippocampal neurones compared to wild-type animals.

For 6-month-old female mice, statistics showed a significant difference in the rostral DG while the caudal DG revealed no difference. Based on these discoveries, conclusions can be made as in 6-month-old female Q331K mutation can more easily affect the rostral DG than the caudal part as poor neurogenesis performance was

observed in this experiment. Intact spatial memory function, with an emphasis on pattern separation, highly depends on the functioning of new adult-born neurons. With reduced neurogenesis, the DG structure may struggle to maintain enough new neurones to perform this function. Indeed, pathological changes may be triggered because of this reduction in immature neurones in the hippocampus. Choi et al.2018 report that mice with fewer new adult-born neurones had an increased susceptibility to neurone cell loss in the later stages of AD leading to cognitive decline (Choi, Bylykbashi, Zena K. Chatila, *et al.*, 2018). The impaired rate of AHN in TDP-$43^{Q331K+/Q331K+}$ mice seem to concentrate on the rostral DG and interfere with important cognitive processes, e.g., spatial learning, memory, etc. This phenomenon in these mice correlates with well-characterised impairments in spatial memory function, as measured by the Marble bury test and 5-choice serial reaction time task (White et al.2018). For FTD disease patients, cognitive decline ranks very highly in causing a severe decrease in living quality. One possible reason for this is a shortage of immature neurons resulting in dysregulated hippocampal function, especially in the rostral pole of the DG. Maria Llorens-Martin's group summarised that FTD patients have DG cell loss (Terreros-Roncal *et al.*, 2022). In a post-mortem human FTD brain sample study, morphologically aberrant DG cells were found in adult-born granule cells. Astrogliosis density was increased. The microglial phagocytic index was reduced. The ratio of RGL (Radial glia-like) cells and proliferating cells changed. Neuroblast proliferation marker, HuC/HuD^{+} shows a decrease. DCX^{+} cell number impaired in DG. The neurogenic niche homeostasis changed. It is evidenced that ageing and neurodegenerative diseases reduce AHN. This process may be through hippocampal dysfunction (Terreros-Roncal *et al.*, 2021). Similarly, AHN impairment was also observed in this project. In addition, clinic-based research recruited 75 FTD patients for analysis of hippocampal volumes quantified through a T-1 weighted MRI signal. Results demonstrated that FTD patients have smaller hippocampi than controls, with the MAPT group having the most atrophic changes. MAPT groups covered 29 cases that have MAPT mutations. These studies suggest that hippocampal impairment exists more widely in FTD patients (Bocchetta *et al.*, 2018).

In contrast, analysis of neurogenesis in the SVZ region of these mice revealed no differences in cell proliferation (Ki67) or immature neurone number (Dcx). These data suggest that TDP-$43^{Q331K+/Q331K+}$ have no deficit in neurogenesis within the SVZ.

However, whilst cell proliferation and neurone differentiation occur at a high rate in this area, new adult-born cells will start their migration from the SVZ along the rostral migratory stream before integrating with circuitry within the olfactory bulb. Here, the new cells perform a similar role within the DG as they enable the formation of new distinct memories relating to olfaction (Sahay, Wilson and Hen, 2011). Accurately quantifying the rate of new neurones in the OB requires a BrdU pulse-chase approach. Therefore, we cannot exclude the possibility that whilst cell division and neurone differentiation processes remain intact in TDP-43$^{Q331K+/Q331K+}$ mice, the rate of migration and maturation in the OB may be altered.

During the counting of immunoreactive cells in the 6-month-old female mice, first, the DCX^{+} cell numbers were collected, and then, using ImageJ, the area of the GCL was quantified for normalisation purposes. Along the rostro-caudal axis of the hippocampus there is a change in the size of the DG and accompanying GCL e.g., the rostral part of the DG is smaller than the caudal part of the DG. To reduce possible sampling bias caused by this, the area of the GCL was collected alongside the quantification of cell numbers. Using an MS Excel spreadsheet, the average DCX^{+} cell number per DG section was divided by the average DG area per DG section. This provides a more accurate comparison between both genotypes of all ages.

This project also compared the dcx^{+} cell number in suprapyramidal and infrapyramidal blades in TDP-43$^{Q331K+/Q331K+}$ mice and their WT littermates. The immature neurone number and morphology were not associated with either the supra- or infra-pyramidal blade of the DG.

The comparison revealed that in TDP-43$^{Q331K+/Q331K+}$ 6-month-old female mice, the rostral hippocampus had fewer immature neurones when compared with the wild-type mice. In 24-month-old male mice, IHC for DCX immunoreactivity revealed very low rates of neurogenesis. The same anti-DCX antibody concentration, 1 in 750, was used to keep consistency across the whole project. After completing the IHC, very few immunopositive cells were present in the hippocampus and other parts of the brain. Microscopy analysis confirmed that the immunoreactivity was not comparable with 6-month-old mice. The density of the immune stain from DCX^{+} cells was relatively weak when compared to that of 6-month-old mice. Quantification of DCX^{+} cell numbers in the 24-month-old mice was performed by manual counting since most of

the sections only contained a few immunostained cells in the GCL. The low DCX^+ cell number may be due to the age of these mice as age accelerates the decline of NSPC activity and subsequent new adult-born neurone formation. The low basal rate of neurogenesis in 24-month-old WT mice may explain why the reduction in DCX^+ cell number in TDP-$43^{Q331K+/Q331K+}$ mice did not reach statistical significance.

In this project, the DCX antibody was widely used throughout the experiments. During optimisation of IHC, the 1 in 750 concentration was shown to consistently stain the immature neurones with little background immunoreactivity, while the antibody protocol suggests 1 in 500. The 1 in 750 dilutions were preferred for my experiments and also saved on the use of antibodies. However, there were still some problems in the process. For 6-month-old animals, the DCX immunoreactivity stained the immature neurones in the DG area. Using light field microscopy, we noticed most of the cells showed a clear and distinct shape from each other, allowing for the efficient collection of data. However, using the same concentration of DCX antibody for 2-week-old animals, the DCX immunoreactivity was very strong. When using light-field microscopy to collect images, we noticed that the DCX^+ cells overlapped with each other. This level of DCX^+ immunostaining made it difficult to collect the data. When the DCX^+ cells cannot be distinguished from each other, it will potentially create less accurate quantification. In contrast to the strong DCX immune activity in 2-week-old animals, 24-month-old mice showed a different result when the same DCX antibody concentration was used. Light field microscopy revealed a weak DCX immune reactivity. This low level of stain can directly affect the accuracy of quantification because the background stain is difficult to exclude and careful analysis is required.

The immune reactivity showed a varied level from 2-week-old to 24-month-old animals, which could indirectly lead to uncontrolled experiment bias. Discussions were performed within our research team about how to reduce this potential bias. However, to keep consistency throughout the whole experiment, the same concentration of DCX antibody was selected. This allowed us to compare the DCX^+ cell number between mice from different age groups.

Furthermore, in peer-reviewed published papers, research consistency is emphasized and encouraged. Maintaining the same antibody concentration throughout the project is considered a key element to completing a successful research project. This also

provides other researchers with a valid reference to compare data sets from different laboratories and emphasises the importance of optimising quantification methods.

Ageing has been shown to play a very important role in adult neurogenesis. In post-natal rodents, neurogenesis starts to decline quickly after the first month (Gillotin *et al.*, 2021). In primates, neurogenesis drops sharply around birth and continues to decrease until a sexually mature age (Gillotin *et al.*, 2021). In mammals, the SVZ and DG have been widely accepted as the 2 main active neurogenic niches (Gillotin *et al.*, 2021). Some researchers indicate that during ageing there is a down-regulation in the rate of cell proliferation and survival of new adult-born neurones, which was shown using the thymidine analogue BrdU. Using IHC, researchers reported that astrocytes showed no change during ageing in the hippocampus. However, oligodendrocytes and microglial cell numbers decreased in the mouse hippocampus (Hayakawa, Kato and Araki, 2007). In this project, DCX was chosen to identify immature neurones and Ki67 was selected to identify proliferating cells. In the DG of TDP-43$^{Q331K/Q331K}$ mice and WT mice, DCX^{+} cell number decreased significantly between 6 and 24 months. There was also a significant decrease in the number of DCX^{+} cells in the SVZ. These results support the notion that ageing affects adult hippocampal neurogenesis in a negative manner. The reduced number of immature neurones could lead to a reduced activity in the function of adult born neurones. Regular brain function relies heavily on the performance of neurones. In elderly rodents, it is common to find brain function degradation, e.g., memory loss, and limb accuracy decline (Mahncke, Bronstone and Merzenich, 2006). Brain diseases like PD and AD are more common in elderly people, which may further exacerbate symptoms of dementia (Deschenes and McCurry, 2009). This might be explained by experiments investigating the loss of immature neurones during ageing (La Rosa, Ghibaudi and Bonfanti, 2019). Within the hippocampal neurogenic niche when older cells go into a state of atrophy, their activities will cease until new mature neurons take their place. In other brain areas, when neurones are damaged, other neurones may adjust to take over the functions. However, this functional replacement is not always fully effective leading to pathologic changes in cellular function (Pekna and Pekny, 2012). A reduction in the number or function of immature neurones in the neurogenic niche could lead to fewer new mature neurones that are needed for spatial memory discrimination. (Scharff, 2000)(Martino, 2004). As time progresses, more neurones die that are not replaced and thus, pathological

changes may appear alongside the degradation in function of the neurological system (Rubinsztein *et al.*, 2005).

This emphasises the need to understand neurodegenerative diseases in the context of ageing. Ageing is a process that can affect the characteristics of cells, including their molecular activities and clearance pathways, which altered the accumulation of proteins within cells. New adult-born neurones integrating with hippocampal circuitry are considered one way to maintain cellular activity and circuit function in the ageing mammalian brain. An age-related decline in new adult-born hippocampal neurones is thought to contribute to the decline in spatial memory performance in aged individuals (Montaron *et al.*, 2006). Indeed, the loss of new adult-born hippocampal neurones was shown to accelerate the loss of neurones in a mouse model of AD (Choi, Bylykbashi, Zena K Chatila, *et al.*, 2018). This report suggests that the paradigm of AHN may be an important and understudied factor in maintaining brain cell health in ageing. Consequently, finding ways to promote AHN during ageing is considered an important aim.

The Tau protein has drawn the attention of academics for years. The function of Tau is related to the structure of the microtubule. In brain disease research, Tau is also considered an important and possible pathogenic factor in bvFTD. Post-mortem analysis of FTD patients has reported a significant accumulation of Tau protein (Neumann and Mackenzie, 2019), which is predominantly made up of 4R-Tau (Ghetti *et al.*, 2015). The accumulation of Tau in cells is considered pathological (Imahori and Uchida, 1997).

In neurodegenerative diseases, abnormal accumulation of tau protein has also been observed (Houben *et al.*, 2021). PHF1-Tau antibody is a mouse monoclonal antibody specific for phosphorylation sites S396 and S404 in tau. It was used to perform the experiments in this project. Colocalization with DCX was used to assist in exploring the relationship between Tau protein and immature hippocampal neurones. The results suggested a correlation between FTD pathology and a decrease in neurogenesis. In this IF work, I found that all DCX^+ cells were PHF1-Tau^+, but there were PHF1-Tau^+ cells that were DCX^-. Tau accumulation occurs mainly in older cells, but this experiment suggests that this phenomenon occurs in new immature DG neurones before they mature. But whether the early stage of Tau accumulation is protective or

toxic is still unclear (Farizatto *et al.*, 2017). The involvement of Tau in AHN was studied here using TDP-43$^{Q331K/Q331K}$ mice where DCX$^{+/}$PHF1-Tau^{+} cells were quantified. The statistical analysis confirmed that the mutation resulted in fewer immature neurones that were PHF1-Tau^{+}.

No matter whether a cell is PHF1-Tau positive or negative, the number of DCX^{+} cells is decreased in TDP-43$^{Q331K/Q331K}$ compared to wild-type mice. This outcome is consistent with the other experiments carried out on the same animals but using nickel-enhanced DAB-IHC for DCX in place of IF. Based on these two experiments, I confirm that there is a significant decrease in the number of immature neurones in the knock-in mice, suggesting that the human TDP-43 homozygous Q331K knock-in mutation decreases neurogenesis in adult mice.

Using the same counting method, cells expressing PHF1-Tau but not DCX were quantified. DCX^{+} cells are considered immature neurones or recently divided neuroblasts, which are distinguished based on their cellular morphology. No significant difference in the number of DCX^{-}/PHF1-Tau^{+} cells in the two groups was reported, suggesting that mature neurones and stem cells which contain accumulated 4R Tau were not affected by TDP-43$^{Q331K/Q331K}$. The average percentage number of DCX^{-} PHF1-Tau^{+} cells in the DG was calculated for wild-type and TDP-43$^{Q331k/Q331k}$ mice. Calculating it this way reduces the impact of the different sizes in DG areas in different sections. Based on this, TDP-43$^{Q331K/Q331K}$ mice contain hippocampal cells, that are Dcx^{-}, with accumulated phospho-tau protein. This may suggest that the homozygous TDP-43 Q331K knock-in causes more cells to start accumulating phospho-tau protein. The aberrant expression of phospho-tau in the hippocampus of this mouse model also coincides with reports of mis-splicing of the tau gene (Kim *et al.*, 2020)(White, Kim, Duffy, Adalbert, Phillips, Peters, Stephenson, Yang, Massenzio, Lin, Andrews, Segonds-Pichon, Metterville, Saksida, Mead, Ribchester, Barhomi, Serre, Coleman, J. Fallon, *et al.*, 2018). In this research, TDP43-Q331K mice showed deficits in motivation and cognition which is similar to the syndrome of FTD (Kim *et al.*, 2020). Apathy-like behaviour was also observed in these mice which were also reported in patients (Kim *et al.*, 2020). In other mouse models of FTD, such as TAU58/2 mice, tau is also observed to accumulate in neurones (Ke *et al.*, 2019). Scholars also reported that tau accumulation can impair axonal plasticity in cell line studies (Sohn *et al.*, 2019).

In my colocalization experiment, most DCX^+ cells showed evidence of PHF1-Tau accumulation. These cells normally refer to immature neurones which go on to replace the older granule cell neurones that have reduced functionality. Further work is needed to determine the molecular mechanism underpinning the reduced AHN observed in TDP-$43^{Q331K/Q331K}$ mice, including the role of inflammation and the mechanisms underpinning the altered appetite reported (Kim *et al.*, 2020).

Researchers discovered that epilepsy could cause a significant cell density difference between the suprapyramidal and infrapyramidal blades of the DG (Snyder, Ferrante and Cameron, 2012)(Scharfman, Helen E et al). It suggested that infrapyramidal blades of the DG have a higher cell density than the suprapyramidal blade (Snyder, Ferrante and Cameron, 2012). This suggests that the two blades are regulated independently and may have distinct contributions to cognition and disease. Further research revealed that mossy fibres have more connections in the infrapyramidal blade in comparison to the suprapyramidal blade (Claiborne, Amaral and Cowan, 1986). Mossy fibres relay frequent electric signals from the GCL of the DG to the CA3 (Haustein *et al.*, 2014), which is important for spatial memory function. Notably, the GCL also receives perforant path inputs from the entorhinal cortex to regulate memory processes (Luna *et al.*, 2019). In my doctoral project, the number of DCX^+ cells in both blades was quantified. Regardless of whether the cells were DCX positive or negative, in TDP43 homozygous Q331K knock-in mice, the number of cells that contain detectable phospho-tau in the suprapyramidal blade was significantly higher than in the infrapyramidal blade. The discrete circuits regulating each blade may account for the observed differences in AHN.

In this project, the influence of sex was also explored in terms of its effect on neurogenesis. The experimental study included 6-month-old WT and TDP-$43^{Q331k/Q331k}$ mice, which provided an indication of hippocampal cell proliferation and immature neurone number without the influence of old age. Based on the number of DCX^+ cells, male WT mice had significantly more DCX^+ cells in SVZ in comparison to female WT mice. A similar trend was seen in TDP-$43^{Q331k/Q331k}$ mice but this was not statistically significant. In the SVZ, a significant decrease in DCX+ cells was observed in both male WT and male TDP-$43^{Q331k/Q331k}$ mice compared to female mice.

This suggests male mice have an increased number of immature neurones. Sex hormones may play an important role in this situation. As it is widely known that testosterone can accelerate the build-up of muscle protein, muscle tissue growth and wound recovery (Jiang, 2019), it may have a similar positive function on hippocampal neurogenesis (Spritzer and Roy, 2020). Furthermore, a higher level of testosterone in the blood can increase physical activity (Eliakim *et al.*, 1998). Since physical movement, e.g., running, increases AHN (Spritzer and Roy, 2020) and cognitive performance (Fanaei *et al.*, 2014), this may be an indirect mechanism that explains these results (Spritzer and Roy, 2020). Lastly, testosterone can affect the cardiovascular system, causing an increased heart rate and blood circulation. I speculate this is a positive contribution to brain activity, especially from a molecular histology point of view (Galea *et al.*, 2013). Conversely, levels of oestrogen are higher in females than males (Viña *et al.*, 2005). In animals, oestrogen accelerates the maturation of reproductive cells in the ovary (Stewart, Mattiske and Pask, 2020). This may have an influence on hippocampal NPCs to speed up the differentiation process (Galea *et al.*, 2013), but further investigations are needed to assess the impact of these hormones on neurogenesis in models of FTD. Furthermore, oestrogen can reduce the risk of cardiovascular incidents by improving vascular permeability (Vin, Allaert and Levardon, 1992), this may potentially attenuate the supply of oxygen (Lee *et al.*, 2013). Some researchers reported that dividing SVZ stem cells are tightly located with blood vessels during regeneration (Tavazoie *et al.*, 2008). An increased supply of oxygen could improve the neurogenic environment for stem cells, but it is unclear whether this will accelerate the maturation process (Segura *et al.*, 2016) (Zhang *et al.*, 1999). Also, the correlation between oxygen and peroxidase in the hippocampus could be another regulator of neurogenesis. Researchers found diet can increase peroxidase approximately four-fold in the rat hippocampus (Ziegler *et al.*, 2003). The authors speculate this may suggest peroxidase plays an important role in hippocampal cell growth (Ziegler *et al.*, 2003). Peroxidase is known to cause damage to the cell cycle, mitochondrial function, and autophagic activity, which will indirectly cause cell death (Bullon, Newman and Battino, 2014)(Boonstra and Post, 2004). I speculate that an improved vascular permeable function may enhance autophagy and increase peroxidase pathway signalling which could contribute to cell differentiation and cell death (Bullon, Newman and Battino, 2014). More investigations into the effect of hormones on neurogenesis during FTD are needed (Stute *et al.*, 2021).

In Chapter 3, I describe that DCX^+ cells contain differently shaped cell bodies and axons. More specifically, the soma of some immature neurones had a round shape whilst others have a more angular structure. With regard to the axons, some cells had no axons, whereas other cells show an elongated custom structure. These findings emphasise the difference in structure between neurones which express DCX. This may suggest that immature neurones are made up of a diverse group of different DCX^+ cell types which have similar but distinct morphology, which can also be referred to as a 'stage'. The morphology of immature neurones with different 'stages' was originally described in 2006 and forms the basis of my structural analysis of the DCX^+ cells (Plümpe *et al.*, 2006). Based on the different structural shapes of the soma and the process all the DCX^+ cells were grouped into 6 categories, from A to F. Categories A and B are defined as being the proliferative stages, and the cell shapes are close to that of NPCs. More specifically, category A includes cells that have a round cell body, which is considered the closest to the stem cell stage. These cells do not have processes or an angled cell body shape. From category B to F, neurones have processes of increasing lengths. Category B was defined as having short, plump processes, and small processes that can extend in different directions. Categories C and D are referred to as the intermediate stages, which cover the medium-length processes, or the process can reach the molecular layer. For most of the immature neurones in these 2 groups, the processes extend to the molecular layer. Some researchers believe the direction of process extension is guided by neuronal molecules (Mikkonen *et al.*, 1998) to ensure the process is sprouting into the molecular layer. The neurons of the postmitotic stage are in categories E and F, which can have one or more dendrites. The dendrites of Category E cells normally reach the molecular layer and have a simple branched structure. The dendrites of category F cells normally have several branches of the secondary dendrites which resemble mature neurone morphology. Interestingly, researchers also found that the DCX^+ cell numbers varied in different maturation stages (Moreno-Jiménez *et al.*, 2019).

All the DCX^+ cells were manually assessed and grouped into these 6 categories. The majority of these cells were of category B, followed by category A. A possible explanation for this is that immature neurones spend longer in this particular stage of differentiation. Another possible explanation is that the cell proliferation and survival rates decrease after they go through stage or category B resulting in fewer cells

continuing into differentiated mature neurones. There is very little difference in the distribution between cells in categories C, D, E and F suggesting that cell survival becomes stable in these stages.

In the DG no significant differences were reported between the number of DCX^+ cells in the 6 categories of neuronal differentiation in 6-month-old WT and TDP-$43^{Q331K/Q331K}$ mice. However, in 6-month-old male TDP-$43^{Q331K/Q331K}$ mice, the rostral infrapyramidal blade contained a significantly greater number of DCX^+ cells in category B in comparison to WT mice. Collectively, these data suggest that the switch from category B to C-F may be vital for immature neurone development into functional new adult-born granule cell neurones. Understanding the molecular pathways regulating this developmental period may allow us to reduce cell death and improve immature neurone survival to enhance hippocampal pattern separation performance (Moreno-Jiménez *et al.*, 2019). Intriguingly, the homozygous TDP-43 Q331K knock-in mutation seems to have a particular effect on the number of category B neurones in the infrapyramidal blade of the rostral pole of the hippocampus. It isn't clear why there may be a spatially restricted effect of this mutation on a discrete part of the hippocampal GCL, however, there is evidence of discrete populations on NSCs residing within the neurogenic niches. For example, the Doetsch lab demonstrated the existence of a discrete subset of NSCs in the ventral SVZ that are stimulated by hypothalamic circuits to generate distinct olfactory bulb neurones (Paul, Chaker and Doetsch, 2017). With the development of single-cell RNA sequencing and spatial transcriptomic assays to identify mRNA expression in brain tissue slices, defining the molecular pathways underpinning this response is technically achievable and is required to delineate the role of TDP43 in this paradigm.

AHN isn't widely studied in models of FTD/ALS. However, AHN in humans was reported to exist throughout life (Moreno-Jiménez *et al.*, 2019). This report focuses on the plasticity of hippocampal circuitry related to AHN. In humans, up to the ninth decade of life, thousands of immature neurones were observed in the DG (Moreno-Jiménez *et al.*, 2019). The authors also explored the different stages of immature neurones, demonstrating that most of the immature neurones achieved a dentate granule cell fate (Moreno-Jiménez *et al.*, 2019). The author also tested that DCX is a valid immature neurones marker (Moreno-Jiménez *et al.*, 2019).

In-vivo experiment, AHN was explored together with tau protein. Data suggests tau protein was not related to regulating AHN (Pallas-Bazarra *et al.*, 2016). However, tau is necessary for newborn granular neurones maturation (Pallas-Bazarra *et al.*, 2016). Stress can cause newborn granule neurones' death, but this process is dependent on the existence of tau protein (Pallas-Bazarra *et al.*, 2016).

5.2 PD

In this chapter, I studied the effect of a unilateral MFB 6-OHDA-lesion on AHN in rats, where SNpc dopamine neurone loss has previously been confirmed (Rees *et al.*, 2022). In order to confirm the lesioned hemisphere in coronal free-floating sections, double immunofluorescence was used, labelling TH^+ and DCX^+ cells. The TH^+ cells allowed the identification of dopaminergic cells within the SNpc, whilst the DCX^+ cells identified immature neurones within the dentate gyrus of the hippocampus. This method was appropriate for assessing the impact of the unilateral loss of SNpc dopaminergic cells on AHN. In this model, we showed that in the lesion group, a reduction in SNpc TH^+ cell number correlated with a reduction in DG DCX^+ from the same brain hemisphere. Compared with previously published data, these results reveal similar depletion of dopaminergic neurones in the SNpc following treatment with 6-OHDA in the rat. Interestingly, a study reported no significant difference in DCX^+ cell numbers in the DG (Worlitzer *et al.*, 2013). Several published papers have reported a significant decrease in DCX^+ cell number in the DG of the 6-OHDA rat model and adopted this model for further experiments (Tajiri *et al.*, 2010)(Krishnamurthi *et al.*, 2009). However, in these studies, 6-OHDA was injected into the striatum rather than the MFB. This route of administration may explain the different results described. Further exploration of the pathways involved may improve our understanding of impaired hippocampal neural stem/progenitor plasticity in models of PD.

These data suggest that loss of SNpc dopamine neurones on the 6-OHDA injected side of the brain results in reduced innervation of the hippocampal neurogenic niche, which is consistent with reports of reduced neurogenesis in the hippocampus of humans diagnosed with PD compared to cognitively intact control patients (Höglinger *et al.*, 2004). Another very interesting element that may need to be taken into consideration

is the potential effect of brain injury caused by the intra-MFB injection of 6-OHDA. In order to maintain experimental consistency, the sham-lesion group received a saline injection, using the same stereotactic coordinates and volume. It is unclear if the injection injury affected the experimental results, however, compared with the toxicity induced by 6-OHDA, the injection injury can be considered mild with recovery within a short time. Analysis of the 3 different groups revealed no statistical differences in DCX^+ cell number. However, given the technical challenges of maintaining tissue section integrity during the free-floating IHC protocol, further exploration of this disease model is needed. For example, it would be beneficial to process the IHC work using single hemispheres, using bilateral 6-OHDA MFB injections to create the lesioned brain or placing the tissue sections directly onto glass slides during the cryo-sectioning, followed by IHC staining. These practical modifications to the protocol would provide more reliable data regarding hippocampal neurogenesis in this rat model of PD.

To determine whether inducing mitochondrial inhibition and subsequent SNpc neurone toxicity would inhibit AHN in the mouse, we used the MPTP model of PD. More specifically, we used a model where MPTP-induced SNpc dopamine neurone loss had been confirmed and the neuroprotective effect of acyl-ghrelin was dependent on AMPK (Bayliss et al.2016). This mouse model of PD has been associated with impaired AHN in published studies (Ahn *et al.*, 2019). Notably, our data revealed that DCX^+ cell numbers were significantly increased in the AG / MPTP group compared to the AG/saline group, in wild-type mice. This comparison revealed that under the same acyl-ghrelin treatment conditions, MPTP increased the DCX^+ cell number. This result seems counterintuitive given MPTP's long-known effect of inhibiting mitochondrial calcium homeostasis, resulting in dopaminergic cell death within the SNpc and cutting the dopamine supply to the hippocampus (Kidd, Hvoslef-Eide and Thomas, 2014). Having said that, saline / MPTP treatment did not affect DCX^+ cell number compared to saline/saline treated mice. Therefore, MPTP only increased DCX^+ cell number in mice that were also treated with acyl-ghrelin. This effect was not observed in mice that lacked AMPK expression in DAT^+ cells. It is unclear why MPTP would exacerbate the neurogenic effect of acyl-ghrelin, one possible reason is that it may be due to its relatively mild toxic impact on cells. Furthermore, mild stress can also trigger a protective response, which is called hormesis. MPTP may be

inducing hormesis in this study by triggering significant – but not total - SNpc dopamine neurone death, with the hippocampal NPCs continuing to receive dopaminergic innervation from the midbrain. This may allow NPCs to achieve a recovery in function after a short time in this model, while the 6-OHDA model induced almost complete (~90%) dopaminergic cell loss in the SNpc. Further validating research such as analysis of TH/DCX at different stages after MPTP are needed to provide evidence for these explanations.

In general, further exploration of AHN is necessary to validate if there is an AHN deficit in other genetic models of PD. Alpha-syn A53T model of PD has been shown to have impaired AHN (Parihar et al., 2008). The generation of iPSC-derived neurones from PD patients is also an interesting area that should be used to determine if the neurogenic function is altered in PD. Interestingly, human NSC models of neurogenesis are shedding light on this form of brain plasticity and could be modified to study the effect of the ghrelin pathway in the context of PD (Dias *et al.*, 2021).

Compared with 6-OHDA, MPTP (1-methyl-4-phenyl-1,2,3,6-tetrahydropyridine) is a relatively mild toxic reagent used to create PD animal models. In particular, the mouse MPTP model is commonly used within the neuroscience research community to study aspects of PD. MPTP selectively targets the dopaminergic neurones in the substantia nigra, induces cell death and decreases dopamine production (Du *et al.*, 2001). Unlike 6-OHDA, MPTP can cross BBB. It can be selectively taken up by astrocytes and converted into MPP+. Dopaminergic neurones can selectively sequester MPP+ where it exerts its neurotoxic effects (Schmidt *et al.*, 1997). At the molecular level, MPTP can alter the free movement of ions and small molecules, which can eventually cause depolarization of the mitochondrial membrane, and ATP depletion followed by cell death (Elustondo *et al.*, 2016). One of the reasons why MPTP has been widely used is its ability to create symptoms of PD in many species, including humans, monkeys and mice (Langston *et al.*, 1983)(Uhl, Javitch and Snyder, 1985). MPTP can be administered via intraperitoneal injection to induce SNpc cell loss, removing any confounding effects of surgery e.g., bleeding, and inflammation. In the clinic, inflammation is regarded as an important aspect driving the progression of dementia. Surgery can generate brain trauma. Brain trauma can cause damage to brain tissue and structures leading to lasting impaired function after the trauma. I speculate that the brain trauma caused by surgery can exacerbate the effect of 6-OHDA. However, brain

repair mechanisms may attenuate the effects of surgical trauma. When these 2 elements happen at the same time, it is difficult to measure the outcome. To limit the impact of trauma on experimental outcomes, surgery should only be performed by fully trained and skilled operators.

In relation to AHN, cell proliferation was reduced in MPTP-treated mice (Höglinger *et al.*, 2004), whilst in the mouse olfactory bulb, MPTP caused a reduction in the number of adult-born neurones (Yamada *et al.*, 2004). In the hippocampus, MPTP reduced the number of adult-born neurones and neural plasticity in this model (Schlachetzki *et al.*, 2016). In two published studies, acyl-ghrelin i.p. injection was reported to attenuate dopaminergic neurone loss (Andrews, 2011)(Moon, H. G. Kim, *et al.*, 2009)(Andrews *et al.*, 2009). Also, when administered with MPTP, ghrelin knockout mice and ghrelin receptor knockout mice had greater neurone loss compared to control mice (Andrews *et al.*, 2005). However, the number of DCX^+ cells was significantly different between the AG/saline group and AG/MPTP groups in wild-type mice. This comparison revealed that under the same acyl-ghrelin condition, MPTP increased the number of DCX^+ cells within the GCL. Given MPTP's long-known function in mitochondrial calcium homeostasis driving pathologic change in transporting energy to cause dopaminergic cell death resulting in reduced dopamine supply for the hippocampus, this result seems counterintuitive and is opposite to what was hypothesised. One possible reason for this is the relatively mild toxic impact on cells. Indeed, mild stress can also trigger a protective response. After causing the death of immature neurons, it is possible that the surviving NSPCs recover their cell function leading to the generation of new DCX^+ cells, whilst 6-OHDA induces an almost complete dopaminergic cell loss in the SNpc. Indeed, NSPCs are reported to attenuate MPTP-mediated toxicity on the behaviour of aged mice (Gnanasegaran *et al.*, 2017). However, further exploration is necessary to validate if there is an AHN deficit in AMPK ko mice, and if other genetic models of PD show a decrease in AHN and related behaviour. The role of iPSC-derived neurones generated from PD patients is also an interesting methodological approach that would allow the assessment of neurogenesis in a tightly controlled experimental environment.

In this project, acyl-ghrelin did not induce an increase in AHN. However, in two experiments using rat models, acyl-ghrelin was reported to increase memory performance. One experiment used intracerebrovascular administration of acyl-

ghrelin (Carlini *et al.*, 2002), whilst the other used an intrahippocampal route (Carlini *et al.*, 2004). The peripheral administration of acyl-ghrelin was also reported to increase spatial memory performance in mice (Diano *et al.*, 2006). In this experiment, acyl-ghrelin also increased neurone synapses formation (Diano *et al.*, 2006). In addition, ghrelin knock-out mice were analysed (Diano *et al.*, 2006). These mice showed a reduced spatial memory performance from their WT littermates (Diano *et al.*, 2006). However, this impairment was attenuated following the administration of acyl-ghrelin intra-peritoneally (Diano *et al.*, 2006). Electrophysiological analysis can also be used to assess hippocampal effects of acyl-ghrelin. Hippocampus excitability was increased by acyl-ghrelin treatment in rats which coincided with improved memory performance following treatment (Carlini *et al.*, 2010). In a rat model of AD, 2-weeks of i.v acyl-ghrelin treatment was reported to improve memory performance (Eslami, Sadeghi and Goshadrou, 2018). Synaptic plasticity was also improved after acyl-ghrelin treatment in this experiment (Eslami, Sadeghi and Goshadrou, 2018). Given the increasing evidence for acyl-ghrelin promoting hippocampal neurogenesis and memory function more research is needed to elucidate the role of both MPTP and AMPK in this context.

5.3 Human AHN

In relation to our exploratory post-mortem human brain IHC work, the DCX antibody-treated tissue sections identified brown-stained immunoreactive cells in the DG. The morphology of some of these cells was similar to the immature neurones reported in rodents, with oval-shaped cell bodies and leading processes. However, the negative control brain tissue, which received saline rather than the primary anti-Dcx antibody, also contained immunoreactive cells. When carefully comparing the cell soma shape, the structure of the leading process, the size of the cells, the nucleus pattern from the staining, and the location of the cells within the DG, we concluded that there were no differences between the stained cells in both anti-Dcx treated and negative control tissues. This result suggests that the DCX antibody used does not reliably identify DCX^+ immature neurones in the specific tissue and conditions of my experiment. The Boldrini et al.2018 study also used anti-DCX to label immature neurones and identify DCX^+ cells with a similar shape. Their experiments revealed that immature neurones

were preserved while the neuroplasticity declined in older patients (Boldrini et al., 2018). A possible reason for our differing results is that their group used a different antibody; anti-DCX from Guinea pig (Millipore) in comparison to Goat anti-DCX (Santa Cruz) which was used in my analysis (Boldrini *et al.*, 2018). Another group recently explored the presence of immature neurones in Alzheimer's disease using human brain samples. Their data demonstrated that AHN was impaired in AD-diagnosed patients (Moreno-Jiménez *et al.*, 2019). Interestingly, from their published images, similar DCX^+ cell shapes were observed. PMI is another key element for Human IHC work (Terstege *et al.*, 2022). Fresh tissue is reported to allow for the detection of DCX via IHC (Terstege *et al.*, 2022). Moreno-Jimenez et al. selected tissues which only have 2.5 hours to 10 hours of PMI (Moreno-Jiménez et al., 2019). This may be the reason that their IHC can detect AHN in the adult human brain.

Another possible explanation for the data obtained in my study is that the DCX antibody is not specific, causing a unknown immune reaction during IHC. However, several experiments were performed using sterile saline that was proved clean and effective. Another explanation is that the DCX antibody used is not applicable to human tissue. The Boldrini group (Boldrini et al.2018) used Rabbit anti-DCX (Sigma-Aldrich) and Guinea pig anti-DCX (Millipore). The Lorens-Martin group used Goat anti- DCX (Santa Cruz Biotechnology), Mouse anti-DCX (Santa Cruz) and Rabbit anti-DCX (Moreno-Jiménez *et al.*, 2019). In this project, Goat anti- DCX (Santa Cruz Biotechnology) was used. However, it also stained neurones in the control tissue. While my doctoral project used Goat anti-DCX (Santa Cruz), future studies will need to select other DXC antibodies used in recently published studies. Further experiments will be needed to clarify the existence of immature neurones in the human hippocampus.

In post-mortem brain tissue from cancer patients aged between 58 – 72 years, researchers detected evidence for the existence of neurogenesis in the adult hippocampal DG. The thymidine analogue, BrdU, was used in these individuals to label dividing cells within tumour biopsies. The scientists demonstrated the uptake of BrdU into cells within the hippocampus, providing evidence for cell division in the adult brain (Eriksson *et al.*, 1998). However, BrdU was later shown to be a mutagen, leading to altered DNA stability and cell death (Taupin, 2007). For this reason, it is no longer used in human research. Another methodological approach that was developed

to assist with birth-dating cells in the human body involved the spike in atmospheric ^{14}C due to above-ground atomic bomb testing in the 1950-1960s. The ^{14}C-^{12}C decay constant allowed researchers at the Karolinska Institute to quantify the age of neurones collected at post-mortem. These studies demonstrated that AHN was still continuing in the adult human brain with a 1.75% annual turnover rate and that the extent of AHN in a human was comparable with mice (Spalding *et al.*, 2013).

Using rat and mouse models in this project, at the cellular level I noticed the phenomenon of neurogenesis is maintained at different levels depending on age. To accurately test neurogenesis in humans, further research needs to be conducted about whether DCX is a unique marker for human immature neurones and whether the phenomenon of AHN exists in humans.

Previously, adult human patient brain samples were reported to have newborn cells in the dentate granular cell layer via BrdU immuno-labelling (Eriksson *et al.*, 1998). Later, radioactive carbon (^{14}C) was used to corroborate the existence of immature neurones in the adult human brain (Spalding *et al.*, 2013)(Ernst *et al.*, 2014). IHC was also used to analyse whether AHN exists in the adult human brain. With evidence for the presence of immature neurones in adult human dentate gyrus (Terreros-Roncal *et al.*, 2021)(Moreno-Jiménez *et al.*, 2019)(Moreno-Jiménez *et al.*, 2021) and evidence against the presence of these cells (Sorrells *et al.*, 2021)(Sorrells *et al.*, 2018)(Cipriani *et al.*, 2018). In these IHC experiments, doublecortin (DCX) was used to detect and label immature neurones. However, in order to avoid reliance on DCX, other proteins that are expressed at different stages of neurogenesis need to be validated in human brain tissue. For example, calretinin is expressed in immature neurones which are small and radial in shape (Kobayashi and Amaral, 1999).

Interestingly, for post-mortem human brain tissues, the preservation of the DCX antigen needs intricate histological protocols in order for it to be targeted effectively (Moreno-Jiménez *et al.*, 2019)(Flor-García *et al.*, 2020). As different brain banks use distinct protocols to process and store human brain tissue, reproducibility problems may exist in experiments using DCX. In these banks, brain tissues are routinely exposed to long-term formalin fixation, whilst some are flash-frozen. These two methods may result in different IHC results when using the same DCX antibody (Moreno-Jiménez *et al.*, 2019). It was reported that flash-frozen human tissue is more

appropriate to detect immature neurones using IHC. Whilst, the formalin-fixed human brain tissue may not be appropriate for the detection of immature neurones by IHC (Moreno-Jiménez *et al.*, 2019). These researchers suggest that in order to detect AHN, it is essential to propose the need for customised brain tissue sample collection and fixation (Moreno-Jiménez *et al.*, 2021). The authors include key factors such as flash-frozen fixation and short post-mortem interval time (Moreno-Jiménez *et al.*, 2021). However, this can be extremely resource-consuming. With current provisions, brain banks will find it difficult to provide these specific conditions for the research community. This technicality, which appears to be essential for detecting AHN in humans, reveals the limitation of current immature neurone detecting technologies.

Single-nuclei RNA sequencing (snRNAseq) was also used to help determine whether AHN exists in human brain tissue. AHN was reported to exist in mice, pigs and macaques by using this technology (Franjic *et al.*, 2022). However, they found no evidence for new neurones in human brain tissue using the same methods, suggesting that AHN may not be present in adult humans (Franjic *et al.*, 2022). In contrast, Wang et al. showed that using snRNAseq, evidence for AHN was present in human adult hippocampi. In their research, AHN declined which age, from 67 to 92 years old (Wang *et al.*, 2021). AHN was again found to exist in these samples and the immature neurones were found to be enriched for stathmin 1 (STMN1) and stathmin 2 (STMN2) which appear to be novel markers in primates (Wang *et al.*, 2021). Interestingly, they emphasised that the number of immature neurones varied widely from donor to donor. They also analysed the snRNAseq datasets from Franjic *et al.*, 2022, confirming the absence of evidence for immature neurones in those data. Wang et al. discovered the increased expression of pro-inflammatory markers in the Franjic et al.2022 dataset, which led them to speculate that neuroinflammation associated with astrocytes may be the reason why immature neurones were not detected (Wang *et al.*, 2021). More recently, snRNAseq and machine learning were applied in exploring AHN in the human brain. In these studies, the authors found evidence for the existence of AHN in human brain samples (Zhou *et al.*, 2022). This approach was complemented with surgical specimens of brain tissue that provided evidence in support of AHN in humans (Zhou *et al.*, 2022).

The use of new research methods is set to deepen our understanding of brain plasticity in many forms, including neurogenesis within the adult mammalian brain. These

studies are essential if we are to develop effective ways to promote healthy brain ageing.

6 Chapter 6 Appendix

Figure 6.1 **The number of immature DCX^{+} neurones in DG decrease between 6 - 24 months in both in TDP-43$^{Q331K+/Q331K+}$ and wild-type mice**

Tukey's multiple comparisons test	Mean Diff.	95.00% CI of diff.	Below threshold?	Summary	Adjusted P Value
6M:WT vs. 6M:Q331K	34.32	19.21 to 49.44	Yes	****	<0.0001
6M:WT vs. 24M:WT	73.18	58.07 to 88.30	Yes	****	<0.0001
6M:WT vs. 24M:Q331K	76.21	61.09 to 91.32	Yes	****	<0.0001
6M:Q331K vs. 24M:WT	38.86	23.75 to 53.98	Yes	****	<0.0001
6M:Q331K vs. 24M:Q331K	41.89	26.77 to 57.00	Yes	****	<0.0001
24M:WT vs. 24M:Q331K	3.023	-12.09 to 18.14	No	ns	0.9428

Test details	Mean 1	Mean 2	Mean Diff.	SE of diff.	N1	N2	
6M:WT vs. 6M:Q331K	82.56	48.24	34.32	5.400	6	6	8.9
6M:WT vs. 24M:WT	82.56	9.374	73.18	5.400	6	6	19
6M:WT vs. 24M:Q331K	82.56	6.351	76.21	5.400	6	6	19
6M:Q331K vs. 24M:WT	48.24	9.374	38.86	5.400	6	6	10
6M:Q331K vs. 24M:Q331K	48.24	6.351	41.89	5.400	6	6	10
24M:WT vs. 24M:Q331K	9.374	6.351	3.023	5.400	6	6	0.79

Figure 6.2**The number of immature DCX^{+} neurones in SVZ decrease between 6 - 24 months in both in TDP-43$^{Q331K+/Q331K+}$ and wild-type mice**

Tukey's multiple comparisons test	Mean Diff.	95.00% CI of diff.	Below threshold?	Summary	Adjusted P Value		
6M:WT vs. 6M:Q331K	5857	-2173 to 13888	No	ns	0.2066		
6M:WT vs. 24M:WT	26729	18699 to 34760	Yes	****	<0.0001		
6M:WT vs. 24M:Q331K	26695	18664 to 34725	Yes	****	<0.0001		
6M:Q331K vs. 24M:WT	20872	12842 to 28903	Yes	****	<0.0001		
6M:Q331K vs. 24M:Q331K	20838	12807 to 28868	Yes	****	<0.0001		
24M:WT vs. 24M:Q331K	-34.58	-8065 to 7996	No	ns	>0.9999		
Test details	Mean 1	Mean 2	Mean Diff.	SE of diff.	N1	N2	
6M:WT vs. 6M:Q331K	26953	21095	5857	2869	6	6	2.8
6M:WT vs. 24M:WT	26953	223.3	26729	2869	6	6	13
6M:WT vs. 24M:Q331K	26953	257.9	26695	2869	6	6	13
6M:Q331K vs. 24M:WT	21095	223.3	20872	2869	6	6	10
6M:Q331K vs. 24M:Q331K	21095	257.9	20838	2869	6	6	10
24M:WT vs. 24M:Q331K	223.3	257.9	-34.58	2869	6	6	0.01

Figure 6.3 **Wild type male mice generate more immature neurones in SVZ compared to females at 6 months of age.**

Tukey's multiple comparisons test	Mean Diff.	95.00% CI of diff.	Below threshold?	Summary	Adjusted P Value		
Male:WT vs. Male:Q331K	5857	-2173 to 13888	No	ns	0.2066		
Male:WT vs. Female:WT	26729	18699 to 34760	Yes	****	<0.0001		
Male:WT vs. Female:Q331K	26695	18664 to 34725	Yes	****	<0.0001		
Male:Q331K vs. Female:WT	20872	12842 to 28903	Yes	****	<0.0001		
Male:Q331K vs. Female:Q331K	20838	12807 to 28868	Yes	****	<0.0001		
Female:WT vs. Female:Q331K	-34.58	-8065 to 7996	No	ns	>0.9999		
Test details	Mean 1	Mean 2	Mean Diff.	SE of diff.	N1	N2	
Male:WT vs. Male:Q331K	26953	21095	5857	2869	6	6	2.8
Male:WT vs. Female:WT	26953	223.3	26729	2869	6	6	13
Male:WT vs. Female:Q331K	26953	257.9	26695	2869	6	6	13
Male:Q331K vs. Female:WT	21095	223.3	20872	2869	6	6	10
Male:Q331K vs. Female:Q331K	21095	257.9	20838	2869	6	6	10
Female:WT vs. Female:Q331K	223.3	257.9	-34.58	2869	6	6	0.01

Figure 6.4 **The TDP-43$^{Q331K/Q331K}$ mutation regulates PHF1-Tau^{+} cell number in the infrapyramidal blade of the DG.**

Šídák's multiple comparisons test	Predicted (LS) mean diff.	95.00% CI of diff.	Below threshold?	S
WT:suprapyramidal blade vs. WT:infrapyramidal blade	3.792	-2.885 to 10.47	No	
WT:suprapyramidal blade vs. Q331K:suprapyramidal blade	-0.2917	-7.757 to 7.174	No	
WT:suprapyramidal blade vs. Q331K:infrapyramidal blade	9.083	1.618 to 16.55	Yes	
WT:infrapyramidal blade vs. Q331K:suprapyramidal blade	-4.083	-11.55 to 3.382	No	
WT:infrapyramidal blade vs. Q331K:infrapyramidal blade	5.292	-2.174 to 12.76	No	
Q331K:suprapyramidal blade vs. Q331K:infrapyramidal blade	9.375	1.197 to 17.55	Yes	

Test details	Predicted (LS) mean 1	Predicted (LS) mean 2	Predicted (LS) mean diff.	S
WT:suprapyramidal blade vs. WT:infrapyramidal blade	13.58	9.792	3.792	
WT:suprapyramidal blade vs. Q331K:suprapyramidal blade	13.58	13.88	-0.2917	
WT:suprapyramidal blade vs. Q331K:infrapyramidal blade	13.58	4.500	9.083	
WT:infrapyramidal blade vs. Q331K:suprapyramidal blade	9.792	13.88	-4.083	
WT:infrapyramidal blade vs. Q331K:infrapyramidal blade	9.792	4.500	5.292	
Q331K:suprapyramidal blade vs. Q331K:infrapyramidal blade	13.88	4.500	9.375	

Figure 6.5 **The TDP-43$^{Q331K/Q331K}$ mutation predominantly reduces DCX^{+} cell number in the suprapyramidal blade of the DG.**

Tukey's multiple comparisons test	Predicted (LS) mean diff.	95.00% CI of diff.	Below threshold?	S
WT:suprapyramidal blade vs. WT:infrapyramidal blade	7.042	0.5122 to 13.57	Yes	
WT:suprapyramidal blade vs. Q331K:suprapyramidal blade	9.083	1.783 to 16.38	Yes	
WT:suprapyramidal blade vs. Q331K:infrapyramidal blade	12.33	5.033 to 19.63	Yes	
WT:infrapyramidal blade vs. Q331K:suprapyramidal blade	2.042	-5.259 to 9.342	No	
WT:infrapyramidal blade vs. Q331K:infrapyramidal blade	5.292	-2.009 to 12.59	No	
Q331K:suprapyramidal blade vs. Q331K:infrapyramidal blade	3.250	-4.747 to 11.25	No	

Test details	Predicted (LS) mean 1	Predicted (LS) mean 2	Predicted (LS) mean diff.	S
WT:suprapyramidal blade vs. WT:infrapyramidal blade	16.83	9.792	7.042	
WT:suprapyramidal blade vs. Q331K:suprapyramidal blade	16.83	7.750	9.083	
WT:suprapyramidal blade vs. Q331K:infrapyramidal blade	16.83	4.500	12.33	
WT:infrapyramidal blade vs. Q331K:suprapyramidal blade	9.792	7.750	2.042	
WT:infrapyramidal blade vs. Q331K:infrapyramidal blade	9.792	4.500	5.292	
Q331K:suprapyramidal blade vs. Q331K:infrapyramidal blade	7.750	4.500	3.250	

Figure 6.6 **The TDP-43$^{Q331K/Q331K}$ mutation reduces the DCX^{+}/PHF1-Tau^{+} cell number predominantly in the suprapyramidal blade of the DG IN 6-month-old female mice.**

Tukey's multiple comparisons test	Predicted (LS) mean diff.	95.00% CI of diff.	Below threshold?	S
WT:suprapyramidal blade vs. WT:infrapyramidal blade	7.542	-1.879 to 16.96	No	
WT:suprapyramidal blade vs. Q331K:suprapyramidal blade	11.02	0.4882 to 21.55	Yes	
WT:suprapyramidal blade vs. Q331K:infrapyramidal blade	14.46	3.926 to 24.99	Yes	
WT:infrapyramidal blade vs. Q331K:suprapyramidal blade	3.479	-7.053 to 14.01	No	
WT:infrapyramidal blade vs. Q331K:infrapyramidal blade	6.917	-3.616 to 17.45	No	
Q331K:suprapyramidal blade vs. Q331K:infrapyramidal blade	3.438	-8.100 to 14.98	No	
Test details	Predicted (LS) mean 1	Predicted (LS) mean 2	Predicted (LS) mean diff.	S
WT:suprapyramidal blade vs. WT:infrapyramidal blade	29.46	21.92	7.542	
WT:suprapyramidal blade vs. Q331K:suprapyramidal blade	29.46	18.44	11.02	
WT:suprapyramidal blade vs. Q331K:infrapyramidal blade	29.46	15.00	14.46	
WT:infrapyramidal blade vs. Q331K:suprapyramidal blade	21.92	18.44	3.479	
WT:infrapyramidal blade vs. Q331K:infrapyramidal blade	21.92	15.00	6.917	
Q331K:suprapyramidal blade vs. Q331K:infrapyramidal blade	18.44	15.00	3.438	

Bibliography

Aarsland, D., Zaccai, J. and Brayne, C. (2005) 'A systematic review of prevalence studies of dementia in Parkinson's disease', *Movement Disorders*, 20(10), pp. 1255–1263. doi: 10.1002/mds.20527.

Abreha, M. H. *et al.* (2021) 'TBK1 interacts with tau and enhances neurodegeneration in tauopathy', *Journal of Biological Chemistry*, 296.

Adusumilli, V. S. *et al.* (2021) 'ROS Dynamics Delineate Functional States of Hippocampal Neural Stem Cells and Link to Their Activity-Dependent Exit from Quiescence', *Cell Stem Cell*, 28(2), pp. 300-314.e6. doi: https://doi.org/10.1016/j.stem.2020.10.019.

Agnihotri, S. K. *et al.* (2019) 'PINK1 deficiency is associated with increased deficits of adult hippocampal neurogenesis and lowers the threshold for stress-induced depression in mice', *Behavioural Brain Research*, 363, pp. 161–172. doi: https://doi.org/10.1016/j.bbr.2019.02.006.

Ahn, S. *et al.* (2019) 'Gami–Chunggan Formula Prevents Motor Dysfunction in MPTP/p-Induced and A53T α-Synuclein Overexpressed Parkinson's Disease Mouse Model Though DJ-1 and BDNF Expression', *Frontiers in Aging Neuroscience*, 11. doi: 10.3389/fnagi.2019.00230.

Ahuja, M. *et al.* (2021) 'Bach1 derepression is neuroprotective in a mouse model of Parkinson's disease', *Proceedings of the National Academy of Sciences*, 118(45), p. e2111643118.

Al-Chalabi, A. (2017) 'Faculty Opinions recommendation of El Escorial World Federation of Neurology criteria for the diagnosis of amyotrophic lateral sclerosis. Subcommittee on Motor Neuron Diseases/Amyotrophic Lateral Sclerosis of the World Federation of Neurology Research Gro', *Faculty Opinions – Post-Publication Peer Review of the Biomedical Literature*. Faculty Opinions Ltd. doi: 10.3410/f.720674161.793529744.

Al-Shaheeb, S. (2019) 'Characterising microglial activation: refinement and validation of primary in vitro models'. Keele University.

ALTMAN, J. and DAS, G. D. (1967) 'Postnatal Neurogenesis in the Guinea-pig', *Nature*, 214(5093), pp. 1098–1101. doi: 10.1038/2141098a0.

Alzheimer, A. (1911) 'Über eigenartige Krankheitsfälle des späteren Alters', *Zeitschrift für die gesamte Neurologie und Psychiatrie*, 4(1), p. 356.

Ames, D. *et al.* (1994) 'Repetitive and compulsive behavior in frontal lobe degenerations', *Journal of Neuropsychiatry and Clinical Neurosciences*, 6(2), pp. 100–113.

An, L. *et al.* (2008) 'The total flavonoids extracted from Xiaobuxin-Tang up-regulate the decreased hippocampal neurogenesis and neurotrophic molecules expression in chronically stressed rats.', *Progress in neuro-psychopharmacology & biological psychiatry*, 32(6), pp. 1484–1490. doi: 10.1016/j.pnpbp.2008.05.005.

Andrews, Z. B. *et al.* (2005) 'Uncoupling protein-2 is critical for nigral dopamine cell survival in a mouse model of Parkinson's disease', *Journal of Neuroscience*, 25(1), pp. 184–191.

Andrews, Z. B. *et al.* (2009) 'Ghrelin promotes and protects nigrostriatal dopamine function via a UCP2-dependent mitochondrial mechanism', *Journal of Neuroscience*, 29(45), pp. 14057–14065.

Andrews, Z. B. (2011) 'The extra-hypothalamic actions of ghrelin on neuronal function', *Trends in Neurosciences*, 34(1), pp. 31–40. doi: https://doi.org/10.1016/j.tins.2010.10.001.

Annenkov, A. (2014) 'Receptor tyrosine kinase (RTK) signalling in the control of neural stem and progenitor cell (NSPC) development', *Molecular neurobiology*, 49(1), pp. 440–471.

Arai, T. *et al.* (2006) 'TDP-43 is a component of ubiquitin-positive tau-negative inclusions in frontotemporal lobar degeneration and amyotrophic lateral sclerosis', *Biochem Biophys Res Commun*, 351(3), pp. 602–611.

Ariyannur, P. S. *et al.* (2021) 'Effects of pyruvate administration on mitochondrial enzymes, neurological behaviors, and neurodegeneration after traumatic brain injury', *Aging and disease*, 12(4), p. 983.

Arnold, E. S. *et al.* (2013) 'ALS-linked TDP-43 mutations produce aberrant RNA splicing and adult-onset motor neuron disease without aggregation or loss of nuclear TDP-43', *Proceedings of the National Academy of Sciences of the United States of America*, 110(8). doi: 10.1073/pnas.1222809110.

Arthur C., J. S. (2008) 'MSK activation and physiological roles', *Frontiers in Bioscience*, Volume(13), p. 5866. doi: 10.2741/3122.

Asanuma, M., Hirata, H. and Cadet, J. L. (1998) 'Attenuation of 6-hydroxydopamine-induced dopaminergic nigrostriatal lesions in superoxide dismutase transgenic mice', *Neuroscience*, 85(3), pp. 907–917. doi: https://doi.org/10.1016/S0306-4522(97)00665-9.

Ash, P. E. A. *et al.* (2010) 'Neurotoxic effects of TDP-43 overexpression in C. elegans', *Human Molecular Genetics*, 19(16), pp. 3206–3218. doi: 10.1093/hmg/ddq230.

Avila, J. *et al.* (2016) 'Tau Structures.', *Frontiers in aging neuroscience*, 8, p. 262. doi: 10.3389/fnagi.2016.00262.

Ayala, Y. M. *et al.* (2011) 'TDP-43 regulates its mRNA levels through a negative feedback loop', *The EMBO Journal*, 30(2), pp. 277–288. doi: https://doi.org/10.1038/emboj.2010.310.

Babić Leko, M. *et al.* (2019) 'Molecular Mechanisms of Neurodegeneration Related to C9orf72 Hexanucleotide Repeat Expansion.', *Behavioural neurology*, 2019, p. 2909168. doi: 10.1155/2019/2909168.

Bae, J. R. and Lee, B. D. (2015) 'Function and dysfunction of leucine-rich repeat kinase 2 (LRRK2): Parkinson's disease and beyond.', *BMB reports*, 48(5), pp. 243–248. doi: 10.5483/bmbrep.2015.48.5.032.

Baloh, R. H. (2012) ‘How do the RNA-binding proteins TDP-43 and FUS relate to amyotrophic lateral sclerosis and frontotemporal degeneration, and to each other?’, *Curr Opin Neurol*, 25(6), pp. 701–707. doi: 10.1097/WCO.0b013e32835a269b.

Banks, W. A. *et al.* (2002) ‘Extent and direction of ghrelin transport across the blood-brain barrier is determined by its unique primary structure’, *Journal of Pharmacology and Experimental Therapeutics*, 302(2), pp. 822–827.

Baralle, M., Buratti, E. and Baralle, F. E. (2013) ‘The role of TDP-43 in the pathogenesis of ALS and FTLD’, *Biochem Soc Trans*, 41(6), pp. 1536–1540. doi: 10.1042/BST20130186.

Barata-Antunes, S. *et al.* (2020) ‘Impact of aging on the 6-OHDA-induced rat model of Parkinson’s disease’, *International journal of molecular sciences*, 21(10), p. 3459.

Barkho, B. Z. *et al.* (2006) ‘Identification of astrocyte-expressed factors that modulate neural stem/progenitor cell differentiation’, *Stem cells and development*, 15(3), pp. 407–421. doi: 10.1089/scd.2006.15.407.

Battista, D. *et al.* (2006) ‘Neurogenic niche modulation by activated microglia: transforming growth factor β increases neurogenesis in the adult dentate gyrus’, *European Journal of Neuroscience*, 23(1), pp. 83–93. doi: 10.1111/j.1460-9568.2005.04539.x.

Bayliss, J. A. *et al.* (2016) ‘Ghrelin-AMPK signaling mediates the neuroprotective effects of calorie restriction in Parkinson’s disease’, *Journal of Neuroscience*, 36(10), pp. 3049–3063.

Bazarian, J. J. *et al.* (2009) ‘Long-term neurologic outcomes after traumatic brain injury’, *The Journal of head trauma rehabilitation*, 24(6), pp. 439–451.

Beckman, J. S. *et al.* (1990) ‘Apparent hydroxyl radical production by peroxynitrite: implications for endothelial injury from nitric oxide and superoxide’, *Proceedings of the National Academy of Sciences of the United States of America*, 87(4), pp. 1620–1624. doi: 10.1073/pnas.87.4.1620.

Belin, A. C. and Westerlund, M. (2008) ‘Parkinson’s disease: A genetic perspective’, *The FEBS Journal*, 275(7), pp. 1377–1383. doi: https://doi.org/10.1111/j.1742-4658.2008.06301.x.

Bergmann, O. *et al.* (2012) ‘The Age of Olfactory Bulb Neurons in Humans’, *Neuron*, 74(4), pp. 634–639. doi: 10.1016/j.neuron.2012.03.030.

Bernheimer, H. *et al.* (1973) ‘Brain dopamine and the syndromes of Parkinson and Huntington. Clinical, morphological and neurochemical correlations.’, *Journal of the neurological sciences*, 20(4), pp. 415–455.

Berry, C., La Vecchia, C. and Nicotera, P. (2010) ‘Paraquat and Parkinson’s disease’, *Cell Death & Differentiation*, 17(7), pp. 1115–1125.

Bettadapur, A., Miller, H. W. and Ralston, K. S. (2020) ‘Biting off what can be chewed: trogocytosis in health, infection, and disease’, *Infection and Immunity*, 88(7), pp. e00930-19.

Betz, W. (1874) ‘Anatomischer nachweis zweier gehirncentra’, *Zentralbl Med Wiss*, 12(578,595).

Beutler, B. (2004) ‘Inferences, questions and possibilities in Toll-like receptor signalling’, *Nature*, 430(6996), pp. 257–263. doi: 10.1038/nature02761.

Beynon, A. L. *et al.* (2013) ‘Ghrelin inhibits LPS-induced release of IL-6 from mouse dopaminergic neurones’, *Journal of neuroinflammation*, 10(1), pp. 1–6.

Bigio, E. H., Brown, D. F. and White, C. L. (1999) ‘Progressive supranuclear palsy with dementia: cortical pathology’, *J Neuropathol Exp Neurol*, 58(4), pp. 359–364.

Bimonte, H. (2003) ‘Age-related deficits as working memory load increases: relationships with growth factors’, *Neurobiology of Aging*, 24(1), pp. 37–48. doi: 10.1016/s0197-4580(02)00015-5.

Bindoff, L. A. *et al.* (1991) ‘Respiratory chain abnormalities in skeletal muscle from patients with Parkinson’s disease’, *Journal of the Neurological Sciences*, 104(2), pp. 203–208. doi: 10.1016/0022-510x(91)90311-t.

Birsa, N., Bentham, M. P. and Fratta, P. (2020) ‘Cytoplasmic functions of TDP-43 and FUS and their role in ALS’, *Seminars in Cell & Developmental Biology*, 99, pp. 193–201. doi: https://doi.org/10.1016/j.semcdb.2019.05.023.

Bloch, A. *et al.* (2006) ‘α-Synuclein pathology of the spinal and peripheral autonomic nervous system in neurologically unimpaired elderly subjects’, *Neuropathology and applied neurobiology*, 32(3), pp. 284–295.

Blochberger, A. and Jones, S. (2011) ‘Parkinson’s disease clinical features and diagnosis’, *Clinical Pharmacist*, 3(11), pp. 361–366. doi: 10.1136/jnnp.2007.131045.

Blum, D. *et al.* (2001) ‘Molecular pathways involved in the neurotoxicity of 6-OHDA, dopamine and MPTP: contribution to the apoptotic theory in Parkinson’s disease’, *Progress in Neurobiology*, 65(2), pp. 135–172. doi: https://doi.org/10.1016/S0301-0082(01)00003-X.

Bocchetta, M. *et al.* (2018) ‘Hippocampal Subfield Volumetry: Differential Pattern of Atrophy in Different Forms of Genetic Frontotemporal Dementia’, *Journal of Alzheimer’s Disease*, 64, pp. 497–504. doi: 10.3233/JAD-180195.

Boka, G. *et al.* (1994) ‘Immunocytochemical analysis of tumor necrosis factor and its receptors in Parkinson’s disease.’, *Neuroscience letters*, 172(1–2), pp. 151–154. doi: 10.1016/0304-3940(94)90684-x.

Boldrini, M. *et al.* (2018) ‘Human Hippocampal Neurogenesis Persists throughout Aging’, *Cell Stem Cell*, 22(4), pp. 589-599.e5. doi: 10.1016/j.stem.2018.03.015.

Bonaguidi, M. A. *et al.* (2012) ‘A unifying hypothesis on mammalian neural stem cell properties in the adult hippocampus’, *Current opinion in neurobiology*. 2012/04/13, 22(5), pp. 754–761. doi: 10.1016/j.conb.2012.03.013.

Bondolfi, L. *et al.* (2004) ‘Impact of age and caloric restriction on neurogenesis in the dentate gyrus of C57BL/6 mice’, *Neurobiology of Aging*, 25(3), pp. 333–340. doi: 10.1016/s0197-4580(03)00083-6.

Bonnet, E. *et al.* (2008) ‘Retinoic acid restores adult hippocampal neurogenesis and reverses spatial memory deficit in vitamin A deprived rats.’, *PloS one*, 3(10), p. e3487. doi: 10.1371/journal.pone.0003487.

Boonstra, J. and Post, J. A. (2004) 'Molecular events associated with reactive oxygen species and cell cycle progression in mammalian cells', *Gene*, 337, pp. 1–13.

Borghero, G. *et al.* (2011) 'A patient carrying a homozygous p.A382T TARDBP missense mutation shows a syndrome including ALS, extrapyramidal symptoms, and FTD', *Neurobiol Aging*, 32(12), pp. 2321–2325. doi: 10.1016/j.neurobiolaging.2011.06.009.

Bosboom, J. L. W., Stoffers, D. and Wolters, E. C. (2004) 'Cognitive dysfunction and dementia in Parkinson's disease', *Journal of Neural Transmission*, 111(10–11), pp. 1303–1315. doi: 10.1007/s00702-004-0168-1.

Bourbouli, M. *et al.* (2017) 'Cerebrospinal Fluid TAR DNA-Binding Protein 43 Combined with Tau Proteins as a Candidate Biomarker for Amyotrophic Lateral Sclerosis and Frontotemporal Dementia Spectrum Disorders', *Dementia and Geriatric Cognitive Disorders*, 44(3–4), pp. 144–152. doi: 10.1159/000478979.

Boxer, A. L. *et al.* (2013) 'Frontotemporal degeneration, the next therapeutic frontier: molecules and animal models for frontotemporal degeneration drug development', *Alzheimers Dement*, 9(2), pp. 176–188. doi: 10.1016/j.jalz.2012.03.002.

Bozoyan, L., Khlghatyan, J. and Saghatelyan, A. (2012) 'Astrocytes control the development of the migration-promoting vasculature scaffold in the postnatal brain via VEGF signaling', *Journal of neuroscience*, 32(5), pp. 1687–1704.

Braak, H. *et al.* (2003) 'Idiopathic Parkinson's disease: possible routes by which vulnerable neuronal types may be subject to neuroinvasion by an unknown pathogen', *Journal of neural transmission*, 110(5), pp. 517–536.

Brigadski, T. and Leßmann, V. (2014) 'BDNF: a regulator of learning and memory processes with clinical potential', *e-Neuroforum*, 20(1), pp. 1–11.

Brion, J. P. and Couck, A. M. (1995) 'Cortical and brainstem-type Lewy bodies are immunoreactive for the cyclin-dependent kinase 5.', *The American journal of pathology*, 147(5), pp. 1465–1476.

Brooks, B. R. (1994) 'El escorial World Federation of Neurology criteria for the diagnosis of amyotrophic lateral sclerosis', *Journal of the Neurological Sciences*, 124, pp. 96–107. doi: https://doi.org/10.1016/0022-510X(94)90191-0.

Brooks, D. J. (2000) 'Dopamine agonists: their role in the treatment of Parkinson{\textquoteright}s disease', *Journal of Neurology, Neurosurgery \& Psychiatry*, 68(6), pp. 685–689. doi: 10.1136/jnnp.68.6.685.

Brooks, D. J. (2004) 'Neuroimaging in Parkinson's disease', *NeuroRX*, 1(2), pp. 243–254. doi: 10.1602/neurorx.1.2.243.

Brown, T. P. *et al.* (2006) 'Pesticides and Parkinson's disease--is there a link?', *Environmental health perspectives*, 114(2), pp. 156–164. doi: 10.1289/ehp.8095.

Brunden, K. R., Trojanowski, J. Q. and Lee, V. M.-Y. (2008) 'Evidence that non-fibrillar tau causes pathology linked to neurodegeneration and behavioral impairments', *Journal of Alzheimer's Disease*, 14(4), pp. 393–399.

Brus, M., Keller, M. and Lévy, F. (2013) 'Temporal features of adult neurogenesis: differences and similarities across mammalian species', *Frontiers in neuroscience*, 7,

p. 135.

Buckwalter, M. S. *et al.* (2006) 'Chronically increased transforming growth factor-beta1 strongly inhibits hippocampal neurogenesis in aged mice', *The American journal of pathology*, 169(1), pp. 154–164. doi: 10.2353/ajpath.2006.051272.

Bullon, P., Newman, H. N. and Battino, M. (2014) 'Obesity, diabetes mellitus, atherosclerosis and chronic periodontitis: a shared pathology via oxidative stress and mitochondrial dysfunction?', *Periodontology 2000*, 64(1), pp. 139–153.

Burrow, G. N. (1993) 'Book Review Cecil Textbook of Medicine 19th edition. Edited by James B. Wyngaarden, Lloyd H. Smith, Jr., and J. Claude Bennett. 2380 pp., illustrated. Philadelphia, W.B. Saunders, 1992. $99. 0-8247-8564-9', *New England Journal of Medicine*, 328(1), pp. 69–70. doi: 10.1056/nejm199301073280122.

Butovsky, O. *et al.* (2006) 'Microglia activated by IL-4 or IFN-γ differentially induce neurogenesis and oligodendrogenesis from adult stem/progenitor cells', *Molecular and Cellular Neuroscience*, 31(1), pp. 149–160. doi: 10.1016/j.mcn.2005.10.006.

Cadet, J. L. and Brannock, C. (1998) 'Invited Review Free radicals and the pathobiology of brain dopamine systems', *Neurochemistry International*, 32(2), pp. 117–131. doi: https://doi.org/10.1016/S0197-0186(97)00031-4.

Cai, H. *et al.* (2013) 'Altered lipid and salt taste responsivity in ghrelin and GOAT null mice', *PLoS One*, 8(10), p. e76553.

Cameron, H. A. and Dayer, A. G. (2008) 'New interneurons in the adult neocortex: small, sparse, but significant?', *Biological psychiatry*. 2007/12/11, 63(7), pp. 650–655. doi: 10.1016/j.biopsych.2007.09.023.

Camicioli, R. *et al.* (2003) 'Parkinson's disease is associated with hippocampal atrophy', *Movement disorders*, 18(7), pp. 784–790.

Cao, L. *et al.* (2004) 'VEGF links hippocampal activity with neurogenesis, learning and memory', *Nature Genetics*, 36(8), pp. 827–835. doi: 10.1038/ng1395.

Cao, X., Li, L.-P., Wang, Q., *et al.* (2013) 'Astrocyte-derived ATP modulates depressive-like behaviors', *Nature Medicine*, 19(6), pp. 773–777. doi: 10.1038/nm.3162.

Cao, X., Li, L.-P., Qin, X.-H., *et al.* (2013) 'Astrocytic Adenosine 5′-Triphosphate Release Regulates the Proliferation of Neural Stem Cells in the Adult Hippocampus', *STEM CELLS*, 31(8), pp. 1633–1643. doi: 10.1002/stem.1408.

Capozzo, R. *et al.* (2017) 'Clinical and genetic analyses of familial and sporadic frontotemporal dementia patients in Southern Italy', *Alzheimer's & dementia : the journal of the Alzheimer's Association*. 2017/03/03, 13(8), pp. 858–869. doi: 10.1016/j.jalz.2017.01.011.

Caproni, S. *et al.* (2014) 'Subclinical visuospatial impairment in Parkinson's disease: the role of Basal Ganglia and limbic system', *Frontiers in neurology*, 5, p. 152. doi: 10.3389/fneur.2014.00152.

Cárdenas, A. *et al.* (2018) 'Evolution of Cortical Neurogenesis in Amniotes Controlled by Robo Signaling Levels.', *Cell*, 174(3), pp. 590-606.e21. doi: 10.1016/j.cell.2018.06.007.

Carlini, V. P. *et al.* (2002) 'Ghrelin increases anxiety-like behavior and memory retention in rats', *Biochemical and biophysical research communications*, 299(5), pp. 739–743.

Carlini, V. P. *et al.* (2004) 'Differential role of the hippocampus, amygdala, and dorsal raphe nucleus in regulating feeding, memory, and anxiety-like behavioral responses to ghrelin', *Biochemical and biophysical research communications*, 313(3), pp. 635–641.

Carlini, V. P. *et al.* (2010) 'Ghrelin induced memory facilitation implicates nitric oxide synthase activation and decrease in the threshold to promote LTP in hippocampal dentate gyrus', *Physiology & behavior*, 101(1), pp. 117–123.

Carpentier, P. A. and Palmer, T. D. (2009) 'Immune influence on adult neural stem cell regulation and function', *Neuron*, 64(1), pp. 79–92. doi: 10.1016/j.neuron.2009.08.038.

Carvalho, M. D. and Swash, M. (2009) 'Awaji diagnostic algorithm increases sensitivity of El Escorial criteria for ALS diagnosis', *Amyotroph Lateral Scler*, 10(1), pp. 53–57. doi: 10.1080/17482960802521126.

Casadesus, G. *et al.* (2004) 'Modulation of Hippocampal Plasticity and Cognitive Behavior by Short-term Blueberry Supplementation in Aged Rats', *Nutritional Neuroscience*, 7(5–6), pp. 309–316. doi: 10.1080/10284150400020482.

Ceccatelli, S. (2013) 'Mechanisms of neurotoxicity and implications for neurological disorders', *Journal of Internal Medicine*, 273(5), pp. 426–428. doi: 10.1111/joim.12053.

Chan, P. *et al.* (1991) 'Rapid ATP Loss Caused by 1-Methyl-4-Phenyl-1,2,3,6-Tetrahydropyridine in Mouse Brain', *Journal of Neurochemistry*, 57(1), pp. 348–351. doi: 10.1111/j.1471-4159.1991.tb02134.x.

Chapman, D. P. *et al.* (2006) 'Dementia and its implications for public health.', *Preventing chronic disease*, 3(2), p. A34.

Chen, M.-K. *et al.* (2008) 'VMAT2 and dopamine neuron loss in a primate model of Parkinson's disease', *Journal of neurochemistry*. 2007/11/05, 105(1), pp. 78–90. doi: 10.1111/j.1471-4159.2007.05108.x.

Cheng, S. T. *et al.* (2014) 'Mental and physical activities delay cognitive decline in older persons with dementia', *Am J Geriatr Psychiatry*, 22(1), pp. 63–74. doi: 10.1016/j.jagp.2013.01.060.

Chinta, S. J. *et al.* (2013) 'Environmental stress, ageing and glial cell senescence: a novel mechanistic link to Parkinson's disease?', *Journal of internal medicine*, 273(5), pp. 429–436. doi: 10.1111/joim.12029.

Choi, S. H., Bylykbashi, E., Chatila, Zena K, *et al.* (2018) 'Combined adult neurogenesis and BDNF mimic exercise effects on cognition in an Alzheimer's mouse model.', *Science (New York, N.Y.)*, 361(6406). doi: 10.1126/science.aan8821.

Choi, S. H., Bylykbashi, E., Chatila, Zena K., *et al.* (2018) 'Combined adult neurogenesis and BDNF mimic exercise effects on cognition in an Alzheimer's mouse model', *Science*, 361(6406), p. eaan8821. doi: 10.1126/science.aan8821.

Choi, W.-S. *et al.* (1999) 'Two distinct mechanisms are involved in 6-hydroxydopamine- and MPP+-induced dopaminergic neuronal cell death: Role of caspases, ROS, and JNK', *Journal of Neuroscience Research*, 57(1), pp. 86–94. doi: https://doi.org/10.1002/(SICI)1097-4547(19990701)57:1<86::AID-JNR9>3.0.CO;2-E.

Chotibut, T. *et al.* (2012) 'Dopamine transporter loss in 6-OHDA Parkinson's model is unmet by parallel reduction in dopamine uptake', *PLoS One*, 7(12), p. e52322.

Chow, T. W. *et al.* (1999) 'Inheritance of frontotemporal dementia', *Arch Neurol*, 56(7), pp. 817–822.

Chow, T. W. *et al.* (2009) 'Apathy symptom profile and behavioral associations in frontotemporal dementia vs dementia of Alzheimer type', *Arch Neurol*, 66(7), pp. 888–893. doi: 10.1001/archneurol.2009.92.

Chu, K., Zhou, X. and Luo, B. (2012) 'Cytokine gene polymorphisms and Parkinson's disease: a meta-analysis.', *The Canadian journal of neurological sciences. Le journal canadien des sciences neurologiques*, 39(1), pp. 58–64. doi: 10.1017/s0317167100012695.

Cipriani, S. *et al.* (2018) 'Hippocampal radial glial subtypes and their neurogenic potential in human fetuses and healthy and Alzheimer's disease adults', *Cerebral Cortex*, 28(7), pp. 2458–2478.

Claiborne, B. J., Amaral, D. G. and Cowan, W. M. (1986) 'A light and electron microscopic analysis of the mossy fibers of the rat dentate gyrus', *Journal of comparative neurology*, 246(4), pp. 435–458.

Clark, L. N. *et al.* (1998) 'Pathogenic implications of mutations in the tau gene in pallido-ponto-nigral degeneration and related neurodegenerative disorders linked to chromosome 17', in *Proceedings of the National Academy of Sciences of the United States of America*, pp. 13103–13107.

Clelland, C. D. *et al.* (2009) 'A functional role for adult hippocampal neurogenesis in spatial pattern separation', *Science (New York, N.Y.)*, 325(5937), pp. 210–213. doi: 10.1126/science.1173215.

Colman, R. J. *et al.* (2009) 'Caloric restriction delays disease onset and mortality in rhesus monkeys', *Science*, 325(5937), pp. 201–204.

Conrad, Chris *et al.* (2007) 'Single molecule profiling of tau gene expression in Alzheimer's disease.', *Journal of neurochemistry*, 103(3), pp. 1228–1236. doi: 10.1111/j.1471-4159.2007.04857.x.

Cook, D. A. *et al.* (2017) 'LRRK2 levels in immune cells are increased in Parkinson's disease.', *NPJ Parkinson's disease*, 3, p. 11. doi: 10.1038/s41531-017-0010-8.

Coppola, G. *et al.* (2012) 'Evidence for a role of the rare p.A152T variant in MAPT in increasing the risk for FTD-spectrum and Alzheimer's diseases', *Hum Mol Genet*, 21(15), pp. 3500–3512. doi: 10.1093/hmg/dds161.

Corniola, R. S. *et al.* (2008) 'Zinc deficiency impairs neuronal precursor cell proliferation and induces apoptosis via p53-mediated mechanisms.', *Brain research*, 1237, pp. 52–61. doi: 10.1016/j.brainres.2008.08.040.

Corrêa, S. A. L. *et al.* (2012) 'MSK1 regulates homeostatic and experience-dependent synaptic plasticity', *The Journal of neuroscience : the official journal of the Society for Neuroscience*, 32(38), pp. 13039–13051. doi: 10.1523/JNEUROSCI.0930-12.2012.

Costall, B., Naylor, R. J. and Pycock, C. (1976) 'Non-specific supersensitivity of striatal dopamine receptors after 6-hydroxydopamine lesion of the nigrostriatal pathway', *European Journal of Pharmacology*, 35(2), pp. 275–283. doi: 10.1016/0014-2999(76)90229-6.

Cowley, M. A. *et al.* (2003) 'The distribution and mechanism of action of ghrelin in the CNS demonstrates a novel hypothalamic circuit regulating energy homeostasis', *Neuron*, 37(4), pp. 649–661.

Coyle-Gilchrist, I. T. S. *et al.* (2016) 'Prevalence, characteristics, and survival of frontotemporal lobar degeneration syndromes.', *Neurology*, 86(18), pp. 1736–1743. doi: 10.1212/WNL.0000000000002638.

Croll, S. D. *et al.* (1998) 'Expression of BDNF and trkB as a function of age and cognitive performance', *Brain Research*, 812(1–2), pp. 200–208. doi: 10.1016/s0006-8993(98)00993-7.

Da Cruz, S. and Cleveland, D. W. (2011) 'Understanding the role of TDP-43 and FUS/TLS in ALS and beyond', *Current Opinion in Neurobiology*, 21(6), pp. 904–919. doi: https://doi.org/10.1016/j.conb.2011.05.029.

Curtis, M. A. *et al.* (2007) 'Human Neuroblasts Migrate to the Olfactory Bulb via a Lateral Ventricular Extension', *Science*, 315(5816), pp. 1243–1249. doi: 10.1126/science.1136281.

Darwish, B. *et al.* (2019) 'Intranigral injection of endotoxin suppresses proliferation of hippocampal progenitor cells', *Frontiers in Neuroscience*, 13, p. 687.

Date, Y. *et al.* (2000) 'Ghrelin, a novel growth hormone-releasing acylated peptide, is synthesized in a distinct endocrine cell type in the gastrointestinal tracts of rats and humans', *Endocrinology*, 141(11), pp. 4255–4261.

Dauer, W. and Przedborski, S. (2003a) 'Parkinson's Disease: Mechanisms and Models', *Neuron*, 39(6), pp. 889–909. doi: https://doi.org/10.1016/S0896-6273(03)00568-3.

Dauer, W. and Przedborski, S. (2003b) 'Parkinson's Disease', *Neuron*, 39(6), pp. 889–909. doi: 10.1016/s0896-6273(03)00568-3.

Deng, H. X. *et al.* (2011) 'Mutations in UBQLN2 cause dominant X-linked juvenile and adult-onset ALS and ALS/dementia', *Nature*, 477(7363), pp. 211–215. doi: 10.1038/nature10353.

Deng, W., Aimone, J. B. and Gage, F. H. (2010) 'New neurons and new memories: how does adult hippocampal neurogenesis affect learning and memory?', *Nature reviews. Neuroscience*. 2010/03/31, 11(5), pp. 339–350. doi: 10.1038/nrn2822.

Deschenes, C. L. and McCurry, S. M. (2009) 'Current treatments for sleep disturbances in individuals with dementia', *Current psychiatry reports*, 11(1), pp. 20–26.

Deumens, R., Blokland, A. and Prickaerts, J. (2002) 'Modeling Parkinson's disease in rats: an evaluation of 6-OHDA lesions of the nigrostriatal pathway', *Experimental neurology*, 175(2), pp. 303–317.

Deuschl, G. *et al.* (2006) 'A Randomized Trial of Deep-Brain Stimulation for Parkinson's Disease', *New England Journal of Medicine*, 355(9), pp. 896–908. doi: 10.1056/NEJMoa060281.

Diano, S. *et al.* (2006) 'Ghrelin controls hippocampal spine synapse density and memory performance', *Nature neuroscience*, 9(3), pp. 381–388.

Diaper, D. C. *et al.* (2013) 'Drosophila TDP-43 dysfunction in glia and muscle cells cause cytological and behavioural phenotypes that characterize ALS and FTLD', *Human Molecular Genetics*, 22(19), pp. 3883–3893. doi: 10.1093/hmg/ddt243.

Dias, G. P. *et al.* (2021) 'Intermittent fasting enhances long-term memory consolidation, adult hippocampal neurogenesis, and expression of longevity gene Klotho.', *Molecular psychiatry*, 26(11), pp. 6365–6379. doi: 10.1038/s41380-021-01102-4.

Diaz, J. *et al.* (1997) 'Selective expression of dopamine D3 receptor mRNA in proliferative zones during embryonic development of the rat brain.', *The Journal of neuroscience : the official journal of the Society for Neuroscience*, 17(11), pp. 4282–92. Available at: http://www.ncbi.nlm.nih.gov/pubmed/9151745.

Dickson, D. and Inc (2011) 'Neurodegeneration the molecular pathology of dementia and movement disorders', p. 477. Available at: http://site.ebrary.com/lib/princeton/Doc?id=10501281.

Dickson, D. W. *et al.* (2002) 'Office of Rare Diseases neuropathologic criteria for corticobasal degeneration', *J Neuropathol Exp Neurol*, 61(11), pp. 935–946.

Doetsch, F. *et al.* (1999) 'Subventricular Zone Astrocytes Are Neural Stem Cells in the Adult Mammalian Brain', *Cell*, 97(6), pp. 703–716. doi: 10.1016/S0092-8674(00)80783-7.

Donaldson, I. (2015) 'James Parkinson's Essay on the Shaking Palsy', *The Journal of the Royal College of Physicians of Edinburgh*, 45(1), pp. 84–86. doi: 10.4997/JRCPE.2015.118.

Dorszewska, J. *et al.* (2014) 'Molecular Effects of L-dopa Therapy in Parkinson's Disease.', *Current genomics*, 15(1), pp. 11–17. doi: 10.2174/1389202914666131210213042.

Du, Y. *et al.* (2001) 'Minocycline prevents nigrostriatal dopaminergic neurodegeneration in the MPTP model of Parkinson's disease', *Proceedings of the National Academy of Sciences*, 98(25), pp. 14669–14674. doi: 10.1073/pnas.251341998.

Dzamko, N., Geczy, C. L. and Halliday, G. M. (2015) 'Inflammation is genetically implicated in Parkinson's disease.', *Neuroscience*, 302, pp. 89–102. doi: 10.1016/j.neuroscience.2014.10.028.

Elabi, O. F. *et al.* (2018) 'The impact of ghrelin on the survival and efficacy of dopaminergic fetal grafts in the 6-OHDA-lesioned rat', *Neuroscience*, 395, pp. 13–21.

Elbaz, A. *et al.* (2002) 'Risk tables for parkinsonism and Parkinson's disease', *Journal of Clinical Epidemiology*, 55(1), pp. 25–31. doi: https://doi.org/10.1016/S0895-4356(01)00425-5.

Eliakim, A. *et al.* (1998) 'Increased physical activity and the growth hormone-IGF-I axis in adolescent males', *American Journal of Physiology-Regulatory, Integrative and Comparative Physiology*, 275(1), pp. R308–R314.

Elustondo, P. A. *et al.* (2016) 'Mitochondrial permeability transition pore induction is linked to formation of the complex of ATPase C-subunit, polyhydroxybutyrate and inorganic polyphosphate', *Cell Death Discovery*, 2(1), p. 16070. doi: 10.1038/cddiscovery.2016.70.

Encinas, J. M. *et al.* (2011) 'Division-coupled astrocytic differentiation and age-related depletion of neural stem cells in the adult hippocampus', *Cell stem cell*, 8(5), pp. 566–579. doi: 10.1016/j.stem.2011.03.010.

Encinas, J. M. and Sierra, A. (2012) 'Neural stem cell deforestation as the main force driving the age-related decline in adult hippocampal neurogenesis', *Behavioural brain research*, 227(2), pp. 433–439.

Erickson, K. I. *et al.* (2010) 'Brain-derived neurotrophic factor is associated with age-related decline in hippocampal volume', *The Journal of neuroscience : the official journal of the Society for Neuroscience*, 30(15), pp. 5368–5375. doi: 10.1523/JNEUROSCI.6251-09.2010.

Eriksson, P. S. *et al.* (1998) 'Neurogenesis in the adult human hippocampus', *Nature Medicine*, 4(11), pp. 1313–1317. doi: 10.1038/3305.

Ernst, A. *et al.* (2014) 'Neurogenesis in the Striatum of the Adult Human Brain', *Cell*, 156(5), pp. 1072–1083. doi: 10.1016/j.cell.2014.01.044.

Eslami, M., Sadeghi, B. and Goshadrou, F. (2018) 'Chronic ghrelin administration restores hippocampal long-term potentiation and ameliorates memory impairment in rat model of Alzheimer's disease', *Hippocampus*, 28(10), pp. 724–734.

Estes, P. S. *et al.* (2011) 'Wild-type and A315T mutant TDP-43 exert differential neurotoxicity in a Drosophila model of ALS.', *Human molecular genetics*, 20(12), pp. 2308–2321. doi: 10.1093/hmg/ddr124.

Fallini, C. *et al.* (2020) 'Traffic jam at the nuclear pore: All roads lead to nucleocytoplasmic transport defects in ALS/FTD', *Neurobiology of Disease*, 140, p. 104835. doi: https://doi.org/10.1016/j.nbd.2020.104835.

Fanaei, H. *et al.* (2014) 'Testosterone enhances functional recovery after stroke through promotion of antioxidant defenses, BDNF levels and neurogenesis in male rats', *Brain research*, 1558, pp. 74–83.

Fanselow, M. S. and Dong, H.-W. (2010) 'Are the dorsal and ventral hippocampus functionally distinct structures?', *Neuron*, 65(1), pp. 7–19. doi: 10.1016/j.neuron.2009.11.031.

Farizatto, K. L. G. *et al.* (2017) 'Aβ42-mediated proteasome inhibition and associated tau pathology in hippocampus are governed by a lysosomal response involving cathepsin B: Evidence for protective crosstalk between protein clearance pathways', *PLoS One*, 12(8), p. e0182895.

Fearnley, Julian M., and A. J. L. (1991) ‘Ageing and Parkinson’S Disease: Substantia Nigra Regional Selectivity’, *Brain*, 114(5), pp. 2283–2301. doi: 10.1093/brain/114.5.2283.

Fecto, F. (2011) ‘<emph type="ital">SQSTM1</emph> Mutations in Familial and Sporadic Amyotrophic Lateral Sclerosis’, *Archives of Neurology*, 68(11), p. 1440. doi: 10.1001/archneurol.2011.250.

Fiesel, F. C. and Kahle, P. J. (2011) ‘TDP-43 and FUS/TLS: cellular functions and implications for neurodegeneration’, *The FEBS Journal*, 278(19), pp. 3550–3568. doi: https://doi.org/10.1111/j.1742-4658.2011.08258.x.

Filigheddu, N. *et al.* (2007) ‘Ghrelin and des-acyl ghrelin promote differentiation and fusion of C2C12 skeletal muscle cells’, *Molecular biology of the cell*, 18(3), pp. 986–994.

Flor-García, M. *et al.* (2020) ‘Unraveling human adult hippocampal neurogenesis’, *Nature Protocols*, 15(2), pp. 668–693. doi: 10.1038/s41596-019-0267-y.

Francardo, V. *et al.* (2011) ‘Impact of the lesion procedure on the profiles of motor impairment and molecular responsiveness to L-DOPA in the 6-hydroxydopamine mouse model of Parkinson’s disease’, *Neurobiology of Disease*, 42(3), pp. 327–340. doi: 10.1016/j.nbd.2011.01.024.

Di Francesco, A. *et al.* (2018) ‘A time to fast’, *Science*, 362(6416), pp. 770–775.

Franjic, D. *et al.* (2022) ‘Transcriptomic taxonomy and neurogenic trajectories of adult human, macaque, and pig hippocampal and entorhinal cells’, *Neuron*, 110(3), pp. 452–469.

Freischmidt, A. *et al.* (2015) ‘Haploinsufficiency of TBK1 causes familial ALS and fronto-temporal dementia’, *Nat Neurosci*, 18(5), pp. 631–636. doi: 10.1038/nn.4000.

Friedland, R. P. *et al.* (2012) ‘Behavioral variant frontotemporal lobar degeneration with amyotrophic lateral sclerosis with a chromosome 9p21 hexanucleotide repeat.’, *Frontiers in neurology*, 3, p. 136. doi: 10.3389/fneur.2012.00136.

Frontotemporal dementia - Treatment - NHS (2022). Available at: https://www.nhs.uk/conditions/frontotemporal-dementia/treatment/ (Accessed: 22 December 2021).

Gage, F. H. (2000) ‘Mammalian Neural Stem Cells’, *Science*, 287(5457), pp. 1433–1438. doi: 10.1126/science.287.5457.1433.

Gagne, J. J. and Power, M. C. (2010) ‘Anti-inflammatory drugs and risk of Parkinson disease: a meta-analysis.’, *Neurology*, 74(12), pp. 995–1002. doi: 10.1212/WNL.0b013e3181d5a4a3.

Galea, L. A. M. *et al.* (2013) ‘Sex, hormones and neurogenesis in the hippocampus: hormonal modulation of neurogenesis and potential functional implications’, *Journal of neuroendocrinology*, 25(11), pp. 1039–1061.

Galpern, W. R. and Lang, A. E. (2006) ‘Interface between tauopathies and synucleinopathies: A tale of two proteins’, *Annals of Neurology*, 59(3), pp. 449–458. doi: 10.1002/ana.20819.

Gao, X. *et al.* (2011) 'Use of ibuprofen and risk of Parkinson disease.', *Neurology*, 76(10), pp. 863–869. doi: 10.1212/WNL.0b013e31820f2d79.

Gasser, T. (2001) 'Genetics of Parkinson's disease', *Journal of Neurology*, 248(10), pp. 833–840. doi: 10.1007/s004150170066.

Geevasinga, N. *et al.* (2016) 'Awaji criteria improves the diagnostic sensitivity in amyotrophic lateral sclerosis: A systematic review using individual patient data', *Clin Neurophysiol*, 127(7), pp. 2684–2691. doi: 10.1016/j.clinph.2016.04.005.

Gendron, T. F., Rademakers, R. and Petrucelli, L. (2013) 'TARDBP mutation analysis in TDP-43 proteinopathies and deciphering the toxicity of mutant TDP-43', *Journal of Alzheimer's disease : JAD*, 33 Suppl 1(Suppl 1), pp. S35–S45. doi: 10.3233/JAD-2012-129036.

Ghetti, B. *et al.* (2015) 'Invited review: Frontotemporal dementia caused by microtubule-associated protein tau gene (MAPT) mutations: a chameleon for neuropathology and neuroimaging', *Neuropathology and applied neurobiology*, 41(1), pp. 24–46. doi: 10.1111/nan.12213.

Ghosh, H. S. (2019) 'Adult Neurogenesis and the Promise of Adult Neural Stem Cells.', *Journal of experimental neuroscience*, 13, p. 1179069519856876. doi: 10.1177/1179069519856876.

Gillotin, S. *et al.* (2021) 'Targeting impaired adult hippocampal neurogenesis in ageing by leveraging intrinsic mechanisms regulating Neural Stem Cell activity', *Ageing Research Reviews*, 71, p. 101447. doi: https://doi.org/10.1016/j.arr.2021.101447.

Ginsberg, S. D. *et al.* (2006) 'Shift in the ratio of three-repeat tau and four-repeat tau mRNAs in individual cholinergic basal forebrain neurons in mild cognitive impairment and Alzheimer's disease.', *Journal of neurochemistry*, 96(5), pp. 1401–1408. doi: 10.1111/j.1471-4159.2005.03641.x.

Glinka, Y., Tipton, K. F. and Youdim, M. B. H. (1996) 'Nature of Inhibition of Mitochondrial Respiratory Complex I by 6-Hydroxydopamine', *Journal of Neurochemistry*, 66(5), pp. 2004–2010. doi: https://doi.org/10.1046/j.1471-4159.1996.66052004.x.

Glinka, Y. Y. and Youdim, M. B. H. (1995) 'Inhibition of mitochondrial complexes I and IV by 6-hydroxydopamine', *European Journal of Pharmacology: Environmental Toxicology and*, 292(3–4), pp. 329–332. doi: 10.1016/0926-6917(95)90040-3.

Gnanasegaran, N. *et al.* (2017) 'Effect of dental pulp stem cells in MPTP-induced old-aged mice model', *European Journal of Clinical Investigation*, 47(6), pp. 403–414. doi: https://doi.org/10.1111/eci.12753.

Golbe, L. I. (2014) 'Progressive supranuclear palsy', in *Seminars in neurology*. Thieme Medical Publishers, pp. 151–159.

Goldman, J. S. *et al.* (2005) 'Comparison of family histories in FTLD subtypes and related tauopathies', *Neurology*, 65(11), pp. 1817–1819.

Gomperts, Stephen N (2016) 'Lewy Body Dementias: Dementia With Lewy Bodies and Parkinson Disease Dementia', *Continuum (Minneapolis, Minn.)*, 22(2 Dementia), pp. 435–463. doi: 10.1212/CON.0000000000000309.

Gomperts, Stephen N. (2016) ‘Lewy Body Dementias’, *CONTINUUM: Lifelong Learning in Neurology*, 22(2, Dementia), pp. 435–463. doi: 10.1212/CON.0000000000000309.

Gorno-Tempini, M. L. *et al.* (2011) ‘Classification of primary progressive aphasia and its variants.’, *Neurology*, 76(11), pp. 1006–1014. doi: 10.1212/WNL.0b013e31821103e6.

Gould, E. *et al.* (1999) ‘Neurogenesis in the Neocortex of Adult Primates’, *Science*, 286(5439), pp. 548–552. doi: 10.1126/science.286.5439.548.

Gould, E. (2007) ‘How widespread is adult neurogenesis in mammals?’, *Nature Reviews Neuroscience*, 8(6), pp. 481–488. doi: 10.1038/nrn2147.

Gould, E. and Gross, C. G. (2002) ‘Neurogenesis in adult mammals: some progress and problems’, *The Journal of neuroscience : the official journal of the Society for Neuroscience*, 22(3), pp. 619–623. doi: 10.1523/JNEUROSCI.22-03-00619.2002.

Graff-Radford, N. and Woodruff, B. (2007) ‘Frontotemporal Dementia’, *Seminars in Neurology*, 27(1), pp. 48–57. doi: 10.1055/s-2006-956755.

Gräff, J. *et al.* (2013) ‘A dietary regimen of caloric restriction or pharmacological activation of SIRT1 to delay the onset of neurodegeneration’, *Journal of Neuroscience*, 33(21), pp. 8951–8960.

Grealish, S. *et al.* (2010) ‘Characterisation of behavioural and neurodegenerative changes induced by intranigral 6-hydroxydopamine lesions in a mouse model of Parkinson’s disease’, *European Journal of Neuroscience*, 31(12), pp. 2266–2278. doi: 10.1111/j.1460-9568.2010.07265.x.

Gross, C. G. (2000) ‘Neurogenesis in the adult brain: death of a dogma’, *Nature Reviews Neuroscience*, 1(1), pp. 67–73. doi: 10.1038/35036235.

Grossman, M. (2010) ‘Primary progressive aphasia: clinicopathological correlations.’, *Nature reviews. Neurology*, 6(2), pp. 88–97. doi: 10.1038/nrneurol.2009.216.

Gu, J. *et al.* (2017) ‘TDP-43 suppresses tau expression via promoting its mRNA instability’, *Nucleic Acids Research*, 45(10), pp. 6177–6193. doi: 10.1093/nar/gkx175.

Gualillo, O. *et al.* (2001) ‘Ghrelin, a novel placental-derived hormone’, *Endocrinology*, 142(2), pp. 788–794.

Guerreiro, P. S. *et al.* (2017) ‘Mutant A53T α-Synuclein Improves Rotarod Performance Before Motor Deficits and Affects Metabolic Pathways’, *NeuroMolecular Medicine*, 19(1), pp. 113–121. doi: 10.1007/s12017-016-8435-5.

Haas, R. H. *et al.* (1995) ‘Low platelet mitochondrial complex I and complex II/III activity in early untreated parkinson’s disease’, *Annals of Neurology*, 37(6), pp. 714–722. doi: 10.1002/ana.410370604.

Hakimi, M. *et al.* (2011) ‘Parkinson’s disease-linked LRRK2 is expressed in circulating and tissue immune cells and upregulated following recognition of microbial structures.’, *Journal of neural transmission (Vienna, Austria : 1996)*, 118(5), pp. 795–808. doi: 10.1007/s00702-011-0653-2.

Halagappa, V. K. M. *et al.* (2007) ‘Intermittent fasting and caloric restriction

ameliorate age-related behavioral deficits in the triple-transgenic mouse model of Alzheimer's disease', *Neurobiology of disease*, 26(1), pp. 212–220.

Hanson, K. A. *et al.* (2010) 'Ubiquilin Modifies TDP-43 Toxicity in a Drosophila Model of Amyotrophic Lateral Sclerosis (ALS)*', *Journal of Biological Chemistry*, 285(15), pp. 11068–11072. doi: https://doi.org/10.1074/jbc.C109.078527.

Hardy, J. *et al.* (2006) 'Genetics of Parkinson's disease and parkinsonism', *Annals of neurology*, 60(4), pp. 389–398.

Hasegawa, E. *et al.* (1990) '1-Methyl-4-phenylpyridinium (MPP+) induces NADH-dependent superoxide formation and enhances NADH-dependent lipid peroxidation in bovine heart submitochondrial particles', *Biochemical and Biophysical Research Communications*, 170(3), pp. 1049–1055. doi: 10.1016/0006-291x(90)90498-c.

Hattiangady, B. and Shetty, A. K. (2008) 'Aging does not alter the number or phenotype of putative stem/progenitor cells in the neurogenic region of the hippocampus', *Neurobiology of aging*. 2006/11/07, 29(1), pp. 129–147. doi: 10.1016/j.neurobiolaging.2006.09.015.

Haustein, M. D. *et al.* (2014) 'Conditions and constraints for astrocyte calcium signaling in the hippocampal mossy fiber pathway', *Neuron*, 82(2), pp. 413–429.

Hayakawa, N., Kato, H. and Araki, T. (2007) 'Age-related changes of astorocytes, oligodendrocytes and microglia in the mouse hippocampal CA1 sector', *Mechanisms of Ageing and Development*, 128(4), pp. 311–316. doi: https://doi.org/10.1016/j.mad.2007.01.005.

Heikkila, R. E. *et al.* (1989) 'Some features of the nigrostriatal dopaminergic neurotoxin 1-methyl-4-phenyl-1,2,3,6-tetrahydropyridine (MPTP) in the mouse', *Molecular and Chemical Neuropathology*, 10(3), pp. 171–183. doi: 10.1007/bf03159727.

Heine, V. M. *et al.* (2004) 'Prominent decline of newborn cell proliferation, differentiation, and apoptosis in the aging dentate gyrus, in absence of an age-related hypothalamus–pituitary–adrenal axis activation', *Neurobiology of Aging*, 25(3), pp. 361–375. doi: 10.1016/s0197-4580(03)00090-3.

Heneka, M. T., Kummer, M. P. and Latz, E. (2014) 'Innate immune activation in neurodegenerative disease', *Nature Reviews Immunology*, 14(7), pp. 463–477.

Hernandez, D. G., Reed, X. and Singleton, A. B. (2016) 'Genetics in Parkinson disease: Mendelian versus non-Mendelian inheritance.', *Journal of neurochemistry*, 139 Suppl(Suppl 1), pp. 59–74. doi: 10.1111/jnc.13593.

Herrmann, N. *et al.* (2012) 'Serotonergic function and treatment of behavioral and psychological symptoms of frontotemporal dementia', *Am J Geriatr Psychiatry*, 20(9), pp. 789–797. doi: 10.1097/JGP.0b013e31823033f3.

Hodge, R. D. *et al.* (2008) 'Intermediate progenitors in adult hippocampal neurogenesis: Tbr2 expression and coordinate regulation of neuronal output', *The Journal of neuroscience : the official journal of the Society for Neuroscience*, 28(14), pp. 3707–3717. doi: 10.1523/JNEUROSCI.4280-07.2008.

Hodges, J. R. *et al.* (2003) 'Survival in frontotemporal dementia.', *Neurology*, 61(3), pp. 349–354. doi: 10.1212/01.wnl.0000078928.20107.52.

Hogan, D. B. *et al.* (2016) 'The Prevalence and Incidence of Frontotemporal Dementia: a Systematic Review.', *The Canadian journal of neurological sciences. Le journal canadien des sciences neurologiques*, 43 Suppl 1, pp. S96–S109. doi: 10.1017/cjn.2016.25.

Höglinger, G. U. *et al.* (2004) 'Dopamine depletion impairs precursor cell proliferation in Parkinson disease', *Nature Neuroscience*, 7(7), pp. 726–735. doi: 10.1038/nn1265.

Houben, S. *et al.* (2021) 'Tau pathology and adult hippocampal neurogenesis: What tau mouse models tell us?', *Frontiers in neurology*, 12, p. 610330.

Huey, E. D. *et al.* (2012) 'FUS and TDP43 genetic variability in FTD and CBS', *Neurobiology of Aging*, 33(5), pp. 1016.e9-1016.e17. doi: https://doi.org/10.1016/j.neurobiolaging.2011.08.004.

Hughes, A. J. *et al.* (1992) 'Accuracy of clinical diagnosis of idiopathic Parkinson ' s disease : a clinico-pathological study of 100 cases', *Journal of neurology, neurosurgery, and psychiatry*, 55, pp. 181–184. doi: 10.1136/jnnp.55.3.181.

Hurtgen, B. J. *et al.* (2016) 'Preclinical identification of vaccine induced protective correlates in human leukocyte antigen expressing transgenic mice infected with Coccidioides posadasii', *Vaccine*, 34(44), pp. 5336–5343.

Hutchison, W. D. *et al.* (1994) 'Differential neuronal activity in segments of globus pallidus in Parkinson's disease patients', *NeuroReport*, 5(12), pp. 1533–1537. doi: 10.1097/00001756-199407000-00031.

Hutton, M. *et al.* (1998) 'Association of missense and 5'-splice-site mutations in tau with the inherited dementia FTDP-17', *Nature*, 393(6686), pp. 702–705.

Iancu, R. *et al.* (2005) 'Behavioral characterization of a unilateral 6-OHDA-lesion model of Parkinson's disease in mice', *Behavioural Brain Research*, 162(1), pp. 1–10. doi: 10.1016/j.bbr.2005.02.023.

Iguchi, Y. *et al.* (2013) 'Loss of TDP-43 causes age-dependent progressive motor neuron degeneration', *Brain*, 136(5), pp. 1371–1382. doi: 10.1093/brain/awt029.

Ikeda, M. *et al.* (2004) 'Efficacy of fluvoxamine as a treatment for behavioral symptoms in frontotemporal lobar degeneration patients', *Dement Geriatr Cogn Disord*, 17(3), pp. 117–121. doi: 10.1159/000076343.

Imahori, K. and Uchida, T. (1997) 'Physiology and pathology of tau protein kinases in relation to Alzheimer's disease', *The Journal of Biochemistry*, 121(2), pp. 179–188.

Ingre, C. *et al.* (2015) 'Risk factors for amyotrophic lateral sclerosis', *Clinical Epidemiology*, 7, pp. 181–193. doi: 10.2147/CLEP.S37505.

Irwin, D. J., Lee, V. M.-Y. and Trojanowski, J. Q. (2013) 'Parkinson's disease dementia: convergence of α-synuclein, tau and amyloid-β pathologies', *Nature Reviews Neuroscience*, 14(9), pp. 626–636. doi: 10.1038/nrn3549.

Jackson-Lewis, V. *et al.* (1995) 'Time course and morphology of dopaminergic neuronal death caused by the neurotoxin 1-methyl-4-phenyl-1,2,3,6-tetrahydropyridine', *Neurodegeneration*, 4(3), pp. 257–269. doi: 10.1016/1055-8330(95)90015-2.

Jagmag, S. A. *et al.* (2016) 'Evaluation of Models of Parkinson's Disease', *Frontiers in Neuroscience*, 9, p. 503. doi: 10.3389/fnins.2015.00503.

Jang, M. *et al.* (2019) 'Oligodendrocytes regulate presynaptic properties and neurotransmission through BDNF signaling in the mouse brainstem', *eLife*. Edited by D. E. Bergles, G. L. Westbrook, and L.-Y. Wang, 8, p. e42156. doi: 10.7554/eLife.42156.

Jankovic, J. (2008) 'Parkinson ' s disease : clinical features and diagnosis', (1957), pp. 368–376. doi: 10.1136/jnnp.2007.131045.

Jankovic, J., Hurtig, H. and Dashe, J. (2014) 'Etiology and pathogenesis of Parkinson disease', *UpToDate. Retrieved from http://www. uptodate. com/home/index. html*.

Janssens, J. *et al.* (2013) 'Overexpression of ALS-Associated p.M337V Human TDP-43 in Mice Worsens Disease Features Compared to Wild-type Human TDP-43 Mice', *Molecular Neurobiology*, 48(1), pp. 22–35. doi: 10.1007/s12035-013-8427-5.

Jasmin, M. *et al.* (2021) 'Netrin-1 and its receptor DCC modulate survival and death of dopamine neurons and Parkinson's disease features', *The EMBO journal*, 40(3), p. e105537.

Jellinger, K. A. (2010) 'Synucleinopathies', *Encyclopedia of Movement Disorders*, pp. 203–207. doi: 10.1016/B978-0-12-374105-9.00291-4.

Jenkins, S. M. and Johnson, G. V (1998) 'Tau complexes with phospholipase C-gamma in situ', *NeuroReport*, 9(1), pp. 67–71.

Jenner, P., Schapira, A. H. V and Marsden, C. D. (1992) 'New insights into the cause of Parkinson's disease', *Neurology*, 42(12), p. 2241. doi: 10.1212/wnl.42.12.2241.

Jiang, H. *et al.* (2008) 'Ghrelin antagonizes MPTP-induced neurotoxicity to the dopaminergic neurons in mouse substantia nigra', *Experimental neurology*, 212(2), pp. 532–537.

Jiang, T. A. (2019) 'Health benefits of culinary herbs and spices', *Journal of AOAC International*, 102(2), pp. 395–411.

Johansson, I. *et al.* (2008) 'Proliferative and protective effects of growth hormone secretagogues on adult rat hippocampal progenitor cells', *Endocrinology*, 149(5), pp. 2191–2199.

Jones, D. C. and Miller, G. W. (2008) 'The effects of environmental neurotoxicants on the dopaminergic system: A possible role in drug addiction', *Biochemical Pharmacology*, 76(5), pp. 569–581. doi: https://doi.org/10.1016/j.bcp.2008.05.010.

Jones Jr, H. R. *et al.* (2013) *The Netter Collection of Medical Illustrations: Nervous System, Volume 7, Part 1-Brain e-Book*. Elsevier Health Sciences.

Josephs, K. A. *et al.* (2006) 'Clinicopathologic analysis of frontotemporal and corticobasal degenerations and PSP', *Neurology*, 66(1), pp. 41–48.

Josephs, K. A. *et al.* (2011) 'Neuropathological background of phenotypical variability in frontotemporal dementia', *Acta Neuropathol*, 122(2), pp. 137–153. doi: 10.1007/s00401-011-0839-6.

Josephs, K. A., Whitwell, J. L. and Jack, C. R. (2008) 'Jr Anatomic correlates of

stereotypies in frontotemporal lobar degeneration', *Neurobiol Aging*, 29(12), pp. 1859–1863. doi: 10.1016/j.neurobiolaging.2007.04.027.

Kabashi, E. *et al.* (2008) 'TARDBP mutations in individuals with sporadic and familial amyotrophic lateral sclerosis', *Nature Genetics*, 40(5), pp. 572–574. doi: 10.1038/ng.132.

Kabashi, E. *et al.* (2009) 'Gain and loss of function of ALS-related mutations of TARDBP (TDP-43) cause motor deficits in vivo', *Human Molecular Genetics*, 19(4), pp. 671–683. doi: 10.1093/hmg/ddp534.

Kalia, L. V. and Lang, A. E. (2015) 'Parkinson's disease', *The Lancet*, 386(9996), pp. 896–912. doi: 10.1016/S0140-6736(14)61393-3.

Van Kampen, J. M., McGeer, E. G. and Stoessl, A. J. (2000) 'Dopamine transporter function assessed by antisense knockdown in the rat: protection from dopamine neurotoxicity', *Synapse*, 37(3), pp. 171–178.

Kane, J. P. M. *et al.* (2018) 'Clinical prevalence of Lewy body dementia', *Alzheimer's Research & Therapy*, 10(1), p. 19. doi: 10.1186/s13195-018-0350-6.

Kannarkat, G. T. *et al.* (2015) 'Common Genetic Variant Association with Altered HLA Expression, Synergy with Pyrethroid Exposure, and Risk for Parkinson's Disease: An Observational and Case-Control Study.', *NPJ Parkinson's disease*, 1, pp. 15002-. doi: 10.1038/npjparkd.2015.2.

Kaplan, M. S. (2001) 'Environment complexity stimulates visual cortex neurogenesis: death of a dogma and a research career', *Trends in Neurosciences*, 24(10), pp. 617–620. doi: 10.1016/s0166-2236(00)01967-6.

Karakaya, T. *et al.* (2012) 'Treatment options for tauopathies', *Curr Treat Options Neurol*, 14(2), pp. 126–136. doi: 10.1007/s11940-012-0168-7.

Karelina, K. *et al.* (2012) 'MSK1 regulates environmental enrichment-induced hippocampal plasticity and cognitive enhancement', *Learning & memory (Cold Spring Harbor, N.Y.)*, 19(11), pp. 550–560. doi: 10.1101/lm.025775.112.

Katoh-Semba, R. *et al.* (1998) 'Age-related changes in levels of brain-derived neurotrophic factor in selected brain regions of rats, normal mice and senescence-accelerated mice: a comparison to those of nerve growth factor and neurotrophin-3', *Neuroscience Research*, 31(3), pp. 227–234. doi: 10.1016/s0168-0102(98)00040-6.

Katoh-Semba, R. *et al.* (2002) 'Distribution of Brain-Derived Neurotrophic Factor in Rats and Its Changes with Development in the Brain', *Journal of Neurochemistry*, 69(1), pp. 34–42. doi: 10.1046/j.1471-4159.1997.69010034.x.

Kawakita, E., Hashimoto, M. and Shido, O. (2006) 'Docosahexaenoic acid promotes neurogenesis in vitro and in vivo.', *Neuroscience*, 139(3), pp. 991–997. doi: 10.1016/j.neuroscience.2006.01.021.

Ke, Y. D. *et al.* (2019) 'CNS cell type–specific gene profiling of P301S tau transgenic mice identifies genes dysregulated by progressive tau accumulation', *Journal of Biological Chemistry*, 294(38), pp. 14149–14162.

Kempermann, G. *et al.* (2003) 'Early determination and long-term persistence of adult-generated new neurons in the hippocampus of mice', *Development*, 130(2), pp.

391–399. doi: 10.1242/dev.00203.

Kempermann, G. *et al.* (2018) 'Human Adult Neurogenesis: Evidence and Remaining Questions', *Cell Stem Cell*, 23(1), pp. 25–30. doi: https://doi.org/10.1016/j.stem.2018.04.004.

Kempermann, G., Gast, D. and Gage, F. H. (2002) 'Neuroplasticity in old age: Sustained fivefold induction of hippocampal neurogenesis by long-term environmental enrichment', *Annals of Neurology*, 52(2), pp. 135–143. doi: 10.1002/ana.10262.

Kempermann, G., Kuhn, H. G. and Gage, F. H. (1997) 'More hippocampal neurons in adult mice living in an enriched environment', *Nature*, 386(6624), pp. 493–495. doi: 10.1038/386493a0.

Kent, B. A. *et al.* (2015) 'The orexigenic hormone acyl-ghrelin increases adult hippocampal neurogenesis and enhances pattern separation', *Psychoneuroendocrinology*, 51, pp. 431–439.

Kertesz, A. (2005) 'Frontotemporal Dementia: One Disease, or Many?', *Alzheimer Disease & Associated Disorders*, 19(Supplement 1), pp. S19–S24. doi: 10.1097/01.wad.0000183080.69196.64.

Kertesz, A. and Munoz, D. G. (2002) 'Frontotemporal dementia', *Medical Clinics of North America*, 86(3), pp. 501–518. doi: 10.1016/s0025-7125(02)00011-1.

Kfoury, N. *et al.* (2012) 'Trans-cellular propagation of Tau aggregation by fibrillar species', *J Biol Chem*, 287(23), pp. 19440–19451. doi: 10.1074/jbc.M112.346072.

Kharkar, S. D. (2013) 'Parkinson ' S Disease', 363(November), pp. 1–6.

Kidd, E. J., Hvoslef-Eide, M. and Thomas, R. S. (2014) 'Anti-amyloid precursor protein antibodies as a potential therapy for Alzheimer's disease', *Neuroreport*, 25(3), p. 145.

Kim, E. *et al.* (2020) 'Coexistence of perseveration and apathy in the TDP-43Q331K knock-in mouse model of ALS–FTD', *Translational Psychiatry*, 10(1), p. 377. doi: 10.1038/s41398-020-01078-9.

Kimonis, V. E. *et al.* (2008) 'VCP disease associated with myopathy, Paget disease of bone and frontotemporal dementia: Review of a unique disorder', *Biochimica et Biophysica Acta (BBA) - Molecular Basis of Disease*, 1782(12), pp. 744–748. doi: https://doi.org/10.1016/j.bbadis.2008.09.003.

Kimura, T. *et al.* (2018) 'Phospho-Tau Bar Code: Analysis of Phosphoisotypes of Tau and Its Application to Tauopathy', *Frontiers in Neuroscience*, 12. doi: 10.3389/fnins.2018.00044.

Knibb, J. A., Kipps, C. M. and Hodges, J. R. (2006) 'Frontotemporal dementia', *Current Opinion in Neurology*, 19(6), pp. 565–571. doi: 10.1097/01.wco.0000247606.57567.41.

Knopman, D. S. and Roberts, R. O. (2011) 'Estimating the number of persons with frontotemporal lobar degeneration in the US population.', *Journal of molecular neuroscience : MN*, 45(3), pp. 330–335. doi: 10.1007/s12031-011-9538-y.

Kobayashi, Y. and Amaral, D. G. (1999) ‘Chapter IV - Chemical neuroanatomy of the hippocampal formation and the perirhinal and parahippocampal cortices’, in Bloom, F. E., Björklund, A., and Hökfelt, T. (eds) *The Primate Nervous System, Part III*. Elsevier (Handbook of Chemical Neuroanatomy), pp. 285–401. doi: https://doi.org/10.1016/S0924-8196(99)80026-8.

Kojima, M. *et al.* (1999) ‘Ghrelin is a growth-hormone-releasing acylated peptide from stomach’, *Nature*, 402(6762), pp. 656–660.

Kokoeva, M. V (2005) ‘Neurogenesis in the Hypothalamus of Adult Mice: Potential Role in Energy Balance’, *Science*, 310(5748), pp. 679–683. doi: 10.1126/science.1115360.

Kopin, I. J. and Markey, S. P. (1988) ‘MPTP Toxicity: Implications for Research in Parkinson’s Disease’, *Annual Review of Neuroscience*, 11(1), pp. 81–96. doi: 10.1146/annurev.ne.11.030188.000501.

Koren, S. A. *et al.* (2019) ‘Tau drives translational selectivity by interacting with ribosomal proteins’, *Acta Neuropathologica*, 137(4), pp. 571–583. doi: 10.1007/s00401-019-01970-9.

Kortte, K. B. and Rogalski, E. J. (2013) ‘Behavioural interventions for enhancing life participation in behavioural variant frontotemporal dementia and primary progressive aphasia’, *Int Rev Psychiatry*, 25(2), pp. 237–245. doi: 10.3109/09540261.2012.751017.

Kovacs, G. G. *et al.* (2009) ‘TARDBP variation associated with frontotemporal dementia, supranuclear gaze palsy, and chorea’, *Mov Disord*, 24(12), pp. 1843–1847. doi: 10.1002/mds.22697.

Kraemer, B. C. *et al.* (2010) ‘Loss of murine TDP-43 disrupts motor function and plays an essential role in embryogenesis’, *Acta Neuropathologica*, 119(4), pp. 409–419. doi: 10.1007/s00401-010-0659-0.

Kramer, J. H. *et al.* (2003) ‘Distinctive neuropsychological patterns in frontotemporal dementia, semantic dementia, and Alzheimer disease’, *Cogn Behav Neurol*, 16(4), pp. 211–218.

Krishnamurthi, R. V. M. *et al.* (2009) ‘A novel diketopiperazine improves functional recovery given after the onset of 6-OHDA-induced motor deficit in rats.’, *British journal of pharmacology*, 156(4), pp. 662–672. doi: 10.1111/j.1476-5381.2008.00064.x.

Kuhn, H. G. and Cooper-Kuhn, C. M. (2007) ‘Bromodeoxyuridine and the Detection of Neurogenesis’, *Current Pharmaceutical Biotechnology*, 8(3), pp. 127–131. doi: 10.2174/138920107780906531.

Kuhn, H. G., Dickinson-Anson, H. and Gage, F. H. (1996) ‘Neurogenesis in the dentate gyrus of the adult rat: age-related decrease of neuronal progenitor proliferation’, *The Journal of neuroscience : the official journal of the Society for Neuroscience*, 16(6), pp. 2027–2033. doi: 10.1523/JNEUROSCI.16-06-02027.1996.

Küppers, E. *et al.* (2000) ‘Estrogen: A multifunctional messenger to nigrostriatal dopaminergic neurons’, *Journal of Neurocytology*, 29(5), pp. 375–385. doi: 10.1023/A:1007165307652.

Kuwabara, T. *et al.* (2009) 'Wnt-mediated activation of NeuroD1 and retro-elements during adult neurogenesis', *Nature neuroscience*. 2009/08/23, 12(9), pp. 1097–1105. doi: 10.1038/nn.2360.

Kuzumaki, N. *et al.* (2010) 'Hippocampal epigenetic modification at the doublecortin gene is involved in the impairment of neurogenesis with aging', *Synapse*, 64(8), pp. 611–616. doi: https://doi.org/10.1002/syn.20768.

Kuzumaki, N. *et al.* (2011) 'Hippocampal epigenetic modification at the brain-derived neurotrophic factor gene induced by an enriched environment', *Hippocampus*, 21(2), pp. 127–132. doi: 10.1002/hipo.20775.

Kwiatkowski, T. J. *et al.* (2009) 'Mutations in the FUS/TLS gene on chromosome 16 cause familial amyotrophic lateral sclerosis', *Science*, 323(5918), pp. 1205–1208. doi: 10.1126/science.1166066.

Lagier-Tourenne, C. *et al.* (2013) 'Targeted degradation of sense and antisense C9orf72 RNA foci as therapy for ALS and frontotemporal degeneration', *Proc Natl Acad Sci U S A*, 110(47), pp. E4530–4539. doi: 10.1073/pnas.1318835110.

Lanata, S. C. and Miller, B. L. (2016) 'The behavioural variant frontotemporal dementia (bvFTD) syndrome in psychiatry.', *Journal of neurology, neurosurgery, and psychiatry*, 87(5), pp. 501–511. doi: 10.1136/jnnp-2015-310697.

Langston, J. W. *et al.* (1983) 'Chronic Parkinsonism in humans due to a product of meperidine-analog synthesis', *Science*, 219(4587), pp. 979–980.

Langston, J. W. and Irwin, I. (1986) 'MPTP', *Clinical Neuropharmacology*, 9(6), pp. 485–507. doi: 10.1097/00002826-198612000-00001.

Lapchak, P. A. *et al.* (1993) 'BDNF and trkB mRNA expression in the hippocampal formation of aging rats', *Neurobiology of Aging*, 14(2), pp. 121–126. doi: 10.1016/0197-4580(93)90087-r.

Lee, E.-J. *et al.* (2010) 'α-Synuclein activates microglia by inducing the expressions of matrix metalloproteinases and the subsequent activation of protease-activated receptor-1', *The Journal of Immunology*, 185(1), pp. 615–623.

Lee, J. *et al.* (2000) 'Dietary restriction increases the number of newly generated neural cells, and induces BDNF expression, in the dentate gyrus of rats.', *Journal of molecular neuroscience : MN*, 15(2), pp. 99–108. doi: 10.1385/JMN:15:2:99.

Lee, V. M., Goedert, M. and Trojanowski, J. Q. (2001) 'Neurodegenerative tauopathies', *Annu Rev Neurosci*, 24, pp. 1121–1159. doi: 10.1146/annurev.neuro.24.1.1121.

Lee, Y.-S. *et al.* (2013) 'Long course hyperbaric oxygen stimulates neurogenesis and attenuates inflammation after ischemic stroke', *Mediators of Inflammation*, 2013.

Lenka, A. *et al.* (2015) 'Structural and functional neuroimaging in patients with Parkinson's disease and visual hallucinations: A critical review', *Parkinsonism & Related Disorders*, 21(7), pp. 683–691. doi: https://doi.org/10.1016/j.parkreldis.2015.04.005.

Letenneur, L. *et al.* (2007) 'Flavonoid Intake and Cognitive Decline over a 10-Year Period', *American Journal of Epidemiology*, 165(12), pp. 1364–1371. doi:

10.1093/aje/kwm036.

Leugers, C. J. and Lee, G. (2010) ‘Tau potentiates nerve growth factor-induced mitogen-activated protein kinase signaling and neurite initiation without a requirement for microtubule binding’, *J Biol Chem*, 285(25), pp. 19125–19134. doi: 10.1074/jbc.M110.105387.

Li, E. *et al.* (2013) ‘Ghrelin directly stimulates adult hippocampal neurogenesis: implications for learning and memory’, *Endocrine journal*, pp. EJ13-0008.

Li, Y. *et al.* (2008) ‘TrkB Regulates Hippocampal Neurogenesis and Governs Sensitivity to Antidepressive Treatment’, *Neuron*, 60(4), p. 730. doi: 10.1016/j.neuron.2008.10.021.

Liachko, N. F., Guthrie, C. R. and Kraemer, B. C. (2010) ‘Phosphorylation Promotes Neurotoxicity in a Caenorhabditis elegans Model of TDP-43 Proteinopathy’, *Journal of Neuroscience*, 30(48), pp. 16208–16219. doi: 10.1523/JNEUROSCI.2911-10.2010.

Lidow, M. S. and Rakic, P. (1995) ‘Neurotransmitter receptors in the proliferative zones of the developing primate occipital lobe’, *Journal of Comparative Neurology*, 360(3), pp. 393–402. doi: 10.1002/cne.903600303.

Lie, D.-C. *et al.* (2005) ‘Wnt signalling regulates adult hippocampal neurogenesis’, *Nature*, 437(7063), pp. 1370–1375. doi: 10.1038/nature04108.

Liljegren, M. *et al.* (2015) ‘Criminal behavior in frontotemporal dementia and Alzheimer disease’, *JAMA Neurol*, 72(3), pp. 295–300. doi: 10.1001/jamaneurol.2014.3781.

Ling, H. *et al.* (2012) ‘Hypokinesia without decrement distinguishes progressive supranuclear palsy from Parkinson’s disease’, *Brain*, 135(4), pp. 1141–1153. doi: 10.1093/brain/aws038.

Lisman, J. E. and Grace, A. A. (2005) ‘The Hippocampal-VTA Loop: Controlling the Entry of Information into Long-Term Memory’, *Neuron*, 46(5), pp. 703–713. doi: https://doi.org/10.1016/j.neuron.2005.05.002.

Litvan, I. *et al.* (1996) ‘Validity and reliability of the preliminary NINDS neuropathologic criteria for progressive supranuclear palsy and related disorders’, *J Neuropathol Exp Neurol*, 55(1), pp. 97–105.

Liu, F. and Gong, C.-X. (2008) ‘Tau exon 10 alternative splicing and tauopathies’, *Molecular neurodegeneration*, 3, p. 8. doi: 10.1186/1750-1326-3-8.

Loganathan, S. *et al.* (2020) ‘To Be or Not To Be…Toxic—Is RNA Association With TDP-43 Complexes Deleterious or Protective in Neurodegeneration?’, *Frontiers in Molecular Biosciences*, 6. doi: 10.3389/fmolb.2019.00154.

Lomen-Hoerth, C. (2011) ‘Clinical phenomenology and neuroimaging correlates in ALS-FTD’, *J Mol Neurosci*, 45(3), pp. 656–662. doi: 10.1007/s12031-011-9636-x.

Lomen-Hoerth, C., Anderson, T. and Miller, B. (2002) ‘The overlap of amyotrophic lateral sclerosis and frontotemporal dementia’, *Neurology*, 59(7), pp. 1077–1079.

Lotharius, J. and Brundin, P. (2002a) ‘Impaired dopamine storage resulting from alpha-synuclein mutations may contribute to the pathogenesis of Parkinson’s disease.’,

Human molecular genetics, 11(20), pp. 2395–2407. doi: 10.1093/hmg/11.20.2395.

Lotharius, J. and Brundin, P. (2002b) 'Pathogenesis of parkinson's disease: dopamine, vesicles and α-synuclein', *Nature Reviews Neuroscience*, 3(12), pp. 932–942. doi: 10.1038/nrn983.

Lotharius, J., Dugan, L. L. and O'Malley, K. L. (1999) 'Distinct mechanisms underlie neurotoxin-mediated cell death in cultured dopaminergic neurons', *The Journal of neuroscience : the official journal of the Society for Neuroscience*, 19(4), pp. 1284–1293. doi: 10.1523/JNEUROSCI.19-04-01284.1999.

Lucin, K. M. and Wyss-Coray, T. (2009) 'Immune activation in brain aging and neurodegeneration: too much or too little?', *Neuron*, 64(1), pp. 110–122. doi: 10.1016/j.neuron.2009.08.039.

Luna, V. M. *et al.* (2019) 'Adult-born hippocampal neurons bidirectionally modulate entorhinal inputs into the dentate gyrus', *Science*, 364(6440), pp. 578–583. doi: 10.1126/science.aat8789.

Lundblad, M. *et al.* (2004) 'A model of l-DOPA-induced dyskinesia in 6-hydroxydopamine lesioned mice: relation to motor and cellular parameters of nigrostriatal function', *Neurobiology of Disease*, 16(1), pp. 110–123. doi: 10.1016/j.nbd.2004.01.007.

Luskin, M. B. (1993) 'Restricted proliferation and migration of postnatally generated neurons derived from the forebrain subventricular zone', *Neuron*, 11(1), pp. 173–189. doi: 10.1016/0896-6273(93)90281-U.

Luthman, J. *et al.* (1989) 'Selective lesion of central dopamine or noradrenaline neuron systems in the neonatal rat: motor behavior and monoamine alterations at adult stage', *Behavioural Brain Research*, 33(3), pp. 267–277. doi: https://doi.org/10.1016/S0166-4328(89)80121-4.

Lutter, M. *et al.* (2008) 'The orexigenic hormone ghrelin defends against depressive symptoms of chronic stress', *Nature neuroscience*, 11(7), pp. 752–753.

M Isaacs, A. *et al.* (2011) 'Frontotemporal dementia caused by CHMP2B mutations', *Current Alzheimer research*, 8(3), pp. 246–251.

MacKenzie, I. R. A. *et al.* (2011) 'Distinct pathological subtypes of FTLD-FUS', *Acta Neuropathologica*, 121(2), pp. 207–218. doi: 10.1007/s00401-010-0764-0.

Mackenzie, I. R. and Neumann, M. (2012) 'FET proteins in frontotemporal dementia and amyotrophic lateral sclerosis', *Brain Res*, 1462, pp. 40–43. doi: 10.1016/j.brainres.2011.12.010.

Macphee, G. J. A. and Stewart, D. A. (2001) 'Parkinson's disease', *Reviews in Clinical Gerontology*, 11(1), pp. 33–49. doi: 10.1017/s0959259801011145.

Magnin, E. *et al.* (2016) 'Primary progressive aphasia in the network of French Alzheimer plan memory centers', *Journal of Alzheimer's Disease*, 54(4), pp. 1459–1471.

Mahncke, H. W., Bronstone, A. and Merzenich, M. M. (2006) 'Brain plasticity and functional losses in the aged: scientific bases for a novel intervention', *Progress in brain research*, 157, pp. 81–109.

Mahul-Mellier, A.-L. *et al.* (2018) 'The making of a Lewy body: the role of α-synuclein post-fibrillization modifications in regulating the formation and the maturation of pathological inclusions', *BioRxiv*, p. 500058.

Mandelkow, E. M. and Mandelkow, E. (2012) 'Biochemistry and cell biology of tau protein in neurofibrillary degeneration', *Cold Spring Harb Perspect Med*, 2(7), p. a006247. doi: 10.1101/cshperspect.a006247.

Maneuf, Y. P. *et al.* (1994) 'On the Role of Enkephalin Cotransmission in the GABAergic Striatal Efferents to the Globus Pallidus', *Experimental Neurology*, 125(1), pp. 65–71. doi: 10.1006/exnr.1994.1007.

Marsh, S. E. *et al.* (2022) 'Dissection of artifactual and confounding glial signatures by single-cell sequencing of mouse and human brain', *Nature Neuroscience*, 25(3), pp. 306–316. doi: 10.1038/s41593-022-01022-8.

Martino, G. (2004) 'How the brain repairs itself: new therapeutic strategies in inflammatory and degenerative CNS disorders', *The Lancet Neurology*, 3(6), pp. 372–378.

Marxreiter, F., Regensburger, M. and Winkler, J. (2013) 'Adult neurogenesis in Parkinson's disease', *Cellular and Molecular Life Sciences*, 70(3), pp. 459–473. doi: 10.1007/s00018-012-1062-x.

Masui, K. *et al.* (2008) 'Evaluation of sensitivity and specificity of doublecortin immunostatining for the detection of infiltrating glioma cells', *Brain tumor pathology*, 25(1), pp. 1–7.

Maswood, N. *et al.* (2004) 'Caloric restriction increases neurotrophic factor levels and attenuates neurochemical and behavioral deficits in a primate model of Parkinson's disease', *Proceedings of the National Academy of Sciences*, 101(52), pp. 18171–18176.

Matcovitch-Natan, O. *et al.* (2016) 'Microglia development follows a stepwise program to regulate brain homeostasis.', *Science (New York, N.Y.)*, 353(6301), p. aad8670. doi: 10.1126/science.aad8670.

Mattison, J. A. *et al.* (2017) 'Caloric restriction improves health and survival of rhesus monkeys', *Nature communications*, 8(1), pp. 1–12.

McDonald, H. Y. and Wojtowicz, J. M. (2005) 'Dynamics of neurogenesis in the dentate gyrus of adult rats', *Neuroscience letters*, 385(1), pp. 70–75.

McKhann, G. M. *et al.* (2001) 'Clinical and Pathological Diagnosis of Frontotemporal Dementia: Report of the Work Group on Frontotemporal Dementia and Pick's Disease', *Archives of Neurology*, 58(11), pp. 1803–1809. doi: 10.1001/archneur.58.11.1803.

McNaught, K. S. P. *et al.* (2002) 'Aggresome-related biogenesis of Lewy bodies', *European Journal of Neuroscience*, 16(11), pp. 2136–2148.

Mendez, M. F., Shapira, J. S. and Miller, B. L. (2005) 'Stereotypical movements and frontotemporal dementia', *Mov Disord*, 20(6), pp. 742–745.

Meredith, G. E. *et al.* (2002) 'Lysosomal malfunction accompanies alpha-synuclein aggregation in a progressive mouse model of Parkinson's disease', *Brain research*, 956(1), pp. 156–165.

Merrilees, J. (2007) ‘A model for management of behavioral symptoms in frontotemporal lobar degeneration’, *Alzheimer Dis Assoc Disord*, 21(4), pp. s64-69. doi: 10.1097/WAD.0b013e31815bf774.

Merrilees, J. *et al.* (2009) ‘Rest-activity and behavioral disruption in a patient with frontotemporal dementia’, *Neurocase*, 15(6), pp. 515–526. doi: 10.1080/13554790903061371.

Mesulam, M.-M. *et al.* (2014) ‘Primary progressive aphasia and the evolving neurology of the language network.’, *Nature reviews. Neurology*, 10(10), pp. 554–569. doi: 10.1038/nrneurol.2014.159.

Mesulam, M. M. (1982) ‘Slowly progressive aphasia without generalized dementia’, *Annals of Neurology*, 11(6), pp. 592–598.

Mesulam, M. M. (1987) ‘Primary progressive aphasia: differentiation from Alzheimer’s disease’, *Ann Neurol*, 37, pp. 1448–1553.

Metrick, M. A. *et al.* (2020) ‘A single ultrasensitive assay for detection and discrimination of tau aggregates of Alzheimer and Pick diseases’, *Acta Neuropathologica Communications*, 8(1), p. 22. doi: 10.1186/s40478-020-0887-z.

Miguel, L. *et al.* (2012) ‘Accumulation of insoluble forms of FUS protein correlates with toxicity in Drosophila.’, *Neurobiology of aging*, 33(5), pp. 1008.e1–15. doi: 10.1016/j.neurobiolaging.2011.10.008.

Mikkonen, M. *et al.* (1998) ‘Remodeling of neuronal circuitries in human temporal lobe epilepsy: increased expression of highly polysialylated neural cell adhesion molecule in the hippocampus and the entorhinal cortex’, *Annals of Neurology: Official Journal of the American Neurological Association and the Child Neurology Society*, 44(6), pp. 923–934.

Minami, S. S. *et al.* (2014) ‘Progranulin protects against amyloid β deposition and toxicity in Alzheimer’s disease mouse models’, *Nature Medicine*, 20(10), pp. 1157–1164. doi: 10.1038/nm.3672.

Miranda, C. J. *et al.* (2012) ‘Aging brain microenvironment decreases hippocampal neurogenesis through Wnt-mediated survivin signaling’, *Aging cell*. 2012/04/04, 11(3), pp. 542–552. doi: 10.1111/j.1474-9726.2012.00816.x.

Mitchell, J. C. *et al.* (2015) ‘Wild type human TDP-43 potentiates ALS-linked mutant TDP-43 driven progressive motor and cortical neuron degeneration with pathological features of ALS’, *Acta neuropathologica communications*, 3(1), pp. 1–16.

Mogi, M. *et al.* (1995) ‘Transforming growth factor-beta 1 levels are elevated in the striatum and in ventricular cerebrospinal fluid in Parkinson’s disease.’, *Neuroscience letters*, 193(2), pp. 129–132. doi: 10.1016/0304-3940(95)11686-q.

Monje, M. L. (2003) ‘Inflammatory Blockade Restores Adult Hippocampal Neurogenesis’, *Science*, 302(5651), pp. 1760–1765. doi: 10.1126/science.1088417.

Montaron, M. F. *et al.* (2006) ‘Lifelong corticosterone level determines age-related decline in neurogenesis and memory’, *Neurobiology of aging*, 27(4), pp. 645–654.

Di Monte, D. A. (1991) ‘Mitochondrial DNA and Parkinson’s disease’, *Neurology*, 41(Issue 5, Supplement 2), pp. 38–42. doi: 10.1212/wnl.41.5_suppl_2.38.

Montembeault, M. *et al.* (2018) 'Clinical, Anatomical, and Pathological Features in the Three Variants of Primary Progressive Aphasia: A Review', *Frontiers in Neurology*, 9. doi: 10.3389/fneur.2018.00692.

Moon, M., Kim, S., *et al.* (2009) 'Ghrelin regulates hippocampal neurogenesis in adult mice', *Endocrine journal*, 56(3), pp. 525–531.

Moon, M., Kim, H. G., *et al.* (2009) 'Neuroprotective effect of ghrelin in the 1-methyl-4-phenyl-1, 2, 3, 6-tetrahydropyridine mouse model of Parkinson's disease by blocking microglial activation', *Neurotoxicity research*, 15(4), pp. 332–347.

Moon, M., Cha, M.-Y. and Mook-Jung, I. (2014) 'Impaired hippocampal neurogenesis and its enhancement with ghrelin in 5XFAD mice', *Journal of Alzheimer's Disease*, 41(1), pp. 233–241.

Mor, D. E., Daniels, M. J. and Ischiropoulos, H. (2019) 'The usual suspects, dopamine and alpha-synuclein, conspire to cause neurodegeneration', *Movement Disorders*, 34(2), pp. 167–179.

Moreno-Jiménez, E. P. *et al.* (2019) 'Adult hippocampal neurogenesis is abundant in neurologically healthy subjects and drops sharply in patients with Alzheimer's disease', *Nature Medicine*, 25(4), pp. 554–560. doi: 10.1038/s41591-019-0375-9.

Moreno-Jiménez, E. P. *et al.* (2021) 'Evidences for adult hippocampal neurogenesis in humans', *Journal of Neuroscience*, 41(12), pp. 2541–2553. doi: 10.1523/JNEUROSCI.0675-20.2020.

Mori, K. *et al.* (2000) 'Kidney produces a novel acylated peptide, ghrelin', *FEBS letters*, 486(3), pp. 213–216.

Morris, M. *et al.* (2011) 'The many faces of tau', *Neuron*, 70(3), pp. 410–426. doi: 10.1016/j.neuron.2011.04.009.

Morrison, S. J. and Kimble, J. (2006) 'Asymmetric and symmetric stem-cell divisions in development and cancer.', *Nature*, 441(7097), pp. 1068–1074. doi: 10.1038/nature04956.

Morshead, C. M. *et al.* (1994) 'Neural stem cells in the adult mammalian forebrain: A relatively quiescent subpopulation of subependymal cells', *Neuron*, 13(5), pp. 1071–1082. doi: 10.1016/0896-6273(94)90046-9.

Mosca, L. *et al.* (2012) 'Wide phenotypic spectrum of the TARDBP gene: homozygosity of A382T mutation in a patient presenting with amyotrophic lateral sclerosis, Parkinson's disease, and frontotemporal lobar degeneration, and in neurologically healthy subject', *Neurobiol Aging*, 33(8), pp. 1841–1844. doi: 10.1016/j.neurobiolaging.2012.01.108.

Mosley, A. D. (2009) *The encyclopedia of Parkinson's disease*. Infobase Publishing.

Nakamura, Y., Si, Q. S. and Kataoka, K. (1999) 'Lipopolysaccharide-induced microglial activation in culture: temporal profiles of morphological change and release of cytokines and nitric oxide', *Neuroscience Research*, 35(2), pp. 95–100. doi: 10.1016/s0168-0102(99)00071-1.

Nakanishi, M. *et al.* (2007) 'Microglia-derived interleukin-6 and leukaemia inhibitory factor promote astrocytic differentiation of neural stem/progenitor cells', *European*

Journal of Neuroscience, 25(3), pp. 649–658. doi: https://doi.org/10.1111/j.1460-9568.2007.05309.x.

Nakazato, M. *et al.* (2001) 'A role for ghrelin in the central regulation of feeding', *Nature*, 409(6817), pp. 194–198.

Narvid, J. *et al.* (2009) 'Of brain and bone: the unusual case of Dr', *A. Neurocase*, 15(3), pp. 190–205. doi: 10.1080/13554790802632967.

National Institute on Aging. (2016) *Parkinson's Disease | National Institute on Aging, U.S. Department of Health and Human Services*. Available at: https://www.nia.nih.gov/health/parkinsons-disease (Accessed: 25 December 2021).

Neary, D., Snowden, J. and Mann, D. (2005) 'Frontotemporal dementia', *The Lancet Neurology*, 4(11), pp. 771–780. doi: 10.1016/s1474-4422(05)70223-4.

Neumann, M. *et al.* (2006) 'Ubiquitinated TDP-43 in frontotemporal lobar degeneration and amyotrophic lateral sclerosis', *Science*, 314(5796), pp. 130–133. doi: 10.1126/science.1134108.

Neumann, M. *et al.* (2011) 'FET proteins TAF15 and EWS are selective markers that distinguish FTLD with FUS pathology from amyotrophic lateral sclerosis with FUS mutations', *Brain*, 134(Pt 9), pp. 2595–2609. doi: 10.1093/brain/awr201.

Neumann, M. and Mackenzie, I. R. A. (2019) 'Neuropathology of non-tau frontotemporal lobar degeneration', *Neuropathology and applied neurobiology*, 45(1), pp. 19–40.

Nicola, Z., Fabel, K. and Kempermann, G. (2015) 'Development of the adult neurogenic niche in the hippocampus of mice', *Frontiers in neuroanatomy*, 9, p. 53.

Nimmerjahn, A. (2005) 'Resting Microglial Cells Are Highly Dynamic Surveillants of Brain Parenchyma in Vivo', *Science*, 308(5726), pp. 1314–1318. doi: 10.1126/science.1110647.

Nithianantharajah, J. and Hannan, A. J. (2006) 'Enriched environments, experience-dependent plasticity and disorders of the nervous system', *Nature Reviews Neuroscience*, 7(9), pp. 697–709. doi: 10.1038/nrn1970.

Njie, E. G. *et al.* (2012) 'Ex vivo cultures of microglia from young and aged rodent brain reveal age-related changes in microglial function', *Neurobiology of aging*. 2010/07/02, 33(1), pp. 195.e1-195.12. doi: 10.1016/j.neurobiolaging.2010.05.008.

Noble, W. *et al.* (2013) 'The importance of tau phosphorylation for neurodegenerative diseases.', *Frontiers in neurology*, 4, p. 83. doi: 10.3389/fneur.2013.00083.

Noufi, P. *et al.* (2019) 'Use of Cholinesterase Inhibitors in Non-Alzheimer's Dementias', *Drugs & Aging*, 36(8), pp. 719–731. doi: 10.1007/s40266-019-00685-6.

Nurk, E. *et al.* (2009) 'Intake of flavonoid-rich wine, tea, and chocolate by elderly men and women is associated with better cognitive test performance.', *The Journal of nutrition*, 139(1), pp. 120–127. doi: 10.3945/jn.108.095182.

Nuytemans, K. *et al.* (2010) 'Genetic etiology of Parkinson disease associated with mutations in the SNCA, PARK2, PINK1, PARK7, and LRRK2 genes: A mutation update', *Human Mutation*, 31(7), pp. 763–780. doi: 10.1002/humu.21277.

O'Keeffe, G. C. *et al.* (2009) 'Dopamine-induced proliferation of adult neural precursor cells in the mammalian subventricular zone is mediated through EGF', *Proceedings of the National Academy of Sciences*, 106(21), pp. 8754–8759. doi: 10.1073/pnas.0803955106.

O'Neill, C. *et al.* (2001) 'Neurofibrillary tangles and tau phosphorylation', *Biochemical Society Symposia*, 67, pp. 81–88. doi: 10.1042/bss0670081.

Ohtani, N. *et al.* (2003) 'Dopamine modulates cell cycle in the lateral ganglionic eminence.', *The Journal of neuroscience : the official journal of the Society for Neuroscience*, 23(7), pp. 2840–2850. doi: 23/7/2840 [pii].

Olney, R. K. *et al.* (2005) 'The effects of executive and behavioral dysfunction on the course of ALS', *Neurology*, 65(11), pp. 1774–1777.

Onyike, C. U. and Diehl-Schmid, J. (2013) 'The epidemiology of frontotemporal dementia.', *International review of psychiatry (Abingdon, England)*, 25(2), pp. 130–137. doi: 10.3109/09540261.2013.776523.

OUH (2022) *MND and ALS - Oxford MND Centre*. Available at: https://www.ouh.nhs.uk/services/departments/neurosciences/neurology/mnd/support/mnd-als.aspx (Accessed: 22 December 2021).

Padiglia, A. *et al.* (1997) 'Modulation of 6-hydroxydopamine oxidation by various proteins', *Biochemical Pharmacology*, 53(8), pp. 1065–1068. doi: https://doi.org/10.1016/S0006-2952(96)00716-2.

Pajares, M. *et al.* (2020) 'Inflammation in Parkinson's disease: mechanisms and therapeutic implications', *Cells*, 9(7), p. 1687.

Pallas-Bazarra, N. *et al.* (2016) 'Novel function of Tau in regulating the effects of external stimuli on adult hippocampal neurogenesis', *The EMBO journal*, 35(13), pp. 1417–1436.

Palmer, T. D. *et al.* (1999) 'Fibroblast growth factor-2 activates a latent neurogenic program in neural stem cells from diverse regions of the adult CNS', *The Journal of neuroscience : the official journal of the Society for Neuroscience*, 19(19), pp. 8487–8497. doi: 10.1523/JNEUROSCI.19-19-08487.1999.

Palmer, T. D., Takahashi, J. and Gage, F. H. (1997) 'The Adult Rat Hippocampus Contains Primordial Neural Stem Cells', *Molecular and Cellular Neuroscience*, 8(6), pp. 389–404. doi: 10.1006/mcne.1996.0595.

Palumbo, A. *et al.* (1999) 'Nitrite- and Peroxide-Dependent Oxidation Pathways of Dopamine: 6-Nitrodopamine and 6-Hydroxydopamine Formation as Potential Contributory Mechanisms of Oxidative Stress- and Nitric Oxide-Induced Neurotoxicity in Neuronal Degeneration', *Chemical Research in Toxicology*, 12(12), pp. 1213–1222. doi: 10.1021/tx990121g.

Pan, H. S., Penney, J. B. and Young, A. B. (1985) ?'-Aminobutyric Acid and Benzodiazepine Receptor Changes Induced by Unilateral 6-Hydroxydopamine Lesions of the Medial Forebrain Bundle', *Journal of Neurochemistry*, 45(5), pp. 1396–1404. doi: 10.1111/j.1471-4159.1985.tb07205.x.

Pan, H. S. and Walters, J. R. (1988) 'Unilateral lesion of the nigrostriatal pathway decreases the firing rate and alters the firing pattern of globus pallidus neurons in the

rat', *Synapse*, 2(6), pp. 650–656. doi: 10.1002/syn.890020612.

Pandey, S. and Srivanitchapoom, P. (2017) 'Levodopa-induced Dyskinesia: Clinical Features, Pathophysiology, and Medical Management.', *Annals of Indian Academy of Neurology*, 20(3), pp. 190–198. doi: 10.4103/aian.AIAN_239_17.

Parihar, M. S. *et al.* (2008) 'Mitochondrial association of alpha-synuclein causes oxidative stress', *Cellular and Molecular Life Sciences*, 65(7), pp. 1272–1284.

Park, J.-H. and Enikolopov, G. (2010) 'Transient elevation of adult hippocampal neurogenesis after dopamine depletion', *Experimental neurology*, 222(2), pp. 267–276.

Park, S. H. *et al.* (2004) 'Activation of NF-κB is involved in 6-hydroxydopamine—but not MPP+-induced dopaminergic neuronal cell death: its potential role as a survival determinant', *Biochemical and biophysical research communications*, 322(3), pp. 727–733.

Parke, D. V (1991) 'Free radicals in biology and medicine (2nd Edition)', *FEBS Letters*, 284(1), pp. 135–136. doi: 10.1016/0014-5793(91)80785-2.

Parkinson's disease - NHS (2022). Available at: https://www.nhs.uk/conditions/parkinsons-disease/ (Accessed: 25 December 2021).

PARKINSON UK (2020) *Reporting on Parkinson's: information for journalists | Parkinson's UK*. Available at: https://www.parkinsons.org.uk/about-us/reporting-parkinsons-information-journalists (Accessed: 25 December 2021).

Parkinsonism vs. Parkinson's Disease: What's The Difference? (2022). Available at: https://parkinsonsdisease.net/answers/parkinsonism-vs-pd (Accessed: 25 December 2021).

Paul, A., Chaker, Z. and Doetsch, F. (2017) 'Hypothalamic regulation of regionally distinct adult neural stem cells and neurogenesis.', *Science (New York, N.Y.)*, 356(6345), pp. 1383–1386. doi: 10.1126/science.aal3839.

Pekna, M. and Pekny, M. (2012) 'The neurobiology of brain injury', in *Cerebrum: the Dana forum on Brain science*. Dana Foundation.

Perlmutter, J. S. (2009) 'Assessment of Parkinson disease manifestations', *Current protocols in neuroscience*, 49(1), pp. 10–11.

Perry, D. C. *et al.* (2012) 'Voxel-based morphometry in patients with obsessive-compulsive behaviors in behavioral variant frontotemporal dementia', *Eur J Neurol*, 19(6), pp. 911–917. doi: 10.1111/j.1468-1331.2011.03656.x.

Perumal, A. S. *et al.* (1989) 'Regional effects of 6-hydroxydopamine (6-OHDA) on free radical scavengers in rat brain', *Brain Research*, 504(1), pp. 139–141. doi: https://doi.org/10.1016/0006-8993(89)91611-9.

Phan, J.-A. *et al.* (2017) 'Early synaptic dysfunction induced by α-synuclein in a rat model of Parkinson's disease.', *Scientific reports*, 7(1), p. 6363. doi: 10.1038/s41598-017-06724-9.

Pick, A. (1892) 'Uber die Beziehungen der senilen Hirnatrophie zur Aphasie', *Prag Med Wochenschr*, 17, pp. 165–167.

Pijnenburg, Y. A. *et al.* (2003) 'Vulnerability to neuroleptic side effects in

frontotemporal lobar degeneration', *Int J Geriatr Psychiatry*, 18(1), pp. 67–72. doi: 10.1002/gps.774.

Plümpe, T. *et al.* (2006) 'Variability of doublecortin-associated dendrite maturation in adult hippocampal neurogenesis is independent of the regulation of precursor cell proliferation', *BMC Neuroscience*, 7(1), p. 77. doi: 10.1186/1471-2202-7-77.

Polymenidou, M. *et al.* (2011) 'Long pre-mRNA depletion and RNA missplicing contribute to neuronal vulnerability from loss of TDP-43', *Nat Neurosci*, 14(4), pp. 459–468. doi: 10.1038/nn.2779.

Poorkaj, P. *et al.* (1998) 'Tau is a candidate gene for chromosome 17 frontotemporal dementia', *Annals of neurology*, 43(6), pp. 815–825. doi: 10.1002/ana.410430617.

Postuma, R. B. *et al.* (2012) 'Identifying prodromal Parkinson's disease: Pre-Motor disorders in Parkinson's disease', *Movement Disorders*, 27(5), pp. 617–626. doi: https://doi.org/10.1002/mds.24996.

Postuma, R. B. (2014) 'Prodromal Parkinson's disease–using REM sleep behavior disorder as a window', *Parkinsonism & related disorders*, 20, pp. S1–S4.

Postuma, R. B., Gagnon, J. F. and Montplaisir, J. (2010) 'Clinical prediction of Parkinson's disease: planning for the age of neuroprotection', *Journal of Neurology, Neurosurgery & Psychiatry*, 81(9), pp. 1008–1013. doi: 10.1136/jnnp.2009.174748.

Pottier, C. *et al.* (2015) 'Whole-genome sequencing reveals important role for TBK1 and OPTN mutations in frontotemporal lobar degeneration without motor neuron disease', *Acta Neuropathol*, 130(1), pp. 77–92. doi: 10.1007/s00401-015-1436-x.

Pottier, C. *et al.* (2016) 'Genetics of FTLD: overview and what else we can expect from genetic studies', *J Neurochem*, 138(Suppl 1), pp. 32–53. doi: 10.1111/jnc.13622.

van Praag, H. *et al.* (2005) 'Exercise enhances learning and hippocampal neurogenesis in aged mice', *The Journal of neuroscience : the official journal of the Society for Neuroscience*, 25(38), pp. 8680–8685. doi: 10.1523/JNEUROSCI.1731-05.2005.

Przedborski, S. *et al.* (1992) 'Transgenic mice with increased Cu/Zn-superoxide dismutase activity are resistant to N-methyl-4-phenyl-1,2,3,6-tetrahydropyridine-induced neurotoxicity', *The Journal of neuroscience : the official journal of the Society for Neuroscience*, 12(5), pp. 1658–1667. doi: 10.1523/JNEUROSCI.12-05-01658.1992.

Puangmalai, N. *et al.* (2020) 'Internalization mechanisms of brain-derived tau oligomers from patients with Alzheimer's disease, progressive supranuclear palsy and dementia with Lewy bodies', *Cell death & disease*, 11(5), pp. 1–16.

Purves, D. *et al.* (2001) 'Circuits within the basal ganglia system', in *Neuroscience. 2nd edition*. Sinauer Associates.

Quintana, J. L. B. *et al.* (2009) 'Parkinson's Disease and Tea : A Quantitative Review', *Journal of the American College of Nutrition*, 28(1), pp. 1–6. doi: 10.1080/07315724.2009.10719754.

Rademakers, R., Cruts, M. and van Broeckhoven, C. (2004) 'The role of tau (MAPT) in frontotemporal dementia and related tauopathies', *Human Mutation*, 24(4), pp. 277–295. doi: https://doi.org/10.1002/humu.20086.

Rakhit, S. *et al.* (2005) 'N-methyl-D-aspartate and brain-derived neurotrophic factor induce distinct profiles of extracellular signal-regulated kinase, mitogen- and stress-activated kinase, and ribosomal s6 kinase phosphorylation in cortical neurons.', *Molecular pharmacology*, 67(4), pp. 1158–1165. doi: 10.1124/mol.104.005447.

Rakic, P. (2002) 'Neurogenesis in adult primate neocortex: an evaluation of the evidence', *Nature Reviews Neuroscience*, 3(1), pp. 65–71. doi: 10.1038/nrn700.

Rakowicz, W. P. and Hodges, J. R. (1998) 'Dementia and aphasia in motor neuron disease: an underrecognised association?', *Journal of Neurology, Neurosurgery \& Psychiatry*, 65(6), pp. 881–889. doi: 10.1136/jnnp.65.6.881.

Ramsay, R. R. *et al.* (1986) 'Energy-driven uptake of N-methyl-4-phenylpyridine by brain mitochondria mediates the neurotoxicity of MPTP', *Life Sciences*, 39(7), pp. 581–588. doi: 10.1016/0024-3205(86)90037-8.

Ramsay, R. R. *et al.* (1987) 'The inhibition site of MPP+, the neurotoxic bioactivation product of 1-methyl-4-phenyl-1,2,3, 6-tetrahydropyridine is near the Q-binding site of NADH dehydrogenase', *Archives of Biochemistry and Biophysics*, 259(2), pp. 645–649. doi: 10.1016/0003-9861(87)90531-5.

Ramsay, R. R., Salach, J. I. and Singer, T. P. (1986) 'Uptake of the neurotoxin 1-methyl-4-phenylpyridine (MPP+) by mitochondria and its relation to the inhibition of the mitochondrial oxidation of NAD+-linked substrates by MPP+', *Biochemical and Biophysical Research Communications*, 134(2), pp. 743–748. doi: 10.1016/s0006-291x(86)80483-1.

Rankin, K. P. *et al.* (2005) 'Self awareness and personality change in dementia', *J Neurol Neurosurg Psychiatry*, 76(5), pp. 632–639.

Ransohoff, R. M. and Cardona, A. E. (2010) 'The myeloid cells of the central nervous system parenchyma', *Nature*, 468(7321), pp. 253–262.

Ransom, B. R. *et al.* (1987) 'Astrocytes convert the parkinsonism inducing neurotoxin, MPTP, to its active metabolite, MPP+', *Neuroscience Letters*, 75(3), pp. 323–328. doi: 10.1016/0304-3940(87)90543-x.

Rascovsky, K. *et al.* (2011) 'Sensitivity of revised diagnostic criteria for the behavioural variant of frontotemporal dementia.', *Brain : a journal of neurology*, 134(Pt 9), pp. 2456–2477. doi: 10.1093/brain/awr179.

Ratcliff, R. *et al.* (2016) 'Diffusion Decision Model: Current Issues and History.', *Trends in cognitive sciences*, 20(4), pp. 260–281. doi: 10.1016/j.tics.2016.01.007.

Ratti, A. and Buratti, E. (2016) 'Physiological functions and pathobiology of TDP-43 and FUS/TLS proteins', *Journal of neurochemistry*, 138, pp. 95–111.

Rees, D. *et al.* (2022) 'Acyl-ghrelin attenuates neurochemical and motor deficits in the 6-OHDA model of Parkinson{\textquoteright}s disease', *bioRxiv*. doi: 10.1101/2022.01.31.478447.

Restivo, L. *et al.* (2015) 'Development of adult-generated cell connectivity with excitatory and inhibitory cell populations in the hippocampus', *Journal of Neuroscience*, 35(29), pp. 10600–10612.

Revest, J. M. *et al.* (2009) 'Adult hippocampal neurogenesis is involved in anxiety-

related behaviors', *Molecular psychiatry*, 14(10), pp. 959–967.

Reynolds, B. a. a and Weiss, S. (1992) 'Generation of neurons and astrocytes from isolated cells of the adult mammalian central nervous system', *Science*, 255(5052), pp. 1707–1710. doi: DOI: 10.1126/science.1553558.

Riku, Y. *et al.* (2021) 'Pathway from TDP-43-Related Pathology to Neuronal Dysfunction in Amyotrophic Lateral Sclerosis and Frontotemporal Lobar Degeneration.', *International journal of molecular sciences*, 22(8). doi: 10.3390/ijms22083843.

Robertson, G. S. and Robertson, H. A. (1989) 'Evidence that L-dopa-induced rotational behavior is dependent on both striatal and nigral mechanisms', *The Journal of neuroscience : the official journal of the Society for Neuroscience*, 9(9), pp. 3326–3331. doi: 10.1523/JNEUROSCI.09-09-03326.1989.

La Rosa, C., Ghibaudi, M. and Bonfanti, L. (2019) 'Newly generated and non-newly generated "immature" neurons in the mammalian brain: a possible reservoir of young cells to prevent brain aging and disease?', *Journal of clinical medicine*, 8(5), p. 685.

Rosen, H. J. *et al.* (2005) 'Neuroanatomical correlates of behavioural disorders in dementia.', *Brain : a journal of neurology*, 128(Pt 11), pp. 2612–2625. doi: 10.1093/brain/awh628.

Rosso, S. M. *et al.* (2001) 'Complex compulsive behaviour in the temporal variant of frontotemporal dementia', *J Neurol*, 248(11), pp. 965–970.

Roychowdhury, S. and Forsyth, D. R. (2012) 'Sleep disturbance in Parkinson disease', *Journal of Clinical Gerontology and Geriatrics*, 3(2), pp. 53–61. doi: https://doi.org/10.1016/j.jcgg.2012.04.002.

Rubchinsky, L. L., Park, C. and Worth, R. M. (2012) 'Intermittent neural synchronization in Parkinson's disease', *Nonlinear dynamics*, 68(3), pp. 329–346.

Rubinsztein, D. C. *et al.* (2005) 'Autophagy and its possible roles in nervous system diseases, damage and repair', *Autophagy*, 1(1), pp. 11–22.

Rudge, J. S. *et al.* (1992) 'Expression of Ciliary Neurotrophic Factor and the Neurotrophins - Nerve Growth Factor, Brain-Derived Neurotrophic Factor and Neurotrophin 3-in Cultured Rat Hippocampal Astrocytes', *European Journal of Neuroscience*, 4(6), pp. 459–471. doi: 10.1111/j.1460-9568.1992.tb00896.x.

Rudge, J. S. *et al.* (1995) 'Changes in neurotrophic factor expression and receptor activation following exposure of hippocampal neuron/astrocyte cocultures to kainic acid', *The Journal of neuroscience : the official journal of the Society for Neuroscience*, 15(10), pp. 6856–6867. doi: 10.1523/JNEUROSCI.15-10-06856.1995.

Sahay, A. *et al.* (2011) 'Increasing adult hippocampal neurogenesis is sufficient to improve pattern separation', *Nature*. 2011/04/03, 472(7344), pp. 466–470. doi: 10.1038/nature09817.

Sahay, A., Drew, M. R. and Hen, R. (2007) 'Dentate gyrus neurogenesis and depression', *The Dentate Gyrus: A Comprehensive Guide to Structure, Function, and Clinical Implications*. Elsevier, pp. 697–822. doi: 10.1016/s0079-6123(07)63038-6.

Sahay, A., Wilson, D. A. and Hen, R. (2011) 'Pattern separation: a common function

for new neurons in hippocampus and olfactory bulb', *Neuron*, 70(4), pp. 582–588. doi: 10.1016/j.neuron.2011.05.012.

Sanai, N. *et al.* (2004) 'Unique astrocyte ribbon in adult human brain contains neural stem cells but lacks chain migration', *Nature*, 427(6976), pp. 740–744. doi: 10.1038/nature02301.

Sanchez-Castaneda, C. *et al.* (2009) 'Correlations between gray matter reductions and cognitive deficits in dementia with Lewy Bodies and Parkinson's disease with dementia', *Movement Disorders*, 24(12), pp. 1740–1746. doi: https://doi.org/10.1002/mds.22488.

Schapansky, J., Nardozzi, J. D. and LaVoie, M. J. (2015) 'The complex relationships between microglia, alpha-synuclein, and LRRK2 in Parkinson's disease', *Neuroscience*, 302, pp. 74–88.

Schapira, A. H. V, Mann, V. M., *et al.* (1990) 'Anatomic and Disease Specificity of NADH CoQ1Reductase (Complex I) Deficiency in Parkinson's Disease', *Journal of Neurochemistry*, 55(6), pp. 2142–2145. doi: 10.1111/j.1471-4159.1990.tb05809.x.

Schapira, A. H. V, Cooper, J. M., *et al.* (1990) 'Mitochondrial Complex I Deficiency in Parkinson's Disease', *Journal of Neurochemistry*, 54(3), pp. 823–827. doi: 10.1111/j.1471-4159.1990.tb02325.x.

Schapira, A. H. V, Holt, I. J., *et al.* (1990) 'Mitochondrial DNA analysis in Parkinson's disease', *Movement Disorders*, 5(4), pp. 294–297. doi: 10.1002/mds.870050406.

Schapira, A. H. V, Chaudhuri, K. R. and Jenner, P. (2017) 'Non-motor features of Parkinson disease', *Nature Reviews Neuroscience*, 18(7), pp. 435–450. doi: 10.1038/nrn.2017.62.

Scharff, C. (2000) 'Chasing fate and function of new neurons in adult brains', *Current opinion in Neurobiology*, 10(6), pp. 774–783.

Schlachetzki, J. C. M. *et al.* (2016) 'Dopaminergic lesioning impairs adult hippocampal neurogenesis by distinct modification of α-synuclein', *Journal of Neuroscience Research*, 94(1), pp. 62–73. doi: https://doi.org/10.1002/jnr.23677.

Schmidt, D. E. *et al.* (1997) 'Attenuation of 1-methyl-4-phenylpyridinium (MPP+) neurotoxicity by deprenyl in organotypic canine substantia nigra cultures.', *Journal of neural transmission (Vienna, Austria : 1996)*, 104(8–9), pp. 875–885. doi: 10.1007/BF01285555.

Schneider, A. and Mandelkow, E. (2008) 'Tau-based treatment strategies in neurodegenerative diseases', *Neurotherapeutics*, 5(3), pp. 443–457. doi: 10.1016/j.nurt.2008.05.006.

Schouten, M. *et al.* (2020) 'Circadian glucocorticoid oscillations preserve a population of adult hippocampal neural stem cells in the aging brain', *Molecular Psychiatry*, 25(7), pp. 1382–1405. doi: 10.1038/s41380-019-0440-2.

Schrag, A. (2008) 'Epidemiology of movement disorders', in. Lippincott Williams & Wilkins.

Schroeter, M. L. *et al.* (2008) 'Neural networks in frontotemporal dementia–a meta-analysis', *Neurobiol Aging*, 29(3), pp. 418–426. doi:

10.1016/j.neurobiolaging.2006.10.023.

Scotter, E. L., Chen, H.-J. and Shaw, C. E. (2015) 'TDP-43 Proteinopathy and ALS: Insights into Disease Mechanisms and Therapeutic Targets', *Neurotherapeutics*, 12(2), pp. 352–363. doi: 10.1007/s13311-015-0338-x.

Seelaar, H. *et al.* (2011) 'Clinical, genetic and pathological heterogeneity of frontotemporal dementia: a review', *Journal of Neurology, Neurosurgery \& Psychiatry*, 82(5), pp. 476–486. doi: 10.1136/jnnp.2010.212225.

Seeley, W. W. *et al.* (2006) 'Early frontotemporal dementia targets neurons unique to apes and humans', *Ann Neurol*, 60(6), pp. 660–667.

Seeley, W. W. *et al.* (2007) 'Dissociable intrinsic connectivity networks for salience processing and executive control', *J Neurosci*.

Seeley, W. W. *et al.* (2008) 'Frontal paralimbic network atrophy in very mild behavioral variant frontotemporal dementia.', *Archives of neurology*, 65(2), pp. 249–255. doi: 10.1001/archneurol.2007.38.

Seeley, W. W., Zhou, J. and Kim, E. J. (2012) 'Frontotemporal Dementia: What Can the Behavioral Variant Teach Us about Human Brain Organization?', *Neuroscientist*, 18(4), pp. 373–385. doi: doi:1073858411410354.

Segura, I. *et al.* (2016) 'The oxygen sensor PHD2 controls dendritic spines and synapses via modification of filamin A', *Cell reports*, 14(11), pp. 2653–2667.

Seo, J. *et al.* (2019) 'A non-human primate model for stable chronic Parkinson's disease induced by MPTP administration based on individual behavioral quantification', *Journal of Neuroscience Methods*, 311, pp. 277–287. doi: https://doi.org/10.1016/j.jneumeth.2018.10.037.

Seress, L. *et al.* (2001) 'Cell formation in the human hippocampal formation from mid-gestation to the late postnatal period', *Neuroscience*, 105(4), pp. 831–843. doi: 10.1016/s0306-4522(01)00156-7.

Seress, L. (2007) 'Comparative anatomy of the hippocampal dentate gyrus in adult and developing rodents, non-human primates and humans', *The Dentate Gyrus: A Comprehensive Guide to Structure, Function, and Clinical Implications*. Elsevier, pp. 23–798. doi: 10.1016/s0079-6123(07)63002-7.

Sha, S. *et al.* (2006) 'Are frontotemporal lobar degeneration, progressive supranuclear palsy and corticobasal degeneration distinct diseases?', *Nature Clinical Practice Neurology*, 2(12), pp. 658–665. doi: 10.1038/ncpneuro0357.

Shahriyari, L. and Komarova, N. L. (2013) 'Symmetric vs. Asymmetric Stem Cell Divisions: An Adaptation against Cancer?', *PLOS ONE*, 8(10), pp. 1–16. doi: 10.1371/journal.pone.0076195.

Shen, R.-S. *et al.* (1985) 'Serotonergic conversion of MPTP and dopaminergic accumulation of MPP+', *FEBS Letters*, 189(2), pp. 225–230. doi: 10.1016/0014-5793(85)81028-0.

Sherer, T. B. *et al.* (2012) 'Overcoming obstacles in Parkinson's disease', *Movement Disorders*, 27(13), pp. 1606–1611. doi: 10.1002/mds.25260.

Shulman, J. M., De Jager, P. L. and Feany, M. B. (2011) 'Parkinson's Disease: Genetics and Pathogenesis', *Annual Review of Pathology: Mechanisms of Disease*, 6(1), pp. 193–222. doi: 10.1146/annurev-pathol-011110-130242.

Sierra, A. *et al.* (2010) 'Microglia shape adult hippocampal neurogenesis through apoptosis-coupled phagocytosis', *Cell stem cell*, 7(4), pp. 483–495. doi: 10.1016/j.stem.2010.08.014.

Sierra, A. *et al.* (2015) 'Neuronal hyperactivity accelerates depletion of neural stem cells and impairs hippocampal neurogenesis.', *Cell stem cell*, 16(5), pp. 488–503. doi: 10.1016/j.stem.2015.04.003.

Silhol, M. *et al.* (2005) 'Age-related changes in brain-derived neurotrophic factor and tyrosine kinase receptor isoforms in the hippocampus and hypothalamus in male rats', *Neuroscience*, 132(3), pp. 613–624. doi: 10.1016/j.neuroscience.2005.01.008.

Silva, J. *et al.* (2018) 'Neuroprotective effects of seaweeds against 6-hydroxidopamine-induced cell death on an in vitro human neuroblastoma model', *BMC complementary and alternative medicine*, 18(1), pp. 1–10.

Šimić, G. *et al.* (2016) 'Tau Protein Hyperphosphorylation and Aggregation in Alzheimer's Disease and Other Tauopathies, and Possible Neuroprotective Strategies.', *Biomolecules*, 6(1), p. 6. doi: 10.3390/biom6010006.

Simon, J. *et al.* (2004) 'Mitogen-and stress-activated protein kinase 1 mediates cAMP response element-binding protein phosphorylation and activation by neurotrophins', *Journal of Neuroscience*, 24(18), pp. 4324–4332.

Skibinski, G. *et al.* (2005) 'Mutations in the endosomal ESCRTIII-complex subunit CHMP2B in frontotemporal dementia', *Nat Genet*, 37(8), pp. 806–808.

Smirnov, D. S. *et al.* (2020) 'Cognitive decline profiles differ in Parkinson disease dementia and dementia with Lewy bodies.', *Neurology*, 94(20), pp. e2076–e2087. doi: 10.1212/WNL.0000000000009434.

Snowden, J. S., Neary, D. and Mann, D. M. A. (2002) 'Frontotemporal dementia.', *The British journal of psychiatry : the journal of mental science*, 180, pp. 140–143. doi: 10.1192/bjp.180.2.140.

Snyder, J. S., Ferrante, S. C. and Cameron, H. A. (2012) 'Late maturation of adult-born neurons in the temporal dentate gyrus', *PloS one*, 7(11), p. e48757.

Sohn, P. D. *et al.* (2019) 'Pathogenic tau impairs axon initial segment plasticity and excitability homeostasis', *Neuron*, 104(3), pp. 458–470.

Song, H., Stevens, C. F. and Gage, F. H. (2002) 'Astroglia induce neurogenesis from adult neural stem cells', *Nature*, 417(6884), pp. 39–44. doi: 10.1038/417039a.

Song, M. *et al.* (2021) 'Diagnostic classification and biomarker identification of Alzheimer's disease with random forest algorithm', *Brain Sciences*, 11(4), p. 453.

Sonne, J., Reddy, V. and Beato, M. R. (2019) 'Neuroanatomy, substantia nigra'.

Sorrells, S. F. *et al.* (2018) 'Human hippocampal neurogenesis drops sharply in children to undetectable levels in adults.', *Nature*, 555(7696), pp. 377–381. doi: 10.1038/nature25975.

Sorrells, S. F. *et al.* (2021) 'Positive controls in adults and children support that very few, if any, new neurons are born in the adult human hippocampus', *Journal of Neuroscience*, 41(12), pp. 2554–2565.

Sotiropoulos, I. *et al.* (2011) 'Stress acts cumulatively to precipitate Alzheimer's disease-like tau pathology and cognitive deficits', *Journal of Neuroscience*, 31(21), pp. 7840–7847.

Soto-Otero, R. *et al.* (2000) 'Autoxidation and Neurotoxicity of 6-Hydroxydopamine in the Presence of Some Antioxidants', *Journal of Neurochemistry*, 74(4), pp. 1605–1612. doi: https://doi.org/10.1046/j.1471-4159.2000.0741605.x.

Spalding, K. L. *et al.* (2013) 'Dynamics of hippocampal neurogenesis in adult humans', *Cell*, 153(6), pp. 1219–1227. doi: 10.1016/j.cell.2013.05.002.

Spillantini, M. G., Crowther, R. A., *et al.* (1998) 'alpha-Synuclein in filamentous inclusions of Lewy bodies from Parkinson's disease and dementia with lewy bodies.', *Proceedings of the National Academy of Sciences of the United States of America*, 95(11), pp. 6469–6473. doi: 10.1073/pnas.95.11.6469.

Spillantini, M. G., Murrell JR, G., *et al.* (1998) 'Mutation in the tau gene in familial multiple system tauopathy with presenile dementia', in *Proceedings of the National Academy of Sciences of the United States of America*, pp. 7737–7741.

Spritzer, M. D. and Roy, E. A. (2020) 'Testosterone and adult neurogenesis', *Biomolecules*, 10(2), p. 225.

Sreedharan, J. *et al.* (2015) 'Age-dependent TDP-43-mediated motor neuron degeneration requires GSK3, hat-trick, and xmas-2', *Current Biology*, 25(16), pp. 2130–2136.

Stallings, N. R. *et al.* (2010) 'Progressive motor weakness in transgenic mice expressing human TDP-43', *Neurobiology of Disease*, 40(2), pp. 404–414. doi: https://doi.org/10.1016/j.nbd.2010.06.017.

Stangl, D. and Thuret, S. (2009) 'Impact of diet on adult hippocampal neurogenesis', *Genes & nutrition*. 2009/08/15, 4(4), pp. 271–282. doi: 10.1007/s12263-009-0134-5.

Steele, N. Z. *et al.* (2018) 'Frequency of frontotemporal dementia gene variants in C9ORF72, MAPT, and GRN in academic versus commercial laboratory cohorts', *Advances in Genomics and Genetics*, Volume 8, pp. 23–33. doi: 10.2147/agg.s164047.

Stewart, M. K., Mattiske, D. M. and Pask, A. J. (2020) 'exogenous oestrogen impacts cell fate decision in the developing gonads: A potential cause of declining human reproductive health', *International Journal of Molecular Sciences*, 21(21), p. 8377.

Stute, P. *et al.* (2021) 'Cognitive health after menopause: Does menopausal hormone therapy affect it?', *Best Practice & Research Clinical Endocrinology & Metabolism*, 35(6), p. 101565.

Sveinbjornsdottir, S. (2016) 'The clinical symptoms of Parkinson's disease', *Journal of Neurochemistry*, pp. 318–324. doi: 10.1111/jnc.13691.

Swartz JR, M. *et al.* (1997) 'Frontotemporal dementia: treatment response to serotonin selective reuptake inhibitors', *J Clin Psychiatry*, 58(5), pp. 212–216.

van Swieten, J. C. and Heutink, P. (2008) ‘Mutations in progranulin (GRN) within the spectrum of clinical and pathological phenotypes of frontotemporal dementia’, *The Lancet Neurology*, 7(10), pp. 965–974. doi: 10.1016/s1474-4422(08)70194-7.

Van Swieten, J. and Spillantini, M. G. (2007) ‘Hereditary frontotemporal dementia caused by Tau gene mutations’, *Brain Pathology*, 17(1), pp. 63–73.

Sydow, A. *et al.* (2011) ‘Reversibility of Tau-Related Cognitive Defects in a Regulatable FTD Mouse Model’, *Journal of Molecular Neuroscience*, 45(3), p. 432. doi: 10.1007/s12031-011-9604-5.

Tajiri, N. *et al.* (2010) ‘Exercise exerts neuroprotective effects on Parkinson’s disease model of rats.’, *Brain research*, 1310, pp. 200–207. doi: 10.1016/j.brainres.2009.10.075.

Talbot, K. (2009) ‘Motor neuron disease’, *Practical Neurology*, 9(5), pp. 303–309. doi: 10.1136/jnnp.2009.188151.

Tansey, M. G. and Romero-Ramos, M. (2019) ‘Immune system responses in Parkinson’s disease: Early and dynamic.’, *The European journal of neuroscience*, 49(3), pp. 364–383. doi: 10.1111/ejn.14290.

Tanti, A. *et al.* (2013) ‘Region-dependent and stage-specific effects of stress, environmental enrichment, and antidepressant treatment on hippocampal neurogenesis’, *Hippocampus*, 23(9), pp. 797–811.

Tashiro, A. *et al.* (2006) ‘NMDA-receptor-mediated, cell-specific integration of new neurons in adult dentate gyrus’, *Nature*, 442(7105), pp. 929–933. doi: 10.1038/nature05028.

Taupin, P. (2007) ‘BrdU immunohistochemistry for studying adult neurogenesis: Paradigms, pitfalls, limitations, and validation’, *Brain Research Reviews*, 53(1), pp. 198–214. doi: https://doi.org/10.1016/j.brainresrev.2006.08.002.

Tavazoie, M. *et al.* (2008) ‘A Specialized Vascular Niche for Adult Neural Stem Cells’, *Cell Stem Cell*, 3(3), pp. 279–288. doi: https://doi.org/10.1016/j.stem.2008.07.025.

Tekin, S. and Cummings, J. L. (2002) ‘Frontal-subcortical neuronal circuits and clinical neuropsychiatry: an update’, *J Psychosom Res*, 2002;53(2), pp. 647–654.

Terreros-Roncal, J. *et al.* (2021) ‘Impact of neurodegenerative diseases on human adult hippocampal neurogenesis’, *Science*, 374(6571), pp. 1106–1113. doi: 10.1126/science.abl5163.

Terreros-Roncal, J. *et al.* (2022) ‘Response to Comment on “Impact of neurodegenerative diseases on human adult hippocampal neurogenesis”’, *Science*, 376(6590), p. eabo0920. doi: 10.1126/science.abo0920.

Terstege, D. J. *et al.* (2022) ‘New neurons in old brains: implications of age in the analysis of neurogenesis in post-mortem tissue’, *Molecular Brain*, 15(1), p. 38. doi: 10.1186/s13041-022-00926-7.

Thibodeau, M.-P. and Miller, B. L. (2013) ‘“Limits and current knowledge of Pick’s disease: its differential diagnosis”. A translation of the 1957 Delay, Brion, Escourolle article.’, *Neurocase*, 19(5), pp. 417–422. doi: 10.1080/13554794.2012.667133.

Thomas, B. and Beal, M. F. (2017) ‘Parkinson ’ s disease’, 16(2), pp. 183–194. doi: 10.1093/hmg/ddm159.

Thompson, A. *et al.* (2008) ‘Changes in adult neurogenesis in neurodegenerative diseases: cause or consequence?’, *Genes, Brain and Behavior*, 7, pp. 28–42.

Tolle, V. *et al.* (2002) ‘Ultradian rhythmicity of ghrelin secretion in relation with GH, feeding behavior, and sleep-wake patterns in rats’, *Endocrinology*, 143(4), pp. 1353–1361.

Tranel, D., Bechara, A. and Denburg, N. L. (2002) ‘Asymmetric functional roles of right and left ventromedial prefrontal cortices in social conduct, decision-making, and emotional processing’, *Cortex*, 2002;38(4), pp. 589–612.

Trinczek, B. *et al.* (1995) ‘Domains of tau protein, differential phosphorylation, and dynamic instability of microtubules.’, *Molecular Biology of the Cell*, 6(12), pp. 1887–1902. doi: 10.1091/mbc.6.12.1887.

Trojano, L. and Papagno, C. (2018) ‘Cognitive and behavioral disorders in Parkinson’s disease: an update. II: behavioral disorders.’, *Neurological sciences : official journal of the Italian Neurological Society and of the Italian Society of Clinical Neurophysiology*, 39(1), pp. 53–61. doi: 10.1007/s10072-017-3155-7.

Tsai, R. M. and Boxer, A. L. (2016) ‘Therapy and clinical trials in frontotemporal dementia: past, present, and future’, *J Neurochem*, 138(Suppl 1), pp. 211–221. doi: 10.1111/jnc.13640.

Tschop, M., Smiley, D. L. and Heiman, M. L. (2000) ‘Ghrelin induces adiposity in rodents. Nature. 2000; 407: 908-13’, *Stainless Steel Pilot Control Valves Pressure Reducing Control Valve Regulator Valve.[Abundant Stock High Capability Resistant Safety Guardrail Road Fence Barrier]*.

Tsuchiya, K. *et al.* (2001) ‘Argyrophilic grain disease mimicking temporal Pick’s disease: A clinical, radiological, and pathological study of an autopsy case with a clinical course of 15 years’, *Acta Neuropathologica*, 102(2), pp. 195–199. doi: 10.1007/s004010100365.

Uhl, G., Javitch, J. and Snyder, S. (1985) ‘Normal MPTP binding in parkinsonian substantia nigra: evidence for extraneuronal toxin conversion in human brain’, *The Lancet*, 325(8435), pp. 956–957.

Ungerstedt, U. and Arbuthnott, G. W. (1970) ‘Quantitative recording of rotational behavior in rats after 6-hydroxy-dopamine lesions of the nigrostriatal dopamine system’, *Brain Research*, 24(3), pp. 485–493. doi: 10.1016/0006-8993(70)90187-3.

Valko, M., Morris, H. and Cronin, M. T. D. (2005) ‘Metals, toxicity and oxidative stress’, *Current medicinal chemistry*, 12(10), pp. 1161–1208.

Vance, C. *et al.* (2009) ‘Mutations in FUS, an RNA processing protein, cause familial amyotrophic lateral sclerosis type 6’, *Science*, 323(5918), pp. 1208–1211. doi: 10.1126/science.1165942.

Vin, F., Allaert, F. A. and Levardon, M. (1992) ‘Influence of estrogens and progesterone on the venous system of the lower limbs in women’, *The Journal of dermatologic surgery and oncology*, 18(10), pp. 888–892.

Viña, J. *et al.* (2005) 'Why females live longer than males? Importance of the upregulation of longevity-associated genes by oestrogenic compounds', *FEBS letters*, 579(12), pp. 2541–2545.

Wang, X. *et al.* (2021) 'Transcriptome dynamics of hippocampal neurogenesis in macaques across the lifespan and aged humans'. doi: 10.21203/rs.3.rs-1015150/v1.

Warren, J. D. *et al.* (2013) 'Molecular nexopathies: a new paradigm of neurodegenerative disease.', *Trends in neurosciences*, 36(10), pp. 561–569. doi: 10.1016/j.tins.2013.06.007.

Warren, J. D., Rohrer, J. D. and Rossor, M. N. (2013) 'Frontotemporal dementia', *BMJ*, 347. doi: 10.1136/bmj.f4827.

Watkins, J. A. *et al.* (2021) 'Extensive phenotypic characterisation of a human TDP-43Q331K transgenic mouse model of amyotrophic lateral sclerosis (ALS)', *Scientific Reports*, 11(1), p. 16659. doi: 10.1038/s41598-021-96122-z.

Watson, G. S. and Leverenz, J. B. (2010) 'Profile of cognitive impairment in Parkinson's disease.', *Brain pathology (Zurich, Switzerland)*, 20(3), pp. 640–645. doi: 10.1111/j.1750-3639.2010.00373.x.

Weerasinghe-Mudiyanselage, P. D. E. *et al.* (2022) 'Structural Plasticity of the Hippocampus in Neurodegenerative Diseases.', *International journal of molecular sciences*, 23(6). doi: 10.3390/ijms23063349.

Weingarten, M. D. *et al.* (1975) 'A protein factor essential for microtubule assembly', in *Proc Natl Acad Sci U S A*, pp. 1858–1862.

Weinhard, L. *et al.* (2018) 'Microglia remodel synapses by presynaptic trogocytosis and spine head filopodia induction.', *Nature communications*, 9(1), p. 1228. doi: 10.1038/s41467-018-03566-5.

Wexler, E. M. *et al.* (2009) 'Endogenous Wnt signaling maintains neural progenitor cell potency', *Stem cells (Dayton, Ohio)*, 27(5), pp. 1130–1141. doi: 10.1002/stem.36.

White, M. A., Kim, E., Duffy, A., Adalbert, R., Phillips, B. U., Peters, O. M., Stephenson, J., Yang, S., Massenzio, F., Lin, Z., Andrews, S., Segonds-Pichon, A., Metterville, J., Saksida, L. M., Mead, R., Ribchester, R. R., Barhomi, Y., Serre, T., Coleman, M. P., Fallon, J. R., *et al.* (2018) 'TDP-43 gains function due to perturbed autoregulation in a Tardbp knock-in mouse model of ALS-FTD', *Nature Neuroscience*, 21(4), pp. 552–563. doi: 10.1038/s41593-018-0113-5.

White, M. A., Kim, E., Duffy, A., Adalbert, R., Phillips, B. U., Peters, O. M., Stephenson, J., Yang, S., Massenzio, F., Lin, Z., Andrews, S., Segonds-Pichon, A., Metterville, J., Saksida, L. M., Mead, R., Ribchester, R. R., Barhomi, Y., Serre, T., Coleman, M. P., Fallon, J., *et al.* (2018) 'TDP-43 gains function due to perturbed autoregulation in a Tardbp knock-in mouse model of ALS-FTD', *Nature Neuroscience*, 21(4), pp. 552–563. doi: 10.1038/s41593-018-0113-5.

Wilhelmsen, K. C. *et al.* (1994) 'Localization of Disinhibition-Dementia-Parkinsonism-Amyotrophy Complex to 17q21-22', *American Journal of Human Genetics*, 55(6), pp. 1159–1165.

Wilhelmsson, U. *et al.* (2012) 'Astrocytes Negatively Regulate Neurogenesis Through the Jagged1-Mediated Notch Pathway', *STEM CELLS*, 30(10), pp. 2320–2329. doi:

10.1002/stem.1196.

Wirenfeldt, M., Dalmau, I. and Finsen, B. (2003) 'Estimation of absolute microglial cell numbers in mouse fascia dentata using unbiased and efficient stereological cell counting principles', *Glia*, 44(2), pp. 129–139. doi: 10.1002/glia.10277.

Witte, A. V *et al.* (2009) 'Caloric restriction improves memory in elderly humans', *Proceedings of the National Academy of Sciences*, 106(4), pp. 1255–1260.

Woodbury, M. E. and Ikezu, T. (2014) 'Fibroblast growth factor-2 signaling in neurogenesis and neurodegeneration.', *Journal of neuroimmune pharmacology : the official journal of the Society on NeuroImmune Pharmacology*, 9(2), pp. 92–101. doi: 10.1007/s11481-013-9501-5.

Woolley, J. D. *et al.* (2011) 'The diagnostic challenge of psychiatric symptoms in neurodegenerative disease: rates of and risk factors for prior psychiatric diagnosis in patients with early neurodegenerative disease.', *The Journal of clinical psychiatry*, 72(2), pp. 126–133. doi: 10.4088/JCP.10m06382oli.

Worlitzer, M. M. A. *et al.* (2013) 'The majority of newly generated cells in the adult mouse substantia nigra express low levels of Doublecortin, but their proliferation is unaffected by 6-OHDA-induced nigral lesion or Minocycline-mediated inhibition of neuroinflammation', *European Journal of Neuroscience*, 38(5), pp. 2684–2692. doi: https://doi.org/10.1111/ejn.12269.

Wu, J. W. *et al.* (2013) 'Small misfolded Tau species are internalized via bulk endocytosis and anterogradely and retrogradely transported in neurons.', *The Journal of biological chemistry*, 288(3), pp. 1856–1870. doi: 10.1074/jbc.M112.394528.

Xapelli, S. *et al.* (2020) 'Editorial: Glial and Neural Stem Cells as New Therapeutic Targets for Neurodegenerative Disorders', *Frontiers in Cellular Neuroscience*, 14. doi: 10.3389/fncel.2020.00071.

Yamada, M. *et al.* (2004) 'Neurogenesis in olfactory bulb identified by retroviral labeling in normal and 1-methyl-4-phenyl-1, 2, 3, 6-tetrahydropyridine-treated adult mice', *Neuroscience*, 124(1), pp. 173–181.

Yamashita, T. *et al.* (2006) 'Subventricular zone-derived neuroblasts migrate and differentiate into mature neurons in the post-stroke adult striatum', *Journal of Neuroscience*, 26(24), pp. 6627–6636.

Yao, S. C., Hart, A. D. and Terzella, M. J. (2013) 'An evidence-based osteopathic approach to Parkinson disease', *Osteopathic Family Physician*, 5(3), pp. 96–101. doi: 10.1016/j.osfp.2013.01.003.

Yassa, M. A. and Stark, C. E. L. (2011) 'Pattern separation in the hippocampus', *Trends in Neurosciences*, 34(10), pp. 515–525. doi: https://doi.org/10.1016/j.tins.2011.06.006.

Yin, Y., Li, Y. and Zhang, W. (2014) 'The growth hormone secretagogue receptor: its intracellular signaling and regulation', *International journal of molecular sciences*, 15(3), pp. 4837–4855.

Yoshida, H. and Ihara, Y. (1993) 'τ in Paired Helical Filaments Is Functionally Distinct from Fetal τ: Assembly Incompetence of Paired Helical Filament-τ', *Journal of Neurochemistry*, 61(3), pp. 1183–1186. doi: https://doi.org/10.1111/j.1471-

4159.1993.tb03642.x.

Yoshida, M. (2006) ‘Cellular tau pathology and immunohistochemical study of tau isoforms in sporadic tauopathies’, *Neuropathology*, 26(5), pp. 457–470. doi: https://doi.org/10.1111/j.1440-1789.2006.00743.x.

Yu, D. X., Marchetto, M. C. and Gage, F. H. (2014) ‘How to make a hippocampal dentate gyrus granule neuron’, *Development*, 141(12), pp. 2366–2375.

Zarei, S. *et al.* (2015) ‘A comprehensive review of amyotrophic lateral sclerosis’, *Surgical Neurology International*, 6(1). doi: 10.4103/2152-7806.169561.

Zbarsky, V. *et al.* (2005) ‘Neuroprotective properties of the natural phenolic antioxidants curcumin and naringenin but not quercetin and fisetin in a 6-OHDA model of Parkinson’s disease’, *Free radical research*, 39(10), pp. 1119–1125.

Zhang, K. Y. *et al.* (2014) ‘Ubiquilin 2: A component of the ubiquitin–proteasome system with an emerging role in neurodegeneration’, *The International Journal of Biochemistry & Cell Biology*, 50, pp. 123–126. doi: https://doi.org/10.1016/j.biocel.2014.02.018.

Zhang, Y. *et al.* (1999) ‘Tissue oxygen levels control astrocyte movement and differentiation in developing retina’, *Developmental Brain Research*, 118(1–2), pp. 135–145.

Zhao, C., Deng, W. and Gage, F. H. (2008) ‘Mechanisms and Functional Implications of Adult Neurogenesis’, *Cell*, 132(4), pp. 645–660. doi: 10.1016/j.cell.2008.01.033.

Zhao, Z. *et al.* (2014) ‘Ghrelin administration enhances neurogenesis but impairs spatial learning and memory in adult mice’, *Neuroscience*, 257, pp. 175–185.

Zhou, Y. *et al.* (2022) ‘Molecular landscapes of human hippocampal immature neurons across lifespan’, *Nature*, 607(7919), pp. 527–533. doi: 10.1038/s41586-022-04912-w.

Zhukareva, V. *et al.* (2002) ‘Sporadic Pick’s disease: a tauopathy characterized by a spectrum of pathological tau isoforms in gray and white matter’, *Ann Neurol*, 51(6), pp. 730–739.

Ziegler, D. R. *et al.* (2003) ‘Ketogenic diet increases glutathione peroxidase activity in rat hippocampus’, *Neurochemical research*, 28(12), pp. 1793–1797.